

Stoichiometric Biology of the Synapse

Dissertation

in partial fulfillment of the requirements for the degree

“Doctor of Natural Sciences (Dr. rer. nat)”

in the Neuroscience Program

at the Georg August University Göttingen,

Faculty of Biology

submitted by

Benjamin G. Wilhelm

born in

Kassel, Germany

Göttingen, March 2013

“Everything which is composed of not one but multiple parts is not just the mere aggregation of parts but a unity.”

Freely translated from Aristotle, Metaphysics (1401 b 11–14)

I hereby declare that I prepared the dissertation entitled "Stoichiometric Biology of the Synapse" on my own with no other sources and aids than quoted.

Benjamin G. Wilhelm

Table of Contents

Table of Contents.....	I
Acknowledgements	IV
Abstract.....	VI
List of Figures.....	VII
List of Tables.....	VIII
List of Abbreviations	IX
<u>1. Introduction</u>	1
1.1 Functional and morphological features of synapses	1
1.1.1 Synaptic vesicle exocytosis	4
1.1.2 Synaptic vesicle endocytosis	6
1.1.3 Need for descriptive approaches	10
1.2 Molecular composition of a synapse	11
1.2.1 The molecular composition of the post-synaptic density.....	11
1.2.2 The molecular composition of a synaptic vesicle	12
1.2.3 The molecular composition of the AZ.....	14
1.3 Scope of this study	16
<u>2. Materials and Methods</u>	17
2.1 Chemicals.....	17
2.2 Buffers and Solutions	17
2.3 Antibodies	17
2.4 Microscopy	24
2.4.1 Epi-fluorescence microscopy	24
2.4.2 Confocal microscopy	24
2.4.2.1 <i>STED microscopy</i>	25
2.4.3 Electron Microscopy	25
2.5 Preparation of synaptosomes.....	26
2.5.1 Comparison of upper (U) and lower (L) synaptosome bands	28

2.5.2 Attempts to further enrich synaptosomes	29
2.6 Processing of synaptosomes for EM	32
2.7 Characterization of synaptosomes	33
2.7.1 Fluorescence-based spin down assay	33
2.7.1.2 <i>Spin down efficiency assay</i>	34
2.7.2 EM-based assay.....	35
2.8 Three dimensional reconstructions of synaptosomes	35
2.9 Determining absolute protein amounts per synaptosome.....	35
2.9.1 Protein standards.....	35
2.9.2 SDS-Page and Western Blotting	38
2.9.2.1 Troubleshooting immunoblots	39
2.9.3 Deriving correction factors for soluble proteins potentially lost from synaptosomes during purification.....	41
2.10 Immunostaining of primary hippocampal cultures	43
2.11 Immunostaining of mouse NMJs	44
2.12 Graphical modeling of the average pre-synaptic terminal.....	45
<u>3. Results</u>	<u>46</u>
3.1 Purification and characterization of synaptosomes	47
3.1.1 Determining the fraction of synaptosome particles using a fluorescence assay.....	48
3.1.2 Determining amount of synaptosomes using electron micrographs	51
3.1.3 The purity of the synaptosome preparations – comparing the two assays	52
3.2 Physical parameters of the synaptosomes.....	54
3.3 Absolute quantification of pre-synaptic proteins.....	57
3.3.1 Control for loss of soluble proteins during synaptosome purification	61
3.3.2 Calculating absolute protein copy numbers per synapse	64
3.4 Investigating the pre-synaptic protein organization.....	71
3.4.1 Pre-synaptic protein organization in primary hippocampal neurons	72
3.4.2 Pre-synaptic protein organization in mouse NMJs	75
3.5 The average pre-synaptic terminal	77
3.5.1 Graphical model of the average pre-synaptic terminal	93

4. Discussion	100
4.1 Quantitative approaches	101
4.1.1 Quantitative mass spectrometry	101
4.1.2 Quantitative microscopy	103
4.1.3 Quantitative immunoblots	105
4.2 Stoichiometric biology of a pre-synaptic terminal	108
4.2.1 Bottlenecks as control elements for pre-synaptic function	130
4.2.2 SV release is blocked everywhere but at distinct sites	131
4.2.3 The synapse – more than just the sum of its parts	133
5. Conclusion and Outlook	135
Bibliography	137
Appendix	185
Curriculum Vitae	187
Publications	188

Acknowledgements

First and foremost, I would like to thank my supervisor Prof. Silvio Rizzoli for outstanding guidance and supervision. Silvio, îți mulțumesc pentru suportul tău constant și pentru că mi-ai oferit șansa de a lucra în cadrul unui proiect atât de interesant. Îți mulțumesc de asemenea pentru că mi-ai ascultat și mi-ai apreciat opiniile. Îți mulțumesc că ai avut grijă de bunăstarea mea (mentală), uneori chiar mai mult decât de a ta. Aș vrea să îți mulțumesc și pentru că mi-ai împărtășit filozofia ta despre viață și știință, precum și bancurile tale foarte amuzante (“The incredible loneliness of his single neuron”). Îți mulțumesc pentru acești 4 ani – m-am simțit grozav lucrând cu tine!

I would like to thank the members of my thesis committee, Prof. Erwin Neher and Prof. Stefan Hell for their support and helpful discussions. I also want to thank Stefan Hallermann for agreeing to be part of my extended thesis committee.

I am grateful to Prof. Michael Hörner for being part of my thesis committee and especially for being the coordinator of the MSc/PhD Neuroscience program. Thank you Sandra and Michael, for your continuous support in the past years and for providing such an excellent study atmosphere.

In addition I would like to thank Prof. Ralf Heinrich who was highly influential during the early stages of my scientific career. Ralf, thank you for your support and the opportunities you gave me.

I would also like to thank the good souls of the ENI: Sissi and Christiane for help with administrative issues, Matthias and Ali for making sure my system was always running properly, Heiko and Robin for excellent technical support and Frank and Sven for helping me to make a very special wooden ring.

I am indebted to Gottfried Mieskes for always having the time to answer my questions although I have never been part of his lab. I also want to thank our collaborators: Prof. Henning Urlaub, Sunit Mandad, Prof. Volker Haucke, Dr. Michael Krauss, Prof. Reinhard Jahn, Ursel Ries, Aurelien Roux, Beat Schwaller and Prof. Christian Griesinger.

I am grateful to the team of the Boehringer Ingelheim Fonds for their personal and financial support in the past three years.

Many thanks to Dr. Teja Grömer. Teja, you are a great scientist and personal physician but I value you most as a friend. Be sure to always get a “Toastpizza” from me anywhere and anytime – thank you for everything.

Ein ausdrücklicher Dank geht an meine Freunde – Ihr wisst wer Ihr seid. Ich bin unglaublich stolz Euch zu haben und freue mich auf viele weitere Jahre mit Euch! Danke für Wambo, Alle machen mit, Call me Maybe, Man Doh, Tu Es und Ohne Hose.

Es wird gesagt, dass man sich seine Familie nicht aussuchen kann, sondern sie so nehmen muss wie sie ist – ich freue mich, dass es so ist und möchte Euch von ganzem Herzen für eure Unterstützung und Zuneigung danken. Ein besonderer Dank geht an meine Eltern, die es sicherlich nie leicht mit mir hatten, aber immer für mich da waren und an mich geglaubt haben. Ich bin dankbar für die Zeit, die ich mit Euch verbringen kann und weiß, dass es zu Hause immernoch am schönsten ist.

Laura, Du bist nun schon über zehn Jahre an meiner Seite, schenkst mir Kraft und Mut, aber auch Vernunft und Einsicht. Dafür möchte ich Dir danken – danke, dass es uns so gut geht, danke, dass Du mein Liebblingsmensch bist.

Abstract

Synaptic transmission at chemical synapses relies on the fusion of neurotransmitter-loaded vesicles with the plasma membrane of the pre-synaptic terminal (exocytosis). The synaptic vesicle material is then retrieved from the plasma membrane (endocytosis) and new vesicles are formed, completing what has been termed synaptic vesicle recycling. Both exo- and endocytosis are tightly regulated processes, involving a plethora of specific proteins. Much is already known about the nature of these proteins and about their interplay during vesicle recycling. However, this is not sufficient for a global understanding of synaptic function. Two critical lines of evidence are still missing: we lack quantitative information on protein numbers in the synapse and we also have limited data on their locations. In other words, the molecular anatomy of the synapse is still unknown.

Here I addressed this problem by integrating several quantitative biochemistry and microscopy approaches. First, I determined the physical parameters (size, shape and organelle composition) of synapses isolated from rat brain (synaptosomes), using three-dimensional reconstructions of ultrathin electron microscopy sections. Second, I performed quantitative immunoblots to determine absolute copy numbers for 59 major proteins involved in synaptic vesicle exo- and endocytosis. Third, I determined the spatial organization of the proteins by imaging them using stimulated emission depletion (STED) microscopy, with a lateral precision of at least 40-50 nm. The information obtained from all of these assays was used to generate a three-dimensional graphical model of the pre-synaptic terminal, placing synaptic proteins in the appropriate locations, at their determined copy numbers.

My findings enable us for the first time to draw conclusions on how the spatio-temporal availability of proteins determines the functional regulation of the synapse. For example, my results suggest that the availability of cysteine-string-protein (CSP) and Complexin controls exocytosis and that the availability of the Clathrin light chain governs endocytosis. Overall, my data imply that synaptic function is primarily regulated by the abundance of specific proteins, rather than by the function of control mechanisms. This type of regulation is much simpler than many models proposed in the past. For example, no negative feedback loops are needed to limit synaptic processes – the limited availability of key components is sufficient for their control. Finally, since most synaptic mechanisms have closely related counterparts in other cellular areas, I suggest that the type of regulation I observed is not restricted to the synapse, but is likely applicable to the entire cell.

List of Figures

Figure 1-1: Different modes of synaptic vesicle retrieval

Figure 1-2: Molecular model of a synaptic vesicle

Figure 2-1: Purification of Synaptosomes

Figure 2-2: Comparing compositions of upper and lower synaptosome fractions

Figure 2-3: Multiple gradient centrifugations damage synaptosomes and cause clumping

Figure 2-4: Comparing amounts of synaptic proteins in different synaptosome preparations

Figure 2-5: Schematic of the spin down experiment

Figure 2-6: Troubleshooting of quantitative immunoblots

Figure 3-1: Experimental outline of the project

Figure 3-2: Fluorescence spin down assay to determine purity of synaptosome fractions

Figure 3-3: Spin down efficiency assay

Figure 3-4: EM-based assay to determine composition of synaptosome preparations

Figure 3-5: EM-based assay confirms findings of the fluorescence spin down assay

Figure 3-6: 3D reconstruction of a synaptosome

Figure 3-7: All 3D reconstructions of synaptosomes

Figure 3-8: Evaluation of certain physical parameters of the synaptosomes

Figure 3-9: Quantitative analysis of the synaptosome preparations

Figure 3-10: Control for loss of soluble proteins during synaptosome purification

Figure 3-11: Schematic for calculating absolute protein numbers#

Figure 3-12: Absolute protein numbers

Figure 3-13: Pre-synaptic protein organization in synapses from hippocampal cultures

Figure 3-14: Protein organization at the mouse NMJ

Figure 3-15: Ultrastructural appearance of the average pre-synaptic terminal

Figure 3-16: Distribution of several soluble proteins within the average pre-synaptic terminal

Figure 3-17: Distribution of membrane proteins within the average pre-synaptic terminal

Figure 3-18: Magnification of a vesicle embedded in a network of cytosolic proteins

Figure 3-19: Magnification of a plasma-membrane area

Figure 3-20: Magnification of the active zone area

List of Tables

Table 2-1: Buffers and Solutions

Table 2-2: Antibodies

Table 2-3: Filter-sets used for epi-fluorescence microscopy

Table 2-4: Objectives used for epi-fluorescence microscopy

Table 2-5: Laser lines of the Leica set-up

Table 2-6: Protein concentration of the synaptosome fractions

Table 2-7: Purified Proteins

Table 2-8: Schagger gel composition

Table 2-9 Proteins investigated with modified immunoblot conditions

Table 2-10: Immunostainings on cortical brain slices and synaptosomes

Table 3-1: Absolute numbers of synaptosomes per nanogram preparation

Table 3-2: Physical parameters of the synaptosomes

Table 3-3: Correction factors for potential loss of soluble proteins

Table 3-4: Absolute protein numbers per synaptosome

Table 4-1: Corrected protein numbers for the calcium buffers

List of Abbreviations

AMPA	α -amino-3-hydroxy-5-methyl-4-isoxazolepropionic acid receptor
AP	Adaptor protein
APD	Avalanche photodiode
APP	Amyloid precursor protein
APS	Ammonium persulfate
AQUA	absolute quantification
ATP	Adenosin triphosphate
AZ	Active zone
BAR	Bin-Amphyphisin-Rvs
BCA	Bicinchoninic acid
BSA	Bovine serum albumin
CALM	Clathrin assembly lymphoid myeloid leukaemia
CAZ	Cytomatrix at the active zone
CCD	Charged coupled device
CSP	Cystein string protein
DIV	Days in vitro
EM	Electron microscopy
FCS	Fetal Calf Serum
GDI	Rab GDP dissociation inhibitor
GTP	Guanosin triphosphate
Hsc70	Heat shock cognate 71 kDa protein
iBAQ	Intensity-based absolute quantification
kDa	Kilo Dalton
KO	Knock out
NMDA	<i>N</i> -Methyl-D-aspartic acid or <i>N</i> -Methyl-D-aspartate
NMJ	Neuromuscular junction
NSF	<i>N</i> -ethylmaleimide-sensitive factor
PAGE	Polyacrylamide gel electrophoresis
PFA	Paraformaldehyde
PIP ₂	Phosphatidylinositol 4,5-bisphosphate

PIPK I γ	Phosphatidylinositol 4-phosphate 5-kinase type-1 gamma
PSD	Postsynaptic density
PVDF	Polyvinylidene difluoride
Rab	Ras related in brain
ROI	Region of interest
SCAMP	Secretory carrier-associated membrane proteins
SDS	Sodium dodecyl sulfate
SEM	Standard error of the mean
SGIP	Src-homology 3-domain growth factor receptor-bound 2-like (endophilin) interacting protein
SH3	Sarcoma homology 3 domain
SNAP	Synaptosomal associated protein
SNARE	Soluble N-ethylmaleimide-sensitive factor attachment protein receptor
STED	Stimulated emission depletion microscopy
SV	Synaptic vesicle
SV2	Synaptic vesicle protein 2
Syndapin	Synaptic dynamin associated protein
TDE	2,2'-thiodiethanol
TEMED	Tetramethylethylenediamine
TIRF	Total internal reflection
TRIS	Tris(hydroxymethyl)aminomethane
TMA-DPH	1-(4-Trimethylammoniumphenyl)-6-Phenyl-1,3,5-Hexatriene <i>p</i> - Toluenesulfonate
VAMP	Vesicle associated membrane protein
vGlut	Vesicular Glutamate transporter

1. Introduction

Our daily life is composed of numerous versatile behaviors, all controlled by our brain – we move, we think, we learn. The ability of the brain to coordinate such actions crucially depends on the information transfer between different neurons. Our brain is a highly complex organ, expected to contain more than 100 billion neurons, with each forming about 1000 connections to neighboring nerve cells (Pakkenberg and Gundersen, 1997). Although the brain has been proposed to house the soul by Hippocrates as early as 400 BC, its functional composition remained elusive until the late 19th century. The first histological description of the brain by Ramon y Cajal revealed that the brain is composed of different highly specialized cells that are connected to one another at distinct sites (Ramon y Cajal, 1894). These connection sites were later termed synapses (from syn = together and haptein = touch, detect) by Foster and Sherrington (Foster and Sherrington, 1897). At first it was assumed that an electrical signal (current) is directly transferred from one cell to the next (electrical synapses) through pores that connect the two cells (today known as gap junctions). However, later findings by Otto Loewi demonstrated that a signal can also be conveyed by chemical substances giving rise to the theory of chemical synapses (Loewi, 1926). In the following section I will briefly outline the two different types of synapses and elaborate more thoroughly on the physiology of chemical synapses, since they are the major synapses in the brain.

1.1 Functional and morphological features of synapses

Synaptic transmission is the basis for every action performed by an organism and takes place at specialized sites – the synapses. We generally differentiate between two distinct types of synapses which differ in function and morphology:

In the case of electrical synapses, the cytoplasm of two neighboring cells are directly connected by small proteinaceous channels (composed of connexins) known as gap junctions. The gap junctions are small hydrophilic pores of approximately 1.2 nm which allow ions and small proteins to flow from one cell into the other (Bennett and Zukin, 2004). Upon arrival of an action potential the current (i.e. the ions) is able flow directly into the postsynaptic cell across the gap junctions (Kandel, 2000). This outlines the major advantages of gap junctions: they are bidirectional (i.e. information can be transferred in both directions) and extremely fast. The latter has been shown to be essential for synchronizing neuronal firing patterns and the direct

functional coupling of nerve cells (Hormuzdi et al., 2004). Electrical synapses were first discovered in crayfish (Furshpan and Potter, 1959) but later also found in vertebrates, where they are expected to function in parallel to chemical synapses in fast pathways (Connors and Long, 2004).

The majority of synapses in the brain are chemical synapses in which the electrical signal is converted into a chemical one prior to transmission to the receiving cell. The incoming action potential triggers the opening of voltage-gated calcium channels in the pre-synaptic terminal of the sending neuron. Thus, calcium ions flow into the terminal and initiate a complex cascade of protein interactions (see next section) which leads to the fusion of vesicles with the plasma membrane. The so called synaptic vesicles (SVs) are small membranous organelles approximately 42 nm in diameter containing the neurotransmitter substance. Fusion generally occurs at so called active zones (AZs) which contain a plethora of proteins, crucial for synaptic transmission and appears electron dense in electron micrographs (Sudhof, 2004). The neurotransmitters are released into the synaptic cleft upon fusion of the SV with the plasma membrane of the pre-synaptic terminal. Here they diffuse through the 20-40 nm wide cleft and dock to specialized receptors at the plasma membrane of the post-synaptic neuron. This triggers the opening of post-synaptic ion channels and leads to a change in post-synaptic membrane potential. Hence, the chemical signal released from the pre-synaptic terminal is retransformed into an electrical signal in the post-synaptic cell. Two major classes of post-synaptic receptors are known: at ionotropic receptors the receptor is also the channel and binding of neurotransmitter causes a conformational change, thus opening of the channel. In contrast, metabotropic receptors activate a G-protein coupled cascade upon binding of neurotransmitter which in turn opens separate ion channels. At the pre-synaptic site the vesicles are retrieved by endocytosis and refilled with neurotransmitter or in other words: the vesicles are made ready for another potential round of exocytosis. Thus, signal transmission at chemical synapses is a far more complex process compared to electrical synapses. This allows tuning and modulating the information processing according to the specific context, which renders chemical synapses substantially more flexible and plastic than electrical synapses (Kandel, 2000).

The above outlined sequence of events fits well to the processes within central chemical synapses. Other types of synapses do vary regarding their precise anatomy, depending on their location and function within the organism. In this study I investigated two different subtypes of chemical synapses – central pre-synaptic terminals and peripheral neuromuscular junctions

(NMJs). NMJs form the connection of the nervous system with muscle fibers. The innervating motor neuron sends a neuritic process onto the muscle where it forms the endplate (i.e. terminal formation of a motor neuron transmitting neural impulses to a muscle). Upon release of the neurotransmitter the muscle is activated and ultimately contracts. Compared to cortical or hippocampal synapses which only contain hundreds of vesicles and a single AZ ((Schikorski and Stevens, 1997) see also 2.7), NMJs can contain several thousand vesicles and have multiple AZs per terminal (Rizzoli and Betz, 2005). The post-synaptic site of the muscle contains large invaginations just opposite the AZ called junctional folds. The post-synaptic receptors are almost exclusively located at the tips of the folds while the flanks and the folds themselves are covered with voltage-gated calcium channels (Flucher and Daniels, 1989). This particular arrangement serves as an amplifier for the incoming signal and ensures the generation of a muscle contraction (Bewick, 2003; Martin, 1994): the folds effectively increase the surface of the post-synaptic site and therefore also the number of voltage-gated sodium channels available. Further, the rather narrow folds serve as a high resistance barrier for the current flow and hence more net current is funneled down the fold along the voltage-gated sodium channels (Vautrin and Mambrini, 1989). In regard to this, the NMJ is specifically designed to ensure reliable signal transmission from the motor neuron to the muscle.

Another type of chemical synapse which is regularly found in sensory cells (e.g. retinal bipolar cells and cochlear hair cells) is the so called ribbon synapse. At sensory synapses information is often conveyed via graded potential which demand high amounts of fusion ready vesicles to sustain long periods of release (Sterling and Matthews, 2005). In ribbon synapses the AZ contains an elongated membranous structure to which approximately 100 SVs are tethered and ready to fuse (Lenzi et al., 1999). This renders ribbon synapses ideal candidates for sensory systems which require relatively long and continuous periods of release (Moser et al., 2006; Pelassa and Lagnado, 2011).

The last chemical synapse subtype briefly outlined here is the Calyx of Held. The Calyx a very well characterized synapse localized to the mammalian auditory nervous system. It is a large glutamatergic synapse containing multiple release sites designed for efficient and fast signal transmission. A major advantage of this synapse for researchers is the easy accessibility of both the pre- and post-synaptic compartment which have delineated this synapse to be particularly practical for patch clamp recordings (Borst and Soria van Hoeve, 2012).

1.1.1 Synaptic vesicle exocytosis

The cycle of exo- and endocytosis of SVs holds a central position in pre-synaptic physiology. The vesicles are small (approximately 42 nm in diameter) and can therefore only hold a limited set of proteins (Takamori et al., 2006). Up to now, not all vesicular proteins are completely characterized but they are expected to be functionally involved in SV cycling (exocytosis, endocytosis or refilling of vesicles). In this section I will provide an overview about the mechanisms governing vesicle fusion and the specific set of proteins involved in it.

Newly synthesized vesicle components are transported down from the cell soma to the terminals along microtubule tracks (Conde and Caceres, 2009). Within the terminal the vesicles are arranged in a cluster of several hundred vesicles (Sudhof, 2004). Most of the vesicles are interconnected and tethered by Synapsin which is known to interact with SVs and vesicular proteins as well as with the Actin cytoskeleton (Cesca et al., 2010). The network formed by Actin and Synapsin to organize the vesicles is further complemented by Septin molecules which are reported to form filaments and regulate the spatio-temporal course of SV fusion (Yang et al., 2010b).

Upon arrival of an action potential, the plasma membrane of the pre-synaptic terminal is depolarized. This ultimately leads to an influx of calcium ions via voltage-gated calcium channels. Increasing the internal calcium concentration has been suggested to have several major pre-synaptic effects (Collin et al., 2005; Neher and Sakaba, 2008) and not all might have been characterized yet. It is for instance known that calcium activates a Calmodulin dependent phosphorylation cascade which among others leads to phosphorylation of Synapsins (Benfenati et al., 1992). Phosphorylation of Synapsin in turn causes it to disassociate from the SVs and thereby freeing them. The vesicles are now in principle able to move within the terminal to reach potential fusion sites (Cesca et al., 2010). Furthermore, calcium influx through channels situated directly at the AZ generates so called calcium micro-domains which are expected to directly trigger SV fusion via the pre-synaptic calcium sensor Synaptotagmin (Serulle et al., 2007).

Prior to fusion vesicles are assumed to be docked and primed ready for release directly at the AZ (Sudhof, 2004). This process is essential for reliable neurotransmission and is expected to be mainly regulated by Munc13 and Munc18 (Ma et al., 2011; Sudhof and Rothman, 2009). In addition, the most prominent synaptic ras-related small monomeric GTPase Rab3 also appears to be involved in vesicle priming but its precise role remains unknown (Fischer von Mollard et

al., 1991; Jahn and Fasshauer, 2012). Recent studies have reported accumulating evidence that RIM proteins serve as a major scaffolds during priming due to their interaction with Munc13 (Deng et al., 2011), Rab3 (Jahn and Fasshauer, 2012) and calcium channels (Kaeser et al., 2011).

After priming the fusion reaction itself is triggered by Synaptotagmin and mediated by the family of soluble N-ethylmaleimide-sensitive factor (NSF) attachment protein receptor (SNARE) proteins. Elevated intracellular calcium levels are detected by the vesicular calcium sensor Synaptotagmin. The protein contains two C2 domains for binding of calcium ions which display increased affinity to phospholipids upon binding of calcium (Matthew et al., 1981; Sudhof and Rizo, 1996). Hence, Synaptotagmin can bind to the plasma membrane and thereby bring the vesicle into close proximity to it (Haucke et al., 2011). In addition, calcium causes dissociation of the functional fusion clamp Complexin from SNARE complexes and therefore enables SNARE mediated exocytosis of SVs (Li et al., 2011; Kummel et al., 2011; Malsam et al., 2012; Martin et al., 2011). Another prominent example for a pre-synaptic calcium sensor is the soluble protein Doc2. This protein similar to Synaptotagmins in structure but lacks the trans-membrane region and has a higher affinity for calcium ions (Groffen et al., 2006). Recently, it has recently been reported that Doc2 is involved in spontaneous neurotransmitter release (Groffen et al., 2010).

Vesicle fusion is mediated by SNARE proteins in all cells and organisms studied to date. The three major synaptic SNAREs are Syntaxin 1, SNAP 25 and VAMP 2 (vesicle associated membrane protein) which is also known as Synaptobrevin 2 (Jahn and Scheller, 2006). During SNARE complex formation the two target (t-) SNAREs Syntaxin and SNAP 25 form a tight complex (SNARE complex) with the vesicular (v-) SNARE VAMP 2. Formation of the SNARE complex is initiated at the amino-terminus and proceeds to the carboxy terminus of the proteins in a zipper-like fashion. This process can be regarded as the driving force for vesicle fusion: zippering bridges the gap between the two opposing membranes and mechanical energy that is freed during this process is used to overcome the energy barrier for merging of the two membranes (Haucke et al., 2011; Jahn and Scheller, 2006; Sudhof, 2004). Recent studies have demonstrated that the formation of one to three SNARE complexes provides sufficient amounts of energy to drive vesicle fusion (Mohrmann et al., 2010; Sinha et al., 2011; van den Bogaart et al., 2010). In order to provide SNARE proteins for multiple fusion cycles, the SNARE complexes need to be disassembled again after fusion. This energy dependent process is mediated by NSF and its partner α -soluble NSF attachment protein (α -SNAP, Jahn and Scheller, 2006).

As outlined in the last paragraph, SNARE complex formation is the central element in SV fusion. In order to be able to interact with their putative partners the individual SNARE proteins need to be present in their functional conformations. Interestingly, this is provided by two different chaperone systems whose impairment has been reported to cause neurodegenerative diseases: (1) a complex composed of CSP, Hsc70 and SGT α (Sharma et al., 2010; Tobaben et al., 2001) and (2) α -Synuclein (Burre et al., 2010). Although both SNARE chaperones known so far aim at stabilizing the unfolded SNAP 25, it cannot be excluded that future studies will find potential chaperones for the other SNARE proteins (Sudhof and Rizo, 2011).

1.1.2 Synaptic vesicle endocytosis

After fusion of the SV with the plasma membrane, the vesicular components – proteins and lipids – are retrieved in a process referred to as endocytosis. This is important in order to maintain the pre-synaptic vesicle pool and to remove excess phospholipids from the plasma membrane. Depending on synaptic activity, several different modes of retrieval have been proposed which seem to coexist in a pre-synaptic terminal. However, it is still controversially debated to what extent the different modes of endocytosis contribute to vesicle recycling in a physiological context. In the following, I will briefly outline the different mechanisms proposed for SV endocytosis, which are also illustrated in Figure 1-1.

Kiss and Run: according to the Kiss and Run model the vesicles fuse only transiently with the plasma membrane and do not completely collapse (see red arrows in Figure 1-1). The neurotransmitters are released through a short lived fusion pore (Smith et al., 2008). Since the vesicle components are not entirely immersed into the membrane this mode of endocytosis is substantially faster compared to Clathrin-mediated endocytosis (Sun et al., 2002). Moreover, the molecular identity of the vesicle is maintained after fusion, rendering post-fusion sorting processes (e.g. endosomal sorting) unnecessary (Rizzoli and Jahn, 2007). Although several studies have reported transient fusion events using different techniques (He et al., 2006; Klingauf et al., 1998; Zhang et al., 2009), the physiological relevance of this release mode is still not clear (Chen et al., 2008; Granseth et al., 2007). In line with this, it has also been claimed that the phenomenon of transient fusion might be an artifact introduced by the techniques used to report it (Granseth et al., 2009).

Bulk endocytosis: unlike Kiss and Run, the occurrence of bulk endocytosis at pre-synaptic terminals is widely accepted in the scientific community. Although it has been reported

for many different preparations (Gennaro et al., 1978; Miller and Heuser, 1984; Clayton et al., 2008; Teng and Wilkinson, 2000; Wu and Wu, 2007), it is only observed during long and intense stimulation paradigms (Clayton and Cousin, 2009). Therefore, it is expected to compensate for the vast amount of membrane which is added to the plasma membrane during intense SV exocytosis. In response to such high stimulations the plasma membrane forms a tubular invagination of which individual vesicles are pinched off via Clathrin mediated endocytosis (Ferguson et al., 2007; see blue arrows in Figure 1-1). Hence, bulk endocytosis could be a cellular mechanism to remove large amounts of membrane quickly from the plasma membrane.

Clathrin mediated endocytosis: in contrast to Kiss and Run, the vesicle collapses entirely into the plasma membrane prior to Clathrin mediated endocytosis (Jung and Haucke, 2007). The vesicular material is then retrieved via the formation of a Clathrin coated vesicle that is pinched off of the plasma membrane (see black arrows in Figure 1-1). Clathrin mediated endocytosis requires several seconds, rather than milliseconds, and is therefore substantially slower compared to Kiss and Run (Granseth et al., 2007). Although it has been demonstrated that the vesicle material remains clustered upon fusion (Willig et al., 2006) it is quite likely that the newly formed vesicles are sorted in an endosomal intermediate (Hoopmann et al., 2010; Rizzoli et al., 2006; Uytterhoeven et al., 2011; see next paragraph on endosomal recycling). Clathrin mediated endocytosis is expected to take place at specific sites next to the AZ termed peri-AZ (Brodin et al., 2000; Haucke et al., 2011; Roos and Kelly, 1999).

Endosomal sorting: as mentioned above, recently endocytosed vesicles might undergo additional sorting steps prior to their integration into the SV cluster (see green arrows in Figure 1-1). Recycling of vesicle material in endosomes is not per se a distinct mode of retrieval but rather a sorting step that may follow retrieval. Sorting of SV material is expected to take place in early endosomes where the specific protein composition of a vesicle (Takamori et al., 2006) is established (Hoopmann et al., 2010; Rizzoli et al., 2006; Uytterhoeven et al., 2011). In line with this, several endosomal marker proteins such as Syntaxin 6 and 13, Rab5 and Vti1a have also been found to be present on SVs (Takamori et al., 2006). However, up to know it is not clear whether all vesicles are subjected to an endosomal sorting step after endocytosis.

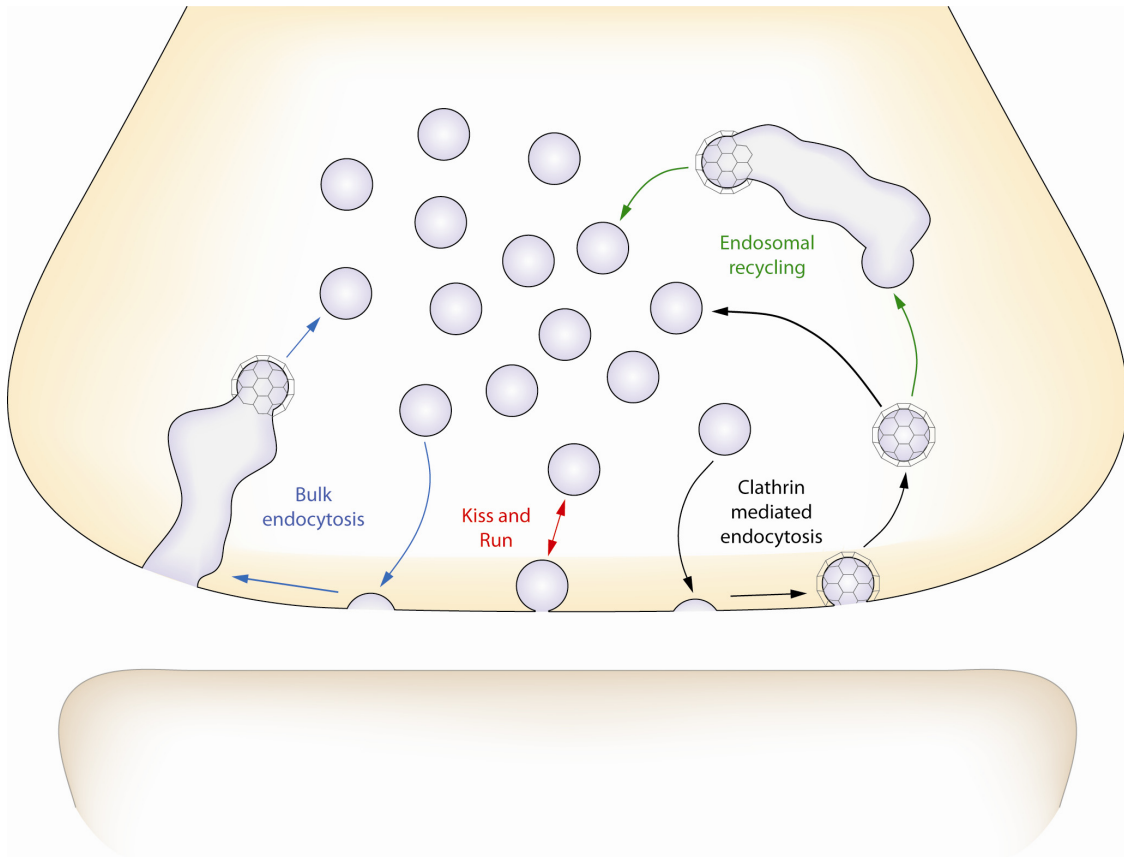


Figure 1-1: Different modes of synaptic vesicle retrieval.

The schematic illustrates the different roads a SV can follow after exocytosis. The vesicle material can be retrieved via classical Clathrin mediated endocytosis (black arrows) potentially followed by an endosomal sorting step (green arrows). An alternative recycling mode which has been proposed is transient fusion of the vesicle better known as Kiss and Run (red arrows). Retrieval of membrane and vesicle proteins during intense stimulation is expected to be mediated by bulk endocytosis (blue arrows).

As outlined in the last paragraphs, different modes of retrieval for vesicle material have been reported. I will now elaborate further on proteins and mechanisms involved in vesicle retrieval on the basis of the predominant retrieval mechanism in synapses: Clathrin-mediated endocytosis (Granseth et al., 2006; Newton et al., 2006; Granseth et al., 2007; Wienisch and Klingauf, 2006; Dickman et al., 2005). In brief, a Clathrin-coated vesicle consists of an inner and an outer layer which are assembled sequentially. While the outer layer is mainly composed of the Clathrin coat, the inner is formed by adaptor and accessory proteins (McMahon and Boucrot, 2011). How these layers are assembled will be outlined in the following paragraphs:

The first step during Clathrin mediated endocytosis is the formation of a membrane invagination referred to as a pit. A crucial component for the formation of such a pit is the

membrane lipid phosphatidylinositol 4,5-bisphosphate (PIP₂) generated via phosphorylation of PIP by phosphatidylinositol 4-phosphate 5-kinase type-1 gamma (PIPK I γ) (Wenk and De Camilli, 2004). Subsequently, proteins like EPS 15, Epsin 1 and Intersectin are recruited to the pit (Saheki and De Camilli, 2012) where they form a nucleation module which is essential for recruitment of adaptor proteins and curvature formation (Henne et al., 2010; Ford et al., 2002; Saheki and De Camilli, 2012).

This module in turn recruits adaptor proteins (AP) to the pit as for example AP 2 (Henne et al., 2010), AP180/CALM (Clathrin assembly lymphoid myeloid leukaemia) and Stonin 2 (Willox and Royle, 2012; Diril et al., 2006) which mediate sorting of specific vesicle cargo (see also speculations on Synaptophysin-mediated cargo sorting in 4.2). In addition, the large adaptor molecules may also use their flexible and unfolded structures which reach into the cytoplasm to capture Clathrin and other accessory proteins (Edeling et al., 2006) (Schmid and McMahon, 2007)- (Saheki and De Camilli, 2012). Particularly AP2 seems to be essential for the maturation of the pit as deletion of the protein causes accumulation of nucleation complexes without Clathrin (Motley et al., 2003) (Boucrot et al., 2010).

After assembly of the adaptor proteins and the completion of the first layer, Clathrin molecules are recruited to the pit to coat the emerging vesicle. The coat is made of Clathrin triskelia which in turn are composed of three Clathrin light and heavy chain molecules respectively (Musacchio et al., 1999). Between 40 (Cheng et al., 2007) and 100 (McMahon and Boucrot, 2011) triskelia are needed for coating of a single SV and the coat further stabilizes the curvature of the membrane (McMahon and Boucrot, 2011; Cocucci et al., 2012). Upon complete assembly of the Clathrin coat the vesicle is ready to be retrieved and pinched off of the membrane.

Scission of the nascent vesicle is mediated by the GTPase Dynamin (Ferguson et al., 2007). Dynamin is recruited to the protein neck via an interaction with the BAR- (Bin-Amphiphysin-Rvs) domain proteins Endophilin and Amphiphysin. These two proteins are curvature sensors and preferably bind to the bare neck of the pit thereby targeting Dynamin directly to the point of scission (Wigge et al., 1997; Sundborger et al., 2011; Ferguson et al., 2009). Scission itself is achieved by polymerization of Dynamin into helical rings around the neck of the vesicle. Upon hydrolysis of GTP, these rings undergo a conformational change which causes the ring to contract and ultimately pinches off the coated vesicle of the plasma membrane (Ferguson and De Camilli, 2012; Roux et al., 2006; Sweitzer and Hinshaw, 1998).

After scission of the vesicle from the plasma membrane the vesicle is not yet ready to be re-integrated in the SV cluster. This can only be done after the vesicle shed off its Clathrin coat. Disassembly of the Clathrin coat is mediated by Auxillin and Hsc70 (heat shock cognate 71 kilo Dalton (kDa) protein) starting at the former neck of the vesicle. The neck region is most likely devoid of Clathrin and thus offers an ideal location to initiate the uncoating (McMahon and Boucrot, 2011; Taylor et al., 2012; Xing et al., 2010). Auxillin binds to this former neck region and recruits Hsc70 which uncoats the vesicle stepwise triskelion by triskelion (Ungewickell et al., 1995; Schlossman et al., 1984).

Following scission, the new vesicle can be subjected to an additional endosomal sorting step (see above) or be directly integrated into the SV cluster. The integration of the vesicle is thought to be mediated by Syndapin in conjunction with the Actin cytoskeleton (Kessels and Qualmann, 2004). In order to obtain release-competent vesicles, they further need to be refilled with neurotransmitter. Depending on the neuronal sub-type, the refilling is regulated by different vesicular transporters. For example, in the case of glutamatergic synapses (major excitatory transmitter in the brain), the refilling is mediated by a protein called vesicular Glutamate transporter (VGlut) 1 or 2 (Bellocchio et al., 2000). The transporters ship Glutamate into the SV along a Proton concentration gradient (high intravesicular concentration) which is established by the ubiquitous vesicle protein vATPase (Saw et al., 2011; Finbow and Harrison, 1997).

Refilling and Integration of the vesicle into the cluster closes the cycle of exo- and endocytosis and the recently endocytosed vesicle is again ready to participate in neurotransmission.

1.1.3 Need for descriptive approaches

In summary, exo- and endocytosis of SVs are complex processes which are tightly regulated and involve plenty different proteins. A great deal of studies has investigated functions of individual proteins and mechanisms which are thought to govern vesicle cycling (Sudhof, 2004). Of these, the above-cited studies only represent a small fraction of what is known. However, the controversies in the field (see for instance Kiss and Run versus Clathrin mediated endocytosis) show that it is extremely difficult to draw reliable conclusions about synaptic function, particularly comprising all different findings about the functions of the proteins involved. Functional information on proteins is certainly indispensable for

understanding synaptic function, but it is also important to know the distinct molecular composition of a synapse. The number/ abundance of a protein as well as its organization within the synapse are likely to substantially determine the function of the protein. This is particularly evident regarding that many synaptic processes are dependent on the spatio-temporal availability of several interaction partners (e.g. SV exo- and endocytosis). Therefore, studies which identify and quantify the individual elements of a synapse could help us to fit the individual pieces of information on protein function together in order to understand the general concepts of synaptic physiology.

1.2 Molecular composition of a synapse

Descriptive studies provide a framework for functional mechanisms by providing types, amounts and possibly also locations of the participating elements. Such studies help to understand the relation of the individual findings to each other and therefore substantially advance our understanding of the system as a whole. Several studies have addressed the synaptic composition in the past and I will summarize some of the main findings in the following sections.

1.2.1 The molecular composition of the post-synaptic density

The post-synaptic density (PSD) is an electron dense region attached to the post-synaptic membrane opposite the AZ. Depending on the activity of the respective synapse the PSD is between 250 and 500 nm in diameter and 25 to 50 nm thick (Spacek and Harris, 1998; Harris et al., 1992). Its major function is the accumulation and organization of neurotransmitter receptors in the plasma membrane of the post-synaptic cell. Further it contains kinases and phosphatases involved in signaling cascades (Ziff, 1997). Several studies have investigated the proteome of the PSD in the past and found between approximately 300 and 500 different proteins (Cheng et al., 2006; Peng et al., 2004; Jordan et al., 2004; Yoshimura et al., 2004 reviewed in Sheng and Hoogenraad, 2007).

Among the identified proteins are for instance the two ionotropic Glutamate receptors AMPA (α -amino-3-hydroxy-5-methyl-4-isoxazolepropionic acid receptor) and NMDA (*N*-Methyl-D-aspartic acid or *N*-Methyl-D-aspartate) which serve complementary functions in synaptic signaling: while AMPA receptors mediate fast synaptic transmission, NMDA receptors are only activated/ recruited upon increased levels of synaptic activity and therefore hold a central

position in controlling synaptic plasticity (Mayer, 2005). Apart from the receptors several other proteins were identified which are essential for the receptor organization in the plasma membrane. One example is the large scaffolding protein Homer which tethers metabotropic Glutamate receptors to proteins of the Shank family (Kammermeier, 2006). The latter are in turn involved in linking the post-synaptic receptor complexes to Actin filaments of the cytoskeleton (Sala et al., 2005). One of the most studied proteins of the post-synapse is presumably PSD-95 (Hunt et al., 1996; Cho et al., 1992). PSD-95 contains different functional domains which are known to bind and localize NMDA receptors and Potassium channels as well as adhesion molecules such as Neuroligins (Han and Kim, 2008; Chen et al., 2011). Many other proteins that were found are related to intracellular signaling pathways. The most prominent example of those is the omnipresent Calmodulin dependent protein kinase II (Hudmon and Schulman, 2002). In analogy to the pre-synaptic terminal, the kinase regulates a signaling cascade which influences protein synthesis in the cell body. Therefore, it can also be regarded as a major regulatory element in learning and memory formation (Yamauchi, 2005). Past studies have also addressed the quantitative composition of PSDs (e.g. Cheng et al., 2006). However, so far only the relative amounts of several proteins to each other have been determined reliably (but see Sugiyama et al., 2005 where fluorescence microscopy is used for quantification – discussed in 4.1.2) and a detailed analysis yielding the absolute copy numbers per PSD are yet missing.

1.2.2 The molecular composition of a synaptic vesicle

A central position in neuronal communication is held by SVs. These small intracellular organelles are the carriers of the neurotransmitters which are released by exocytosis during synaptic activity. As outlined in section 1.1, each vesicle is equipped with a specific set of proteins that are involved in vesicular trafficking and are crucial for the function of the SV – i.e. to release neurotransmitters. Several studies have investigated the proteome of SVs using purified brain vesicles (Coughenour et al., 2004; Burre et al., 2006). A comprehensive picture of the SV architecture was recently provided by an elegant study investigating the physical as well as the molecular characteristics of a trafficking organelle (Takamori et al., 2006). Takamori and colleagues reported that SVs have an average diameter of approximately 42 nm, contain about 1790 neurotransmitter molecules and have a dry mass of 17.8 MDa ($29.6 \cdot 10^{-18}$ g).

Interestingly, they found Cholesterol to be substantially enriched in vesicles (see also (Benfenati et al., 1989) compared to the rest of the neuronal plasma membrane (Vincendon et

al., 1972; Pfrieger, 2003). Therefore, it could be speculated, that the formation of Cholesterol-rich plasma membrane patches is involved in sorting of SV components prior to vesicle retrieval (Bonanomi et al., 2006; see also discussion of Synaptophysin in 4.2).

Probably the most stunning finding of this study was how dense a SV is packed with integral membrane proteins (see Figure 1-2). They found almost 200 different proteins co-purifying with SVs. Over 80 of these were integral membrane proteins of which 40 were known to be localized to vesicular membranes. Furthermore, they determined absolute copy numbers for 15 SV proteins. By far the most abundant protein with almost 70 copies per vesicle was the v-SNARE VAMP 2. This number is particularly interesting, regarding that one to three SNARE complexes are sufficient for reliable vesicle fusion (Mohrmann et al., 2010; Sinha et al., 2011; van den Bogaart et al., 2010). Surprisingly, they also found the t-SNAREs Syntaxin 1 and SNAP 25 on the vesicle, although in low amounts with approximately 6 and 2 copies respectively. Besides the well known SNAREs involved in synaptic transmission, they also found several endosomal SNARE proteins such as Vti1a, Syntaxin 6 and 13. These findings were interpreted as further indication for the proposed endosomal sorting step during SV endocytosis (Takamori et al., 2006; see also Hoopmann et al., 2010; Rizzoli et al., 2006; Uytterhoeven et al., 2011). The second most abundant protein they found was Synaptophysin, with approximately 32 copies. Although Synaptophysin is the most prominent marker for SVs, its precise function is not yet completely understood (see 4.2). The major vesicular calcium sensor Synaptotagmin 1 was reported to contribute an average of 15 molecules to the vesicle. Interestingly, they also found an about 8 Synapsin molecules per SV. As mentioned above, Synapsin tethers SVs to the cytoskeleton but it is not a membrane protein and only associates with the vesicle. Similar to Synapsin they found 10 copies of Rab3a which is also only an associated protein and released upon activity (Fischer von Mollard et al., 1991). For both proteins it is likely that substantially more molecules were associated with the vesicle initially that were lost during purification (see 4.2).

It is important to mention that another study, investigating absolute copy numbers per vesicle using quantitative fluorescence microscopy, reported divergent numbers for some of the proteins (Mutch et al., 2011a; Mutch et al., 2011b). However, as the use of fluorescence microscopy for absolute quantification is prone to labeling-artifacts, these results will not be presented here but are discussed in section 4.1.2.

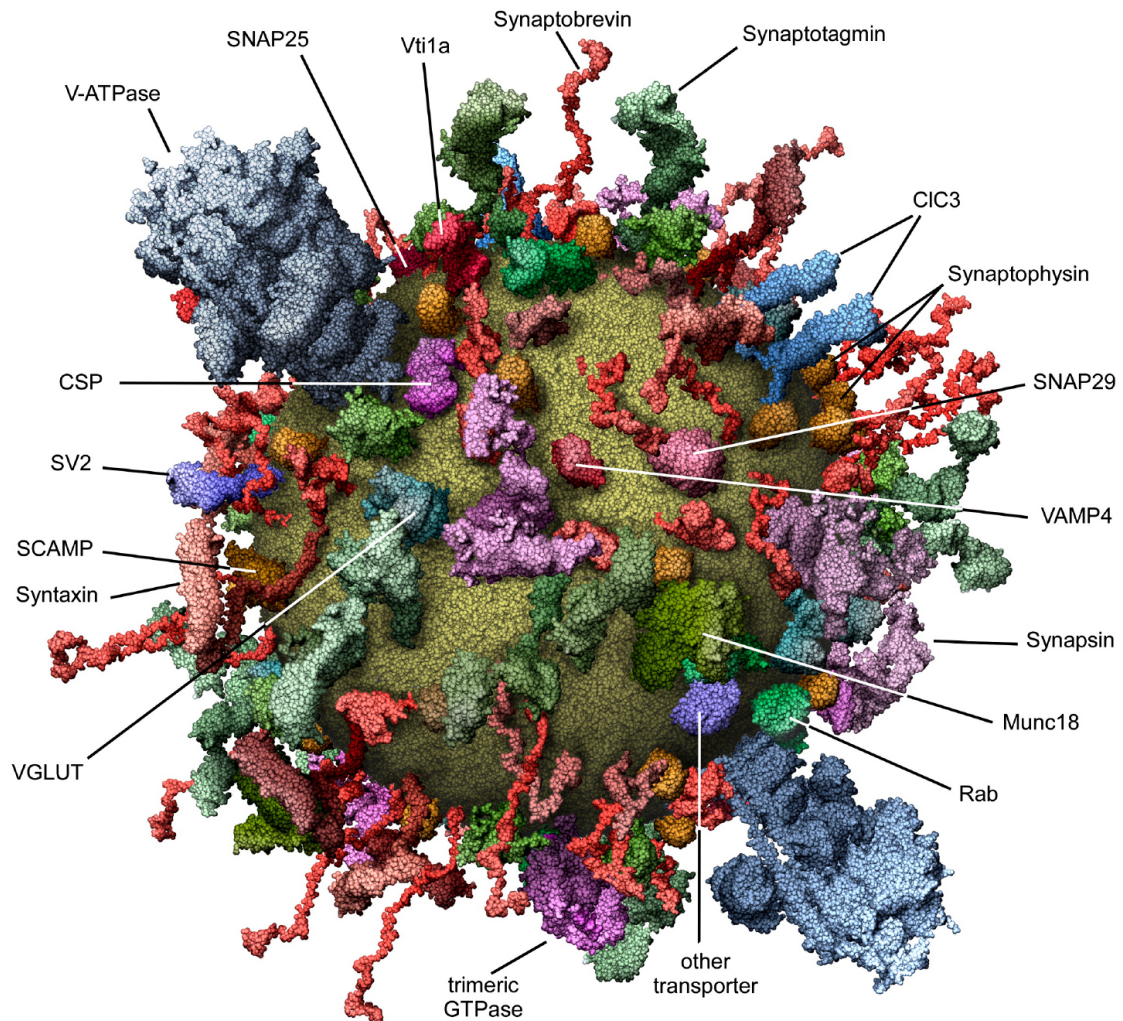


Figure 1-2: Molecular model of a synaptic vesicle

Graphical model illustrating the average brain SV containing the most abundant integral membrane and associated proteins (modified from Takamori et al., 2006).

1.2.3 The molecular composition of the AZ

At the pre-synaptic terminal the AZ is the region where the SVs fuse with the plasma membrane to release their neurotransmitter content into the synaptic cleft (Couteaux and Pecot-Dechavassine, 1970). The AZ is composed of a distinct collection of proteins referred to as the cytomatrix at the AZ (CAZ) (Sudhof, 2012). Due to its high protein concentration the AZ can be seen as an electron dense area in electron micrographs. The most prominent functions of the CAZ are to mediate neurotransmitter release (recruiting, docking, priming and fusion of SVs) and organization of voltage-gated calcium channels at the AZ (Gundelfinger and Fejtova, 2011). Size,

shape and numbers of active zones depend entirely on the type of the synapse (Cano et al., 2013).

To reliably determine the proteome of a certain cellular compartment always implies that it is actually possible to isolate this particular compartment from the rest of the cell. Since the AZ is per definition not strictly separated from the rest of the terminal (by a membrane for instance) it has long been difficult to precisely address its exact composition (Phillips et al., 2005; Phillips et al., 2001). However, a recent study succeeded in purifying AZs by capturing docked vesicles with anti SV2 antibodies. Using this approach they found approximately 240 specific proteins (Morciano et al., 2009; reviewed in Volkhardt and Karas, 2012). Besides cytoskeletal proteins and adhesion molecules, they also found proteins of the exo- and endocytosis machinery (outlined in section 1.1) as well as specific CAZ proteins. Two prominent examples of those are Bassoon and Piccolo. Both proteins are huge multi-domain proteins which are expected to team up as scaffolds of the exo- and endocytosis machinery as well as for other elements in the pre-synaptic terminal (Fejtova and Gundelfinger, 2006). Interestingly, they seem to have a preferred orientation in the synapse (Dani et al., 2010) indicating that specific domains of the proteins regulate specific synaptic processes (Dresbach et al., 2003). Another CAZ protein expected to regulate the organization of the active zone particularly during development is α -Liprin (Dai et al., 2006). One of its binding partners is ELKS (also known as ERC or CAST) which is expected to provide a platform for vesicle fusion downstream of vesicle docking (Inoue et al., 2006; Kaeser et al., 2009).

Unfortunately, up to now there is no quantitative information available on the precise molecular composition of the active zone which is most likely due to the difficult purification procedure (see above).

In summary, the past three sections on the molecular composition of different synaptic compartments have demonstrated that although there is already a base of proteomic (reviewed in Bai and Witzmann, 2007) and quantitative information it is not yet sufficient to provide a thorough overview about the entire terminal. The data presented in this thesis is supposed to add a couple of pieces to the puzzle of the molecular anatomy of a synapse.

1.3 Scope of this study

Although several studies have addressed the proteome of compartments within and the pre-synaptic terminal, a complete analysis concerning its molecular composition is yet missing. Therefore, the ultimate aim of this study is to provide a concise picture of the molecular anatomy of a pre-synaptic terminal providing its physical (size and organelle composition) and molecular (absolute proteins numbers and organization) composition.

To address this question I used isolated brain synapses (from cortex and cerebellum) – referred to as synaptosomes – as a model system (see 3.1). I first determined the physical characteristics of the average brain terminal such as size as well as number and distribution of active zone, mitochondria, endosomes and SVs performing 3D reconstructions of electron micrographs (see 3.2). Next, I determined the molecular parameters of the average synapse i.e. the absolute protein composition and the organization of these proteins. The former was done using quantitative immunoblots for 59 synaptic and 5 reference proteins (see 3.3) while the latter was done using super resolution STED (stimulated emission depletion) microscopy in two model systems (see 3.4). The quantification results were further validated using quantitative mass spectrometry, which displayed results similar to the quantitative immunoblots. Since this work was performed by our collaborators Prof. Dr. Henning Urlaub and Sunit Mandad (Max-Planck Institute for biophysical chemistry) it is not included in this thesis.

The different information obtained in these three approaches – synapse ultrastructure, protein copy numbers and protein localization – was then used to generate a graphical model of the average pre-synaptic terminal (see 3.5).

The results I present in this study provide exciting insights into the pre-synaptic architecture. Thereby, the ultrastructural and proteomic information can be used to generate a comprehensive picture of the molecular composition of a pre-synaptic terminal that could serve as a frame-work for functional synaptic studies. Furthermore I provide – for the first time ever – a quantitative approach covering the most important proteins of an entire cellular compartment. In this regard, my findings do not only enhance our general understanding of the synapse but also allow drawing conclusions on the correlation of cellular function and protein abundance/ composition in general (see 4.2).

2. Materials and Methods

2.1 Chemicals

Unless otherwise stated all chemicals were purchased from VWR (Hannover, Germany), Merck (Darmstadt, Germany) or Sigma (Taufkirchen, Germany).

2.2 Buffers and Solutions

All buffers and solutions that were used in this study can be found in Table 2-1.

Table 2-1: Buffers and Solutions

Buffer or Solution	Composition
Anode buffer	200 mM TRIS (pH 8.9)
Blocking buffer	PBS + 5% milk powder (low fat) + 0.1% Tween-20
Cathode buffer	100 mM TRIS, 100 mM Tricin, 1% SDS
Gel buffer	3 M TRIS, 0.3% SDS (pH 8.45)
High salt PBS	500 mM NaCl, 20 mM Na ₂ HPO ₄ (pH 7.4)
Mouse buffer	154 mM NaCl, 5 mM KCl, 2 mM CaCl ₂ , 11 mM Glucose, 5 mM HEPES (pH 7.4)
Phosphate buffer	22 mM NaH ₂ PO ₄ , 78 mM Na ₂ HPO ₄ (pH 7.2)
Phosphate buffered saline (PBS)	150 mM NaCl, 20 mM Na ₂ HPO ₄ (pH 7.4)
Sample buffer	50 mM TRIS, 4% SDS, 0.01 % Serva Blue G, 12% Glycerol, 2% β-Mercaptoethanol (pH 6.8)
Sodium buffer	10 mM Glucose, 5 mM KCl, 140 mM NaCl, 1.2 mM Na ₂ HPO ₄ , 5 mM NaHCO ₃ , 20 mM HEPES (pH 7.4)
Sucrose buffer	320 mM Sucrose, 5 mM HEPES (pH 7.4)
Transfer buffer	200 mM Glycin, 25 mM TRIS, 20% Methanol, 0.04% SDS
Wash buffer	PBS + 0.05% Tween-20

2.3 Antibodies

Several experiments of this study employed antibodies to label proteins of interest via immunolabeling. A complete list of all antibodies that were used is provided in Table 2-2. The

table further indicates in which experiments a particular antibody was used and at which dilution: immunoblot (see 3.3), immunostaining of primary hippocampal cultures (ICC, see 3.4.1), of NMJs (IHC, see 3.4.2), of synaptosomes alone (Syn, see 3.1.1) and of cortical brain slices and synaptosomes in parallel (Slice/Syn, both 3.3.1).

Table 2-2: Antibodies

Target protein	Antibody	Application	Supplier
Actin	mouse monoclonal	immunoblot 1:500	Novus Biologicals (NB600-535)
	mouse monoclonal	ICC 1:100 IHC 1:100	Sigma (A1978)
Alpha-SNAP	mouse monoclonal, 77.2	immunoblot 1:1000 ICC 1:100 IHC 1:50 Slice/Syn 1:500	Synaptic Systems
Alpha-Synuclein	rabbit polyclonal	immunoblot 1:1000 ICC 1:100 IHC 1:2000 Slice/Syn 1:500	Synaptic Systems (128 002)
Amphiphysin	rabbit polyclonal	immunoblot 1:1000 ICC 1:100 IHC 1:200 Slice/Syn 1:500	Synaptic Systems
AP 180	rabbit polyclonal	immunoblot 1:1000 ICC 1:100 IHC 1:1000 Slice/Syn 1:500	Synaptic Systems
AP2	rabbit monoclonal	immunoblot 1:500 Slice/Syn 1:500	Abcam (ab75995)
	rabbit polyclonal	ICC 1:100	Santa Cruz (sc-99026)
	mouse monoclonal	IHC 1:400	Sigma (A5441)
APP	mouse monoclonal, 22C11	immunoblot 1:1000 ICC 1:100 IHC 1:2000	Millipore (MAB-348)
BACE1	rabbit polyclonal	immunoblot 1:500 ICC 1:100 IHC 1:100	Santa Cruz (sc-10748)
Bassoon	mouse monoclonal	ICC 1:100 IHC 1:200 Syn 1:200	Stressgene (ADI-VAM-PS003-D)
	rabbit polyclonal	ICC 1:500	Synaptic Systems

2. Materials and Methods

Calbindin	rabbit polyclonal	immunoblot 1:1000 ICC 1:500 Slice/Syn 1:500	Swant (CB-38)
CALM	goat polyclonal	immunoblot 1:1000 Slice/Syn 1:500	Santa Cruz (sc6433)
Calmodulin	rabbit monoclonal	immunoblot 1:1000 ICC 1:100 Slice/Syn 1:500	Novus Biologicals (NB110-55649)
Calretinin	rabbit polyclonal	immunoblot 1:1000 ICC 1:500 Slice/Syn 1:500	Swant (7699/3H)
Clathrin heavy chain	mouse monoclonal, TD.1	immunoblot 1:100	Volker Haucke (FMP, Berlin, Germany)
	mouse monoclonal	ICC 1:100 IHC 1:200 Slice/Syn 1:500	BD Biosciences (610499)
Clathrin light chain	goat polyclonal	immunoblot 1:500	Novus Biologicals (NBP1-05035)
	mouse monoclonal, 57.4	ICC 1:100 Slice/Syn 1:500	Synaptic Systems
Complexin-1/2	rabbit polyclonal	immunoblot 1:1000 ICC 1:100 IHC 1:500 Slice/Syn 1:500	Synaptic Systems (122 002)
CSP	rabbit polyclonal	immunoblot 1:1000 ICC 1:100 IHC 1:1000 Slice/Syn 1:500	Synaptic Systems
Doc2 A/B	rabbit polyclonal	immunoblot 1:1000 ICC 1:100 IHC 1:1000 Slice/Syn 1:500	Synaptic Systems
Dynamamin 1,2,3	rabbit polyclonal	immunoblot 1:1000 Slice/Syn 1:500	Synaptic Systems (115 002)
	mouse monoclonal	ICC 1:100	BD Bioscience (610245)
	rabbit polyclonal	IHC 1:100	Abnova (PAB9596)
Endophilin I,II,III	mouse monoclonal	immunoblot 1:500	Santa Cruz (sc-46702)
	rabbit polyclonal	ICC 1:100 IHC 1:200 Slice/Syn 1:500	Synaptic Systems
Epsin 1	rabbit polyclonal	immunoblot 1:1000	Abcam (ab82688)
	rabbit polyclonal, EPR3023	ICC 1:100 IHC 1:200 Slice/Syn 1:500	Novus Biologicals (NBP1-40602)

2. Materials and Methods

Hsc70	mouse monoclonal, uncoating ATPase	immunoblot 1:1000	Synaptic Systems
	mouse monoclonal	ICC 1:100 IHC 1:2000 Slice/Syn 1:500	Santa Cruz (sc-7298)
Intersectin-1	rabbit polyclonal	immunoblot 1:1000 ICC 1:100 IHC 1:400 Slice/Syn 1:500	Volker Haucke (FMP, Berlin, Germany)
Munc13a	rabbit polyclonal	immunoblot 1:1000 ICC 1:100	Akonline (ABIN571921)
	rabbit polyclonal	IHC 1:200 Slice/Syn 1:500	Synaptic Systems (126 103)
Munc18a	rabbit polyclonal	immunoblot 1:1000 Slice/Syn 1:500	Synaptic Systems (116 002)
	mouse monoclonal	ICC 1:100 IHC 1:50	BD Biosciences (610336)
Myelin Basic Protein	goat polyclonal	immunoblot 1:500	Santa Cruz (sc-13912)
NSF	mouse polyclonal, 83.11	immunoblot 1:1000	Synaptic Systems
	rabbit polyclonal	ICC 1:100 IHC 1:1000 Slice/Syn 1:500	Synaptic Systems
Parvalbumin	rabbit polyclonal	immunoblot 1:1000 ICC 1:100 Slice/Syn 1:500	Swant (PV 25)
PIP Kinase I γ	rabbit polyclonal	immunoblot 1:1000 ICC 1:100 IHC 1:200 Slice/Syn 1:500	Volker Haucke (FMP, Berlin, Germany)
PSD-95	mouse monoclonal	immunoblot 1:1000	Synaptic Systems (124 011)
	mouse monoclonal	Syn 1:200	Sigma (P246)
Rab3a	mouse monoclonal, 42.2	immunoblot 1:1000	Synaptic Systems
	mouse monoclonal	ICC 1:100	BD Biosciences (610379)
	rabbit polyclonal	IHC 1:1000 Slice/Syn 1:500	Synaptic Systems
Rab5a	mouse monoclonal, 621.3	immunoblot 1:1000	Synaptic Systems
	rabbit polyclonal	ICC 1:100 IHC 1:200 Slice/Syn 1:500	Cellsignaling (3547)
Rab7a	rabbit polyclonal	immunoblot 1:1000 ICC 1:100	Novus Biologicals (NBP1-05048)

2. Materials and Methods

	mouse monoclonal	IHC 1:100 Slice/Syn 1:500	Santa Cruz (sc81922)
SCAMP 1	rabbit polyclonal	immunoblot 1:1000 ICC 1:100 IHC 1:200	Synaptic Systems
Septin 5	rabbit polyclonal	immunoblot 1:1000 ICC 1:1000 IHC 1:300 Slice/Syn 1:500	Volker Haucke (FMP, Berlin, Germany)
SGIP	rabbit polyclonal	immunoblot 1:1000 ICC 1:200 IHC 1:300 Slice/Syn 1:500	Volker Haucke (FMP, Berlin, Germany)
SNAP 23	rabbit polyclonal	immunoblot 1:1000 ICC 1:100 IHC 1:500	Synaptic Systems
SNAP 25	mouse monoclonal, 71.1	immunoblot 1:1000 ICC 1:100 Slice/Syn 1:500	Synaptic Systems
	rabbit polyclonal	IHC 1:500	Reinhard Jahn (MPI bpc, Göttingen, Germany)
SNAP 29	rabbit polyclonal	immunoblot 1:1000	Synaptic Systems
	rabbit polyclonal	ICC 1:300	Abcam (ab68824)
SV2 A/B	mouse monoclonal, C10H4	immunoblot 1:1000 ICC 1:100 IHC 1:2000	Reinhard Jahn (MPI bpc, Göttingen, Germany)
Synapsin I/II	mouse polyclonal	immunoblot 1:500	Novus Biologicals (H00006854-A01)
	rabbit polyclonal	immunoblot 1:1000 IHC 1:200 Slice/Syn 1:500	Synaptic Systems
	mouse polyclonal, Sy4	ICC 1:100	Reinhard Jahn (MPI bpc, Göttingen, Germany)
Synaptogyrin	rabbit polyclonal	immunoblot 1:1000	Novus Biologicals (NBP1-77371)
	rabbit polyclonal	ICC 1:100 IHC 1:200	Synaptic Systems
Synaptophysin	mouse monoclonal, 7.2	immunoblot 1:1000	Synaptic Systems
	rabbit polyclonal, G96	ICC 1:1500 IHC 1:500	Reinhard Jahn (MPI bpc, Göttingen, Germany)
	guinea pig polyclonal	ICC 1:500 IHC 1:200	Synaptic Systems

2. Materials and Methods

		Slice/Syn 1:500	
Synaptotagmin 1	mouse monoclonal, 41.1	immunoblot 1:1000	Synaptic Systems
	mouse monoclonal, 604.1 Atto647N	ICC 1:100	Synaptic Systems
	rabbit polyclonal, luminal domain	IHC 1:200 Syn 1:1000	Synaptic Systems
Synaptotagmin 2	mouse monoclonal	immunoblot 1:1000 IHC 1:500	Abcam (ab60716)
	rabbit polyclonal	ICC 1:100	Synaptic Systems
Synaptotagmin 7	rabbit polyclonal	immunoblot 1:500 ICC 1:100 IHC 1:200	Synaptic Systems
Syndapin	mouse polyclonal	immunoblot 1:1000 ICC 1:100	Novus Biologicals (H00029993-B01)
	rabbit polyclonal	IHC 1:200 Slice/Syn 1:500	Synaptic Systems
Syntaxin 1	mouse monoclonal, HPC-1	immunoblot :1000 IHC 1:1000 Slice/Syn 1:500	Reinhard Jahn (MPI bpc, Göttingen, Germany)
	mouse monoclonal, 78.2	ICC 1:100	Synaptic Systems
Syntaxin 6	rabbit polyclonal	immunoblot 1:1000	Synaptic Systems
	mouse polyclonal	ICC 1:100 IHC 1:200	Reinhard Jahn (MPI bpc, Göttingen, Germany)
Syntaxin 7	rabbit polyclonal	immunoblot 1:1000 ICC 1:100	Synaptic Systems
	mouse polyclonal, 109.1	IHC 1:1000	Reinhard Jahn (MPI bpc, Göttingen, Germany)
Syntaxin 13	rabbit polyclonal	immunoblot 1:1000 IHC 1:200	Synaptic Systems
	mouse polyclonal	ICC 1:100	Synaptic Systems
Syntaxin 16	rabbit polyclonal	immunoblot 1:1000 ICC 1:100 IHC 1:200	Synaptic Systems
Tubulin	rabbit polyclonal	immunoblot 1:1000 ICC 1:3000 IHC 1:200	Synaptic Systems
VAMP 1	rabbit polyclonal	immunoblot 1:1000 ICC 1:100 IHC 1:4000	Synaptic Systems

2. Materials and Methods

VAMP 2	mouse monoclonal, 69.1	immunoblot 1:1000 ICC 1:200 IHC 1:200 Slice/Syn 1:500	Synaptic Systems
VAMP 4	rabbit polyclonal	immunoblot 1:1000 ICC 1:100	Synaptic Systems
vATPase	rabbit polyclonal	immunoblot 1:500	Santa Cruz (sc-28801)
	rabbit polyclonal	ICC 1:100 IHC 1:300	Synaptic Systems
VDAC 1	rabbit polyclonal	immunoblot 1:500	Abcam (ab15895)
	rabbit polyclonal	ICC 1:100	Santa Cruz (sc-98708)
VGlut 1/2	rabbit polyclonal	immunoblot 1:500 ICC 1:100	Synaptic Systems
Vti1 A	rabbit polyclonal	immunoblot 1:1000	Synaptic Systems
	mouse monoclonal	ICC 1:100 IHC 1:200	BD Biosciences (611220)
Bungarotoxin	labeled with tetramethylrhodamin	IHC 1:50	Sigma (T0195)
donkey anti guinea pig	labeled with AlexaFluor488	IHC 1:100 Slice/Syn 1:500	Dianova (706-545-148)
	labeled with Cy3	ICC 1:100 Slice/Syn 1:500	Dianova (706-165-148)
donkey anti goat	IRDye 800 CW	immunoblot 1:10 000	LI-COR (926-32214)
goat anti mouse	labeled with Cy2	ICC 1:100	Dianova (115-225-146)
	labeled with Cy5	Slice/Syn 1:500 Syn 1:200	Dianova (115-175-146)
	labeled with ATTO647N	ICC 1:100 IHC 1:100	Synaptic Systems
	IRDye 800 CW	immunoblot 1:10 000	LI-COR (926-32210)
goat anti rabbit	labeled with Cy2	ICC 1:100	Dianova (111-225-144)
	labeled with Cy3	Syn 1:1000	Dianova (115-165-146)
	labeled with Cy5	Slice/Syn 1:500	Dianova (111-175-144)
	labeled with ATTO647N	ICC 1:100 IHC 1:100	Synaptic Systems
	IRDye 800 CW	immunoblot 1:10 000	LI-COR (926-32211)
mouse anti goat	labeled with Cy3	Slice/Syn 1:500	Dianova (205-165-108)

2.4 Microscopy

2.4.1 Epi-fluorescence microscopy

For most standard applications an inverted Olympus IX71 microscope (Olympus, Hamburg, Germany) equipped with an F-View II CCD camera (12 bit; 6.54 μm pixel size) was used. All filters used in this set up were purchased from Chroma Technology Corporation (Below Falls, VT, USA) and are described in Table 2-3. The microscope is further equipped with a set of Olympus objectives which are listed in Table 2-4.

Table 2-3: Filter-sets used for epi-fluorescence microscopy

Filter	Exciter	Beamsplitter	Emitter
DAPI	350/50 D	400 DCLP	460/50 D
Alexa 488	480/40 HQ	505 LP Q	527/30 HQ
TRITC	545/30 HQ	570 LP Q	610/75 HQ
Cy5	620/60 HQ	660 LP Q	700/75 HQ

Table 2-4: Objectives used for epi-fluorescence microscopy

Lens type	Magnification	Numerical Aperture
UPlanSApo	100x (Oil)	1.40
UPlanSApo	60x (Oil)	1.35
UPlanFL N	40x (Dry)	0.75
UPlanFL N	20x (Dry)	0.5

2.4.2 Confocal microscopy

Confocal microscopy was performed using a Leica TCS STED microscope (Leica Microsystems GmbH, Wetzlar, Germany) equipped with a Leica 100x, 1.4 NA STED oil immersion objective and an acousto-optical tunable filter/ beamsplitter. The laser lines used in this set-up are listed in Table 2-4 and signals were detected using a photomultiplier.

Table 2-5: Laser lines of the Leica set-up

Laser	Excitation lines
Argon (100 mW)	458 nm, 476 nm, 488 nm, 496 nm, 514 nm
HeliumNeon (1 mW)	543 nm
HeliumNeon (2 mW)	594 nm
HeliumNeon (10 mW)	633 nm
Spectraphysics Mai Tai	750 nm (depletion beam in STED mode)

2.4.2.1 STED microscopy

In order to localize the proteins of interest with the highest precision available (see 3.4), super resolution STED microscopy was used. Unlike conventional microscopy, STED is not limited by the diffraction of light (Hell and Wichmann, 1994). In STED microscopy the excitation beam is superimposed with a torus shaped depletion beam which depletes the fluorescence in the periphery but not in the very center of the excitation spot. The resolution is no longer determined by the diffraction of light (in conventional microscopy to approximately 200 nm) but by the intensity of the depletion beam (Willig et al., 2006). The commercially available STED set-up from Leica, which was used in this study, achieves a lateral resolution of approximately 40-50 nm. However, in specialized applications it is possible to obtain resolutions well below 40 nm with STED microscopy (see Schmidt et al., 2008 and Rittweger et al., 2009). Apart from STED, several other super-resolution techniques have emerged in the past. A concise overview about these techniques can be found in (Toomre and Bewersdorf, 2010).

In this study STED imaging was performed using a pulsed 635 nm diode and a 750 nm Mai Tai laser (Newport Spectra-Physics GmbH, Darmstadt, Germany) for excitation and depletion respectively. Signal detection was carried out using an avalanche photodiode (APD).

2.4.3 Electron Microscopy

All electron microscopy (EM) performed in this study except the reconstructions of the synaptosomes (see 3.2) was done using a Zeiss transmission EM 902A (Zeiss, Jena, Germany) equipped with an 8-bit, 1024x1024 CCD camera (Proscan CCD HSS 512/1024; Proscan elektronische Systeme, Scheuring, Germany).

The serial electron micrographs which were used to reconstruct entire synaptosomes (3.2) were obtained using a JEOL JEM1011 EM (JEOL GmbH, Eching, Germany) equipped with an Orius SC1000A 1 (Gatan GmbH, München, Germany) with 14-bit and 4008x2672 pixels.

2.5 Preparation of synaptosomes

Synaptosomes from 6-week old wistar rats were isolated according to a modified protocol based on Gray and Whittaker, 1962 and Nicholls, 1978 (see also Fischer von Mollard et al., 1991). After decapitation of the animals the cortices and cerebella were dissected and homogenized in 12 ml per brain of ice-cold sucrose buffer using approximately 10 strokes at 9000 rpm in a glas-teflon homogenizer. For every set of synaptosomes (N=4) the homogenate of six animals was combined. As indicated in Figure 2-1A, the homogenate (H) was subjected to a round of centrifugation at 3000 g for 3 min (in Beckmann SS34) in order to remove coarse cell debris. The resulting supernatant (S1) was further centrifuged for 12 min at 12 000 g (again Beckmann SS34) which led to pelleting of the synaptosome containing fraction (P2). This pellet was re-suspended in 2 ml per brain of ice-cold sucrose buffer carefully avoiding re-suspending the dark brown mitochondrial precipitate at the very bottom of the tube. This solution was loaded onto a discontinuous Ficoll gradient composed of 3 ml 13%, 1 ml of 9% and 3 ml of 6% Ficoll in sucrose buffer (for six animals a total of six gradients was needed). The gradients were then centrifuged for 35 min at 86 000 g in a swing-out rotor (Thermo Scientific TH 641). The described gradient centrifugation separates the P2 in four different fractions: one containing mostly myelin at the top of the gradient (My), one upper synaptosome fraction between the 6 and 9% interface (U) as well as a lower between the 9 and 12% interface (L) and a dark brown pellet mostly composed of mitochondria (Mt). Representative EM images of the four different fractions can be found in Figure 2-1B. A small portion of all fractions was then processed for EM (see 2.6) while the majority of it was aliquoted, frozen in liquid N₂ and stored at -80°C for later experiments. The protein concentration of the synaptosome fractions U and L was determined using a BCA assay (results are displayed in Table 2-5). Several independent synaptosome preparations were performed of which Table 2-5 only displays those which were used within this study. Although both U and L fractions are predominantly composed of synaptosomes (Nicholls, 1978) only the L fraction was further used for doing quantitative biochemistry. A detailed discussion about why fraction L was preferred over U can be found in the next section.

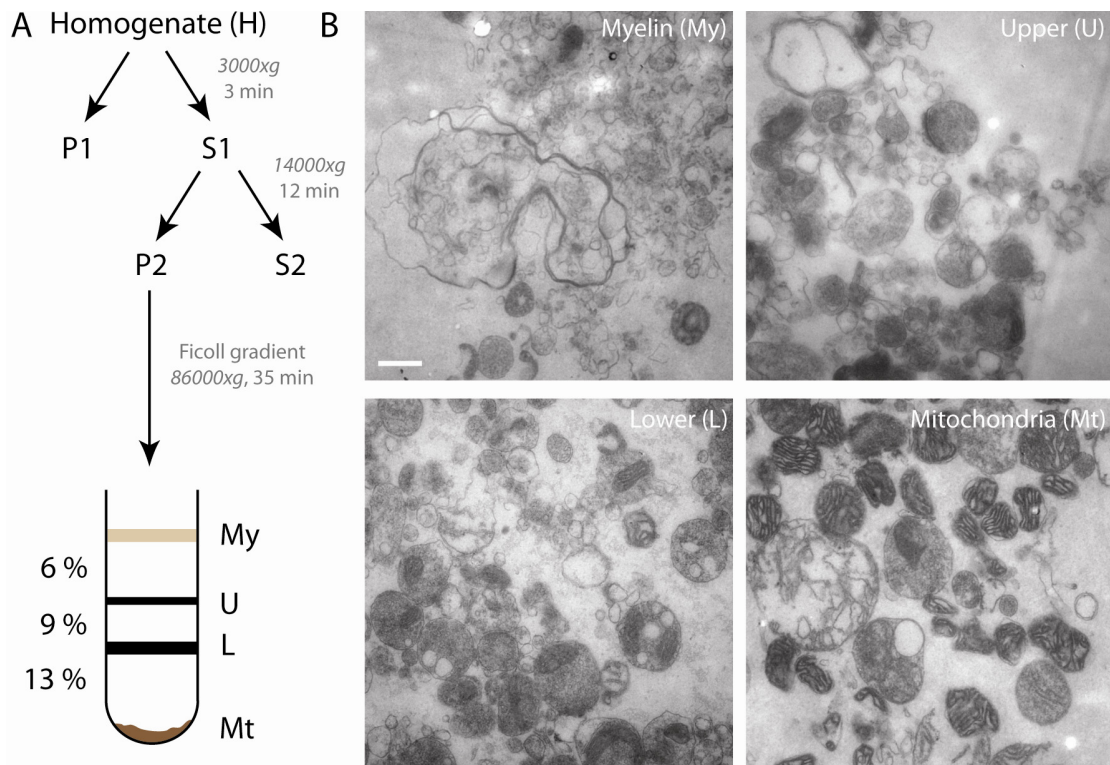


Figure 2-1: Purification of Synaptosomes.

(A) Schematic of the synaptosome purification protocol: synaptosomes are isolated from brain homogenate during a set of two differential (H to S1 and S1 to P2) and one gradient centrifugation steps (Ficoll gradient). The gradient centrifugation delivers four different fractions which are enriched in different cell brain fragments (from top to bottom): My – myelin, U – upper synaptosome, L – lower synaptosome and Mt – mitochondrial fraction.

(B) Representative electron micrographs of the four different fractions obtained via the gradient centrifugation step. Size bar is 250 nm.

Table 2-6: Protein concentration of the synaptosome fractions

Preparation date	Denomination	Fraction	Protein concentration [mg/ml]
23.11.2011	---	U	6.0 mg/ml
	S1	L	11.5 mg/ml
02.03.2011	---	U	8.8 mg/ml
	S2	L	10.5 mg/ml
03.03.2011	---	U	7.8 mg/ml
	S3	L	11.8 mg/ml
08.03.2011	---	U	9.1 mg/ml
	S4	L	13.6 mg/ml

2.5.1 Comparison of upper (U) and lower (L) synaptosome bands

As described in the previous section both upper (U) and lower (L) synaptosome fractions are indeed enriched in synaptosomes (Nicholls, 1978). In order to determine which fraction would be better suited for quantitative experiments, the composition of these fractions was investigated at the EM level. Determining the composition of the two samples using EM (refer to 2.7.2 for a description of the procedure) indeed showed that the majority of the particles in the sample are synaptosomes. However, comparing the two fractions in terms of composition reveals significant differences between them (see Figure 2-2). While the lower band contains more synaptosomes and mitochondria the upper band had more particles which were described as myelin or not identifiable at all (unknown). The increased abundance of myelin in the upper and mitochondria in the lower is not surprising in regard of the composition of the gradient: light particles such as Myelin will stay in lower and heavy particles such as mitochondria will stay in higher Ficoll concentrations (see Figure 2-1A). The presence of mitochondria in a sample is not expected to bias the quantification results as mitochondria are known to be devoid of any pre-synaptic proteins and are anyways present within synapses. In regard of the relatively large amount of unknown particles in U and synaptosomes in L, the latter fraction was used for all following experiments in this study while U was ignored.

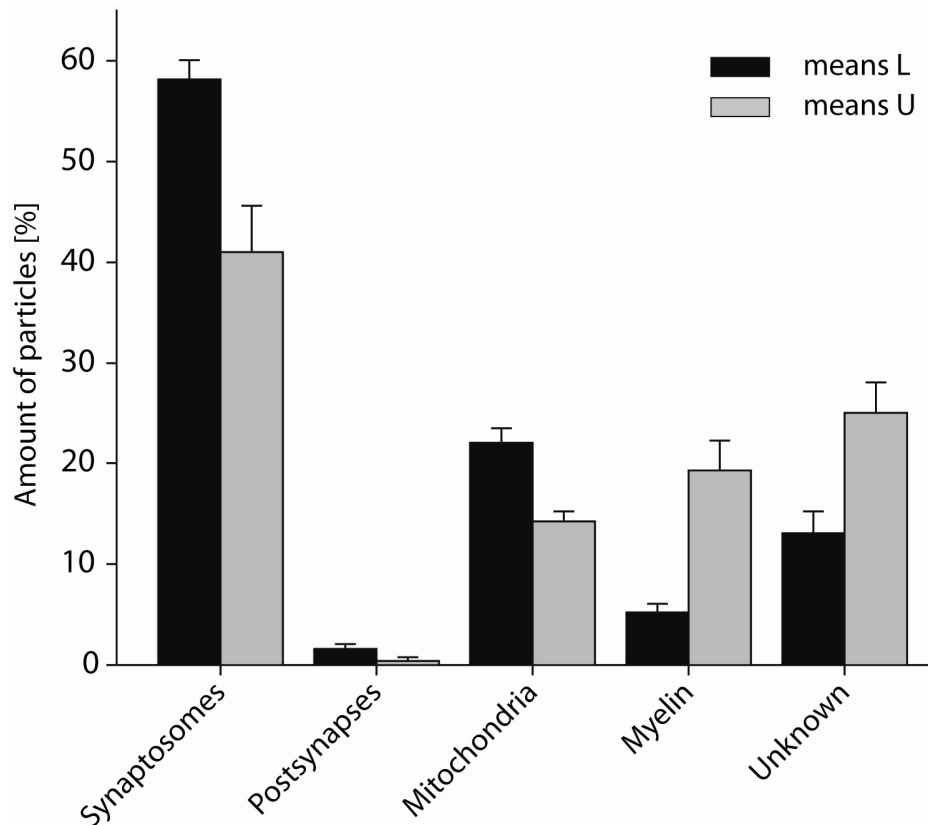


Figure 2-2: Comparing compositions of upper and lower synaptosome fractions.

This graph shows the relative abundance of synaptosomes, post-synapses (i.e. post-synaptic densities), mitochondria, myelin and unidentifiable particles in the upper and lower synaptosome fraction as investigated by EM. Black bars represent means for lower and grey for upper synaptosome bands. Graphs show mean \pm SEM from 4 independent experiments.

2.5.2 Attempts to further enrich synaptosomes

In an attempt to further enrich synaptosomes, the synaptosome fraction L was subjected to two additional rounds of gradient centrifugation (same discontinuous Ficoll gradient as in 2.5) yielding fractions LL and LLL (see Figure 2-2A). Prior to the second and third gradient centrifugation the fractions were washed in order to get rid of the remaining Ficoll which could potentially bias the separation during centrifugation. For this, the synaptosomes were re-suspended in approximately 10 ml sucrose buffer and again pelleted for 12 min at 12000 g (Beckmann SS34). Just as outlined for the synaptosome fractions in 2.5, the resulting fractions were also examined on the ultrastructural level using EM (see Figure 2-2B). Although it seemed as if fractions LL and LLL would actually contain fewer impurities (i.e. particles which could not be identified as synaptosomes, PSDs, mitochondria or myelin – see also 2.7.2) it also seemed as if many of the synaptosomes had actually opened and lost most of their contents.

Further, a fluorescence-based purity assay (described in 2.7.1) revealed that the synaptosomes were substantially more clumped when exposed to multiple gradient centrifugation steps (see Figure 2-2C), which would complicate following experiments to determine the absolute amount of synaptosomes (see 3.1)

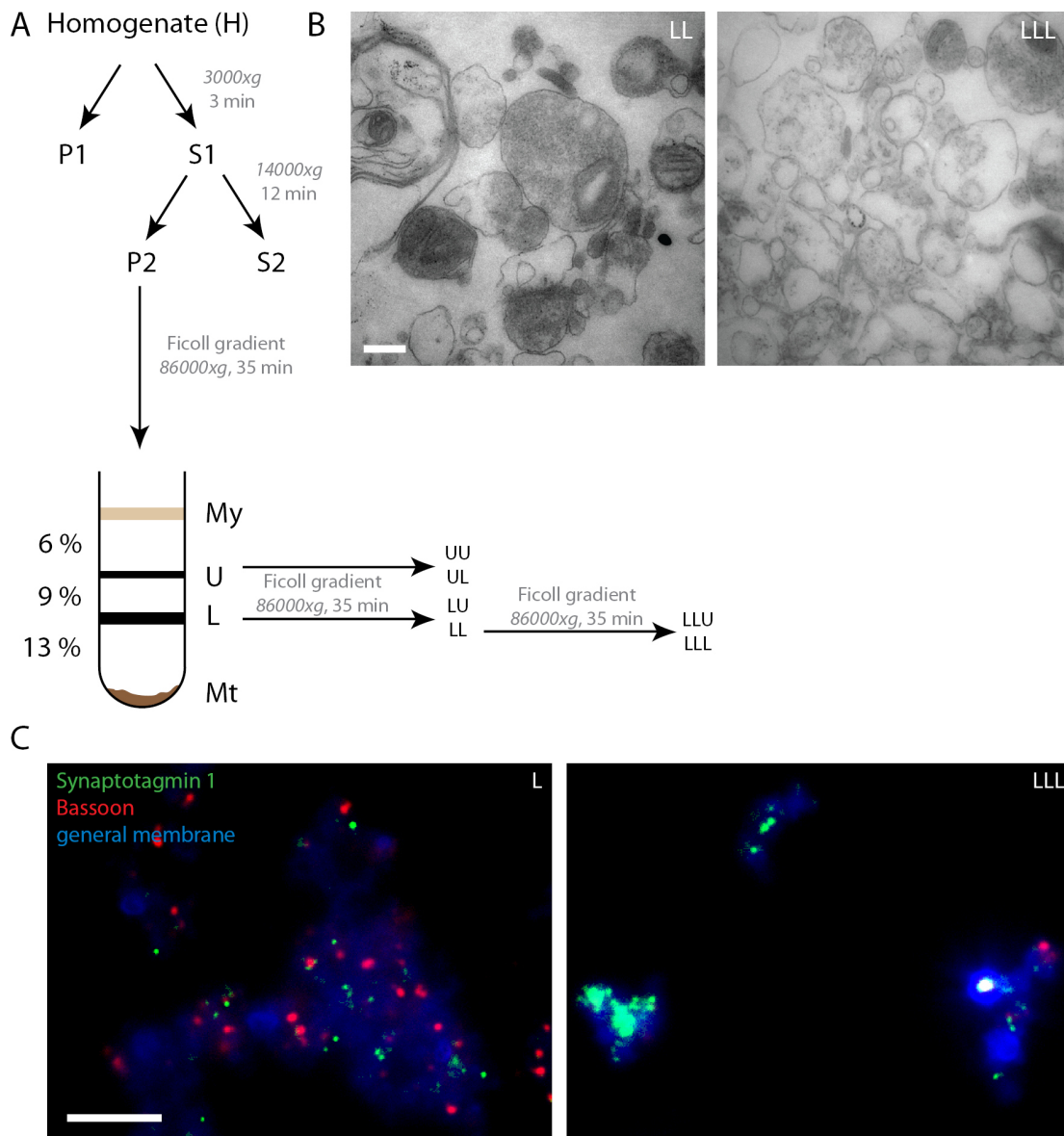


Figure 2-3: Multiple gradient centrifugations damage synaptosomes and cause clumping
 (A) Schematic of the synaptosome purification protocol with two additional gradient centrifugations to obtain enriched synaptosomes. Preparation of synaptosome fractions U and L is identical to Figure 2-1A. In this approach there were two additional gradient centrifugations performed which yielded the fractions LL and LLL.

(B) Representative electron micrographs of the two major fractions obtained via multiple gradient centrifugation steps (see A). Images show that additional gradient centrifugations can damage the synaptosomes (compare with Figure 2-1). Size bar is 250 nm.

(C) Representative fluorescent images from spin down experiments (see 2.7.1). The left image shows an example of a conventionally prepared fraction with only one gradient centrifugation (L) while the image on the right shows an example of preparation subjected to three consecutive gradient centrifugations (LLL). In both images the synaptosomes were stained for Synaptotagmin 1 (green), Bassoon (red) and general membrane/all particles (blue). Please note, that spots positive for the pre-synaptic markers (i) appear clumped in the right while they are separated in the left image and (ii) contain substantially less Bassoon. Size bars is 5 μ m.

To ultimately test whether the additional gradient centrifugations would lead to an enrichment of synaptosomes and therefore also of synapse specific proteins, protein blots (described in 2.9.3) were performed. The results depicted in Figure 2-3 indicate that multiple gradient centrifugations do not lead to a major increase in synaptic proteins. Therefore, it had to be concluded that this procedure did not further enrich synaptosomes. In addition, it was observed that the synaptosomes in the LLL fraction lost substantial amounts of Bassoon during the additional gradients compared to the L fraction (see Figure 2-3 C). Although this finding was not further characterized within this study, it could be assumed that the synaptosomes actually lose their active zones during multiple gradient centrifugation steps.

In conclusion, the additional gradient centrifugation steps did not enrich synaptosomes further but rather altered the ultrastructure of the synaptosomes. Hence, only preparations objected to a single gradient centrifugation (L) were used for the rest of the study.

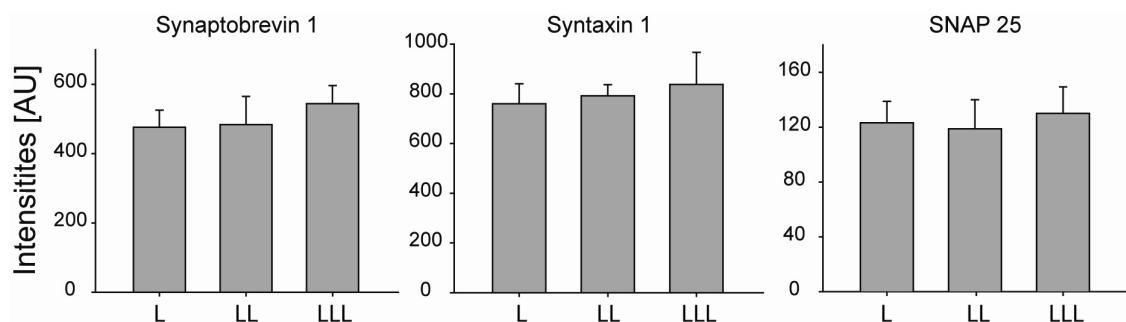


Figure 2-4: Comparing amounts of synaptic proteins in different synaptosome preparations. The figure shows the results of the immunoblots performed for three major synaptic proteins – Synaptobrevin 1, Syntaxin 1 and SNAP 25 – on different synaptosome preparations. The three bars represent different amount of gradient centrifugation steps (1-3) as described in 2.5.1. The bars within one graph are not significantly different, which indicates that multiple gradient centrifugations do not increase the relative amount of synaptic protein. Graphs show mean \pm SEM from 7 independent experiments.

2.6 Processing of synaptosomes for EM

Directly after purification a small amount (approximately 200 μ l) of each fraction was fixed in PBS containing 2.5% Glutaldehyde for 15 min on ice followed by 45 min at room temperature. As the synaptosomes are generally in solution, the particles had to be pelleted (15 000 rpm for 1 min in a tabletop centrifuge from Eppendorf) prior to every buffer change (washing etc.). Before the samples were quenched using PBS containing 100 mM NH_4Cl for 25 min they were briefly washed (twice) with PBS. After two additional washing steps in PBS, the synaptosomes were incubated for 60 min in approximately 400 μ l sterile filtered PBS containing 1% osmium (prepared fresh from a 4% stock solution). After osmication the samples were again washed four to five times with PBS and embedded in small Agarose blocks (warm low melt Agarose was added to the samples, mixed and allowed to solidify). The blocks could then be cut in small pieces and stored in PBS at 4° C over night if desired. Dehydration of the samples was performed according to the following scheme:

30% Ethanol	5 min
50% Ethanol	5 min
70% Ethanol	5 min
90% Ethanol	10 min
95% Ethanol	10 min
100% Ethanol	3x 10 min
1:1 Ethanol:Propylene oxide	10 min
Propylene oxide	3x 10 min
1:1 Propylene oxide:Epon	12-18 hours

In order to allow complete evaporation of organic solvents the samples were kept in Epon for approximately 8 hours prior to embedding in fresh resin. Polymerization of the Epon was achieved by incubating the samples for 24 to 48 hours at 60°C. All samples were cut into 70-90 nm thin sections using a Leica EM UC 6 microtome (Leica, Heidelberg, Germany).

2.7 Characterization of synaptosomes

2.7.1 Fluorescence-based spin down assay

One possibility to determine the absolute number of synaptosomes is to investigate the amount of total particles per volume synaptosomes and which fraction of these are actually synaptosomes. For this the synaptosomes were substantially diluted (100 ng/ml) which is important to avoid clumping of the individual particles and 3 μ g of synaptosomes (total protein) were centrifuged onto 18 mm glass cover-slips for 50 min at 2900 g and 4°C. Prior to this the cover-slips were incubated in PBS with 5% BSA at 37°C overnight and coated with 0.2 μ m TetraSpeck™ beads (Invitrogen, 1 ml of 1:10⁶ diluted beads in PBS for 50 min at 2900 g and 4°C). The beads were used to align the images taken from the synaptosomes as they are visible in all channels. Afterwards, the synaptosomes were fixed for 10 min on ice and 45 min at room temperature with PBS containing 4% PFA (Paraformaldehyde) followed by quenching in PBS + 100 mM NH₄Cl for 30 min at room temperature. Subsequently, after a brief wash in PBS, the samples were blocked and permeabilized for 30 min in PBS + 0.1% Triton X100 + 5% BSA followed by a 1 h incubation with the primary antibodies in the same solution. The synaptosomes were incubated with antibodies against Synaptotagmin 1 for labeling SVs and Bassoon or PSD-95 for labeling pre- and postsynaptic densities respectively. After the antibody incubation the samples were washed briefly in PBS. Secondary antibodies against the respective primaries were applied under the same conditions as the primary antibody. Hence, Synaptotagmin 1 was labeled with Cy3 while Bassoon/PSD-95 was labeled with Cy5. To remove excess antibodies the samples were washed consecutively with high salt and regular PBS prior to imaging (see Figure 2-5 for a schematic of the procedure).

Directly after labeling the samples were imaged in a 1:20 dilution of a saturated solution of 1-(4-Trimethylammoniumphenyl)-6-Phenyl-1,3,5-Hexatriene *p*-Toluenesulfonate (TMA-DPH) in ddH₂O. TMA-DPH is an amphiphilic dye, which emits fluorescence around 440 nm rendering it an ideal candidate for labeling membranes in parallel to the immunostaining. Hence, TMA-DPH labels all particles of the samples serving as a positive labeling control for this assay. Imaging was performed at the before described Olympus set-up (see 2.4.1) with the 100x objective using all available channels: DAPI for TMA-DPH, TRITC for Synaptotagmin 1, Cy5 for Bassoon/ PSD-95 and Alexa488 for beads. As mentioned above, the beads are fluorescent in all four channels and Alexa488 images (where only beads were visible) were used as a reference to align the images during analysis.

Image analysis was performed using custom written MATLAB (MathWorks, Natick, MA, USA) routines (by Silvio O. Rizzoli). The position of the beads was used to align the images obtained in the different channels. The amount of total particles was derived by counting the number of blue spots while the amount of synaptosomes was derived from the fraction of blue spots which were also positively labeled for Synaptotagmin 1. However, this approach assumes that all synaptosomes that were initially centrifuged onto the cover-slips actually went down and attached to it. To control for a potential bias introduced by particles not attaching to the cover-slip a control experiment was designed which is outlined in the next section.

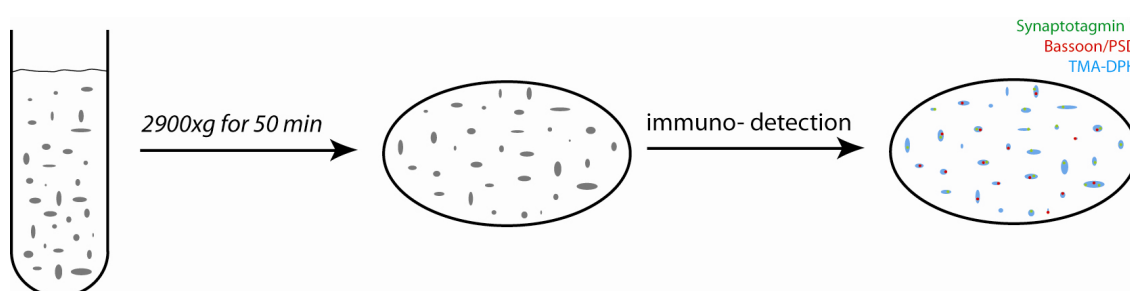


Figure 2-5: Schematic of the spin down experiment.

Synaptosomes are diluted and centrifuged onto a glass cover-slip which was previously coated with BSA and tetraspec beads. After fixation of the sample the synaptosomes are stained for a synaptic vesicle marker (Synaptotagmin 1), a pre- or post-synaptic density marker (Bassoon or PSD) and imaged in the general membrane marker TMA-DPH.

2.7.1.2 Spin down efficiency assay

To determine the bias introduced by synaptosomes which do not attach to the glass cover-slip during centrifugation, samples of the supernatant were taken before and after centrifugation. These samples were immunoblotted (for a detailed description of immunoblots and the respective analysis refer to 2.9.3) for two abundant pre-synaptic proteins – Syntaxin 1 and Synaptobrevin 1 detected with the Synaptic Systems antibodies 78.2 (used 1:10 000) and 69.1 (used 1:1000) respectively. Other than described in 2.9.3 an enhanced chemiluminescence system (Perkin Elmer) was used for visualization of the proteins. The ratio of the protein amounts post over pre centrifugation was used as a correction factor for the determination of the number of synaptosomes in the spin down assay (see 3.3.1).

2.7.2 EM-based assay

The validity of the results obtained from the spin down assay (2.7.1) was further tested on an ultrastructural level using electron micrographs of the synaptosomes. EM samples and images were obtained as described in 2.5 using the EM specified in 2.4.3. Electron micrographs were then individually analyzed concerning their composition. All visible particles were manually selected and assigned to one of five groups: synaptosomes, post-synapses, mitochondria, myelin or unknown. The results of this assay can be found in 3.3.2 while a comparison of the fluorescence and EM-based assay is presented in 3.3.3.

2.8 Three dimensional reconstructions of synaptosomes

The 3D reconstructions of the synaptosomes were obtained from serial sections. After imaging, the sections were manually aligned in Photoshop (Adobe Systems, San Jose, CA, USA). A semi-automated MATLAB routine (written by Silvio O. Rizzoli) was used to analyze the consecutive sections. The different parts of a synaptosome – plasma membrane, vesicles, mitochondria and AZs – were manually selected in each frame. The information obtained from this analysis (sizes, distances etc.) was used by the routine to generate a 3D model of the synapse. Further information gained by this analysis is (i) synapse size/shape and (ii) number as well as position of vesicles, AZs and mitochondria.

2.9 Determining absolute protein amounts per synaptosome

One major aspect of this study was the quantification of pre-synaptic proteins. The following sections outline the methods applied to obtain absolute protein copy numbers per synapse.

2.9.1 Protein standards

All purified proteins that were used in this study as standard proteins for quantitative Western Blots (see 2.9.2) were either kindly provided by collaborators or purchased from different distributors. Protein concentrations were either provided by the manufacturer or determined using a spectrophotometer (Nanodrop ND1000; Peqlab, Erlangen, Germany). Table 2-2 provides an overview of these proteins as well as information on their origin.

Table 2-7: Purified Proteins

Protein	Source and sequence information	Supplier
Actin	from bovine heart muscle	Cytoskeleton Inc. (AD99)
Alpha-SNAP	recombinant rat, 1-295	Reinhard Jahn (MPI bpc, Göttingen, Germany)
Alpha-Synuclein	recombinant human, 1-140	Christian Griesinger (MPI bpc, Göttingen, Germany)
Amphiphysin	recombinant human, 1-696	Novus Biologicals (H00000273-P01)
AP 180	recombinant human, 1-907	Novus Biologicals (H00009892-P01)
AP2 (μ 1)	Recombinant human, 1-435	Novus Biologicals (H00001173-P01)
APP	Recombinant human, 1-306	Novus Biologicals (H00000351-P02)
BACE1	Recombinant human, 1-870	Abnova (H00023621-P01)
Calbindin	Recombinant rat, 1-261	Beat Schwaller (University of Fribourg, Switzerland)
CALM	Recombinant rat, 228-829 (without 645-646 and 684-688)	Volker Haucke (FMP, Berlin, Germany)
Calmodulin	Recombinant human, 1-149	Novus Biologicals (NBC1-18401)
Calretinin	Recombinant rat, 1-271	Beat Schwaller (University of Fribourg, Switzerland)
Clathrin heavy chain	Recombinant rat, 1-364	Volker Haucke (FMP, Berlin, Germany)
Clathrin light chain	Recombinant human, 1-219	Novus Biologicals (H00001211-P01)
Complexin-1	Recombinant human, 1-134	Novus Biologicals (NBC1-18349)
CSP	Recombinant human, 1-198	Novus Biologicals (H00080331-P01)
Doc2 B	Recombinant human, 1-412	Novus Biologicals (H00008447-P01)
Dynamin 1	Recombinant human, 1-864	Aurelien Roux (University of Geneva, Switzerland)
Endophilin I	Recombinant human, 1-352	Novus Biologicals (H00006456-P02)
Epsin 1	Recombinant human, 1-550	Novus Biologicals (H00029924-P01)
Hsc70	Recombinant human, 1-646	Novus Biologicals (NBP1-30278)
Intersectin-1	Recombinant rat, 1-440	Volker Haucke (FMP, Berlin, Germany)
Munc13a	Recombinant rat, 859-1531 (without 1415-1437)	Reinhard Jahn (MPI bpc, Göttingen, Germany)
Munc18a	Recombinant rat, 1-594	Reinhard Jahn (MPI bpc, Göttingen, Germany)

2. Materials and Methods

Myelin Basic Protein	Collected from human brain	Novus Biologicals (NB810-73234)
NSF	Recombinant rat, 1-744	Reinhard Jahn (MPI bpc, Göttingen, Germany)
Parvalbumin	Recombinant rat, 1-110	Beat Schwaller (University of Fribourg, Switzerland)
PIPK I γ	Recombinant rat, 451-668	Volker Haucke (FMP, Berlin, Germany)
PSD-95	Recombinant rat, 64-247	Synaptic Systems (124-01P)
Rab3a	Recombinant human, 1-221	Novus Biologicals (H00005864-P01)
Rab5a	Recombinant human, 1-215	Novus Biologicals (NBC1-18504)
Rab7a	Recombinant human, 1-207	Novus Biologicals (NBP1-50961)
SCAMP 1	Recombinant human, 1-339	Novus Biologicals (H00009522-P01)
Septin 5	Recombinant rat, 1-369	Volker Haucke (FMP, Berlin, Germany)
SGIP	Recombinant rat, 1-222	Volker Haucke (FMP, Berlin, Germany)
SNAP 23	Recombinant human, 1-211	Novus Biologicals (NBC1-18347)
SNAP 25a	Recombinant rat, 1-206	Reinhard Jahn (MPI bpc, Göttingen, Germany)
SNAP 29	Recombinant human, 1-259	Novus Biologicals (H00009342-P01)
SV2 B	Recombinant human, 1-683	Novus Biologicals (H00009899-P01)
Synapsin II	Recombinant human, 348-449	Novus Biologicals (H00006854-Q01)
Synaptogyrin	Recombinant human, 1-192	Novus Biologicals (H00009145-P01)
Synaptophysin	Recombinant human, 1-314	Novus Biologicals (H00006855-P01)
Synaptotagmin 1	Recombinant rat, 1-421	Reinhard Jahn (MPI bpc, Göttingen, Germany)
Synaptotagmin 2	Recombinant human, 311-419	Novus Biologicals (H00127833-Q01)
Synaptotagmin 7	Recombinant human, 41-140	Novus Biologicals (H00009066-Q01)
Syndapin	Recombinant human, 1-445	Novus Biologicals (H00029993-P01)
Syntaxin 1	Recombinant rat, 1-288	Reinhard Jahn (MPI bpc, Göttingen, Germany)
Syntaxin 6	Recombinant rat, 1-255	Reinhard Jahn (MPI bpc, Göttingen, Germany)
Syntaxin 7	Recombinant rat, 1-261	Reinhard Jahn (MPI bpc, Göttingen, Germany)
Syntaxin 13	Recombinant rat, 1-274	Reinhard Jahn (MPI bpc, Göttingen, Germany)

		Germany)
Syntaxin 16	Recombinant mouse, 1-326	Reinhard Jahn (MPI bpc, Göttingen, Germany)
Tubulin	Purified from porcine brain	Cytoskeleton Inc. (T240)
VAMP 1	Recombinant human, 1-91	Novus Biologicals (NBC1-18336)
VAMP 2	Recombinant rat, 1-116	Reinhard Jahn (MPI bpc, Göttingen, Germany)
VAMP 4	Recombinant rat, 1-141	Reinhard Jahn (MPI bpc, Göttingen, Germany)
vATPase (6v0a1)	Recombinant human, 1-831	Novus Biologicals (H00000535-P01)
VDAC 1	Recombinant human, 1-283	Novus Biologicals (H00007416-P01)
VGlut 1	Recombinant human, 1-560	Novus Biologicals (H00057030-P01)
Vti1 A	Recombinant mouse, 1-217	Reinhard Jahn (MPI bpc, Göttingen, Germany)

2.9.2 SDS-Page and Western Blotting

In various experiments throughout this study immunoblotting was used for determining relative and absolute amounts of proteins. Proteins were separated using SDS-PAGE similar to Schagger and von Jagow, 1987 (see also Schagger, 2006). Unless otherwise stated all steps were done at room temperature. First, samples were boiled for 5-10 min at 95°C and then loaded on 10% denaturing Tris/Tricin SDS polyacrylamide gels (see recipe in Table 2-8). Separation of the proteins was carried out in a discontinuous buffer system (separate anode and cathode buffer, for recipes see Table 2-1) at 70 V for 15 min followed by 60-90 min (depending on protein size) at 120 V. Importantly, the purified proteins were always mixed with a defined amount of fetal calf serum (FCS) prior to loading. As these samples were always run in parallel to the synaptosomes (see 3.3), the amount of FCS was chosen to be equivalent to the amount of synaptosomes assuring that all pockets were loaded with approximately the same amount of total protein.

Immunoblotting of the separated proteins was performed similar to a protocol described by Towbin et al., 1989. The proteins were transferred to a nitrocellulose membrane by applying 2 Amp for 2 h at 4°C in a wet blotting tank containing transfer buffer. Following the transfer, membranes were blocked for 45 min and then incubated in the primary antibodies for 1 h, both in blocking buffer. After washing the membranes twice for 15 min they were incubated in the secondary antibody for 45 min, again, both in blocking buffer. Prior to imaging the

membranes were washed three times for 15 min in wash buffer. Detection was performed using the LI-COR Odyssey imaging system (LI-COR Biosciences, Lincoln, NB, USA) at a high resolution and highest possible sensitivity (settings within the imaging software).

Custom written MATLAB routines (by Silvio O. Rizzoli) were used to measure average band intensities which were corrected for local background (mean from average intensities immediately above and below the protein band).

Table 2-8: Schagger gel composition.

Ingredient	Stacking Gel (1x)	Separation Gel (1x)
Gelbuffer	375 μ l	1.675 ml
ddH ₂ O	925 μ l	570 μ l
50% Glycerol	---	1.060 ml
TEMED	2 μ l	3 μ l
10% Ammonium persulfate (APS)	10 μ l	25 μ l
Acrylamide	200 μ l	1.660 ml

2.9.2.1 Troubleshooting immunoblots

Several proteins demanded modified conditions in order to be separated and immunoblotted reliably. This section will address the conditions which were altered and provide a comprehensive table (see table 2-9) including all effected proteins.

FCS: A major component of FCS is bovine serum albumin (BSA), a globular protein of approximately 69 kDa. Unfortunately, several of the proteins that were investigated had similar molecular weights. In these cases the highly abundant BSA (from the FCS that was added to the samples) did mask the epitopes of the purified proteins which therefore could not be detected in the immunoblot. In these cases no FCS was added to the purified protein samples to ensure proper separation and transfer (for an example see Figure 2-6 A).

Boiling: Several, mainly large proteins, tend to aggregate upon boiling which led to an unspecific smear or no signal at all on the membrane. In these cases boiling of the samples was avoided (refer to Figure 2-6 B for an example).

PVDF membrane: Only one protein was blotted on PVDF membranes, namely CALM. The purified protein was kindly provided by Prof. Dr. Volker Haucke (FMP, Berlin, Germany). He

had performed several studies dealing with CALM (Koo et al., 2012; Maritzen et al., 2012) and had strongly suggested the use of these membranes for this particular protein.

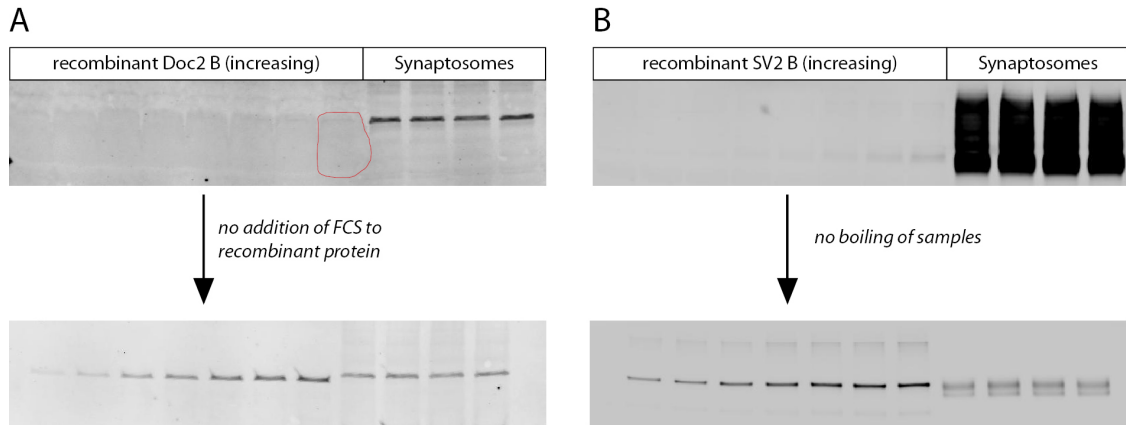


Figure 2-6: Troubleshooting of quantitative immunoblots.

(A) Representative immunoblots of Doc2 B with (upper) and without (lower) the addition of FCS to the recombinant protein. The specific Doc2 B band is only visible without the FCS (lower) while the epitopes are masked by the FCS in the upper immunoblot (red outline).

(B) Representative immunoblots of SV2 B with (upper) and without (lower) boiling of the samples prior to loading on the gel. While boiling may potentially lead to aggregation of some proteins (see thick bands in the upper immunoblot) these can clearly be separated and visualized if samples are not boiled.

Table 2-9 Proteins investigated with modified immunoblot conditions.

Protein	Protocol modification
AP 2	without FCS
CALM	PVDF membrane
Clathrin heavy chain	without FCS
Clathrin light chain	without FCS
Doc2	without FCS
Endophilin	without FCS
Munc13a	without FCS
Munc18a	without FCS
SV2	no boiling of samples
vATPase	without FCS, no boiling of samples

VDAC	without FCS
VGlut	no boiling of samples

2.9.3 Deriving correction factors for soluble proteins potentially lost from synaptosomes during purification

During the process of synaptosome purification it is possible to lose soluble proteins from the pre-synaptic terminals. As this would bias the quantification results obtained from these terminals (3.3), an experiment that would provide correction factors for the loss of soluble proteins was designed. Briefly, synaptosomes and cortical brain slices were immunostained in parallel for (1) Synaptophysin as a trans-membrane reference protein and (2) the soluble protein of interest. The fluorescent ratio obtained from Synaptophysin over protein of interest from the native state (cortical slice) was compared with the same ratio derived from the artificial condition (synaptosome). Comparing the two ratios with each other could then be used to calculate a correction factor if necessary.

Synaptosomes: the synaptosomes were stained as described in 2.7.1 with the exception that 2 μg were centrifuged onto 12 mm glass cover-slips. At the end of the staining the synaptosomes were embedded in Mowiol.

Cortical slices: cortical brain slices from 6 week old wistar rats were prepared by Dr. Meike Pedersen (Max Planck Institute for biophysical chemistry, Department of Membrane Biophysics, Göttingen, Germany) as described in (Vervaeke et al., 2010). Prior to blocking for 1 h in PBS + 10% BSA the slices were briefly washed with Phosphate buffer. Incubation of the primary antibodies was performed for 12 h at room temperature in PBS + 2% BSA + 0.1% Triton X100. After primary antibody incubation the slices were washed twice for 10 min in PBS and incubated with the secondary antibodies for 2 h at room temperature in PBS + 2% BSA. Next, slices were washed twice with PBS, once with high salt PBS and finally once with Phosphate buffer and embedded in Mowiol.

A detailed list of all stainings performed on synaptosomes and slices can be found in Table 2-10. For a comprehensive list of antibodies and dilutions used refer to Table 2-2.

The samples were imaged using a Leica confocal microscope (see 2.4.2). Importantly the imaging conditions (in particular laser intensity and gain) were chosen to be identical for every slice and its respective synaptosome sample to allow a direct comparison of the two different preparations. Images were analyzed using custom written Matlab routines (Silvio O. Rizzoli). In

both preparations the Synaptophysin signals were used to automatically identify pre-synaptic terminals. At these defined regions of interest (ROI) the fluorescence intensity of the particular protein of interest was divided by the Synaptophysin fluorescence to obtain a ratio for protein of interest over Synaptophysin. In order to obtain the correction factor, the ratio Synaptosomes was then divided by the ratio Slices.

Table 2-10: Immunostainings on cortical brain slices and synaptosomes.

Soluble protein of interest	Reference protein
Alpha-SNAP + Cy5	Synaptophysin + Cy3
Alpha-Synuclein + Cy5	Synaptophysin + Cy3
Amphiphysin + Cy5	Synaptophysin + Cy3
AP 180 + Cy5	Synaptophysin + Cy3
AP2 (μ 1) + Cy5	Synaptophysin + Cy3
Calbindin + Cy5	Synaptophysin + Cy3
CALM + Cy2	Synaptophysin + Alexa488
Calmodulin + Cy5	Synaptophysin + Cy3
Calretinin + Cy5	Synaptophysin + Cy3
Clathrin heavy chain + Cy5	Synaptophysin + Cy3
Clathrin light chain + Cy5	Synaptophysin + Cy3
Complexin + Cy5	Synaptophysin + Cy3
CSP + Cy5	Synaptophysin + Cy3
Doc2 B + Cy5	Synaptophysin + Cy3
Dynamin + Cy5	Synaptophysin + Cy3
Endophilin + Cy5	Synaptophysin + Cy3
Epsin 1 + Cy5	Synaptophysin + Cy3
Hsc70 + Cy5	Synaptophysin + Cy3
Intersectin-1 + Cy5	Synaptophysin + Cy3
Munc13a + Cy5	Synaptophysin + Cy3
Munc18a + Cy5	Synaptophysin + Cy3

NSF + Cy5	Synaptophysin + Cy3
Parvalbumin + Cy5	Synaptophysin + Cy3
Phosphatidylinositol 4-kinase I γ + Cy5	Synaptophysin + Cy3
Rab3a + Cy5	Synaptophysin + Cy3
Rab5a + Cy5	Synaptophysin + Cy3
Rab7a + Cy5	Synaptophysin + Cy3
Septin 5 + Cy5	Synaptophysin + Cy3
SGIP + Cy5	Synaptophysin + Cy3
SNAP 25 + Cy5	Synaptophysin + Cy3
Synapsin + Cy5	Synaptophysin + Cy3
Syndapin + Cy5	Synaptophysin + Cy3
Syntaxin 1 + Cy5	Synaptophysin + Cy3
VAMP 2 + Cy5	Synaptophysin + Cy3

2.10 Immunostaining of primary hippocampal cultures

Primary hippocampal cultures were obtained from P1-P3 wistar rats as described in (Willig et al., 2006) After dissection and dissociation of the hippocampi the neurons were plated on an astrocyte feeding layer which had been grown for one week prior to seeding. Cells were kept at 37°C and 5% CO₂ and medium was replaced two days after plating.

To determine the organization of the proteins of interest within the synapse, neurons were stained after 15-20 days in vitro (DIV) for these proteins in parallel with Bassoon and Synaptophysin. After fixation of the neurons in PBS + 4% PFA for 45 min the samples were washed in PBS, quenched with PBS + 100 mM NH₄Cl and washed again with PBS. Prior to incubating with the primary antibodies (for 1 h in PBS + 1.5% BSA + 0.1% Triton X100) the samples were permeabilized in PBS + 0.1% Triton X100. After further washes with PBS + 0.1% Triton X100 the secondary antibodies were applied again in PBS + 1.5% BSA + 0.1% Triton X100 for 1 h. Last, the samples were washed consecutively in high salt PBS and PBS and embedded in 2,2'-thiodiethanol (TDE, Staudt et al., 2007). Embedding in TDE was done via a dilution series of 30, 50, 70 and 90% TDE in PBS followed by 3x 100% TDE (10 min each).

Imaging of the samples was performed using the STED microscope (see 2.4.2). Image analysis was done using semi automatic Matlab routines (written by Silvio O. Rizzoli). The center of mass of a Bassoon spot was determined and assumed to represent the AZ of a synapse. All spots from the protein of interest were assigned to the nearest synapse (i.e. Bassoon spot) while spots found beyond 800 nm were ignored. This procedure was performed for every synapse and the resulting density profiles were rotated and aligned according to their assumed axis. This axis represents the orientation with the weighted maximum overlap of (a) the protein of interest and (b) the Synaptophysin signal between different synapses. The described alignment in orientation was performed to eliminate bias introduced by differently oriented synapses which would have led to random scattering of the spots around the center of the synapse. The aligned density profiles were then used to generate the average density distribution of the protein of interest in respect to the AZ (see also 3.6).

2.11 Immunostaining of mouse NMJs

Mouse *levator auris longus* muscles were dissected in standard Mouse buffer (Angaut-Petit et al., 1987). Prior to fixation in PBS + 4% PFA the muscles were incubated for 15 min in Bungarotoxin and washed for another 15 min in Mouse buffer. After fixation the muscles were washed twice with PBS and quenched for 30 min in PBS + 100 mM NH₄Cl. After another washing step in PBS the muscles were permeabilized in PBS + 0.5% Triton + 2.5% BSA 3x10 min followed by incubation with the primary antibodies in the same buffer for 2 h. Subsequently, muscles were washed in PBS + 0.5% Triton + 2.5% BSA and incubated for 1 h with the secondary antibodies (in PBS + 0.5% Triton + 2.5% BSA). After incubation with the secondary antibodies the muscles were washed twice with high salt PBS + 2.5% BSA over night. The next day, the muscles were washed thoroughly in PBS and embedded via a TDE dilution series as described for the hippocampus cultures in 2.10.

Certain proteins demanded more rigorous blocking conditions in order to achieve a specific staining, thus the following proteins were blocked using PBS + 5% BSA + 5% Trypton/Pepton: BACE, Epsin 1, Munc13a, Syndapin, PIPK 1 γ , Septin 5, SGIP, SNAP 23, SNAP 25, Synaptotagmin 2, Syntaxin 16, VAMP 2, vATPase (A1).

Imaging was performed identical to the hippocampal cultures but image analysis was slightly modified: in addition to the signals from Synaptophysin the protein of interest also the signal from the Bungarotoxin was used to align the images. This was necessary due to the

anatomy of the NMJ where the AZ is not a single diffraction limited spot but an elongated structure.

2.12 Graphical modeling of the average pre-synaptic terminal

The graphical model of the average pre-synaptic terminal including all data acquired in this study was done by Burkhard Rammner (Scimotion, Hamburg, Germany) using custom written plug-ins and scripts in the 3D software Autodesk Maya (Autodesk Inc., Mill Valley, USA)

3. Results

The ultimate goal of this study is to gain a more thorough understanding of the pre-synaptic composition and architecture. To do so, I performed several consecutive experiments integrating several quantitative biochemistry and microscopy approaches (see outline in Figure 3-1).

First, I obtained four different synaptosome preparations (S1-4) from rat brains which I characterized concerning their general composition and the absolute amount of synaptosomes (refer to part 3.1). Second, I determined the physical parameters of the synaptosomes using 3D reconstructions of ultrathin EM sections obtained from the synaptosomes (see part 3.2). Third, I investigated the pre-synaptic protein composition by performing quantitative immunoblots. Here, I used defined amounts of a purified version of the respective protein of interest as a standard in comparison to defined amounts of synaptosomes. Since the absolute number of synaptosomes per μg of synaptosome fraction is known (from 3.1), I could use the results from the immunoblots to calculate absolute protein numbers per synaptosome. This approach allowed me to quantify 59 different pre-synaptic proteins (see part 3.3). Next, I investigated the spatial distribution of these proteins within the pre-synapse using super resolution STED microscopy. This was done in two different preparations: (1) rat hippocampal cultures and (2) mouse NMJs from the *levator auris longus* muscle (refer to part 3.5). Finally, the structural information (3.2) as well as the protein quantification (3.3) and localization (3.4) were used to generate a 3D graphical model of the average brain synapse (see part 3.5).

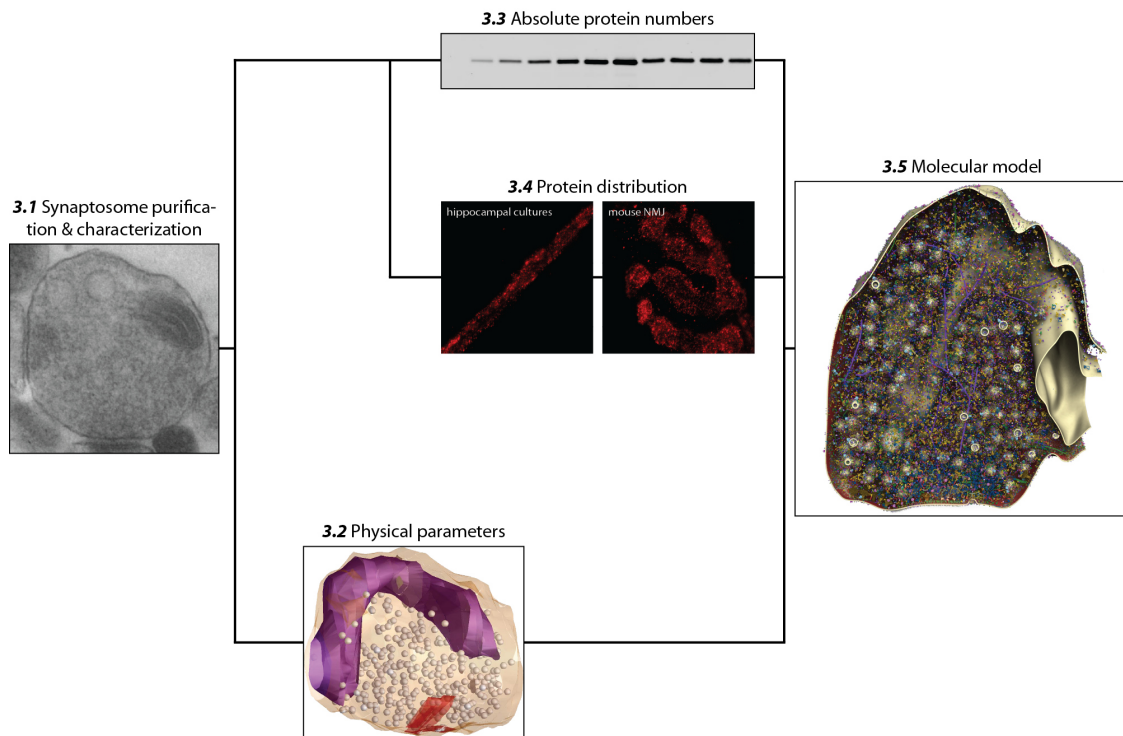


Figure 3-1: Experimental outline of the project.

The schematic illustrates the experimental flow performed to determine the pre-synaptic architecture: synaptosomes were purified and characterized (3.1). Next, their physical characteristics were determined using 3D reconstruction EM (3.2) followed by absolute protein quantification per synapse (3.3) and determining the organization of the proteins within the synapse (3.4). The information obtained from these sets of experiments was then used to generate a graphical model of the average pre-synaptic terminal (3.5).

3.1 Purification and characterization of synaptosomes

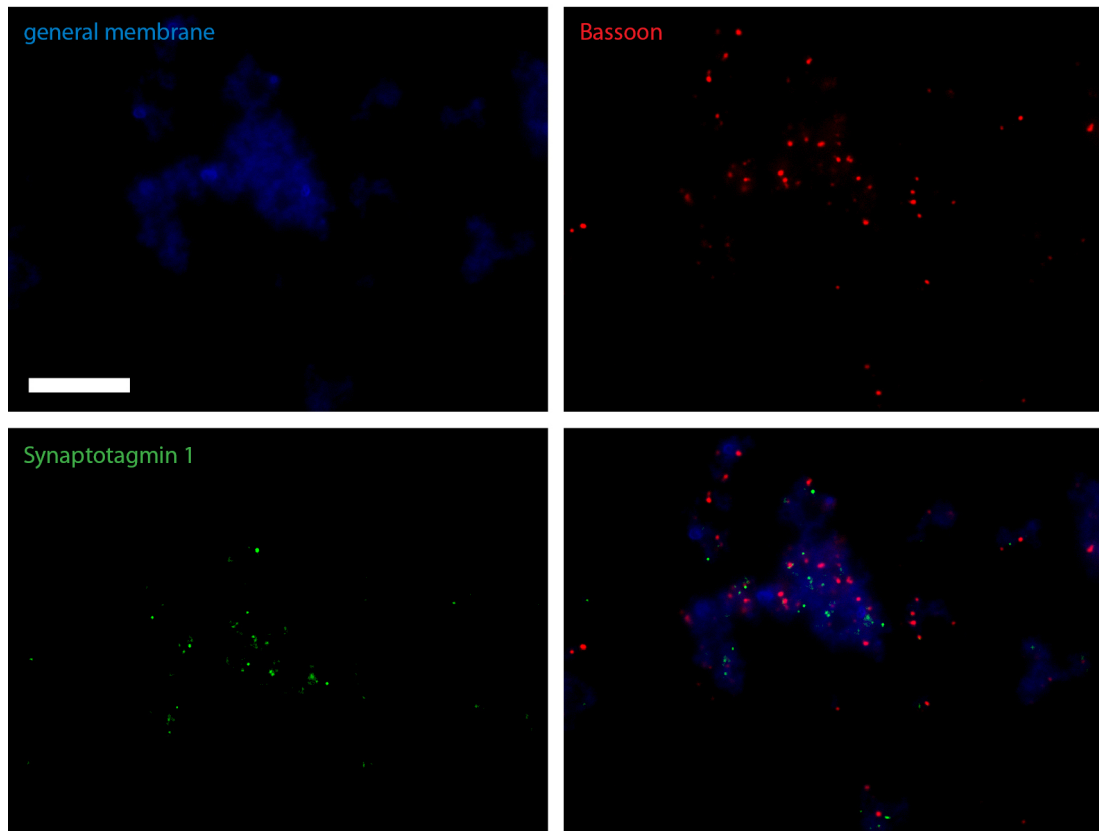
As outlined in the previous section, the main goal of this study was to investigate the molecular architecture of a pre-synaptic terminal. The model system I used to address this question was isolated nerve terminals – so called synaptosomes – from rat brains. During homogenization of the brain material, the pre-synaptic terminals get ripped off of the neuronal processes. These are then isolated via consecutive differential and gradient centrifugation steps (see detailed protocol in 2.5). In principle, the synaptosomes are intact and maintain their neurophysiological properties (Fischer von Mollard et al., 1991). For this study I used only cortex and cerebellum as starting brain material. By using only these two areas of the brain I was able to limit the variability of synapse populations to a certain extent and ensured that I still had enough brain material per animal to perform multiple quantification experiments.

For the purpose of investigating the molecular architecture of the terminal, it was not crucial to work with ultra-pure synaptosome preparation (Dunkley et al., 2008). As outlined in the next sections, the contaminations I found in the synaptosome preparations were mainly of mitochondrial and myelin origin. These types of contamination neither biased the determination of the physical characteristics (3.2) nor the protein quantification (3.3, as all proteins investigated are majorly pre-synaptic). However, especially the latter depended entirely on actually knowing *how* pure the fractions were – i.e. how many synaptosomes are present per μg of total protein. To address this question I developed two different assays. The first relied on determining the amount of synaptosome particles in a fluorescence-based assay and the second on identifying the different components per fraction in an ultrastructural assay. The results of these two approaches are outlined in the next paragraphs (for detailed protocols refer to section 2.7) while a comparison of the two assays as well as an evaluation of the results is provided in 3.1.3.

3.1.1 Determining the fraction of synaptosome particles using a fluorescence assay

The first assay relied on determining the amount of synaptosomes from all particles in a synaptosome fraction using fluorescence microscopy. For this purpose, defined amounts of the synaptosome fractions were immobilized on glass cover-slips via centrifugation (spin down) and immunolabeled for different marker proteins: (i) Synaptotagmin 1 as a marker for SVs and ultimately synaptosomes, (ii) Bassoon or PSD-95 as markers for the pre- or the post-synaptic compartment respectively. As a positive control – i.e. a marker which labels all particles – I used TMA-DPH which is a hydrophobic fluorescent probe used to label membranes (Illinger et al., 1989). This allowed me to determine the total number of particles (TMA-DPH labeling) and the fraction of synaptosome particles (defined as Synaptotagmin 1 positive particles). Knowing the amount of starting material which was spun onto the cover-slips as well as the imaging area, it is possible to calculate the absolute amount of synaptosomes in each preparation. Representative images from this assay can be found in Figure 3-2 A. Analyzing the images from seven to eight independent experiments per condition showed that all synaptosome preparations (S1-4) contained between 51 and 54 % of synaptosome particles.

A



B

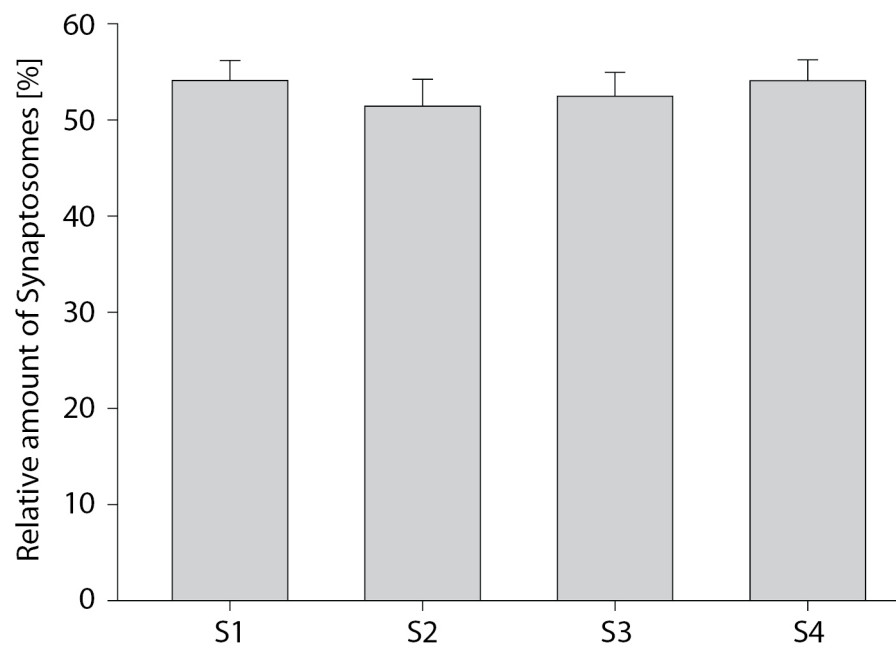


Figure 3-2: Fluorescence spin down assay to determine purity of synaptosome preparations.

(A) Representative images from the fluorescence spin down assay. The immobilized particles are immunolabeled for Bassoon (red) and Synaptotagmin (green). The total pool of particles is labeled with TMA-DPH (blue). Size bar is 2.5 μm .

(B) Quantification of the data obtained in the fluorescence spin down assay. Bars represent the fraction of synaptosome particles in the four different preparations (S1-4). Graph show mean \pm SEM from at least 7 independent experiments.

However, as this assay is critically dependent on how efficient the particles are immobilized (spun down) on the cover-slips it is necessary to determine the efficiency of the spin down. This was done comparing the amount of two prominent pre-synaptic marker proteins – Syntaxin 1 and Synaptobrevin 2 – in the supernatant after spin down (sample) with the input material prior to spin down (control). The results of this control experiment are displayed in Figure 3-3: the average efficiency of the spin down was 98.68 % (mean of 99.63 % for Syntaxin 1 and 97.74% for Synaptobrevin 2) indicating that there was hardly any synaptosomes which did not get immobilized on the cover-slips. Nevertheless, this value was used as a correction factor for determining the amount of synaptosomes per fraction (i.e. values in Table 3-1 are corrected for the loss during centrifugation).

Although the synaptosomes are substantially diluted – and therefore well separated – before being immobilized it is still possible that some particles might have been aggregated into clumps. In this case it would have been difficult to discern them using diffraction limited microscopy, hence aggregation of synaptosomes pose a substantial bias to the quantification of the number of synaptosomes per preparation. To test if this is the case I designed a second assay, which relies on EM to determine the absolute amount of synaptosomes. The results of this assay are outlined in the following section.

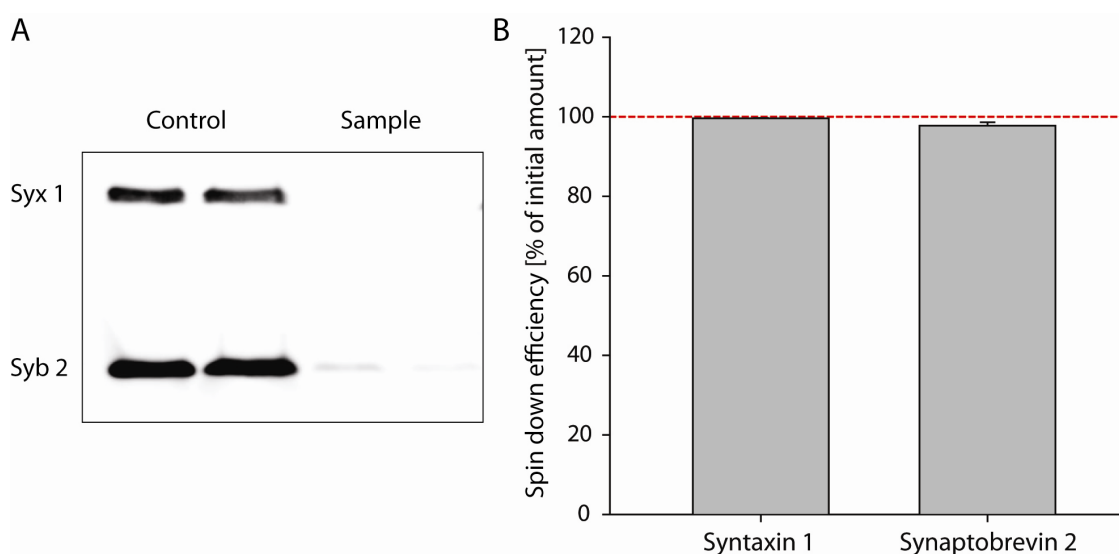


Figure 3-3: Spin down efficiency assay.

(A) Example blot showing the abundance of two pre-synaptic marker proteins – Syntaxin 1 (Syx 1) and Synaptobrevin 2 (Syb 2) – in the supernatant prior to (Control) and after (Sample) centrifugation. As indicated by the blots, there is hardly any protein detected in the supernatant after spin down indicating that most of the synaptosomes are immobilized on the cover-slip.

(B) Graph shows the spin down efficiency for the two marker proteins Syntaxin 1 and Synaptobrevin 2. The dotted red line marks 100% spin down efficiency i.e. that all synaptosomes are immobilized on the cover-slip. Graph shows mean \pm SEM from 8 independent experiments.

3.1.2 Determining amount of synaptosomes using electron micrographs

In order to test the results obtained by the fluorescence spin down assay I investigated electron micrographs of the synaptosome preparations. As described in 2.7.2, all visible particles in the EM images were first manually outlined/ selected and identified. This showed that besides the synaptosomes the majority of the sample was composed of mitochondria, myelin and post-synapses. However, a small amount of objects (~14%) could not be identified as they were either too small or unspecific in appearance.

This data could further be used to control the quantification results obtained previously from the fluorescence spin down assay. Unlike the spin down assay, this assay was not biased by an accumulation of particles into clumps as all objects could be discerned individually in EM. In order to determine the amount of synaptosomes per fraction, the relative volume of each particle group (synaptosome, post-synapses, mitochondria, myelin and unknown) was determined (see Figure 3-4). The fraction obtained for synaptosomes (i.e. the relative volume occupied by synaptosomes in the fraction) could then be used as a control for the results of the spin down assay.

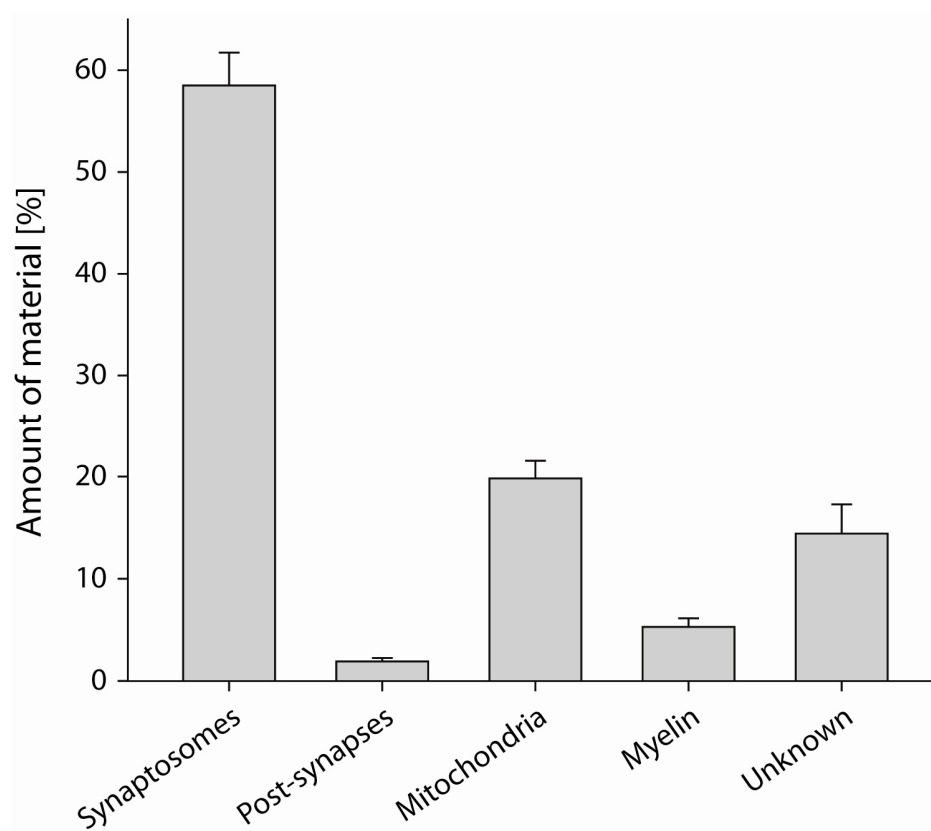


Figure 3-4: EM-based assay to determine composition of synaptosome preparations.

Graph shows the relative composition of the synaptosome preparations. Results are derived by analyzing thin sectioned electron micrographs. Graph shows mean \pm SEM of the four different synaptosome preparations.

3.1.3 The purity of the synaptosome preparations – comparing the two assays

As outlined in the previous two sections, two different assays were employed to determine the amount of synaptosomes per preparation. The first assay depended on fluorescence microscopy to identify the amount of synaptosome particles from all particles. Results obtained with this assay were then validated using an EM-based assay in which the relative volume occupied by the synaptosomes in the preparation was analyzed. In Figure 3-5, the results of these two assays are compared with each other: the bars represent the relative amount of synaptosomes determined with the fluorescence (black) and the EM-based (grey) assay.

In summary, both assays delivered strikingly similar results concerning the amount of synaptosomes per preparation. In addition, the EM-based assay allowed characterization of other components of the synaptosome fractions. The results (i.e. absolute numbers of

synaptosomes) of the assays are summarized in Table 3-2. These values are crucial for further quantitative experiments using the synaptosomes and will be used later to determine absolute protein numbers per pre-synaptic terminal (see 3.3).

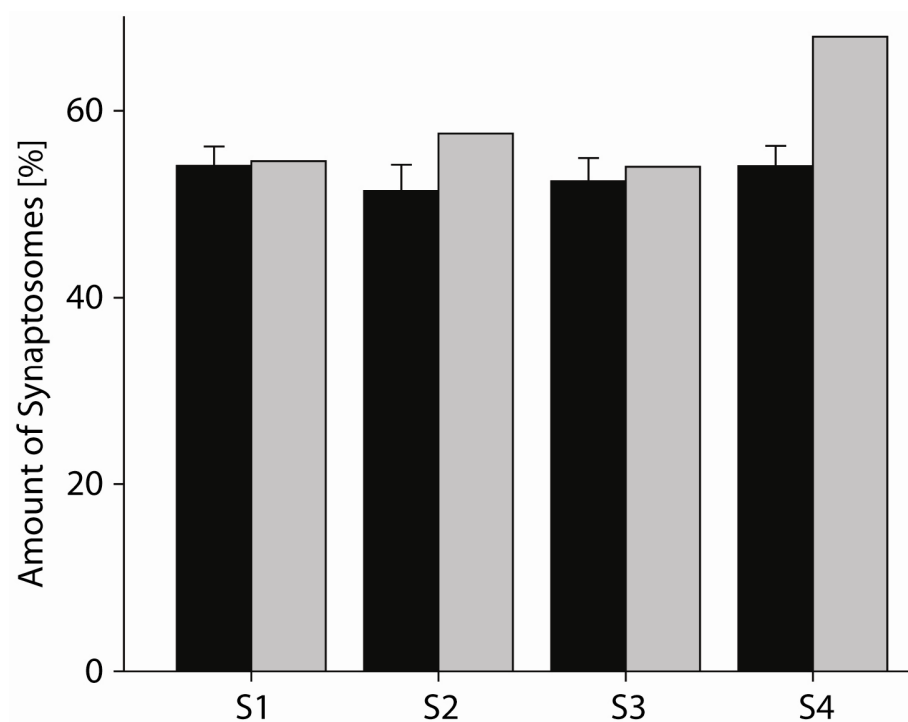


Figure 3-5: EM-based assay confirms findings of the fluorescence spin down assay.

Graph shows the fraction of synaptosomes per preparation (S1-4) as determined with the fluorescence spin down assay (black bars) compared to the EM-based assay (grey bars). For the fluorescence assay, bars represent mean \pm SEM of at least 7 independent experiments. The bars of the EM assay (grey) do not have error bars as they are derived from several images of only a single experiment each (i.e. the respective preparation).

Table 3-1: Absolute numbers of synaptosomes per nanogram of preparation.

Preparation	Synaptosomes per ng
S 1	8532
S 2	10602
S 3	10518
S 4	10096

3.2 Physical parameters of the synaptosomes

In order to draw a complete picture of the average brain synapse, it is important to investigate the physical properties – such as size and organelle composition – of the synaptosomes (Schikorski and Stevens, 1997). To do so, consecutive electron micrographs of the same synaptosome were captured in different ultrathin sections (serial sectioning). These sections were oriented accordingly, aligned and merged into a 3D model of the respective synaptosome (as described in 2.8). Figure 3-5 shows several consecutive images of the same synaptosome (A) and the respective 3D reconstruction (B). The synaptosome displayed here was also used as a template for the graphical model of the average brain synapse (see 3.5).

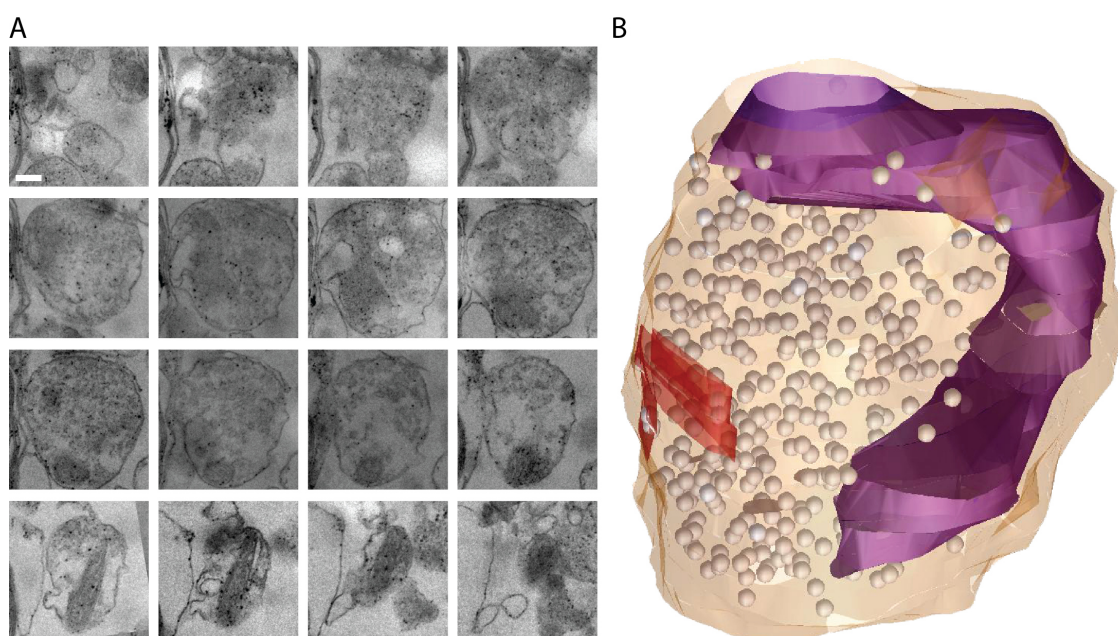


Figure 3-6: 3D reconstruction of a synaptosome.

(A) Consecutive electron micrographs obtained from the same synaptosome. Size bar is 300 nm.
(B) 3D reconstruction of the synaptosome depicted in (A). Images were oriented and aligned respectively in order to generate the reconstruction of the synaptosome.

In total 66 synaptosomes from the four different preparations were reconstructed (between 11 and 22 reconstructions each) which are all depicted in Figure 3-6. The physical information obtained from the reconstructions (size, shape, organelle composition) was used to determine the physical parameters of the average synaptosome (see Table 3-1). As expected, the synaptosomes displayed a rather broad range of SV numbers ranging from as few as 79 up to as many as 1944 SVs per synapse (Figure 3-8 A). Also the size (volume) of the reconstructed

synaptosomes varied between 0.2 and 6.1 μm^3 (Figure 3-8 B). Both these parameters were not surprising, as different studies have reported similar results concerning the heterogeneity of synapse size and vesicle number (Schikorski and Stevens, 1997; Welzel et al., 2011). Interestingly, I found a linear relationship between the size of the synapse and the amount of vesicles – or in other words: the bigger the synapse the more SVs (Figure 3-8 C). In addition, I also found a linear relationship between size of the synapse (surface area) and size of the AZ (Figure 3-8 D). These findings point to the conclusion that function and size of a synapse are going hand in hand in the adult brain: with increasing size, also the availability of the major functional units of a synapse – SVs and AZs – are increasing in numbers and size respectively.

Table 3-2: Physical parameters of the synaptosomes.

Parameter	Value
Volume	$1.1 \pm 0.1 \mu\text{m}^3$
Surface	$4.4 \pm 0.3 \mu\text{m}^2$
Number of Vesicles	383.7 ± 37.9
Volume occupied by vesicles	$0.015 \pm 0.001 \mu\text{m}^3$
Number of AZs per synapse	0.71 ± 0.09
Average size of AZ	$0.21 \pm 0.04 \mu\text{m}^2$
Number of mitochondria per synapse	0.65 ± 0.08
Average size of mitochondria	$0.18 \pm 0.04 \mu\text{m}^3$

A

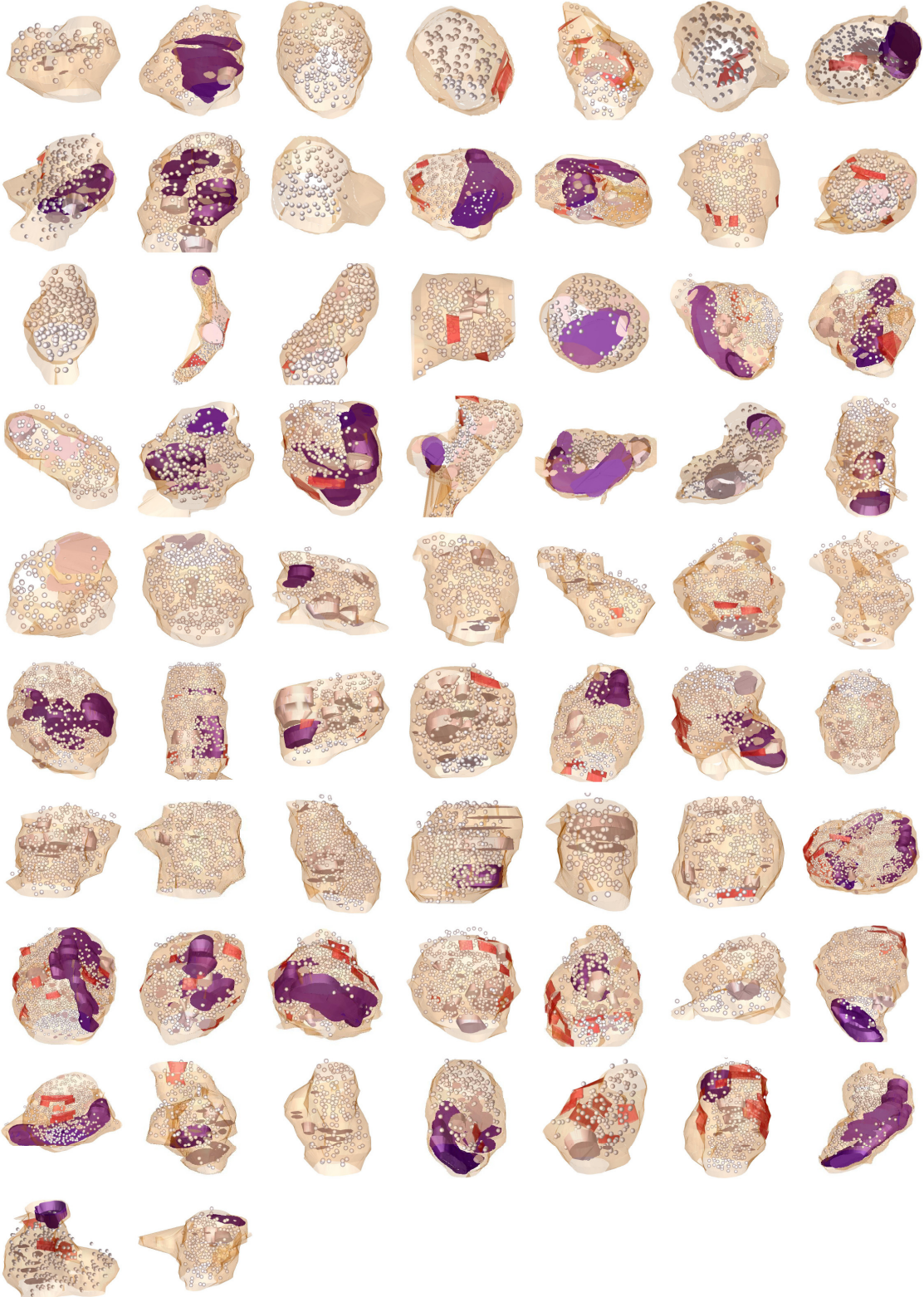
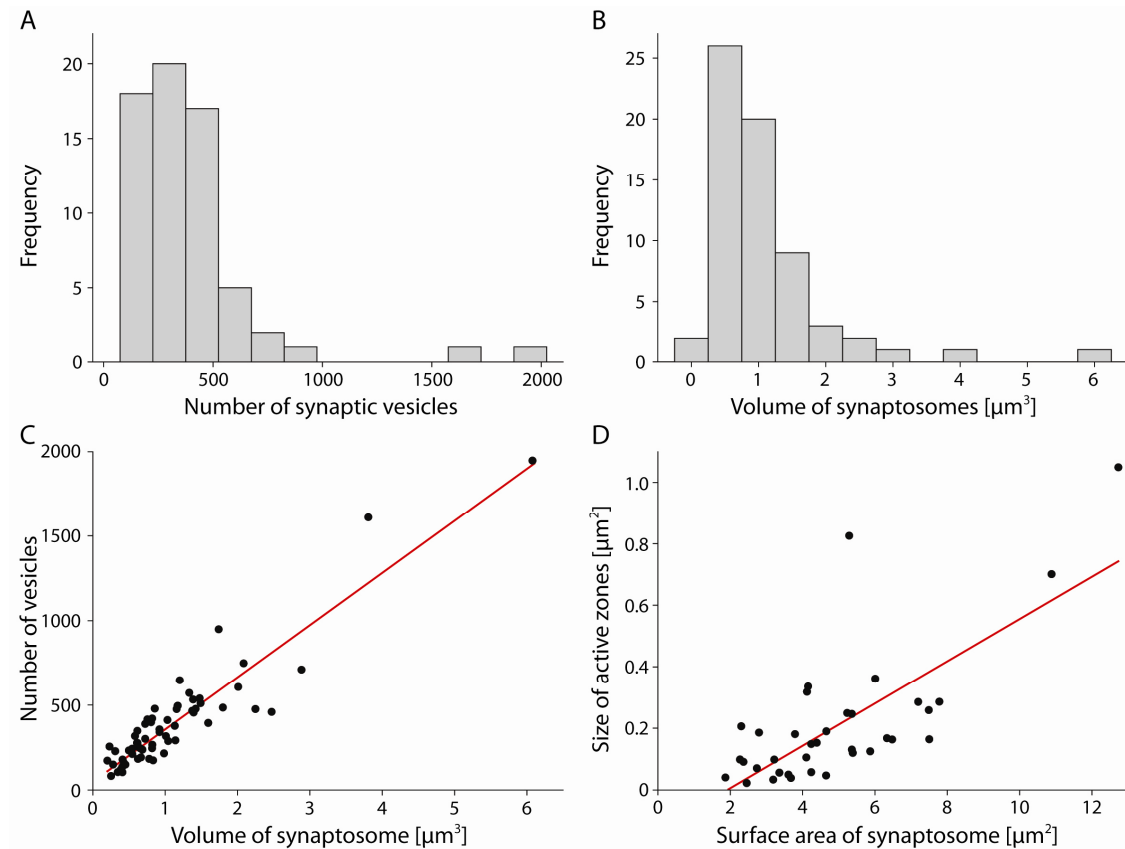


Figure 3-7: All 3D reconstructions of synaptosomes.

(A) A total of 65 synaptosomes (11 to 22 for each preparation) were reconstructed from electron micrographs. The morphological data derived from these reconstructions was used to determine the physical characteristics of the average synaptosome. The plasma-membrane is depicted in beige while mitochondria are purple, SVs white and AZs red. Images are not scaled identically but to maximum size available due to space limitations. Size of a vesicle (i.e. 42 nm) can be used as a reference.

**Figure 3-8: Evaluation of certain physical parameters of the synaptosomes.**

(A) Histogram showing the distribution of SV numbers in the reconstructed synaptosomes.
 (B) Histogram showing the distribution of different synaptosome sizes (by volume).
 (C) Relationship of the number of vesicles and the volume of the synaptosome.
 (D) Relationship between size of the AZ and the surface area of the synaptosome. Both (C) and (D) display a linear dependence of the respective parameters (red line).

3.3 Absolute quantification of pre-synaptic proteins

Characterizing the synaptosome preparations in regard to their composition with a particular focus on determining the absolute number of synaptosomes (3.1) allowed me to further quantify the absolute protein composition of a pre-synaptic terminal. To do so, I made

use of quantitative immunoblotting (similar to Takamori et al., 2006) as outlined in the following paragraph using SNAP 25 as an example:

Defined amounts of synaptosomes were separated (SDS-PAGE with 10% TRIS-Tricin/Schägger gels, (Schagger, 2006; Schagger and von Jagow, 1987) and blotted in parallel with defined amounts of purified SNAP 25. The protein blots were further immunolabeled for SNAP 25 (for a detailed protocol see 2.9). Handling the synaptosomes and the purified SNAP 25 in parallel (i.e. run on the same gel/ blotted on the same membrane) enabled me to directly compare the amount of SNAP 25 detected in the synaptosomes with defined amounts of purified SNAP 25 (see Figure 3-8 A). I then used different amounts of purified SNAP 25 covering a certain range of protein amounts to generate a regression curve. The shape of such a regression curves predominantly depends on the affinity of the primary antibody (used to detect the protein of interest) to its target. However, all such regression curves have a section in which the signal (from immunolabeling) is linearly dependent on the amount of purified protein (loaded on the gel). Adjusting the amount of purified SNAP 25 to cover this section and scaling the amount of synaptosomes to be within this section made it possible to use a linear regression line for determining the amount of SNAP 25 molecules per synaptosomes. The readout of this assay was basically amount (in ng) of SNAP 25 per amount of synaptosomes (in μg). Since the absolute number of synaptosomes per μg of preparation was determined in 3.1 it is now possible to determine the number of SNAP 25 molecules per synaptosome. For a detailed description how the absolute copy numbers were calculated refer to section 3.3.2.

As mentioned previously, the shape of the regression curve depends on the affinity of the particular primary antibody which is used to detect the protein of interest. Therefore, these curves are a unique feature of the protein-antibody interaction and have to be determined individually for every protein which ought to be quantified.

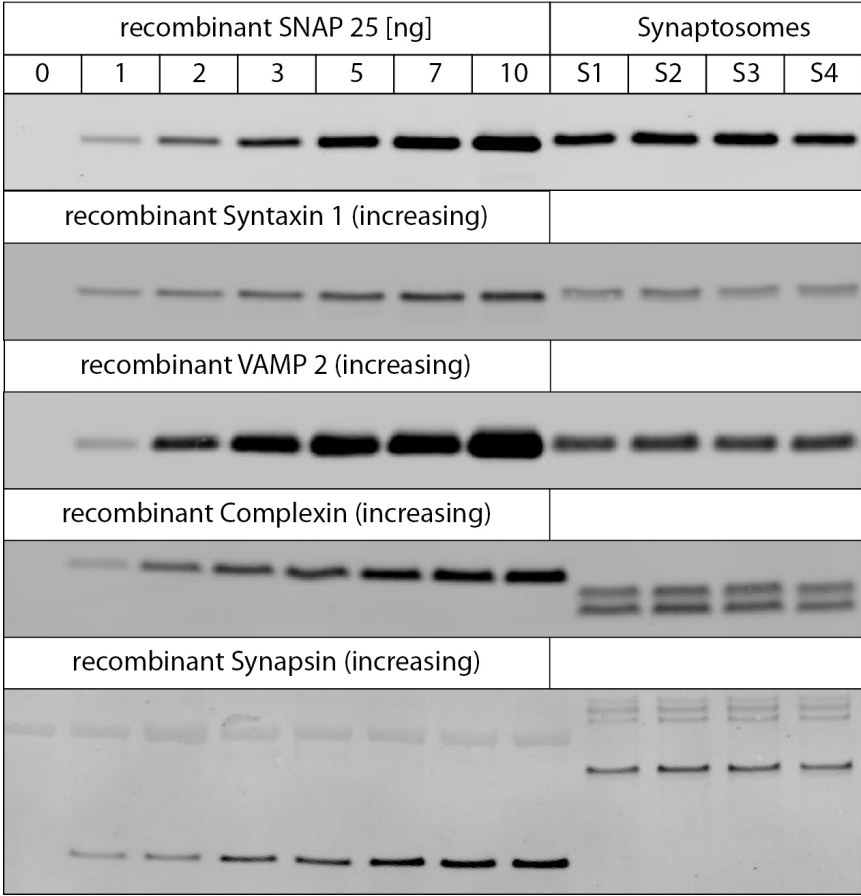
For certain proteins it was possible to quantify more than one isoform with the same purified protein. This worked in cases where the primary antibody, which was used to detect the protein, was raised against a peptide that is conserved in the respective isoforms (so called pan-antibodies). Two examples where this is the case are presented in Figure 3-8 A: both Complexin and Synapsin have multiple isoforms (see bands at different molecular weights) which can be detected equally well with the same antibody. In these cases the regression line derived from the purified protein could be used to quantify all other detectable isoforms.

Importantly only proteins which are known to be predominantly pre-synaptic were quantified in this study. This ensures that contaminants in the synaptosome preparation (see 3.1.2) did not bias the absolute quantification. Using the above outlined approach I determined the absolute copy number of 59 different pre-synaptic proteins. Further, I determined the relative amount of five marker proteins for reference: Actin and Tubulin as the major components of the cytoskeleton, VDAC as a prominent mitochondrial protein, PSD-95 as a post-synaptic protein and myelin basic protein (MBP) as a major protein component of the myelin sheets. All absolute and relative quantification results can be found in Table 3-2.

So far only few studies have addressed quantifying pre-synaptic proteins. One study from Reinhard Jahn's group (Walch-Solimena et al., 1995) investigated the relative abundance of SNARE molecules in synaptosomes and actually found values for SNAP 25 and VAMP 2 which are remarkably similar to my findings. Another study from the same lab used a similar approach to the one followed in this study to examine the molecular anatomy of a trafficking organelle (Takamori et al., 2006). Besides determining the physical parameters and the lipid composition of trafficking vesicles, they also quantified 15 SV proteins. Many of these proteins were also addressed in this study and I found similar amounts for several of the trans-membrane proteins (e.g. CSP, Rab3a, VAMP 2 and vGlut1/2), when taking the number of vesicles in an average synapse into consideration. However, I would like to point out that such a comparison has to be done with certain caution, since it is quite likely that these proteins are not solely present on SVs.

The limiting factors for the amount of different proteins which could be quantified by the assay are the availability of a purified version of the particular protein as well as the existence of an antibody which is able to detect the purified and the endogenous protein equally well. Unfortunately this was not the case for all proteins I was initially interested in, which is why the quantification results are limited to the 59 proteins listed in Table 3-2.

A



B

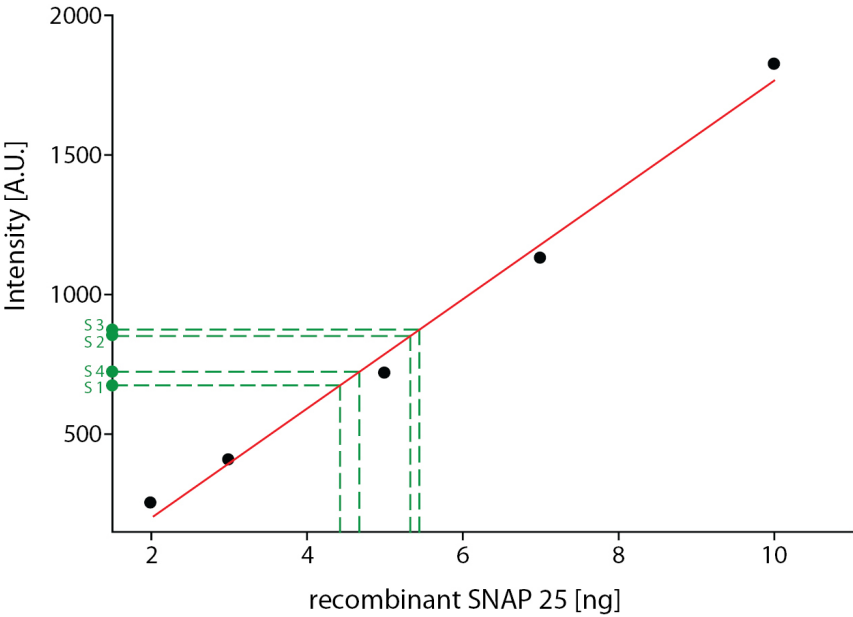


Figure 3-9: Quantitative analysis of the synaptosome preparations.

(A) Example immunoblots comparing the four synaptosome preparations (S1-4) with an increasing amount of the protein of interest in a purified form (first seven lanes). The amount of synaptosomes was chosen to lie within the range covered by the purified protein. The synaptosomes labeled for Complexin and Synapsin display two and four bands respectively. These bands represent different isoforms which are also detected by the primary antibody that was used for labeling and can therefore be quantified as well.

(B) Graph shows the data points (black dots) derived from the SNAP 25 blot in (A). The red line represents the linear regression line which can be used to determine the absolute amount of protein in the synaptosome preparation (indicated by the dotted green lines).

3.3.1 Control for loss of soluble proteins during synaptosome purification

In the course of the synaptosome purification the pre-synaptic terminals are ripped off of their respective neuronal process. In principle, the synaptosomes are expected to reseal afterwards and the EM data indeed shows that this is the case for many synaptosomes (see for instance reconstructions in Figure 3-7). Nevertheless, this process holds the potential of losing proteins unrecoverable from the synapse. Independent of the resealing of the synaptosomes there is a certain time span in which the synaptosomes are open and could in principle lose proteins. Although this should not affect trans-membrane proteins it could be a significant bias for soluble proteins. This is a difficult question to address and there is – at least to my knowledge – no biochemical approach that would allow estimating the loss of proteins from a synaptosome during the purification process. Therefore, a fluorescence-based assay was designed in which I compared the protein amounts of the initial situation (cortical brain slice) with the final preparation (synaptosome).

Both synaptosomes and cortical brain slices were immunolabeled in parallel for the soluble protein of interest as well as for the vesicle marker Synaptophysin, which served as a reference (see Figure 3-10 B for example images). Since Synaptophysin is a trans-membrane protein that is not expected to diffuse out of the synapse during the purification I assumed the amounts of Synaptophysin in both cortical synapses (slice and synaptosome) to be identical. This enabled me to use the synaptic Synaptophysin signal as a reference and to put the synaptic signal from the soluble protein of interest in relation to it (both signals as fluorescence in AU). The ratio of the signals from the protein of interest over Synaptophysin was determined for both preparations. Comparing the two ratios with each other i.e. calculating the ratio of ratios from the slices over the synaptosomes yielded the correction factor for this particular protein (see Figure 3-10 A). Interestingly, I found that only seven proteins (AP180, Clathrin light chain, CALM, Epsin 1, PIPK 1 γ , Rab3a and Rab7a) were lost in significant amounts from the

synaptosomes during purification (see Figure 3-10 C). The correction factors calculated for these proteins can be found in Table 3-3 and were further used to determine the absolute amount of protein per pre-synaptic terminal (see 3.3.2). It is important to mention that for these experiments imaging of the sample pairs (synaptosomes and slice with the same staining) were performed in parallel under the same imaging conditions (illumination and detection parameters).

Finding only seven proteins which significantly diffused out of the synapses during the synaptosome purification suggests that (i) either the fractionation is too fast to allow diffusion of many soluble proteins or (ii) that the synapse has an intrinsic mechanism which prevents the proteins from disusing out of it. The latter idea is supported by recent findings which show that only a small fraction of vesicles is actually needed to maintain synaptic function (Denker et al., 2011a; Marra et al., 2012) while the rest of the vesicles serve as a molecular buffer which retains proteins within the pre-synaptic terminal (Denker et al., 2011b).

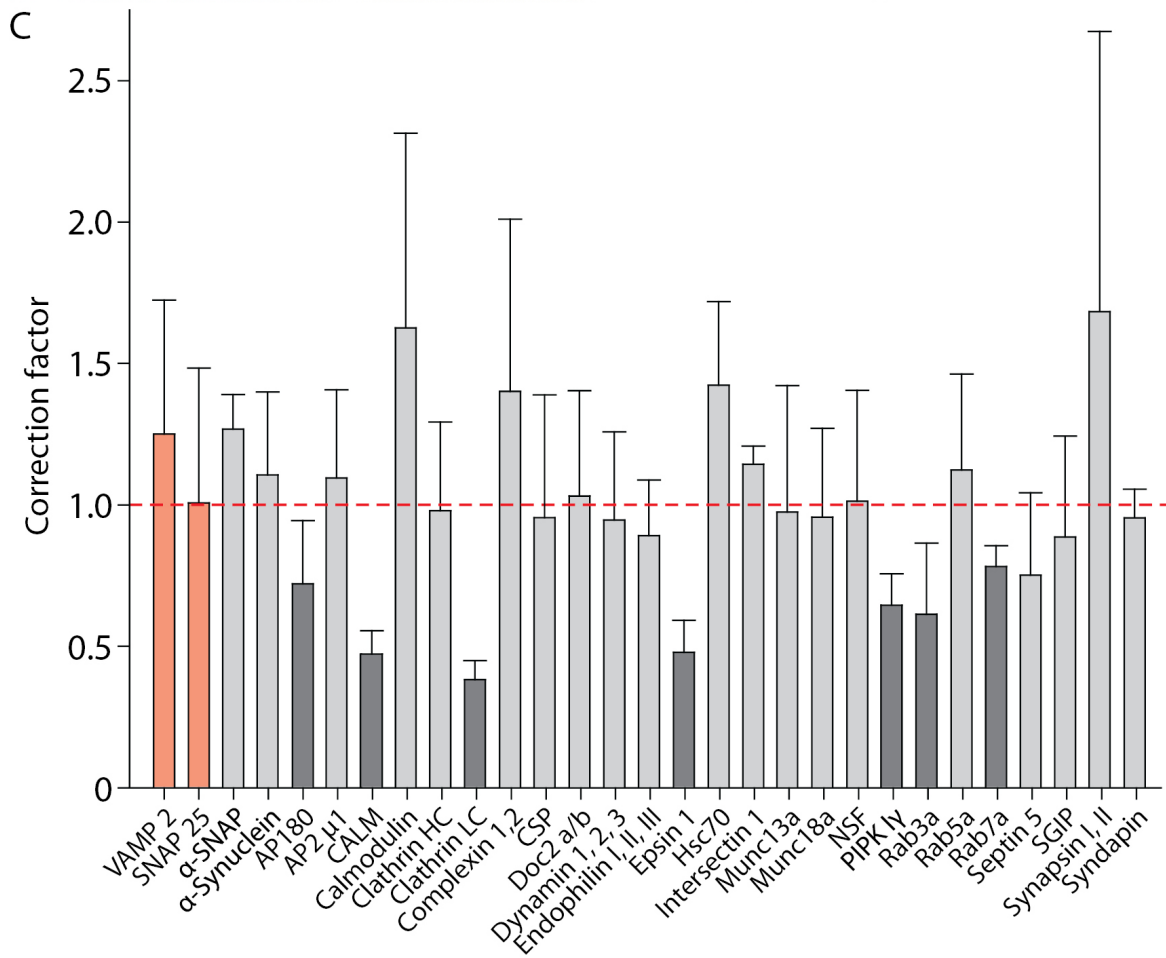
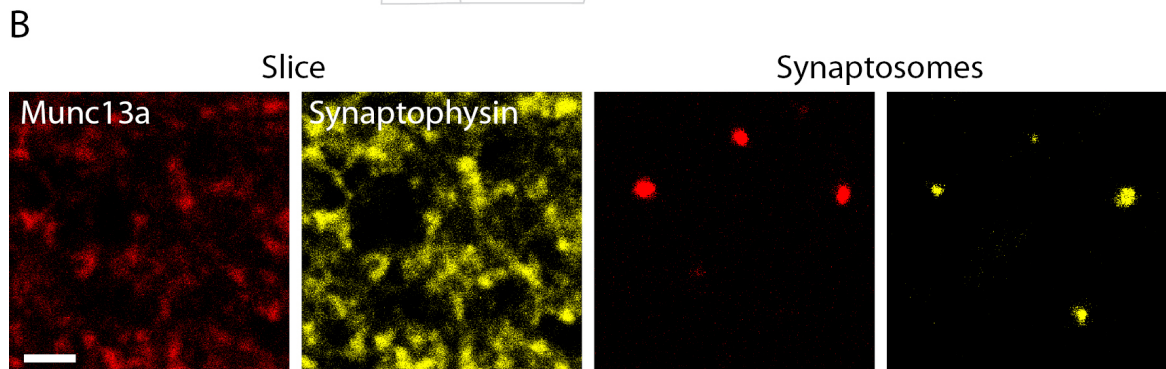
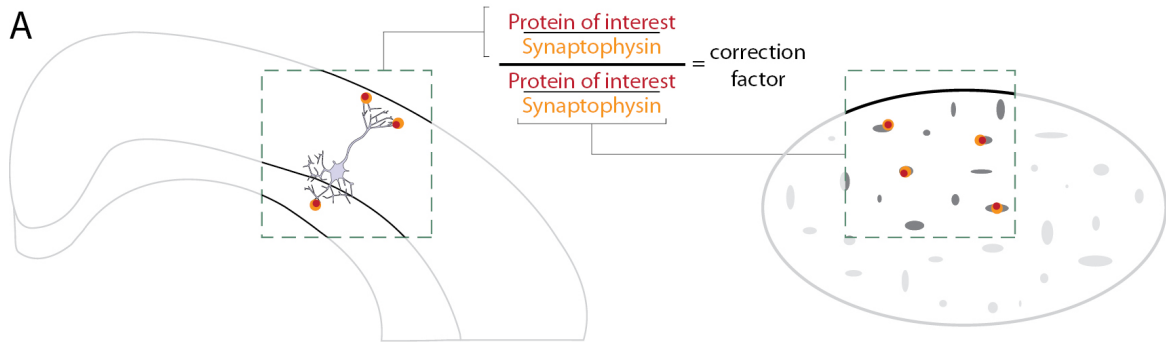


Figure 3-10: Control for loss of soluble proteins during synaptosome purification.

(A) Schematic of the experiment to determine a protein specific correction factor for the potential loss of soluble proteins during synaptosome preparation. Cortical brain slices and synaptosomes were immunostained in parallel for the soluble protein of interest and Synaptophysin. For both preparations the synaptic signal of the soluble protein of interest was divided by the signal obtained from synaptic Synaptophysin (both fluorescence in AU). The two ratios were then used to determine the correction factor for this particular soluble protein by dividing the ratio from the slices by the ratio from the synaptosomes.

(B) Representative images from cortical brain slices (left panel) and synaptosomes (right panel) immunostained for Munc13a (upper row, red) as a soluble and Synaptophysin (lower row, yellow) as reference protein. Size bar is 2 μm

(C) Bar graph displaying the correction factors determined for the different soluble proteins (procedure outlined in (A)). The first two proteins, VAMP 2 and SNAP 25 (pale red bars), are trans-membrane or membrane anchored proteins respectively and served as a control. The dashed red line indicates a correction factor of 1 – i.e. no loss of protein during synaptosome purification. In total, only very few proteins (dark grey bars) are lost from the synaptosomes in significant amounts. Bars represent mean \pm SEM of 2 to 3 independent experiments.

Table 3-3: Correction factors for potential loss of soluble proteins.

Protein	Correction factor
AP180	1.39
CALM	2.12
Clathrin light chain	2.62
Epsin 1	2.09
PIP K I γ	1.55
Rab3a	1.63
Rab7a	1.28

3.3.2 Calculating absolute protein copy numbers per synapse

The experiments outlined in the sections above mostly aimed at determining the amount of a certain protein per pre-synaptic terminal (in grams). In this section I will describe how all these information were used to calculate the absolute number of proteins per synaptosome, again using SNAP 25 as an example.

As described in 3.3, the relative amount of SNAP 25 could be determined by comparing the amount of SNAP 25 in a defined amount of synaptosomes with a protein standard (i.e. purified SNAP 25).

To calculate the number of SNAP 25 molecules per μg of synaptosomes, I needed to know (i) the amount of SNAP 25 in a μg of synaptosomes and (ii) the weight of a single SNAP 25 molecule. While the first was determined in 3.3 using quantitative immunoblots the second could be calculated dividing the molecular weight of SNAP 25 (23315 Da, weight of 1 mol of SNAP 25 in grams) by Avogadro's number (6.023×10^{23} , number of molecules per mol). The number of molecules per μg of synaptosomes was then obtained by multiplying (i) with (ii). In order to obtain the absolute copy number of SNAP 25 per synaptosome, the number of SNAP 25 molecules per amount (in grams) of synaptosomes had to be divided by the previously determined (see 3.1) number of synaptosomes per μg of preparation. A graphical outline of the above described calculations is displayed in Figure 3-11. To obtain the final results I also needed to take the correction factors for the potential loss of soluble proteins during purification into consideration (see 3.3.1). Where applicable the calculated copy numbers were multiplied with the correction factors to obtain the real number (see Table 3-3). A graph illustrating the relative abundances of the proteins is depicted in Figure 3-12 (see also Table 3-4).

Since the average volume of the synaptosomes is also known (from 3.2) I was able to calculate the synaptic molar concentration (molarity) of every protein we quantified (moles of SNAP 25 per synaptosome divided by the average volume of a synaptosome, $1.1 \mu\text{m}^3$). All quantification results are summarized in Table 3-4. For some of the proteins certain correction factors need to be applied due to their differential distribution within the brain regions that were investigated. These proteins are marked by an asterisk (*) and the corrected estimates are discussed and presented in section 4.2.

In addition to the proteins which were known to be predominantly pre-synaptic I also determined the relative amounts of several other proteins as references. However, for these proteins only relative amounts could directly be calculated since they are not predominantly pre-synaptic. Besides the two major components of the cellular cytoskeleton, Actin and Tubulin, I also quantified VDAC, PSD 95 and Myelin Basic Protein which are known to be very abundant in Mitochondria, post-synaptic densities and Myelin respectively.

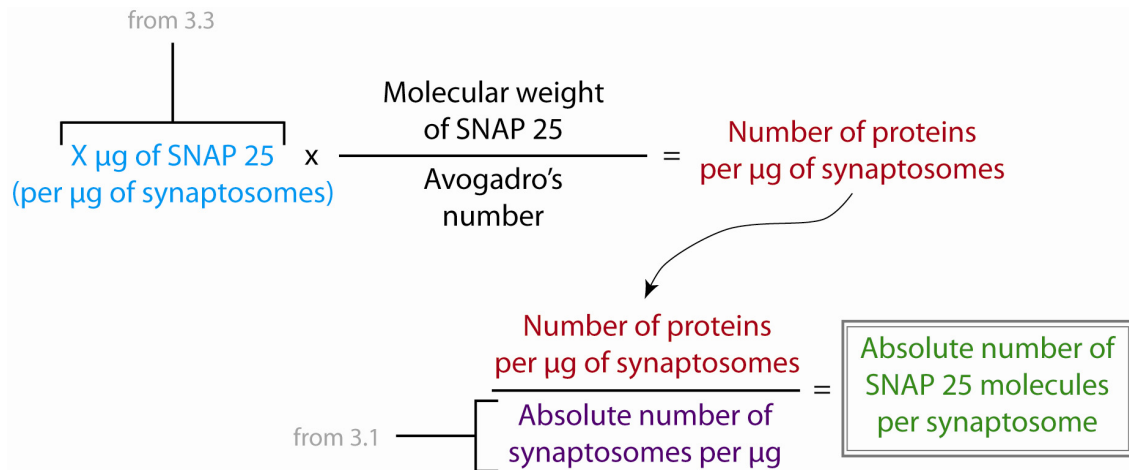


Figure 3-11: Schematic for calculating absolute protein numbers.

Using the example of SNAP 25 this schematic outlines the calculations done in order to obtain the absolute copy numbers of proteins per synaptosomes.

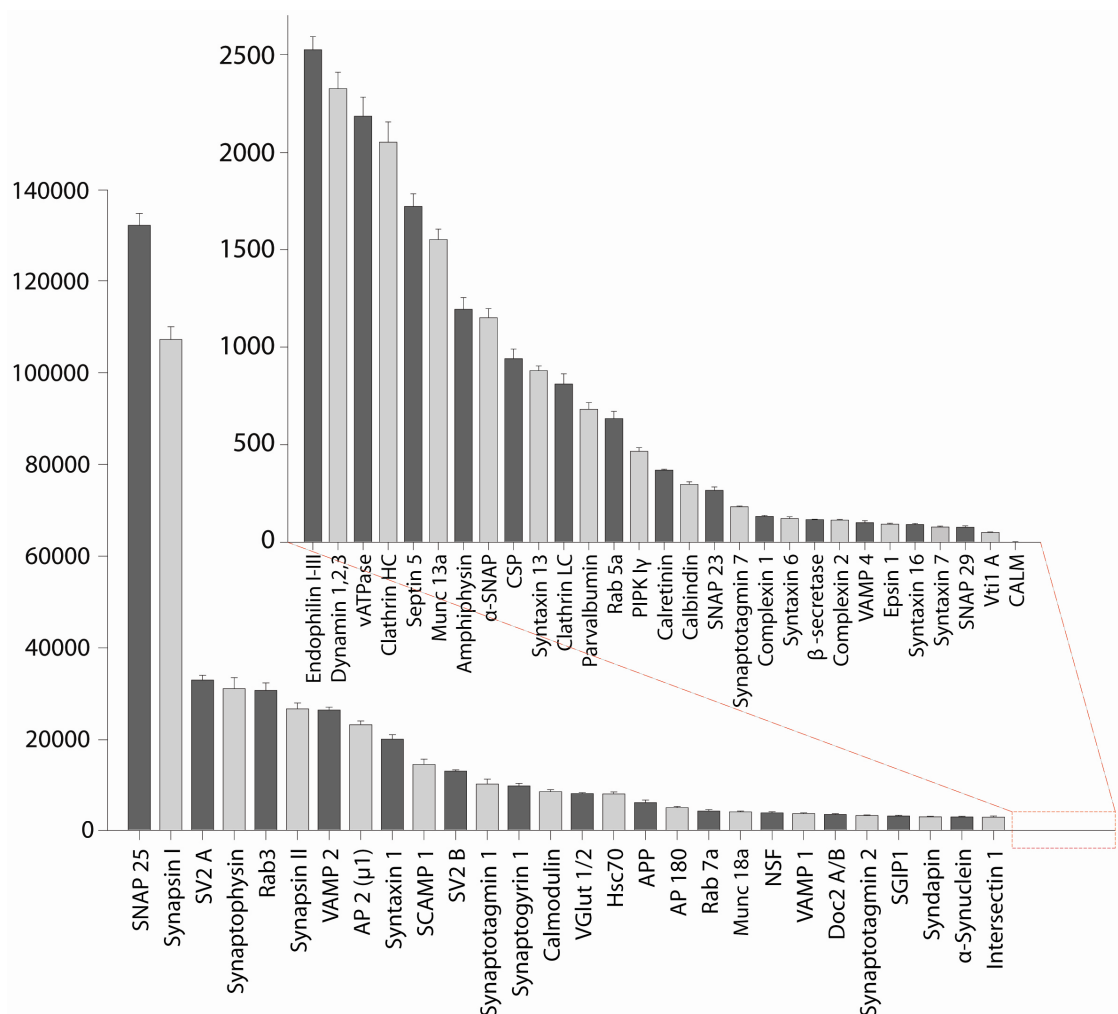


Figure 3-12: Absolute protein numbers.

The graph represents the absolute protein numbers calculated for the different proteins as outlined in section 3.3. The bars represent mean \pm SEM of at least 4 independent experiments. For a detailed list with all protein numbers refer to table 3-4.

Table 3-4: Absolute protein numbers per synaptosome

Protein	Percent of total	Molecules per synapse	Molarity [μM]
α -SNAP	0.06	1150.7 \pm 46.6	1.74
α -Synuclein	0.08	3167.8 \pm 167.7	4.78
Amphiphysin	0.20	1194.2 \pm 60.0	1.80
AP180	0.73	5182.0 \pm 288.0	7.82
AP2 μ 1	2.88	23247.0 \pm 819.9	35.09
APP	0.61	6283.6 \pm 584.5	9.48
β -secretase	0.01	115.8 \pm 2.8	0.17
Calbindin*	0.01	296.9 \pm 13.2	0.45
CALM	0.0002	2.7 \pm 0.2	4.04*10 ⁻³
Calmodulin	0.24	8659.9 \pm 445.5	13.07
Calretinin*	0.02	369.2 \pm 5.5	0.56
Clathrin heavy chain	0.14	2053.5 \pm 103.3	3.10
Clathrin light chain	0.03	810.6 \pm 52.8	1.22
Complexin 1	0.004	132.4 \pm 5.7	0.20
Complexin 2	0.003	113.6 \pm 3.2	0.17
CSP	0.07	941.2 \pm 48.9	1.42
Doc2 a/b	0.34	3696.5 \pm 164.2	5.58
Dynamin 1, 2, 3	0.37	2326.4 \pm 83.9	3.51
Endophilin I, II, III	0.28	2524.4 \pm 67.3	3.81
Epsin 1	0.006	92.9 \pm 4.3	0.14
Hsc70	0.99	8210.1 \pm 404.5	12.39
Intersectin1	0.26	3096.5 \pm 277.6	4.67
Munc13a	0.19	1551.3 \pm 53.2	2.34
Munc18a	0.47	4253.4 \pm 207.1	6.42
NSF	0.55	4064.7 \pm 213.0	6.14
Parvalbumin*	0.01	681.1 \pm 34.3	1.03

PIPK I γ	0.01	465.7 \pm 18.9	0.70
Rab3	1.55	30735.7 \pm 1624.3	46.39
Rab5a	0.02	633.6 \pm 37.3	0.96
Rab7a	0.19	4457.2 \pm 319.8	6.73
SCAMP 1	1.50	14595.0 \pm 1155.3	22.03
Septin 5	0.13	1726.2 \pm 64.4	2.61
SGIP1 α	0.29	3382.2 \pm 158.7	5.11
SNAP 23	0.01	265.6 \pm 17.8	0.40
SNAP 25	5.08	132090.0 \pm 2581.6	199.37
SNAP 29	0.007	77.5 \pm 6.5	0.12
SV2 A	5.63	33006.0 \pm 1034.6	49.82
SV2 B	2.25	13160.0 \pm 256.5	19.86
Synapsin Ia	2.10	34656.0 \pm 2190.6	52.31
Synapsin Ib	4.38	72566.0 \pm 599.7	109.53
Synapsin IIa	0.29	4727.7 \pm 45.3	7.14
Synapsin IIb	1.33	22005.0 \pm 1220.3	33.21
Synaptogyrin 1	0.76	9926.5 \pm 575.7	14.98
Synaptophysin	3.06	31102.0 \pm 2411.0	46.94
Synaptotagmin 1	0.80	10332.0 \pm 1079.2	15.60
Synaptotagmin 2	0.21	3456.8 \pm 132.2	5.22
Synaptotagmin 7	0.01	182.6 \pm 3.5	0.28
Syndapin 1	0.39	3201.0 \pm 131.3	4.83
Syntaxin 1	1.09	20096 \pm 999.4	30.33
Syntaxin 6	0.006	121.7 \pm 9.0	0.18
Syntaxin 7	0.004	78.6 \pm 4.5	0.12
Syntaxin 13	0.05	879.1 \pm 24.3	1.33
Syntaxin 16	0.006	91.3 \pm 5.7	0.14
VAMP1	0.08	3884.3 \pm 182.0	5.86

VAMP2	0.55	26448.0 ± 661.6	39.92
VAMP4	0.003	100.6 ± 10.0	0.15
vATPase	0.44	2186.2 ± 97.1	3.30
vGlut 1/2	1.20	8254.1 ± 224.3	12.46
Vti1 A	0.002	50.6 ± 2.5	0.08
Actin	2.13		
Myelin Basic Protein	0.75		
PSD 95	0.92		
Tubulin	1.53		
VDAC 1	3.67		
Sum	50.96		

As indicated in Table 3-4 the proteins that were quantified added up to approximately 51% of the total protein of the synaptosome preparation. Regarding that all preparations contained a good amount of non-synaptosome material, this number is quite impressive. The sum of all pre-synaptic proteins that were quantified (total sum minus reference proteins) is approximately 42% of the entire synaptosome preparation. In comparison to that the entire amount of proteins which could potentially be synaptic can be estimated from the EM data (see 3.2): adding the extra-synaptic mitochondria (approximately 20%), post-synapses (approximately 1.9%), myelin (approximately 5.3%), unknown material (approximately 14.4%) and intra-synaptic mitochondria (approximately 8.7%, estimated from electron micrographs in 3.2) results in 49.7% of material in the preparation which could in principle be pre-synaptic. Dividing the amount of quantified synaptic material (42%) by the total amount of material that could be synaptic (49.7%) reveals that actually 84.5% of the synaptic material in the synaptosome preparation was quantified.

The absolute copy numbers presented above were further tested by a quantitative mass spectrometry technique termed intensity-based absolute quantifications (iBAQ, Schwanhauser et al., 2011). The experiments showed no major differences for almost all proteins investigated and can yield further estimates for proteins which were not addressed with the quantitative

immunoblots. As this data was acquired by our collaborators Prof. Dr. Henning Urlaub and Sunit Mandad from the Max-Planck Institute for biophysical chemistry it is not included in this thesis.

3.4 Investigating the pre-synaptic protein organization

In order to obtain a concise picture of the pre-synaptic architecture I did not only quantify the absolute amounts of 59 pre-synaptic proteins but was also interested in their organization within the terminal. To investigate the pre-synaptic protein organization I employed super resolution STED microscopy (40 – 50 nm resolution) to analyze the synaptic protein organization in two prominent model systems: (a) primary hippocampal cultures (see 3.4.1) and (b) NMJs of the *levator auris longus* muscle in mice (see 3.4.2).

Admittedly, the most obvious choice for investigating the pre-synaptic protein organization would have been the purified synaptosomes which were used to quantify the proteins. Unfortunately, this was not possible due to several technical and biological limitations:

(1) In the course of the purification the synaptic terminals will face rather unusual biological conditions. It has to be assumed that the ionic environment of the synapse will change drastically during homogenization. The changes in intracellular ion concentrations (i.e. elevated calcium levels etc.) in turn trigger biological processes, which could influence the pre-synaptic protein organization.

(2) Synaptosomes are fragile in terms of structural stability. Subjecting them to the rather harsh conditions (continuous washing steps, permeabilization etc.) of an immunolabeling would most likely alter their synaptic ultra-structure and/or lead to further loss of pre-synaptic proteins and could therefore bias protein distribution in the terminal.

(3) It is technically impossible to perform immunostainings for all proteins on the synaptosomes directly after the preparation, as these would be too many experiments to handle in parallel. Hence, I would have had to use stored synaptosomes – i.e. synaptosomes which had at least been thawed and refrozen once. Multiple cycles of freezing and thawing are commonly used to generate cell ghosts (empty plasma membranes, Urushihara and Yanagisawa, 1987). Therefore, I could not afford using the thawed synaptosomes for investigating protein organization as any round of freezing and thawing is expected to change the composition of the synaptosomes. This was not an issue for the immunoblots as all samples were denatured prior to separation with the SDS-PAGE.

The two preparations I choose represent good model systems to study general protein organization at mammalian synapses. While the hippocampal cultures are very well characterized central synapses, the NMJs allowed me to investigate protein arrangements at a peripheral synapse. Another advantage of these particular synapses is their relatively large size: conventional confocal imaging provides an axial resolution of approximately 500 nm (Conchello and Lichtman, 2005). Regarding the small size of synapses in hippocampal cultures (approximately 600 nm according to Schikorski and Stevens, 1997) it has to be assumed that in many images, vesicles as well as the plasma-membrane will be recorded in the same focal plane. In contrast to this the mouse NMJ is substantially larger (up to several micrometers, see for example Denker et al., 2011a), thus allowing to image the vesicle cluster separately without the plasma-membrane. The following two sections summarize the results obtained from experiments investigating the pre-synaptic protein organization in these two model systems starting with the hippocampal cultures.

3.4.1 Pre-synaptic protein organization in primary hippocampal neurons

Primary hippocampal neurons (DIV 10 – 20) were fixed and immunostained for the respective protein of interest in parallel to the AZ marker Bassoon and the SV protein Synaptophysin (Willig et al., 2006). Both Bassoon and Synaptophysin were imaged with conventional confocal resolution while the protein of interest was imaged in STED mode providing a lateral resolution of approximately 40 – 50 nm. In the analysis the Bassoon signal was used as an indicator for the location of the AZ and the synaptic distribution of the proteins of interest was determined in respect to this marker. The resulting density distributions represent the average synaptic organization of the respective proteins (Figure 3-13).

Representative images of SNAP 25 as well as the corresponding density distribution can be found in Figure 3-13 A. Images of all other proteins can be found in Appendix 1 while the respective density distributions are displayed in Figure 3-13 B. The density distributions in Figure 3-13 B are all centered to the Bassoon signal (i.e. the AZ), marked by a blue circle.

The fact that the density distributions of the different proteins (see Figure 3-13 B) are rather unique for every single protein is a good indicator that this approach is indeed capable to determine to pre-synaptic organization of the various proteins. Although the localization in this approach is still far from the level of the single protein, it is state-of-the-art super resolution

imaging and allows identifying organizational patterns in which the individual proteins are arranged (Loschberger et al., 2012).

In summary, the density distributions obtained with this assay provide good estimates of the synaptic organization of the proteins of interest. Together with the structural information on the pre-synaptic morphology (see 3.2) and the quantitative information on synaptic protein numbers (see 3.3), this data was used to generate a graphical model of the average pre-synaptic terminal (see 3.5). A thorough discussion of the different protein organizations as well as their numbers (from 3.3) can be found in section 3.5 in combination with a discussion of the density distributions from the NMJs.

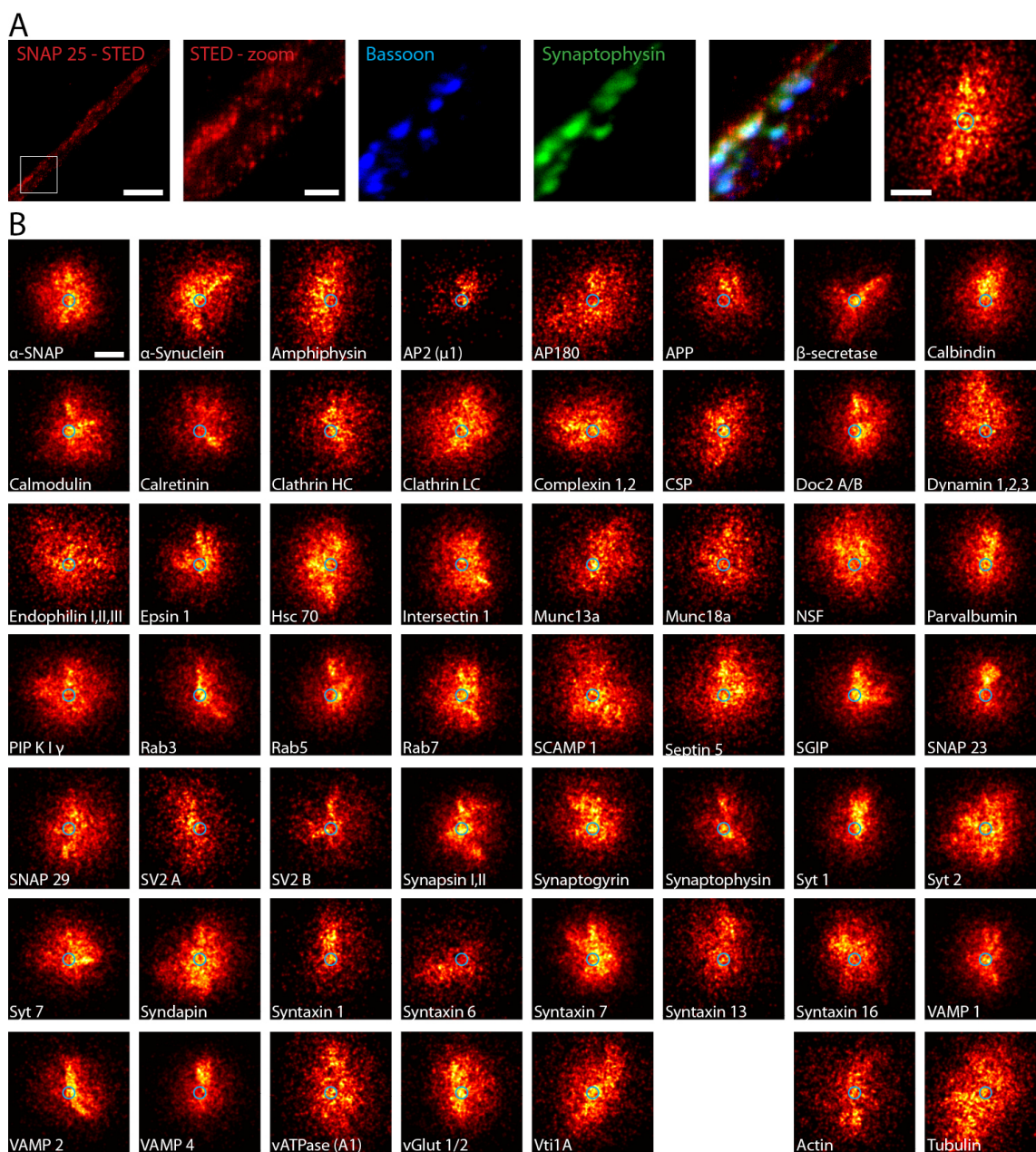


Figure 3-13: Pre-synaptic protein organization in synapses from hippocampal cultures.

(A) Primary hippocampal neurons were immunostained in parallel for a protein of interest (in this case SNAP 25, red), Bassoon (blue) and Synaptophysin (green). Both Bassoon and Synaptophysin were imaged using conventional confocal microscopy while the protein of interest was imaged with super resolution STED microscopy. The dispersion of the SNAP 25 spots in relation to the AZ (Bassoon signal, blue circle in center of the image) was used to generate a density distribution representing the average pre-synaptic SNAP 25 dispersion (last image). Size bars are 5 μm , 1 μm and 250 nm from left to right.

(B) Density distributions for the other proteins investigated. Staining, imaging and analysis was performed as for SNAP 25. Representative images from the different stainings can be found in Appendix 1. Size bars are 250 nm.

3.4.2 Pre-synaptic protein organization in mouse NMJs

The mouse *levator auris longus* was used for investigating the protein organization at a peripheral synapse. Each muscle was freshly dissected prior to every experiment (Angaut-Petit et al., 1987). After fixation the muscles were immunostained for the protein of interest as well as for Synaptophysin (SV marker) and Bungarotoxin. The latter is a toxin originally found in venomous snakes and blocks signal transmission at the NMJ by binding competitively and irreversibly to nicotinic acetylcholine receptors (Morley et al., 1979). In this experiment Bungarotoxin was labeled with tetramethylrhodamin and therefore served as a tag for the post-synapse (directly opposing the pre-synaptic AZ, see e.g. Wu and Betz, 1999).

Identical to the stainings of the hippocampal neurons super resolution STED microscopy (approximately 40 to 50 nm resolution) was used to investigate the organization of the protein of interest and conventional confocal microscopy for imaging the two markers – Synaptophysin and Bungarotoxin. Again, representative images of SNAP 25 can be found in Figure 3-14 A while images of remaining proteins are displayed in Appendix 2.

Using an analysis similar to the one outlined for the hippocampal neurons the distribution of the protein of interest we analyzed in relation to the vesicle cluster (Synaptophysin) and the post-synaptic density (Bungarotoxin) to generate density distributions for every single protein (Figure 3-14 B).

In terms of synaptic organization and morphology, the previously described hippocampal cultures are expected to represent a system, which is closest to the cortical synaptosomes characterized and quantified previously (see 3.1 to 3.3). Nevertheless, as mentioned before, one major advantage of using the NMJs as a model to investigate protein distributions is their relatively large size. The individual synapses are actually bigger than the diffraction limit of the confocal Synaptophysin and Bungarotoxin images. This allowed me to define the precise area covered by the SV cluster (green outline, Synaptophysin) and the post-synaptic zone (blue outline, Bungarotoxin) for every protein individually (see Figure 3-14 B) which was not possible for the rather small synapses of the hippocampal cultures.

In conclusion, the mouse NMJs represent (i) an ideal system to investigate protein organization at a peripheral mammalian synapse and (ii) a good comparison to the hippocampal cultures as the larger size of the synapses allows a more accurate localization of the different proteins. All density distributions displaying the organization of the different proteins at the

mouse NMJ will be discussed together with the corresponding distributions from the hippocampal neurons and the respective protein number per synapse in the following section.

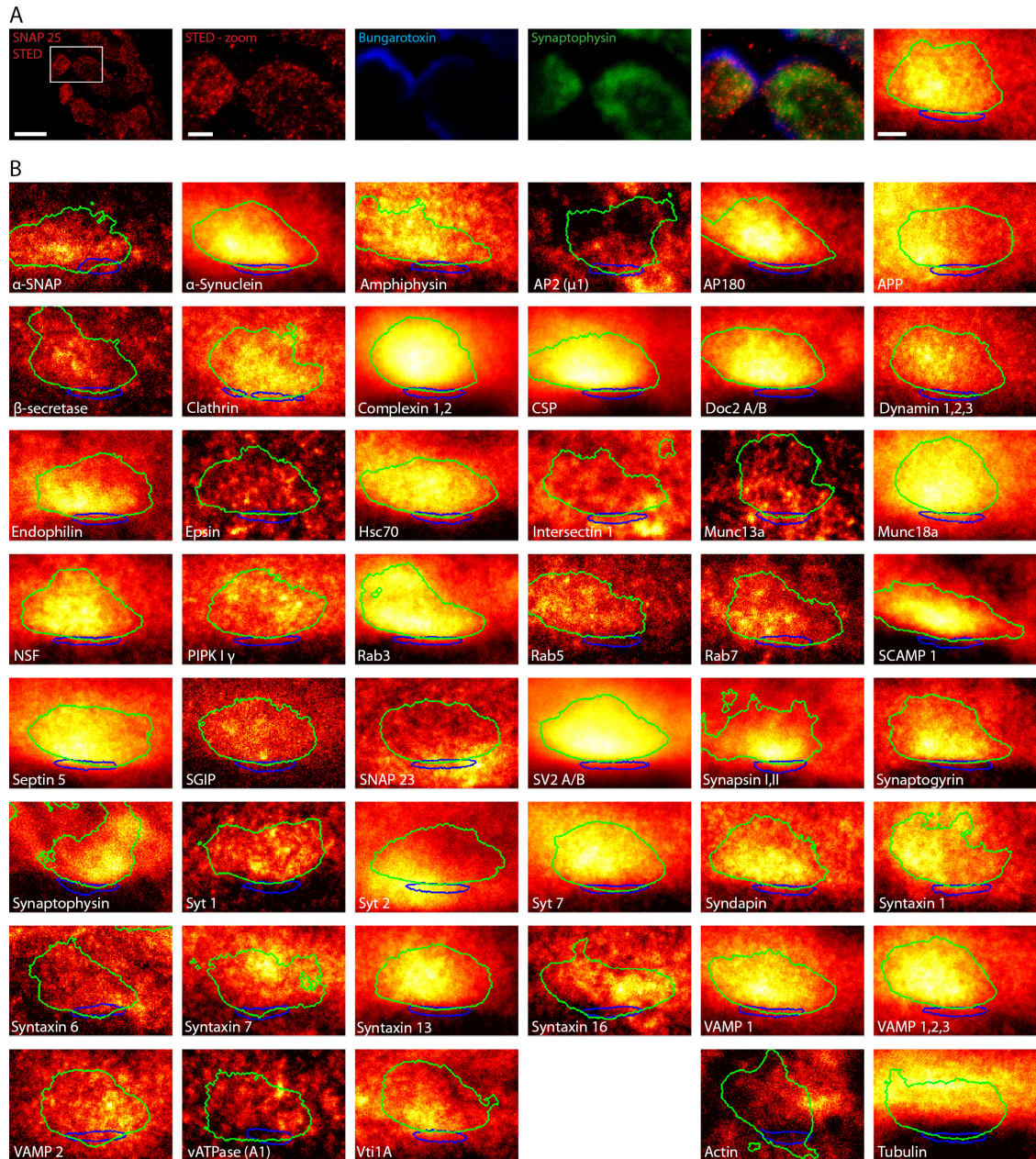


Figure 3-14: Protein organization at the mouse NMJ.

(A) Mouse NMJs were acutely prepared and immunostained in parallel for a protein of interest (in this case SNAP 25, red), nicotinic acetylcholine receptors (via tetramethylrhodamin tagged Bungarotoxin, blue) and Synaptophysin (green). Both Bungarotoxin and Synaptophysin were imaged using conventional confocal microscopy while the protein of interest was imaged with super resolution STED microscopy. The dispersion of the SNAP 25 spots in relation to the post-synapse (Bungarotoxin signal, blue outline) and the SV cluster (Synaptophysin signal, green

outline) was used to generate a density distribution representing the average pre-synaptic SNAP 25 dispersion (last image). Size bars are 5 μm , 1 μm and 500 nm from left to right.

(B) Density distributions for the other proteins investigated. Staining, imaging and analysis was performed as for SNAP 25. Representative images from the different stainings can be found in Appendix 2. Size bars are 250 nm.

3.5 The average pre-synaptic terminal

So far I performed several experiments to determine the physical characteristics of a pre-synaptic terminal (3.2) and the copy numbers for 59 major synaptic proteins (3.3) as well as their distribution (3.4). As noted earlier, the aim of this study is to combine all information on the pre-synaptic architecture in order to generate a graphical model of the average pre-synaptic terminal. Instead of simulating the average synapse I decided to take a representative synapse from the reconstruction dataset (see Figure 3-6). The reconstruction I chose resembled the average synaptosome closely in the most important parameters: volume (1.5 compared to $1.1 \pm 0.1 \mu\text{m}^3$), surface (4.9 compared to $4.4 \pm 0.3 \mu\text{m}^2$), number of vesicles (375 compared to 383.7 ± 37.9), size of the AZ (0.15 compared to $0.21 \pm 0.04 \mu\text{m}^2$), and size of the mitochondria (0.16 compared to $0.18 \pm 0.04 \mu\text{m}^3$). In this particular pre-synaptic terminal the proteins I investigated were placed in the appropriate locations, at their determined copy numbers.

In the following, all proteins that I quantified are listed with their respective copy number \pm SEM in brackets behind the name of each protein. Apart from the protein function I also describe the distribution of the proteins obtained from the STED assay. The later information was used in conjunction with previous information from other studies to place the copy numbers in the graphical model of the synapse (see 3.5.1).

α -SNAP (1150.7 ± 46.6): α -SNAP is an important co-factor for SNARE complex disassembly. After SV fusion, the SNARE complex (cis) resides in the plasma membrane. Binding of two α -SNAP molecules to the middle of the complex recruits and activates NSF which mediates the disassembly of the complex (Marz et al., 2003; Scales et al., 2001; Sollner et al., 1993b; Jahn and Scheller, 2006).

Distribution according to Figures 3-13 and 3-14: present mainly within the SV cluster and in close proximity to the AZ.

α -Synuclein (3167.8 ± 167.7): although α -Synuclein has been shown to be important for synaptic plasticity in song birds (George et al., 1995) its major role in mammals is still highly controversial. Potential functions might be molecular chaperoning of the SNARE complex

formation (Burre et al., 2012; Burre et al., 2010) or even a neuro-protection (Chandra et al., 2005). However, its most discussed role is probably its involvement in neurodegenerative diseases called synucleinopathies (e.g. Parkinson's disease). Its aggregates and deposits are thought to cause neuronal dysfunction and degeneration (Marques and Outeiro, 2012).

Distribution according to Figures 3-13 and 3-14: α -Synuclein is consistently localized to SVs in both mouse NMJs and hippocampal cultures (see also Scott and Roy, 2012).

Amphiphysin (1194.2 \pm 60.0): Amphiphysin contains a BAR (Bin-Amphiphysin-Rvs, reported to bend membranes) domain and has been reported to recruit Dynamin to Clathrin coated pits (Wigge et al., 1997). It is expected to play a crucial role in vesicle scission since introducing its SH3 (Sarcoma Homology 3 Domain) domain into living cells causes a block of SV recycling at the stage of invaginated coated pits (Shupliakov et al., 1997).

Distribution according to Figures 3-13 and 3-14: Amphiphysin can be found within as well as around the vesicle cluster, probably localized to peri-AZs. It also displays substantial overlap with its putative partner during SV endocytosis – Dynamin.

AP180 (5182.0 \pm 288.0): accessory protein during Clathrin coat formation demonstrated to accelerate the AP2 mediated recruitment of Clathrin to the pit (Morgan et al., 2000). Further, it has been shown to regulate size and protein composition of SVs in *Caenorhabditis elegans* (Nonet et al., 1999).

Distribution according to Figures 3-13 and 3-14: localized to vesicles but also to the area around it.

AP2 μ 1 (23247.0 \pm 819.9): is the medium adaptin subunit of the hetero-tetramer AP2 complex. The AP2 complex can be regarded as the major interaction hub during Clathrin mediated endocytosis: it interacts with most of the accessory factors as well as with Clathrin and specific cargo proteins (Honing et al., 2005; Collins et al., 2002; Henne et al.). The latter outlines its significance for the cargo selection of vesicles – either directly (via binding specific cargo molecules) or indirectly by recruiting the respective cargo adaptor proteins (Motley et al., 2003; Boucrot et al.; Huang et al., 2004).

Distribution according to Figures 3-13 and 3-14: the major adaptor protein during endocytosis of SVs displays a similar distribution as AP180. It can be found in the vesicle cluster as well as around it (the latter being particularly evident in the NMJs). Interestingly, AP2 is present at relatively high copy numbers in the synapse (e.g. approximately 4-fold more than AP180).

APP (6283.6 ± 584.5): the amyloid precursor protein (APP) is a ubiquitously expressed integral membrane protein with highest concentration in neuronal synapses. Although its main function is still debated, it has been suggested to play a role in neuronal plasticity (Turner et al., 2003) and synapse formation (Priller et al., 2006). On the other hand it is expected to be a key factor during Alzheimer's disease pathogenesis. Sequential cleavage of APP by the β - and γ -secretases leads to the generation of amyloid beta ($A\beta$) peptides. $A\beta$ aggregates into amyloid plaques, which have been suspected to be the main cause of neurodegeneration in dementia (Haass and Selkoe, 2007).

Distribution according to Figures 3-13 and 3-14: colocalizing with the synaptic vesicle cluster but also present at the edges of the cluster where it is assumed to reside on endosomes (see Groemer et al., 2011). Regarding the fact that the precise function of APP is still unclear, it is surprisingly abundant in a pre-synaptic terminal of an adult rat (see copy number).

β -secretase (115.8 ± 2.8): enzyme involved in the pathogenic cleavage of APP. As mentioned for APP, the generation of the potentially toxic $A\beta$ needs two sequential cleavage steps of APP (1) by the β -secretase and (2) by the γ -secretase. Cleavage via the β -secretase generates a membrane bound fragment referred to as C99 which is further cleaved by the γ -secretase to $A\beta$. Concerning the cleavage of APP, the β -secretase competes with the α -secretase. In contrast, cleavage by the latter marks the beginning of the non-pathogenic pathway that does not lead to $A\beta$ production (Willem et al., 2009; Vassar et al., 1999).

Distribution according to Figures 3-13 and 3-14: the APP cleaving enzyme is predominantly present on membranes close to the SV cluster most likely on vesicles, endosomes and the plasma membrane. Although, APP and β -secretase are reported to be transported in separate carrier vesicles (Goldsbury et al., 2006) they are expected to reside in overlapping organelle populations within the synaptic terminals in order to allow processing of APP (Groemer et al., 2011). Therefore, it is not surprising to have overlapping distributions for the two proteins in the synapse. The low copy number I found is probably due to the fact that the β -secretase is an enzyme and only needed in small amounts as a single molecule can catalyze multiple reactions sequentially.

Calbindin (296.9 ± 13.2): calcium binding protein containing four active binding domains allowing it to hold up to four Calcium ions. Expression of Calbindin is not limited to neurons but within the nervous system it is majorly expressed in Purkinje cells. In general, they regulate cellular activity by buffering calcium influx (Schwaller et al., 2002; Schwaller, 2010) and in

comparison to Calretinin and Parvalbumin it displays medium calcium affinity (Cheung et al., 1993).

Distribution according to Figures 3-13: broad distribution within the pre-synaptic compartment but seems to avoid the vesicle cluster. Calbindin is present at relatively low concentration at the average pre-synaptic terminal. However, the protein is not evenly distributed in the synapses used in this study which inevitably leads to underestimating the copy number.

CALM (2.7 ± 0.2): the Clathrin assembly lymphoid myeloid leukaemia (CALM) protein is the ubiquitously expressed functional homolog of AP180 (Tebar et al., 1999). It is expected to be up regulated during early brain development and down regulated again during further development. Therefore, the expression of CALM appears to be anti-correlated with the one of AP180 (personal communication from Prof. Dr. Volker Haucke) and can be regarded as a negative control in the quantification experiments. Just like AP180, also CALM is not essential for Clathrin mediated endocytosis (Maritzen et al., 2012) although it has recently proposed to be a cargo specific adaptor for VAMP 2 together with AP180 (Koo et al., 2012; Koo et al., 2011).

Calmodulin (8659.9 ± 445.5): Calmodulin is a calcium binding messenger protein best known for its essential role as an intermediate messenger for calcium evoked signaling cascades (Chin and Means, 2000). Several studies also found evidence for a possible role of Calmodulin in SV recycling by controlling the SNARE mechanism (Quetglas et al., 2002; Igarashi and Watanabe, 2007).

Distribution according to Figures 3-13: highly concentrated within the SV cluster.

Calretinin (369.2 ± 5.5): calcium buffering protein similar to Calbindin. However, it has a total of five active calcium binding domains and is predominantly found in granule cells within the nervous system (Schwaller et al., 2002; Schwaller, 2010). Calretinin has the lowest affinity to calcium compared to Calbindin and Parvalbumin (Schwaller et al., 1997; Stevens and Rogers, 1997).

Distribution according to Figure 3-13: Similar to Calbindin it is highly concentrated around the vesicle cluster. Calretinin is not expected to be present in all cerebral synapses which might bias the absolute copy number determined for this protein.

Clathrin heavy chain (2053.5 ± 103.3) and **Clathrin light chain** (810.6 ± 52.8): Clathrin is an essential protein for the formation of coated vesicles. Within neurons it is not only involved in the formation of trafficking vesicles but also in the recycling of SVs (Royle and Lagnado, 2010).

Three molecules of each Clathrin heavy chain and light chain assemble into one triskelion which is the major component of the Clathrin coat on an endocytosing vesicle. The coat of a single SV is composed of approximately 40 (Cheng et al., 2007) to 100 triskelia (Wigge et al., 1997) which are polymerized into penta- and hexagons (Musacchio et al., 1999). During pit formation the pre-formed triskelia are recruited to the membrane by AP2 in a 1:2 fashion (Cocucci et al., 2012). Assembly of further triskelia as well as specific cargo proteins (coat assembly) causes successive invagination of the membrane and finally formation of a coated vesicle which is pinched off of the membrane in a Dynamin-dependent manner (Slepnev and De Camilli, 2000; Wigge et al., 1997).

Distribution according to Figures 3-13 and 3-14: both Clathrin heavy and light chain are partly localized to SVs and to areas around it close to the AZ (especially in the hippocampal cultures). These areas are presumably peri-AZs where compensatory endocytosis of SVs occurs. Interestingly, other than expected from the stoichiometry of a Clathrin triskelion I found about 2.5 fold more Clathrin heavy than light chain. This finding as well as its implications for the regulation of SV endocytosis is further discussed in section 4.2.

Complexin 1 (132.4 ± 5.7) and **Complexin 2** (113.6 ± 3.2): Complexins are small proteins in the neuronal cytoplasm which are able to bind SNARE complexes (Chen et al., 2002; Bracher et al., 2002). Deletion of both Complexin 1 and 2 causes a strong reduction in calcium dependent exocytosis which points to a potential function in triggering SV release (Xue et al., 2010; Yang et al., 2010a). Studies by Rothman and colleagues further confirmed the central role of Complexins in controlling the fusion of SVs. They have found evidence for Complexins acting as a fusion blocker by clamping SNARE complexes. The clamp is then released by increased calcium levels which is expected to be indirectly triggered through Synaptotagmin as Complexins themselves are devoid of calcium binding sites (Kummel et al., 2011; Li et al., 2011).

Distribution according to Figures 3-13 and 3-14: Complexins show striking overlap with vesicles in terms of synaptic localization. This finding is in agreement with previous studies on the functional organization of Complexins demonstrating that this protein is buffered and sequestered by the SV cluster (Denker et al., 2011b; Wragg et al., 2013).

CSP (941.2 ± 48.9): cystein string protein (CSP) alpha is an abundant SV protein acting as a co-chaperone for SNAP 25. Homozygous CSP α KO mice show significant increases in neurodegeneration and mortality rate (Fernandez-Chacon et al., 2004). Later, it has been demonstrated, that deletion of CSP α causes a reduction of SNAP 25 levels. The reduced SNAP 25

levels in turn lead to an impairment of SNARE complex assembly which is expected to be the major cause of neurodegeneration in CSP α KO mice (Sharma et al., 2011; Sharma et al., 2010). Interestingly, SNARE complex assembly is rescued by application of α -Synuclein while SNAP 25 levels remain low (Burre et al., 2010).

Distribution according to Figures 3-13 and 3-14: as a vesicle protein CSP is localized to SVs but also to the plasma membrane (i.e. lateral signals not overlapping with the vesicle cluster).

Doc2 a/b (3696.5 \pm 164.2): Doc2 molecules contain two C-terminal calcium binding domains (C2A and C2B, similar to Synaptotagmins) and a short N-terminal domain which can bind Munc13. The two isoforms – a and b – addressed in this study are predominantly expressed in the brain and are expected to be involved in calcium triggered exocytosis of SVs (Groffen et al., 2006; Verhage et al., 1997). In particular, Doc2 b is expected to function as a high affinity calcium sensor during spontaneous vesicle fusion (Groffen et al., 2010).

Distribution according to Figures 3-13 and 3-14: the majority of the protein is localized to SVs. However, the signals outside and at the edge of the vesicle cluster indicate a potential localization to endosomes as well.

Dynamin 1, 2, 3 (2326.4 \pm 83.9): Dynamins are cytosolic proteins containing an N-terminal GTPase domain. Dynamin 1 is the predominant isoform in synapses while Dynamin 2 is ubiquitously expressed and Dynamin 3 present in brain and testis only. Dynamins have an essential role for Clathrin mediated endocytosis (Ferguson and De Camilli, 2012): during budding of the Clathrin coated vesicle, Dynamin forms a spiral around the neck of the vesicle. Constriction of the spiral via GTP hydrolysis then leads to pinching off of the vesicle from the membrane (Roux et al., 2006). Studies on Dynamin 1 KO mice have shown that the animals develop a severe neurological phenotype and die within a few weeks after birth (Ferguson et al., 2007). Further, temperature sensitive *Drosophila melanogaster* mutants (*shibire*) show complete paralysis as well as a depletion of SVs upon stimulation at the non-permissive temperature (Koenig and Ikeda, 1989; van der Bliek and Meyerowitz, 1991; Chen et al., 1991).

Distribution according to Figures 3-13 and 3-14: Dynamin associates with SVs and is widely distributed in the pre-synaptic terminal. Note also its overlap with putative interaction partners such as Amphiphysin and Endophilin.

Endophilin I, II, III (2524.4 \pm 67.3): Endophilin is a cytosolic protein required for SV endocytosis (Schuske et al., 2003; Sundborger et al., 2011). It has a preference for the curvature

of the vesicle neck and has been reported to recruit Dynamin to the budding vesicle and to assist Synaptojanin in the uncoating of the newly formed vesicle (Kjaerulff et al., 2010).

Distribution according to Figures 3-13 and 3-14: similar distribution as Dynamin or Amphiphysin – associated with SVs as well as with structures around it, presumably the AZ and peri-AZ.

Epsin 1 (92.9 ± 4.3): Epsin 1 is a cytosolic protein predominantly localized to pre-synaptic nerve terminals. It interacts with Intersectin and is an important factor for generating membrane curvature during SV endocytosis (Horvath et al., 2007; Ford et al., 2002).

Distribution according to Figures 3-13 and 3-14: In the hippocampal cultures Epsin is localized to the vesicle cluster. Unfortunately the signal in the mouse NMJs does not seem to be specific enough for an unbiased localization of the protein.

Hsc70 (821.0 ± 40.5): Hsc70 is responsible for disassembling the Clathrin coat and therefore uncoating recently endocytosed SVs. The protein is also known as uncoating ATPase (Schlossman et al., 1984). It is recruited to the vesicle by its cofactor Auxillin and the uncoating procedure is expected to be initiated by scission of the vesicle. Upon scission the former neck of the vesicle is devoid of Clathrin offering an ideal setting for Auxillin and Hsc70 to start the uncoating process. A maximum of one Auxillin and three Hsc70 molecules are required for the complete disassembly of one Clathrin triskelion (Rothnie et al., 2011; Cremona et al., 1999).

Distribution according to Figures 3-13 and 3-14: several molecules are associated with the vesicle cluster while the majority is distributed freely in the cytosol around the cluster.

Intersectin1 (3096.5 ± 277.6): large scaffolding protein connecting several components of the Clathrin machinery (e.g. Clathrin, Epsin and AP2) during SV endocytosis. It therefore is an important element controlling the spatio-temporal organization of Clathrin mediated endocytosis (Pechstein et al., 2010a; Pechstein et al., 2010b).

Distribution according to Figures 3-13 and 3-14: present in the SV cluster and around the AZ most likely at sites of SV endocytosis (peri-AZs).

Munc13a (1551.3 ± 53.2): three different Munc13 isoforms (a, b, c) are known in the brain of which Munc13a shows the largest expression pattern. It binds to RIM proteins and Syntaxin 1 (Deng et al., 2011; Betz et al., 1997) and is indispensable for priming of the SV and therefore ultimately for synaptic vesicle fusion (Varoqueaux et al., 2002).

Distribution according to Figures 3-13 and 3-14: although Munc13a is localized to SVs it sits predominantly at the AZ. Unfortunately, the signal in the mouse NMJs is not specific and can therefore not be used to determine the synaptic localization of Munc13.

Munc18a (4253.4 ± 207.1): similar to Munc13a, Munc18a is also involved in SV vesicle docking and priming. Munc18a binds to Syntaxin 1 with high affinity and is expected to stabilize it during the SNARE complex formation (Burgoyne et al., 2009). Deletion of Munc18 also leads to complete inhibition of neuronal exocytosis underlining its importance for vesicle priming (Verhage et al., 2000).

Distribution according to Figures 3-13 and 3-14: highly localized to SVs, particularly to those in close proximity to the AZ.

NSF (4064.7 ± 213.0): disassembly of SNARE complexes after fusion requires substantial amounts of metabolic energy which is provided by the hexameric ATPase NSF. A complete untangling of the SNARE complexes might require several rounds of NSF activity. The interaction of NSF with the SNARE complex crucially depends on the co-factor α -SNAP (Sollner et al., 1993a; Sollner et al., 1993b; Jahn and Scheller, 2006).

Distribution according to Figures 3-13 and 3-14: NSF displays a certain affinity to SVs but is otherwise ample distributed in the entire pre-synaptic terminal. The active form of the protein during disassembly of the SNARE complex is a hexamer of which I found approximately 677 sets per pre-synaptic terminal.

Parvalbumin (681.1 ± 34.3): similar to Calbindin and Calretinin involved in intracellular calcium buffering. Parvalbumin contains two active calcium binding domains and is highest expressed in Purkinje cells and a specific population of inhibitory interneurons. (Schwaller et al., 2002; Schwaller, 2010). In comparison to the previously described Calbindin and Calretinin it has the highest calcium affinity (Haiech et al., 1979; Eberhard and Erne, 1994).

Distribution according to Figure 3-13: Unlike Calbindin and Calretinin, Parvalbumin is highly localized to synaptic vesicles. Also Parvalbumin is specific for certain neuronal subtypes. Thus, not all synapses in the synaptosome preparation actually contained Parvalbumin. Therefore, it has to be assumed that the actual copy number per pre-synaptic terminal is probably substantially higher.

PIPK I γ (465.7 ± 18.9): the full name of this enzyme is Phosphatidylinositol 4-phosphate 5-kinase type-1 gamma (Giudici et al., 2004). Activated by ARF6 it catalyzes the phosphorylation of PIP to PIP₂ which is expected to play a role of the spatio-temporal control of vesicle

endocytosis. Several endocytic proteins such as AP2, AP180 and Epsin 1 directly interact with PIP and PIP₂ in particular. Therefore, PIPK ly activity leads to recruitment of these endocytic proteins to synaptic membranes (Krauss et al., 2003).

Distribution according to Figures 3-13 and 3-14: the enzyme apparently avoids the vesicle cluster as well as the AZ and is organized in clusters to their sides.

Rab3 (30735.7 ± 1624.3): Rab proteins belong to the family of ras-related small monomeric GTPases and are generally involved in regulating intracellular trafficking. The GTP bound form is the active form and generally recognized by multiple effector proteins. The hydrolysis of GTP to GDP inactivates the protein and the re-phosphorylation is regulated by a Rab escort protein and GDI (Darchen and Goud, 2000; Stenmark, 2009). Of the four Rab3 isoforms known (a, b, c, d), Rab3a is the most prominent pre-synaptic protein and specific to SVs. Single and multiple mutations in Rab3 show impaired neurotransmission but are vital as long as Rab3a is present (Schluter et al., 2004). Rab3a is released from SVs upon exocytosis (Fischer von Mollard et al., 1991) and involved in controlling SV exocytosis since Rab3a deletion results in impaired synaptic transmission while over-expression leads to inhibition of calcium evoked exocytosis (Schluter et al., 2002).

Distribution according to Figures 3-13 and 3-14: entirely associated with SVs in both hippocampal cultures and mouse NMJs.

Rab5a (633.6 ± 37.3): ubiquitously expressed protein, regulating homotypic fusion of early endosomes as well as fusion of endocytic vesicles with early endosomes (Stenmark et al., 1995). Due to its high concentration in early endosomes it is widely used as a specific marker for these organelles (Stenmark et al., 1994).

Distribution according to Figures 3-13 and 3-14: similarly distributed as Rab3a but with several molecules residing just outside of the vesicle cluster on endosomes.

Rab7a (4457.2 ± 319.8): similar to Rab5 but involved in the endocytic pathway of late endosomes i.e. it mediates maturation of the late endosome and its fusion with the lysosome (Bucci et al., 2000).

Distribution according to Figures 3-13 and 3-14: basically identical to Rab5a

SCAMP 1 (14595.0 ± 1155.3): secretory carrier-associated membrane proteins (SCAMPs) are ubiquitously expressed and involved in recycling of cell surface components (Castle and Castle, 2005). SCAMP 1 is present in small amounts on SVs (Takamori et al., 2006) and has been

implied to play a role in recruitment of the Clathrin coat during SV endocytosis due to its interaction with e.g. Intersectin 1 (Fernandez-Chacon et al., 2000).

Distribution according to Figures 3-13 and 3-14: localized to SVs and loosely arranged in the plasma membrane surrounding the cluster.

Septin 5 (1726.2 ± 64.4): Septins are highly conserved in eukaryotes. They form complex hetero-oligomeric structures including rings and filaments and are therefore regarded as a novel part of the cytoskeleton (Mostowy and Cossart, 2012). The ubiquitously expressed Septin 5 participates in targeting and exocytosis of vesicles and has been reported to interact with the SNARE complex (Beites et al., 2005; Amin et al., 2008).

Distribution according to Figures 3-13 and 3-14: it seems to be highly associated with vesicles in the mouse NMJs. However, for the molecular model presented in 3.5.1 we mostly used the distribution information from the hippocampal cultures where Septin 5 is mostly avoiding, almost encircling the cluster.

SGIP1 α (3382.2 ± 158.7): both membrane tubulating and binding protein demonstrated to play a role in Clathrin mediated endocytosis by recruiting essential proteins for proper assembly of the Clathrin coat (Trevaskis et al., 2005; Uezu et al., 2007).

Distribution according to Figures 3-13 and 3-14: predominantly present at the SV cluster and around the AZ.

SNAP 23 (265.6 ± 17.8): ubiquitously expressed functional homolog to SNAP 25 (Jahn and Scheller, 2006). However, expression of SNAP 23 does not rescue SNAP 25 deletion completely (Sorensen et al., 2003).

Distribution according to Figures 3-13 and 3-14: SNAP 23 can be found partly on vesicles and endosomes, mostly on the plasma membrane.

SNAP 25 (132090.0 ± 2581.6): SNAP 25 is a membrane anchored protein (via palmitoyl side chains in the middle of the protein) and part of the SNARE protein family. Together with Syntaxin 1 and VAMP 2 it forms a SNARE complex which is the core component mediating SV exocytosis (Jahn and Scheller, 2006). Although, SNAP-25 is a t-SNARE it is not only localized to the plasma membrane but also to trafficking organelles of pre-synaptic terminals (Walch-Solimena et al., 199; Takamori et al., 2006).

Distribution according to Figures 3-13 and 3-14: according to the stainings SNAP 25 is localized to vesicles, the AZ and the plasma-membrane in general. For the model we assumed approximately 70% of the SNAP 25 on the plasma-membrane to be organized in clusters of

approximately 130 nm (Bar-On et al., 2012) and the remaining 30% to single molecules. In the quantification assay I found SNAP 25 to be extremely abundant within pre-synaptic terminals. This is in line with previous studies (Walch-Solimena et al., 1995) (Knowles et al., 2010) and might point to other potential functions (direct or indirect) of SNAP 25 in synaptic physiology.

SNAP 29 (77.5 ± 6.5): ubiquitously expressed functional homolog to SNAP 25. SNAP 29 has been reported to interfere with SNARE complex disassembly and thereby modulating neurotransmitter release negatively (Su et al., 2001; Peng et al., 2004).

Distribution according to Figure 3-13: SNAP 29 shows a similar distribution to SNAP 23 as it is mainly associated with vesicles and endosomes. However, a substantial fraction also seems to reside on the plasma membrane.

SV2 A (33006.0 ± 1034.6) and **SV2 B** (13160.0 ± 256.5): highly glycosylated integral membrane protein localized to secretory vesicles (Buckley and Kelly, 1985; Bajjalieh et al., 1992). SV2 has been demonstrated to regulate expression and trafficking of the vesicular calcium sensor Synaptotagmin (Yao et al., 2010). In line with this, several studies have found SV2 to be involved in maintaining a pool of vesicles available for calcium mediated exocytosis (Xu and Bajjalieh, 2001; Chang and Sudhof, 2009) suggesting that SV2 regulates pre-synaptic calcium levels (Janz et al., 1999a; Wan et al., 2010). Interestingly, SV2 is also high-jacked by tetanus neurotoxins: the toxin binds to SV2 of recycling vesicles to enter central inhibitory neurons where it inhibits SV release causing rigid muscle paralysis (Yeh et al., 2010).

Distribution according to Figures 3-13 and 3-14: almost completely localized to SVs with several molecules in the plasma membrane and on endosomes. I found a large amount of SV2 A/B molecules at pre-synaptic terminals. It is difficult to compare these results to a previous study that found 2 copies per vesicle (Takamori et al., 2006). As mentioned before, SV2s are highly glycosylated proteins which are likely to bias quantitative immunoblotting and therefore lead to higher or lower results.

Synapsin Ia (34656.0 ± 2190.6), **Synapsin Ib** (72566.0 ± 599.7), **Synapsin IIa** (4727.7 ± 45.3), **Synapsin IIb** (22005.0 ± 1220.3): Synapsins are almost exclusive to neurons and solely associated with SVs. They are known to tether vesicles within the pre-synaptic terminal by interacting both with the SV membrane and elements of the cytoskeleton. Although the precise mechanisms are still debated, current studies imply that binding of Synapsin to SVs is dependent on phosphorylation. The calcium influx following an action potential at a pre-synaptic terminal activates a signaling cascade – involving among others also Calmodulin – which ultimately leads

to phosphorylation of Synapsin. Upon phosphorylation, Synapsin releases the SVs, which are now free to move and fuse with the plasma membrane (Cesca et al., 2010; Fornasiero et al., 2012; Evergren et al., 2007a; Shupliakov et al., 2011).

Distribution according to Figures 3-13 and 3-14: present in the cytosol of the pre-synaptic terminal with its highest concentration in the vesicle cluster. The data on the absolute amount of Synapsin molecules per synapse presented here sheds new light onto the consistency of the synaptic cytoplasm. The extremely large amounts of Synapsin molecules render the entire cytoplasm more rigid possibly comparable to a gel-like matrix (Siksou et al., 2007; Hirokawa et al., 1989). It is likely that this matrix is also involved in retaining vesicles as well as synaptic proteins within the limited space of the pre-synaptic terminal (Denker et al., 2011b; Shupliakov et al., 2011).

Synaptogyrin 1 (9926.5 ± 575.7): ubiquitous neuronal protein localized primarily to SV membranes (Baumert et al., 1990; Jahn et al., 1985). It has been demonstrated to be involved in synaptic plasticity without being crucial for neurotransmitter release but its precise function is still unknown (Janz et al., 1999b).

Distribution according to Figures 3-13 and 3-14: only partly found on SVs. The remaining molecules are localized to the plasma membrane and to endosomes.

Synaptophysin (31102.0 ± 2411.0): membrane bound glycoprotein highly concentrated on SVs (Jahn et al., 1985). It is one of the most widely used markers for pre-synaptic nerve terminals. Nevertheless, its exact function is still elusive. It is known to interact with VAMP 2 (Reisinger et al., 2004) and has been proposed to be involved in synaptic plasticity (Janz et al., 1999b) but not essential for neurotransmitter release (McMahon et al., 1996). Further, a potential function in SV endocytosis has been suggested since it forms a complex with Dynamin at high calcium concentrations (Daly and Ziff, 2002).

Distribution according to Figures 3-13 and 3-14: Synaptophysin is predominantly localized to SVs. However, according to Takamori et al., 2006 approximately two thirds of the molecules found have to be sitting in the plasma membrane, most likely at and around the AZ according to the density distributions.

Synaptotagmin 1 (10332.0 ± 1079.2): Synaptotagmins are integral membrane glycoproteins anchored to SVs. The cytosolic tail of the protein contains two C2-domains for binding calcium ions (Matthew et al., 1981; Sudhof and Rizo, 1996). Synaptotagmin 1 is the major calcium sensor governing evoked neurotransmitter release. Upon binding of calcium its

C2 domain binds to the plasma membrane thereby bringing target and vesicle membrane together. This ultimately brings v- and t-SNAREs into close proximity and therefore initiates the fusion process (Chapman, 2008; Bommert et al., 1993).

Distribution according to Figures 3-13 and 3-14: consistently found on vesicles in both preparations. However, in agreement with previous studies we conclude that a substantial fraction (approximately 20%) of Synaptotagmin 1 molecules also resides in the plasma membrane (see for instance Opazo et al., 2010) and on recycling endosomes (Hoopmann et al., 2010).

Synaptotagmin 2 (3456.8 ± 132.2): very similar to Synaptotagmin 1 in structure and function but predominantly localized to caudal brain areas (Geppert et al., 1991). It has been demonstrated to act jointly with Synaptotagmin 1 during calcium evoked neurotransmitter release (Pang et al., 2006a; Pang et al., 2006b).

Distribution according to Figures 3-13 and 3-14: similarly distributed as Synaptotagmin 2 but with relatively more molecules in the plasma membrane and on endosomes.

Synaptotagmin 7 (182.6 ± 3.5): Synaptotagmin 7 is the most abundant Synaptotagmin isoform following 1 and 2. Interestingly, Synaptotagmin 7 also seems to function as a calcium sensor during exocytosis, however not localized on the vesicle but rather to the plasma membrane (Fernandez et al., 2001).

Distribution according to Figures 3-13 and 3-14: the majority of the molecules seem to be distributed on the plasma membrane while the rest is equally distributed between SVs and endosomes.

Syndapin 1 (3201.0 ± 131.3): Syndapin 1 interacts with Dynamin, Synaptojanin and Synapsin. It is proposed to link vesicle endocytosis to the Actin cytoskeleton which allows the newly formed vesicle to leave the donor membrane after fission (Kessels and Qualmann, 2006; Anggono et al., 2006; Kessels and Qualmann, 2004).

Distribution according to Figures 3-13 and 3-14: majorly found in and around the vesicle cluster and the AZ at potential peri-AZs. Syndapin further shows substantial colocalization with its interaction partner Dynamin.

Syntaxin 1 (20096 ± 999.4): Syntaxins are small integral membrane proteins participating in vesicle fusion as an essential part of the SNARE complex (Bennett et al., 1993). Syntaxin 1 is the most important isoform in SV exocytosis. Together with SNAP 25 and VAMP 2 it forms a SNARE complex mediating SV fusion during neuronal activity. Syntaxin 1 is

predominantly present in 50 – 60 nm clusters (approximately 75 molecules) on the plasma membrane where the molecules are in a dynamic equilibrium with freely diffusing ones (Sieber et al., 2007). Despite its partners in vesicle fusion Syntaxin 1 interacts with Synaptotagmin 1 (Chapman et al., 1995), Munc18 (Zilly et al., 2006) and Ca²⁺-channels (Bergsman and Tsien, 2000).

Distribution according to Figures 3-13 and 3-14: Syntaxin 1 molecules are present on SVs, and in clusters of approximately 75 molecules on the plasma-membrane (Sieber et al., 2007).

Syntaxin 6 (121.7 ± 9.0): SNARE protein involved in vesicle exocytosis primarily at the trans-Golgi network and endosomal compartments. Potential partners for SNARE complex assembly are e.g. Syntaxin 16, VAMP 4 and Vti1a (Jung et al., 2012).

Distribution according to Figures 3-13 and 3-14: predominantly present on endosomes and few on SVs. Interestingly, Syntaxin 6 shows a large overlap in localization with its putative SNARE partners in endosomal trafficking – Syntaxin 16, VAMP4 and Vti1a.

Syntaxin 7 (78.6 ± 4.5): SNARE protein participating in the fusion of late endosomes and lysosomes by forming complexes with Endobrevin (Mullock et al., 2000) and Vti1b (Schluter et al., 2002).

Distribution according to Figure 3-13 and 3-14: similar to Syntaxin 6 having most molecules present on endosomes and a few on vesicles.

Syntaxin 13 (879.1 ± 24.3): The SNARE proteins Syntaxin 12 and 13 are orthologues of the same gene and are predominantly localized to early endosomes (Prekeris et al., 1998; Tang et al., 1998).

Distribution according to Figure 3-13 and 3-14: similar to Syntaxin 6 and 7. Interestingly, when comparing the localization of Syntaxin 7 (specific for late endosomes) and Syntaxin 13 (specific for early endosomes) in the NMJs the early and late endosomes seem to have preferential locations within the pre-synaptic terminal.

Syntaxin 16 (91.3 ± 5.7): SNARE protein operating at the Golgi stack regulating trafficking of the trans-Golgi network (Simonsen et al., 1998). It has been reported to interact with VAMP 3, 4 and Vti1a (Chen et al., 2010). Further, it was proposed to be enriched in neuronal dendrites and to be involved in neurite outgrowth (Chua and Tang, 2008).

Distribution according to Figure 3-13 and 3-14: similar to Syntaxin 6, 7 and 13

VAMP 1 (3884.3 ± 182.0): vesicle associated membrane proteins (VAMPs, also known as Synaptobrevins) are an essential element of the exocytic fusion machinery (v-SNAREs; Jahn and Scheller, 2006). VAMP 1 is highly concentrated on SVs but also present on other secretory granules (Trimble et al., 1988). The function of VAMP 1 and 2 are largely overlapping and they display distinct distributions within the brain (Raptis et al., 2005; Elferink et al., 1989).

Distribution according to Figures 3-13 and 3-14: same distribution as VAMP2.

VAMP 2 (26448.0 ± 661.6): VAMP 2 is the most abundant t-SNARE in the mammalian brain. It is a small integral membrane protein predominantly present on SVs (Baumert et al., 1989). In its function as a t-SNARE it interacts with the two v-SNAREs, SNAP 25 and Syntaxin 1 to form the SNARE complex which mediates SV exocytosis and ultimately neurotransmitter release (Jahn and Scheller, 2006). Although, mice lacking VAMP 2 are vital they show an approximately 10-fold reduction of spontaneous and more than 100-fold reduction of evoked vesicle release (Schoch et al., 2001).

Distribution according to Figures 3-13 and 3-14: VAMP 2 is one of the most reliable markers for SVs and its signal was used as a reference for the localization of the vesicle cluster in all other protein distributions. Therefore, almost all VAMP 2 proteins will be placed on SVs. Comparing the numbers of the putative SNARE partners during SV exocytosis (i.e. VAMP 2, Syntaxin 1 and SNAP 25) it is evident that SNAP 25 is more than 5-fold more abundant than VAMP 2 and Syntaxin 1 adding further interest to a possible function of the SNAP 25 superabundance.

VAMP 4 (100.6 ± 10.0): vesicular SNARE protein similar to VAMP 1 and 2 in function but majorly involved in trans-Golgi network trafficking (Steehmaier et al., 1999; Mallard et al., 2002). Recently, it also has been proposed that VAMP 4 is specific to a fraction of SVs which maintain asynchronous neurotransmitter release (Raingo et al., 2012).

Distribution according to Figure 3-13: same distribution as Syntaxin 6.

vATPase (2186.2 ± 97.1): the vacuolar protein pump is a large protein complex composed of 10 subunits (Perin et al., 1991). It is responsible for acidification of most intracellular organelles and therefore also present in small amounts on SVs (Takamori et al., 2006).

Distribution according to Figures 3-13 and 3-14: present on all intracellular organelles.

vGlut 1/2 (8254.1 ± 224.3): the vesicular glutamate transporters (vGLUTs) are in charge of glutamate uptake and storage in vesicles of glutamatergic synapses. The different isoforms

(vGlut 1 and 2) are differentially expressed in different neuronal populations (Bellocchio et al., 2000; Takamori et al., 2000).

Distribution according to Figure 3-13: entirely localized to vesicles. The transporter is not present in the mouse NMJ as this is a cholinergic synapse.

Vti1 A (50.6 ± 2.5): v-SNARE which is mainly involved in SNARE complex formation at the cis- and trans-Golgi network (Mallard et al., 2002; Kreykenbohm et al., 2002). Has been reported to interact with VAMP4, Syntaxin 6 and 16 (see above). A recent study on the nature of spontaneous versus evoked neurotransmission reported that Vti1 A is selectively involved in spontaneous neurotransmitter release arguing that the two types of release are maintained by distinct vesicle populations (Ramirez et al., 2012) but see also (Wilhelm et al., 2010; Groemer and Klingauf, 2007).

Distribution according to Figures 3-13 and 3-14: mainly found in endosomes with a few molecules present on SVs as well.

Besides the synaptic proteins listed above I also quantified the relative amounts of several reference proteins: Actin, MBP, PSD 95, Tubulin and VDAC1. All of these proteins are not exclusively present in pre-synaptic terminals and therefore served as references to get a rough overview of the general composition of the synaptosome preparations. However, the two cytoskeletal elements Actin and Tubulin are known to not only provide structural stability but are also involved in pre-synaptic function. Actin is for example known to function in clustering of SVs (Dillon and Goda, 2005) while microtubules are necessary for almost every transport in and out of the synapse (Conde and Caceres, 2009). Therefore, I estimated synaptic Actin and Tubulin amounts and inserted them into the graphical model respectively (see 3.5.1). The estimates were obtained considering the following assumptions: in 3.1 we learned that 58.5% of the synaptosome preparations are actually synaptosomes. Since both Actin and Tubulin are not present in mitochondria this fraction could be subtracted from the total resulting in approximately 71% of synaptosomes per sample. Assuming that the two proteins are more or less equally distributed throughout all particles I thus concluded that approximately 71% of the molecules that were found (see Table 3-4) are localized to pre-synaptic terminals. According to this, 22074 Actin and 12056 Tubulin molecules are present in the average pre-synaptic terminal. Concerning the arrangement of these two molecules (see graphical models in next section) we decided that approximately 20% of Tubulin and 70% of Actin (Sankaranarayanan et al., 2003) are

monomeric while the remaining molecules are sufficient to form approximately 4 μm of synaptic microtubule (Chretien and Fuller, 2000) and 18 μm of Actin filaments (Murakami et al., 2010).

3.5.1 Graphical model of the average pre-synaptic terminal

As stated previously, the ultrastructural information of the synaptosomes (see 3.2) was used in combination with the protein quantification (see 3.3) and localization (see 3.4) results to generate a graphical model of the average pre-synaptic terminal. The model was computed by Burkhard Rammner (www.scimotion.com). In the following I will show different views of the synapse also including only subsets of proteins for better visualization:

Figure 3-15 shows only the ultrastructure of the terminal including the Actin and Microtubule filaments. The next image (Figure 3-16) represents the same synapse, but this time including all soluble proteins besides Synapsins. Synapsin is present in such large amounts in a synapse that it would cover all other proteins in this view (see also Figure 3-18). In parallel to this, the next image depicts the terminal including all proteins attached or integral to the membrane (see Figure 3-17). After showing general overviews about the entire synapse the next three images display zooms of certain regions with a selected protein composition. Figure 3-18 shows a synaptic vesicle embedded into a tight network of soluble proteins (in particular Synapsins). After a more detailed view into the cytosol I also provide a closer view on the plasma-membrane. Figure 3-19 shows a zoomed view of a part of the plasma-membrane containing protein complexes and cluster. At last, I wanted to show the AZ in more detail in Figure 3-20. This image only contains proteins of the plasma-membrane as well as those that are associated with the AZ.

An interesting finding which is nicely visualized by the below presented images is how crowded the synapse actually is. It has been known already that a SV is densely packed with different integral membrane proteins (Takamori et al., 2006) but apparently this is a concept which also holds true for the entire pre-synaptic compartment. Both membrane and in particular soluble proteins are present in vast amounts and densely packed in the terminal. This makes it tempting to speculate on the function of the vast amount of proteins in general as well as specifically for some of the proteins. For a thorough discussion of the relation between synaptic protein number and function refer to section 4.2.

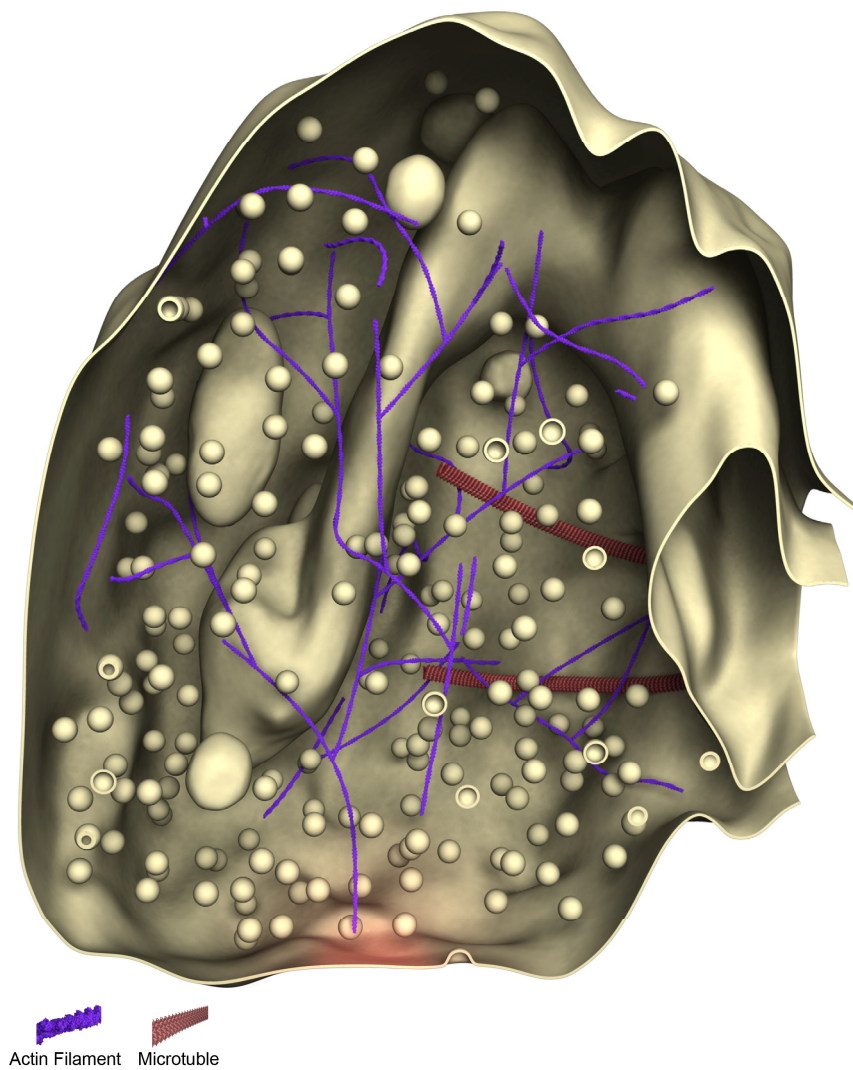


Figure 3-15: Ultrastructural appearance of the average pre-synaptic terminal
Graphical model obtained from data presented in 3.1 to 3.4 displaying only the ultrastructure of the terminal (AZ displayed in red) and the cytoskeletal filaments of Actin and Tubulin.

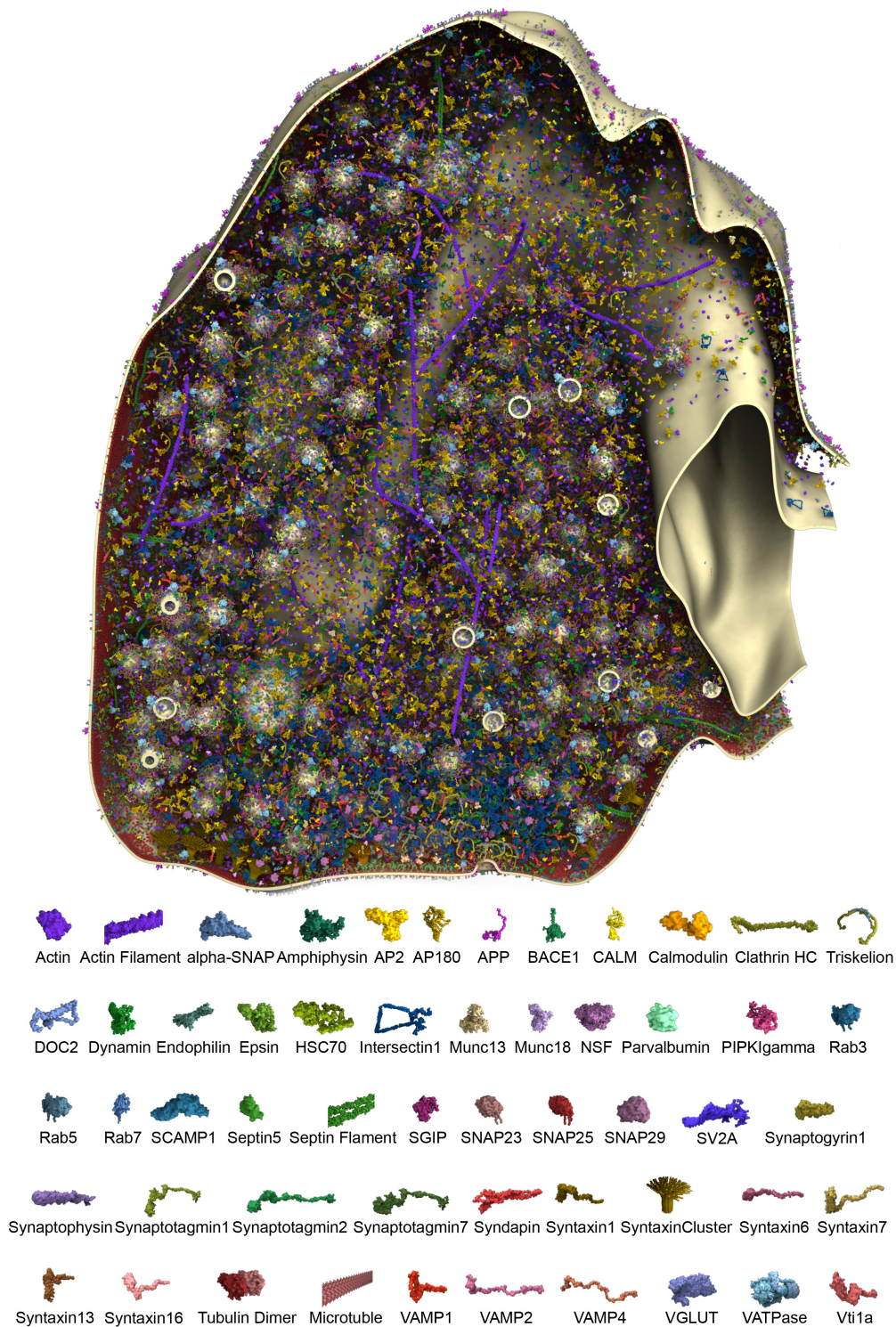


Figure 3-16: Distribution of several soluble proteins within the average pre-synaptic terminal
 Graphical model obtained from data presented in 3.1 to 3.4 displaying only cytosolic proteins with the exception of Synapsins. The proteins included in this image are all listed in the legend underneath it.

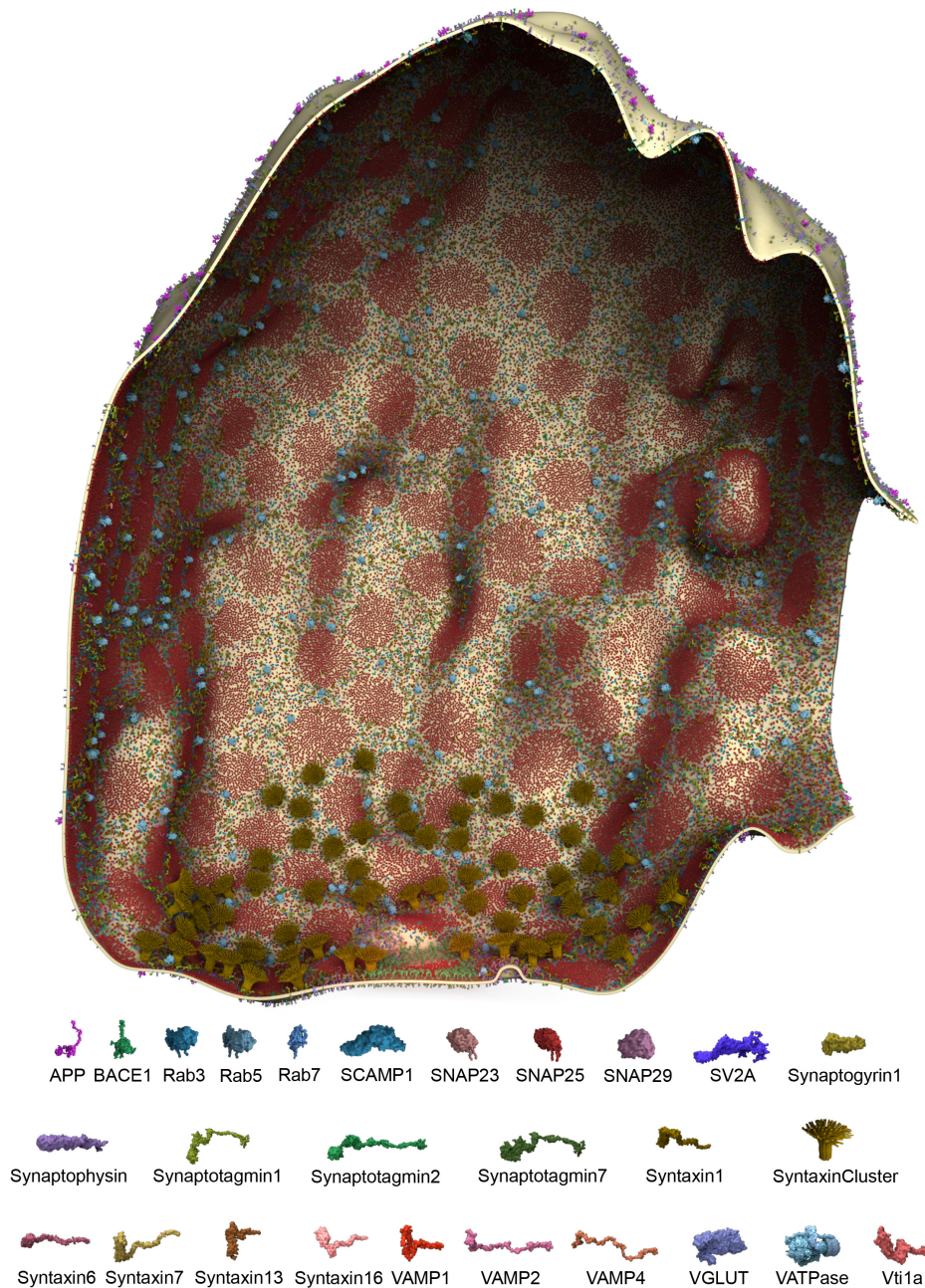


Figure 3-17: Distribution of membrane proteins within the average pre-synaptic terminal

Graphical model obtained from data presented in 3.1 to 3.4 displaying all membrane bound (integral or attached) addressed in this study. The proteins included in this image are all listed in the legend underneath it.

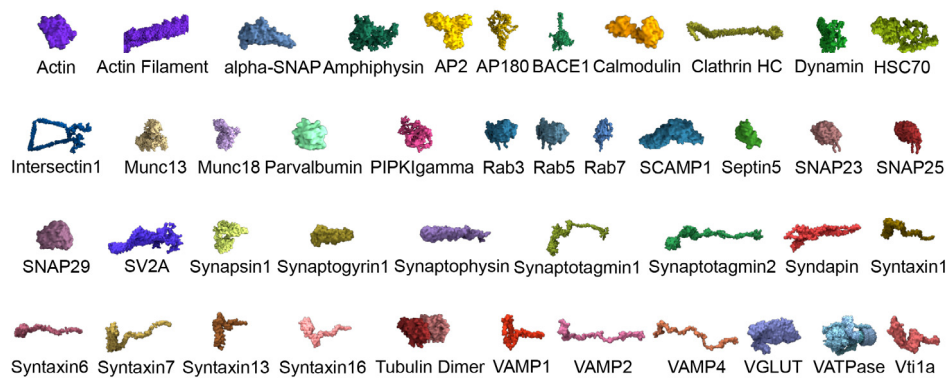
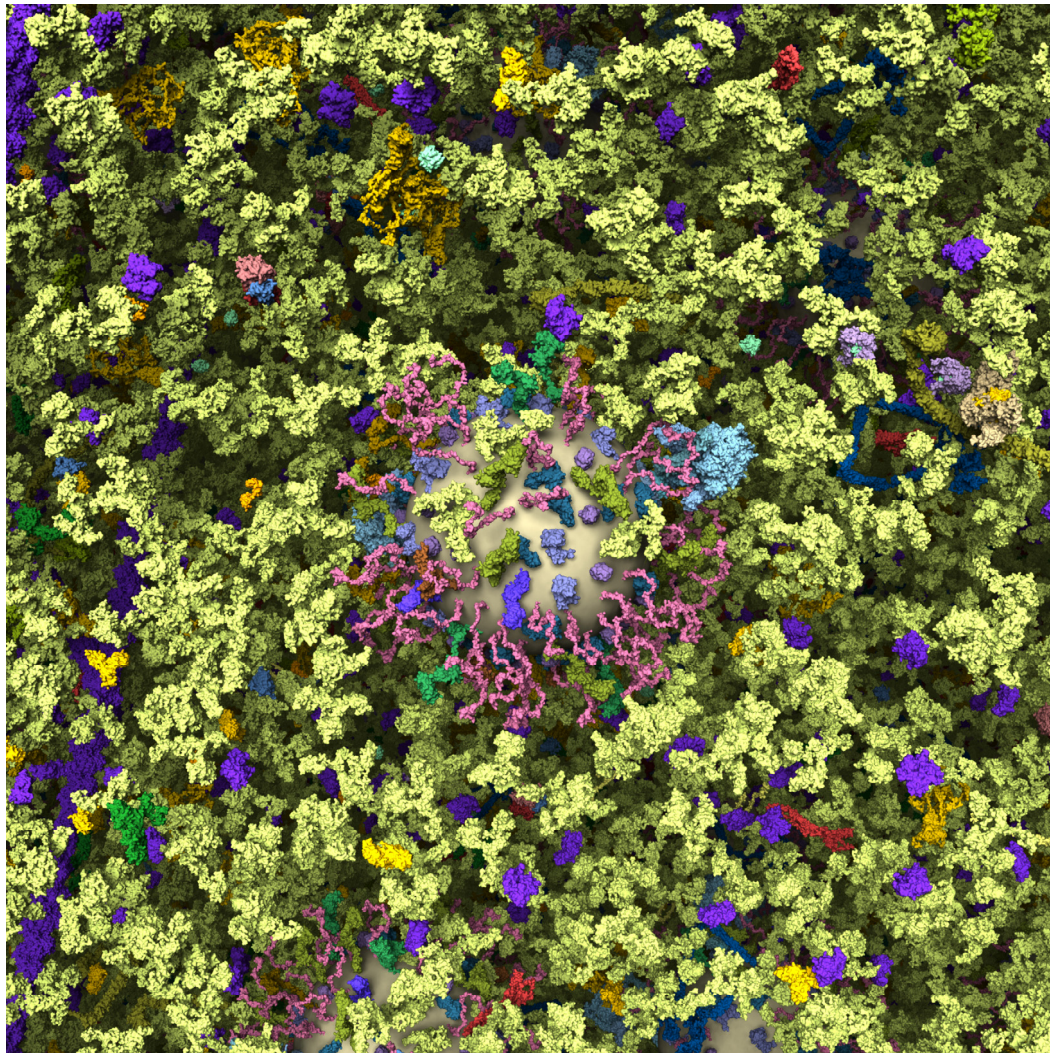


Figure 3-18: Magnification of a vesicle embedded in a network of cytosolic proteins

Graphical model obtained from data presented in 3.1 to 3.4 showing a zoom on a vesicle immersed in soluble proteins. The proteins included in this image are all listed in the legend underneath it.

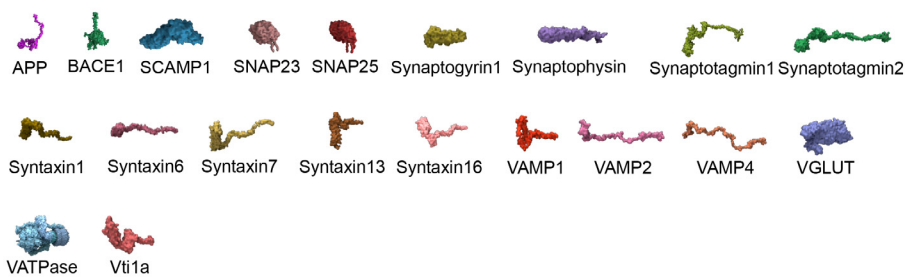
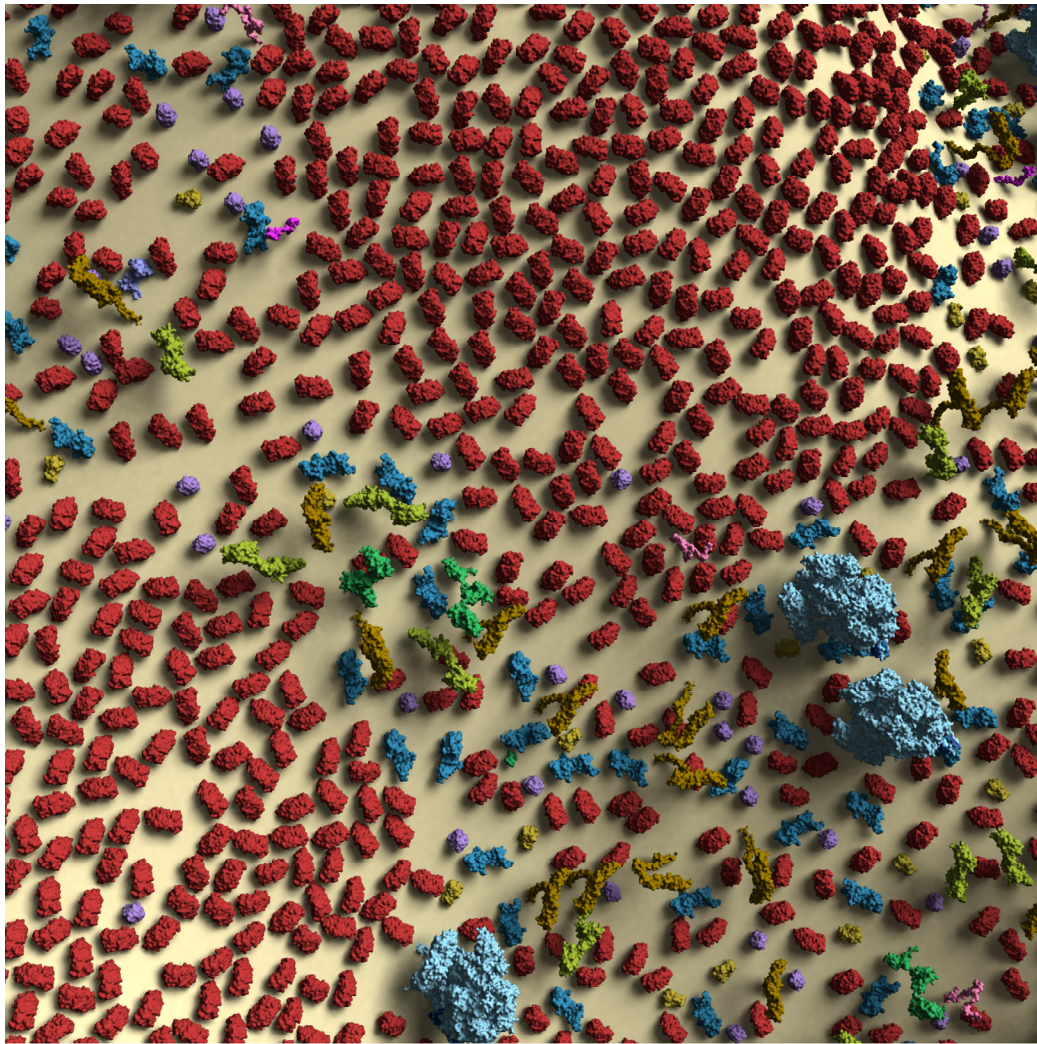


Figure 3-19: Magnification of a plasma-membrane area

Graphical model obtained from data presented in 3.1 to 3.4 showing a zoom on a plasma-membrane area. The proteins included in this image are all listed in the legend underneath it.

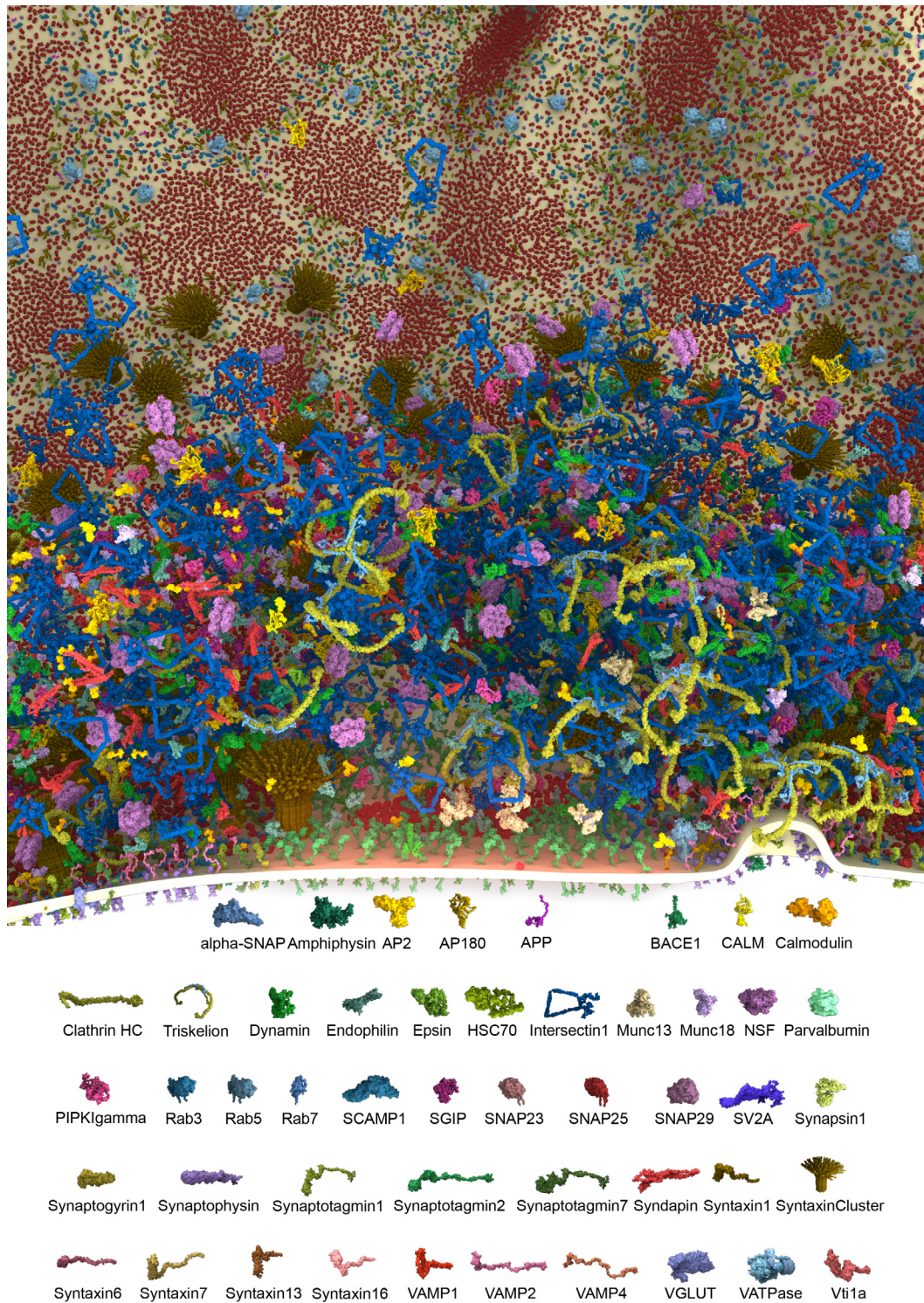


Figure 3-20: Magnification of the active zone area

Graphical model obtained from data presented in 3.1 to 3.4 showing a zoom on the AZ. The proteins included in this image are all listed in the legend underneath it.

4. Discussion

The ability of a multi-cellular organism to react to a stimulus is crucially dependent on the information exchange between at least two different cells. In the mammalian brain the major interface for information exchange between two neurons are the chemical synapses (see 1.1). Basically all complex behavior is mediated and controlled by a cascade of events within the pre-synaptic terminal which leads to transmission of the signal to the next cell. A dysfunction in this cascade can lead to a severe disorder or – in the worst case – to death. With regard to this it is not surprising that investigating the processes involved in signal transmission were a central element of molecular neurophysiological research in the past five decades. Numerous studies have investigated the synaptic composition throughout the years (e.g. Bai and Witzmann, 2007; Schikorski and Stevens, 1997; Takamori et al., 2006; Burre and Volkandt, 2007). However, a complete description of the synaptic architecture, its protein composition and their organization within the synapse is yet missing.

The ultimate aim of my work is to provide a comprehensive characterization of a pre-synaptic terminal of a brain synapse. I used isolated nerve terminals, so called synaptosomes (see 3.1) to investigate the ultrastructural architecture and molecular composition of a cortical pre-synaptic terminal. Consecutive electron micrographs were used for 3D reconstructions of the synaptosomes (see 3.2). These experiments provided all physical characteristics of the synaptosomes (such as size, shape, number and position of vesicles etc.) and allowed modeling the average pre-synaptic terminal. I further performed quantitative immunoblots to determine absolute copy numbers of 59 major synaptic proteins (see 3.3). In order to investigate the synaptic distribution and organization of these proteins, super-resolution STED microscopy was performed on immunolabeled primary hippocampal neurons and mouse NMJs (see 3.4). Finally, all information obtained concerning the pre-synaptic architecture (i.e. terminal structure, protein numbers and distribution) was combined to generate a graphical model of the average pre-synaptic terminal (see 3.5).

Although the claim of this study is to provide a model of the average brain synapse I am well aware that the “average” synapse is a theoretical construct which most likely does not exist as we describe it. Even though I choose to work with synaptosomes from only two distinct brain regions – cortex and cerebellum - it has to be expected that the individual synapses differ substantially in shape, composition and function. All assays of this study using synaptosomes

investigate this heterogeneous population of synapses at once and do not differentiate between different neuronal and synaptic subtypes. Nevertheless, this is not just the only feasible approach available today to quantify synaptic proteins but it also provides a considerable database of the general architecture of a pre-synaptic terminal. The majority of the proteins that were investigated in this study are abundant proteins, widely distributed over different neuronal populations and crucial for synaptic function in general, hence variations between different synapses can be expected to be rather small.

A comprehensive understanding of synaptic physiology can not be achieved by solely investigating individual protein functions but demands to regard the synapse as a whole. The findings presented in this work on the molecular composition of a pre-synaptic terminal allow for the first time to draw conclusions on the functional organization of a synapse. A thorough discussion of the implications of the spatio-temporal availability of proteins is provided in section 4.2. Prior to this I will elaborate on technical aspects concerning protein quantification in the following paragraphs.

4.1 Quantitative approaches

A central aspect of this study is the absolute quantification of pre-synaptic proteins using quantitative immunoblots I decided to use this technique for protein quantification as it is a robust and well established approach which has successfully been applied to similar questions in the past (Walch-Solimena et al., 1995; Takamori et al., 2006). However, there are two other technical approaches which could be used for protein quantification: mass spectrometry and quantitative microscopy. All three approaches as well as their applicability for quantitative studies will briefly be discussed in the following sections.

4.1.1 Quantitative mass spectrometry

Mass spectrometry has long been used as an analytical tool to qualitatively determine the protein composition of a certain sample (proteomics). Proteomic analysis of the brain started approximately 15 years ago (Fountoulakis et al., 1999) and has provided a wealth of data so far (Bai and Witzmann, 2007). Various studies have elucidated the qualitative protein composition of different neuronal sub compartments (see also 1.2) such as the postsynaptic density (Cheng et al., 2006; Hunt et al., 1996), the AZ (Volkhardt and Karas, 2012; Morciano et al., 2009), and the SV (Takamori et al., 2006; Burre et al., 2006). All these studies have

contributed significantly to our understanding of synaptic protein composition and ultimately synaptic function.

Recent advances, particularly in the sensitivity of mass spectrometers have opened the door towards absolute quantification of proteins by mass spectrometry (Nikolov et al., 2012; Schmidt and Urlaub, 2012). The existing approaches for quantitative mass spectrometry can be divided in two categories: label-based and label-free techniques.

Label-based techniques depend on either labeling the sample or the protein standard with stable isotopes (e.g. ^{13}C , ^{15}N , ^{18}O and ^2H). The labeled peptides are thus heavier than unlabeled ones which can be used for quantification (Boersema et al., 2009). Obviously, label-based techniques which required labeling of the proteins in the sample were no alternative for this study as native rat synapses were used as starting material. The most accurate method for absolute quantification is called absolute quantification (AQUA) and depends on chemically synthesized standard peptides which are labeled with stable isotopes. The AQUA peptides are added in defined amounts to the sample prior to ionization. Due to the different mass of the AQUA peptides compared to the native peptides, they can be distinguished in the mass spectrum and knowing the absolute amount of AQUA peptides used allows quantification of the native protein (Gerber et al., 2003; Desiderio and Kai, 1983; Kirkpatrick et al., 2005). Although this technique seems promising for future quantification studies it has one major pitfall: a specific AQUA peptide is required for every single protein ought to be quantified in a sample. This means that prior information about the proteins to be quantified is indispensable and that this technique is extremely cost intensive when applied to large protein sets since individual AQUA peptides are relatively expensive (Nikolov et al., 2012; Schmidt and Urlaub, 2012).

One of the most accurate label-based techniques is iBAQ (Schwanhausser et al., 2011). This technique is similar to the AQUA method outlined above. In iBAQ, peptides derived from standard proteins are used instead of the labeled AQUA peptides (see above). As the concentration of the standard protein and hence also of the peptides is known, the resulting intensity in the mass spectrum can be used to quantify the protein number in the sample (Schwanhausser et al., 2011). Also in this approach peptides of every protein of interest have to be available but as they are not labeled they are substantially easier and cheaper to obtain. However, since the peptides derived from the standard proteins are – unlike AQUA peptides – not labeled with stable isotopes the iBAQ technique is less sensitive compared to AQUA.

Nevertheless, iBAQ offers a feasible and reliable approach for protein quantification using mass spectrometry.

The major issue for reliable mass spectrometry derived quantification data is proper digestion of the proteins. Especially membrane proteins are difficult to digest due to their amphipathic nature (Santoni et al., 2000, but see also Rabilloud, 2009). Studies have shown that approximately 30% of the mammalian genome encodes for trans-membrane proteins (Stevens and Arkin, 2000). The pre-synaptic terminal also contains many integral membrane proteins which fulfill crucial functions during neurotransmission (e.g. SNARE proteins, Synaptotagmins etc.) and were quantified in this study. In regard to this, I concluded that using mass spectrometry for determining absolute protein amounts in the synaptosomes would not necessarily be more accurate and reliable than using quantitative immunoblots (discussed in 4.1.3) but it would offer an alternative approach to validate data obtained by quantitative immunoblots. Hence, iBAQ was used in collaboration with Prof. Dr. Henning Urlaub and Sunit Mandad and largely confirm most of the results presented here (data not shown).

4.1.2 Quantitative microscopy

Microscopy traditionally is a qualitative technique mainly used to investigate the structural composition of a sample. Advances in labeling, imaging and detection technology opened an avenue for quantitative studies using microscopy. The general concept common to all microscopy-based quantification assays is that the absolute number is determined by comparing the signal obtained by the sample to a signal obtained by a standard. Most commonly, antibody labeling is used to visualize the protein of interest. In this context the signal obtained from a single protein-antibody complex (representing one protein) is used as the reference for quantification and all signals obtained from the sample are hence integral multiples of it (Mutch et al., 2011a).

Quantitative mass spectrometry and immunoblots are bulk biochemistry methods which determine the protein amount of entire populations of organelles/ compartments (depending on the purification procedure). In contrast to this the major advantage of microscopy-based quantification methods is that these techniques are able to address single units of a sample individually. Thus, microscopy-based quantification assays are not only capable of determining the average copy number but also the degree of variation in protein numbers between the different units (Mutch et al., 2011a).

The first steps towards quantitative microscopy were taken in the field of microfluorometry. Here, quantitative immunofluorescence was used to determine the composition of different solutions (Jongsma et al., 1971). In neurons the first study performing quantitative microscopy employed immunogold EM to determine the copy number of different receptors at the post-synaptic density (Nusser, 1999; Tanaka et al., 2005). Later studies used fluorescence microscopy instead of EM to address the copy number of post- (Sugiyama et al., 2005) as well as pre-synaptic proteins (Chiu et al., 2002; Chiu et al., 2001).

The most recent study using fluorescence imaging for quantifying protein amounts partially revisited the composition of the SV (Mutch et al., 2011b). Interestingly, they found – compared to Takamori et al., 2006 – varying copy numbers for several proteins. They determined the vesicular copy numbers of vATPase, SV2, VGlut1, Synaptotagmin 1, Synaptogyrin 1, VAMP 2 and Synaptophysin. All but vATPase varied significantly from previous results (Takamori et al., 2006) ranging from 6.6-fold less to 3.4-fold more protein. Furthermore, they were able to determine the variance of these seven proteins revealing that VAMP 2, Synaptophysin and Synaptogyrin 1 have a high inter-vesicle variability (Mutch et al., 2011b).

As mentioned before the biggest advantage of microscopy-based quantification assays is that every unit of a sample is addressed individually making it possible to draw conclusions on the variability of the units. Providing not only the average but also a reliable variance for each unit renders microscopy a powerful tool for quantification studies. Unfortunately, microscopy-based quantification approaches are suffering from two technical limitations which will bias the results substantially:

The first problem comes along with the fact that quantitative microscopy relies on characterizing individual elements rather than bulk samples (compare with quantitative immunoblots and mass spectrometry). Therefore, the applicability of quantitative microscopy crucially depends on (a) investigate only well separated particles as accumulations would render it impossible to quantify individual elements and/ or (b) an imaging system with superior 3D resolution. The latter is for example provided in recently developed 3D super-resolution microscope systems such as 3D-STED (Schmidt et al., 2008) and 3D-STORM (Huang et al., 2008, reviewed in Huang et al., 2010).

The second problem of quantitative microscopy is inherent to the nature of an antibody labeling. In most quantification assays based on microscopy a combination of primary and secondary antibody is used to label the protein of interest. A single antibody is approximately

150 kDa and 10 nm in diameter (Galbraith and Galbraith, 2011; Blondeau et al., 2004). This is already substantially larger than most synaptic proteins. For a comparison: a SV has an average outer diameter of approximately 42 nm and the most abundant vesicle protein VAMP 2 weights less than 20 kDa (Takamori et al., 2006). Recently, two independent studies using super-resolution microscopy have shown that the labeling efficiency of proteins in close proximity is crucially dependent on the size of the label. In both studies the use of smaller labels (so called Aptamers and Nanobodies respectively) led to a higher labeling density of the same samples. This demonstrates that antibodies – and in particular a complex consisting of primary and secondary – are unable to label proteins which are in close proximity to each other (Opazo et al., 2012; Ries et al., 2012). Therefore, it has to be assumed that quantitative microscopy-based on immunolabeling will underestimate the copy numbers for densely packed proteins substantially. These findings shed new light onto the differences in copy numbers of SV proteins reported by quantitative immunoblots (Takamori et al., 2006) and quantitative microscopy (Mutch et al., 2011b). In agreement with this concept, for all proteins which were found to be highly abundant on SVs the number obtained by quantitative microscopy is substantially lower compared to quantitative immunoblotting (Synaptophysin, VAMP 2, VGlut and Synaptotagmin 1). In contrast, estimates for less abundant proteins were equal or higher when quantified with fluorescence microscopy (vATPase, SV2 and Synaptogyrin 1).

In summary, protein quantification based on microscopy has the advantage to quantify individual units of a sample rather than a bulk composition but is not suitable for determining copy numbers of proteins which are densely packed.

4.1.3 Quantitative immunoblots

Quantifying proteins using western immunoblotting is probably one of the oldest techniques for protein quantification (Schiavini et al., 1989). So called western blotting is in general a very well established and widely used technique for qualitative protein detection (Towbin et al., 1989). The difference to quantitative western blots is that the latter involves a protein standard which is processed in parallel to determine the absolute amount of a certain protein in the sample (Takamori et al., 2006). This in turn implies that the respective protein standard has to be obtained for every protein which is to be quantified. Generally, these standards are purified proteins or peptides oftentimes recombinantly expressed and isolated from heterologous expression systems. Unfortunately, not all proteins can be purified equally

well yet, which is why the amount of different proteins quantified in this study is limited to the 59 proteins listed in 3.3. A reliable and reproducible quantification of proteins using western blots generally faces two major challenges: (1) antibody specificity and (2) efficient transfer of the proteins onto the membrane.

(1) The antibody used for detection of the protein of interest has to be able to detect the standard protein and the endogenous protein in the sample equally well. This is particularly difficult if the standard protein is a recombinantly expressed and purified version of the protein of interest. These recombinant proteins might only contain a part of the original protein sequence or might even be derived from a different species. In these cases it is extremely important that the selected antibody was raised against a specific immunogen which is conserved in both the recombinant and the endogenous protein. Another factor which is extremely difficult to address is the effect of protein glycosylation on antibody binding. Glycosylation is a major protein modification following translation and some synaptic proteins are known to be glycosylated prior to their integration into the synapse (e.g. Kwon and Chapman, 2012). Glycosylation is not only involved in proper sorting and trafficking of the respective protein but also affects its tertiary structure (Kittler and Moss, 2003; Vagin et al., 2009). Since it is easier to express proteins in prokaryotic organisms, most recombinant expression systems rely on bacteria as expression hosts. Unfortunately, bacteria lack eukaryotic post-translational modifications such as formation of disulfide bonds and glycosylation (Baneyx, 1999). Therefore, recombinant proteins which are used as standard proteins could in principle have an altered affinity to the antibody compared to the endogenous protein. As mentioned before, this is an almost impossible bias to address. The only possibility in my view is to use antibodies raised against a part of the protein which is not (neither directly nor indirectly) affected by glycosylation (providing all glycosylation sites are known). Finally, one aspect which could also bias antibody detection lies in the process of separating the proteins (SDS-PAGE). The endogenous protein is part of a mixture of different proteins (in this case the synaptosome preparation) and usually accounts for only a small percentile of the entire protein amount. On the other side, the protein standard which is separated in parallel to the endogenous protein is naturally not present in a protein mixture and ideally makes up close to 100% of the total protein. The general protein density is therefore a lot higher in the sample than in the protein standard. This could in principle influence separation as well as transfer onto the membrane and ultimately detection of the protein of interest. To overcome this bias I decided to mix the

protein standard with an equal amount of FCS to imitate the total protein concentration in the sample (see also 3.3).

(2) Efficient transfer of the immobilized proteins from the polyacrylamide gel onto the nitrocellulose membrane is crucial for reliable quantification of different protein amounts. Incomplete transfer of a protein band will inevitably lead to biased results. Also, proteins with different molecular weights are transferred differently – the higher the molecular weight the slower the transfer. This is particularly important as some standard proteins (when recombinantly expressed with tags or as shorter sequences) might have higher or lower molecular weights compared to the native protein. This bias was avoided in this study by (i) using only standard proteins which had similar molecular weights and (ii) using wet transfer conditions with field electrodes (providing a homogeneous electrical field) and rather strong transfer conditions to ensure complete protein transfer (see 2.9). A good indicator whether a certain protein range is transferred properly is the protein ladder run in parallel to the samples. If marker bands are entirely transferred the same can be assumed for the proteins in the samples. Another good intrinsic control is the linearity of the signal obtained from the standard protein. If the blot shows a linear dependence between amount of standard protein loaded and signal obtained over a certain range of protein it can safely be assumed that varying protein amounts are transferred reliably and also that varying protein amounts are detected properly (see (1)). It is important to mention again, that such standard curves depend on the affinity of the antibody to the protein and represent a sigmoid curve when looking at a large range of protein amounts. However, all such curves have a linear part which can be used for determining the amount of protein (see 3.3).

Besides taking care of the issues outlined in (1) and (2) I also used near infrared dyes for detection of the primary antibody (see 2.9). These dyes are highly sensitive and show a wide linear detection range (Weldon et al., 2008; Wang et al., 2007). However, their major advantage is that the signal is detected in a range (i.e. around 800 nm) which naturally detects less auto-fluorescence (Monici, 2005) providing hardly any noise which could bias the signal.

In summary, I choose to use immunoblots for the absolute quantification of pre-synaptic proteins. This approach has proven numerous times in the past to be able provide reliable quantitative data (e.g. Takamori et al., 2006) and was – at least in my hands – as accurate as quantitative mass spectrometry by iBAQ (data not shown). An approach based on quantitative microscopy would have provided substantially more information on the inter-synaptic variability

but it was not worth to trade this for a reduction in accuracy which would render the rest of the quantification useless. In regard to this, I am convinced that quantitative immunoblotting is still the most reliable and robust technique to determine the absolute protein amount of a biological sample and thus perfectly suited to investigate the molecular composition of a pre-synaptic terminal.

4.2 Stoichiometric biology of a pre-synaptic terminal

A main part of this study dealt with the determination of absolute protein copy numbers per pre-synaptic terminal in which I quantified 59 pre-synaptic proteins. In the next section these proteins are grouped to my best knowledge according to overt function within the synapse. Further, every proteins abundance and distribution is discussed in context of synaptic physiology. All copy numbers mentioned for individual proteins in this section are rounded from Table 3-4.

Cytoskeletal and associated proteins

The main elements of the cellular cytoskeleton are microtubules and Actin filaments. The former is composed of Tubulin molecules and functions as neuronal highways which transport cargo vesicles down axons into the pre-synaptic terminal (and vice versa). The amount of Tubulin we estimated is sufficient for approximately 4 μm of synaptic microtubules – a number which seems reasonable assuming 4-5 microtubule tracks entering a pre-synaptic terminal and approximately 20% monomeric molecules (Conde and Caceres, 2009).

On the other hand, Actin filaments are known not only to reach into the synapse but to form a complex network within and especially around the vesicle cluster. It is expected to function as a passive scaffolding system for vesicles and regulatory molecules (Dillon and Goda, 2005). Assuming 30% of all Actin molecules being in filaments and 70% monomeric (Sankaranarayanan et al., 2003) yields 15452 free molecules and approximately 18 μm of Actin filament according to my calculations. At a first glance these values seem rather high for a cytoskeletal protein within the synapse. However, since Actin does not only serve as a network for connecting vesicles (Bloom et al., 2003) but is also involved in the scission and re-integration of vesicles into the cluster (Taylor et al., 2012; Merrifield et al., 2002), these findings are plausible.

Septin 5 is localized to the periphery of AZs in mature brain neurons and has been suggested to regulate the spatio-temporal organization of neurotransmitter release (Yang et al., 2010b). In terms of copy numbers, I found an equivalent of approximately 11 μm of pure Septin 5 filament in the synaptosomes. Within the native synapse it is expected that Septin filaments are not solely composed of Septin 5 but also other Septin isoforms (e.g. Septin 7). Further, these filaments are predominantly located around the AZ and their lengths are multiples of 25 nm (Hsu et al., 1998). The Septin oligomers might bind to Syntaxin molecules and thereby preventing release outside of the AZ (Beites et al., 1999; Beites et al., 2005). However, binding to Syntaxin has been reported for various proteins ranging from calcium channels (Sheng et al., 1994) to Ribosomes (unpublished observations from Silvio O. Rizzoli). Therefore, it is uncertain whether this is a physiologically relevant binding or a biochemical artifact. Unfortunately, too little is known about the specific role of Septin 5 in the synapse in order to speculate further on the number of molecules in a physiological context.

Synapsins are cytosolic proteins and their role in the pre-synaptic terminal has been extensively investigated in the past two decades. They have been demonstrated to be involved in reversible tethering of SVs to the Actin cytoskeleton and in maintaining the reserve pool of vesicles cross-linked and immobile. Following stimulation Synapsin is phosphorylated and dissociates from the SVs. The freed vesicles can now move within the synapse for instance to reach potential fusion sites. More recent studies have suggested that some Synapsin molecules actually remain on the vesicles and are involved in docking and priming steps preceding exocytosis. Further, free Synapsins can potentially stimulate the formation of Actin filaments and therefore also assist in reintegrating recently endocytosed vesicles into the vesicle cluster (Cesca et al., 2010). In their characterization of the molecular composition of the SV, Takamori and colleagues found approximately 8 Synapsins to be present on a vesicle after purification. However, due to the harsh conditions during SV purifications it can be assumed that this number is not representative for the actual amount of Synapsin molecules linked directly or indirectly to a single vesicle. In this study I found substantially more Synapsin molecules per pre-synaptic terminal: 107222 Synapsin I and 26732 Synapsin II molecules resulting in a total of 133954 Synapsins per synapse rendering it one of the most abundant proteins addressed in this study. Containing such a large amount of Synapsin molecules certainly has an influence on the viscosity of the synaptic cytosol. Under these circumstances, it can be assumed that the cytosol has the consistency of a gel-like matrix (see Figure 3-18, see also Siksou et al., 2007; Hirokawa et

al., 1989). This matrix might be crucial in maintaining the SVs in the terminal (Orenbuch et al., 2012) were these in turn function as a molecular buffer in maintaining accessory proteins in the synapse (Denker et al., 2011b). In this respect, the cyto-matrix created by the Synapsin molecules and the large vesicle cluster might complement one another in retaining themselves as well as other soluble proteins in the pre-synaptic terminal. Surprisingly, however, a Synapsin triple KO mouse model failed to display any severe synaptic phenotype (Fornasiero et al., 2012; Gitler et al., 2004). This is difficult to explain especially regarding the high abundance of Synapsin in a pre-synaptic terminal. In case of its potential function as a molecular buffer in conjunction with the SV cluster it could be assumed that the cluster is sufficient for retaining crucial amounts of protein but that the system is of course more efficient with Synapsin in addition.

Calcium buffers

The three calcium buffers investigated in this study – Calbindin (297 copies), Calretinin (369 copies) Parvalbumin (681 copies) – regulate the precise spatio-temporal course of calcium signals. Studies using transgenic mouse models have outlined their significance for signaling pathways involved in neuronal network formation (Schwaller, 2011). All three were found in similar amounts in the synaptosomes. However, as mentioned in 3.5 they are differentially expressed within cortical and cerebella synapses (Schwaller, 2010) which will naturally lead to an underestimation of their synaptic abundance in this assay. In this respect, it has to be assumed that at most 5% of the synapses in the preparations contain Calbindin, Calretinin and Parvalbumin (personal communication with Prof. Beat Schwaller). Hence, neurons that express one of the three proteins have at least 20-fold more molecules per synapse than I estimated previously (see section 3.3). This is particularly evident regarding the high endogenous buffer capacities reported for central neurons (Helmchen et al., 1996; Aponte et al., 2008). Therefore, it has to be assumed that the numbers in table 3-4 have to be corrected by this factor to obtain a more accurate minimal estimate (see Table 4-1).

Table 4-1: Corrected protein numbers for the calcium buffers.

Protein	Molecules per synapse	Molarity [μM]
Calbindin	5938.0 \pm 264.0	9.00
Calretinin	7384.0 \pm 110.0	11.20
Parvalbumin	13622 \pm 686	20.06

Calcium binding messenger protein

Calmodulin is not only an important intermediate messenger in calcium dependent signaling cascades but accumulating evidence also outlines its involvement in regulating SV recycling (Igarashi and Watanabe, 2007; Halling et al., 2005). Interestingly, the protein has been suggested to play a role during short term plasticity being crucial for refilling of the readily releasable pool of vesicles after stimulation (Sakaba and Neher, 2001). In line with these findings I have reported Calmodulin to be highly abundant in the SV cluster (see Figure 3-13). Also the amount of protein I found (8660 molecules) seems reasonable in regard of a protein which is (i) equally distributed within the entire vesicle cluster (ii) and expected to interact with highly abundant proteins such as VAMP 2 (Quetglas et al., 2002) and Rab3 (Coppola et al., 1999).

Calcium sensors

In this study I determined the absolute abundance of four synaptic calcium sensing molecules: the three most abundant Synaptotagmin isoforms - 1 (10332 molecules), - 2 (3457 molecules) and - 7 (183 molecules) as well as Doc2 (3697 molecules). Generally it is expected that the different calcium sensors found in secretory cells work together and most likely also interact to regulate vesicle fusion (Walter et al., 2011).

As expected, I found Synaptotagmin 1 to be the most abundant calcium sensing protein (Geppert et al., 1994). The amount of molecules I found per pre-synaptic terminal is well in agreement with previous studies on the functional organization of the protein within the synapse: the majority of the 10332 molecules most likely reside on SVs (15 molecules per vesicle according to Takamori et al., 2006), a substantial fraction on the plasma membrane (approximately 20% according to Opazo et al., 2010) and the remaining molecules on recycling endosomes (Hoopmann et al., 2010; Rizzoli et al., 2006; Uytterhoeven et al., 2011). I therefore conclude that the amount of Synaptotagmin I found as well as its synaptic organization confirms

previous findings about the functional organization of Synaptotagmin 1 in the pre-synaptic terminal.

Doc2 has recently been reported to function as a calcium sensor during spontaneous neurotransmitter release (Groffen et al., 2010, but see also Pang et al., 2011 and Yao et al., 2011). However, regarding the rather low frequency of spontaneous release in most neurons (Geppert et al., 1994; Frerking et al., 1997) it is difficult to understand why this protein is so abundant (3697 molecules) in a pre-synaptic terminal. The following hypothesis could provide a possible explanation for this: Doc2 is a soluble protein and its function as a calcium sensor to initiate vesicle fusion depends on coincidence detection of calcium and a fusion-competent vesicle (Groffen et al., 2010). The widespread distribution of vesicles within almost the entire terminal (see Figure 3-6) demands either site specific recruitment of Doc2 in case of a spontaneous fusion event or a large amount of molecules which cover the entire area. The latter scenario seems easier to implement for the cell and could therefore provide an explanation for the high amount of Doc2 per pre-synaptic terminal. The distribution of Doc2 throughout the entire vesicle cluster (see Figure 3-13) could further be interpreted as indirect evidence for a single pool of SVs that maintains active and spontaneous release (Wilhelm et al., 2010; Groemer and Klingauf, 2007; Hua et al., 2010). In case of a separate pool of vesicles for spontaneous release it would not be expected to find the potential spontaneous fuser molecule equally distributed amongst all vesicles.

Integral vesicle proteins

The precise function of SV2 is still under debate. Recent studies suggest that the protein is involved in (i) mediating expression and trafficking of Synaptotagmin (Yao et al., 2010) and (ii) regulating calcium mediated exocytosis in general (Wan et al., 2010; Chang and Sudhof, 2009). In agreement with studies reporting SV2 to be present on SVs (Bajjalieh et al., 1992) both of the stainings show a highly vesicular organization (see Figure 3-13 and 3-14 respectively). In the quantification experiments I found 46166 molecules of SV2 per single synaptosome. Regarding the study of Takamori et al., 2006 who found approximately 2 copies of SV2 per single SV, it could be assumed that my determined copy number is a significant overestimate of the real amount. As mentioned previously, functional SV2 contains many post-translational glycosylations (Buckley and Kelly, 1985) which are known to influence protein folding and therefore also detection on immunoblots (see 4.1.3). In this case the different glycosylation

patterns of (a) the purified SV2 used as standard for the immunoblot and (b) the native protein in the sample did most likely result in altered binding affinities of the antibody for the two versions of the protein. Therefore, a lowered affinity of the antibody for the purified standard protein will naturally cause an overestimation of the actual protein (since more standard protein is needed to obtain a signal equal to the signal of the sample). However, in regard of the fact that SV2 has reliably been used for immunoisolation of SVs (e.g. Morciano et al., 2005) it is also difficult to accept that every vesicle should only be equipped with two copies of it. In line with this, the enrichment blot for SV2 in the study of Takamori et al. (part of the supplementary material) shows the most prominent enrichment of all 85 proteins tested for enrichment during SV purification. Therefore, I expect our number to be an over- and their number to be an underestimate of the actual synaptic SV2 amounts.

Interestingly, I also found rather large amounts of Synaptogyrin (9927 copies per synapse), which was also shown to be rather scarce on SVs (2 copies according to Takamori et al., 2006). However, unlike SV2 it is not exclusively localized to SVs but also present on the plasma membrane and on endosomes (see Figure 3-13). Up to now, only very little is known about the function of this protein. It has been proposed to fulfill an essential function during synaptic plasticity together with Synaptophysin (Janz et al., 1999a). However, the fact that Synaptogyrin is so abundant in a pre-synaptic terminal delineates it an interesting candidate to hold an important function in synaptic physiology. It will be interesting to follow future studies on this particular protein and especially how its function could be related to its number and distribution.

Synaptophysin is a specific component of SVs accounting for approximately 10% of their total protein content (Takamori et al., 2006). Although its precise function is still debated it is frequently used as the most reliable marker for SVs (Thiel, 1993) and has been used for immunoisolation of SVs (Burger et al., 1989). Although studies with transgenic mice failed to report a synaptic phenotype (McMahon et al., 1996) the protein is expected to be involved in SV recycling (Bonanomi et al., 2006). One of the most prominent theories is based on its interaction with cholesterol (Thiele et al., 2000): it is known that cholesterol is enriched in the membrane of SVs compared to the neuronal plasma membrane (Takamori et al., 2006; Vincendon et al., 1972; Pfrieger, 2003). In line with this it has been proposed that the enrichment in cholesterol is the underlying mechanism for sorting of the vesicular material into patches prior to endocytosis. The cholesterol depending micro-domains, which among other proteins also contained

Synaptophysin, are thought to be the lateral organizer of SV endocytosis (Jia et al., 2006). In this regard the formation of Synaptophysin homo-oligomers (dimers to hexamers, see Pennuto et al., 2002 and Johnston and Sudhof, 1990) could be envisioned to facilitate the formation of cholesterol enriched micro-domains. On the other hand, the ability of Synaptophysin to form hetero-oligomers (again dimers to hexamers) with, for instance, VAMP 2 (Pennuto et al., 2002; Calakos and Scheller, 1994) or vATPase (Galli et al., 1996) might initiate the gathering of specific vesicle proteins at the cholesterol pit (see for example Gordon et al., 2011). Interestingly, Synaptophysin has also been found to be trafficked to SVs with high precision – more specific than any other SV protein (Pennuto et al., 2002) a trait likely to be linked to its binding to cholesterol (Thiele et al., 2000). Summing up these observations it could be speculated that Synaptophysin holds a leading position in the formation of SV pits on the plasma membrane, which are ready for endocytosis. In line with this only few SV proteins have been demonstrated to be sorted by classical adaptor proteins such as AP2 and AP180 (McMahon and Boucrot, 2011) and this gap could at least partially be closed by Synaptophysin-mediated pre-sorting of proteins in the pit. In respect to this theory one would expect Synaptophysin to be present in large amounts on SVs (31.5 copies per vesicle according to Takamori et al., 2006), the plasma membrane (particularly around the AZ) as well as in recycling endosomes (Cameron et al., 1991). I found approximately 31102 copies of Synaptophysin per pre-synaptic terminal. According to the stainings (see Figure 3-13) and in agreement with the above outlined literature a third of the protein is expected to reside directly on vesicles, half on the plasma membrane and the rest in endosomal compartments.

Exocytosis – docking and priming of vesicles

Two important proteins for docking and priming of SVs are Munc13 and -18 (Verhage and Sorensen, 2008). The latter is expected to bind Syntaxin 1 forming a stable complex likely serving as an early docking platform for vesicles (Gulyas-Kovacs et al., 2007; Toonen et al., 2006a). Munc13 on the other hand is proposed to prime the SNARE complex for fusion (Varoqueaux et al., 2002; Augustin et al., 1999). Hence, both proteins are apparently involved in preparing the fusion of the vesicle with Munc13 being downstream of M18 in this process (Verhage and Sorensen, 2008). As depicted in Figure 3-13, both proteins seem to be similarly organized within the pre-synaptic terminal. Interestingly, I found substantially more Munc18 (4253) than -13 (1551) molecules per synapse. Regarding that Munc13 functions downstream of

Munc18, this stoichiometry can be meaningful for regulating vesicle priming: having Munc13 (i.e. the downstream element) as the rate-limiting factor has the advantage that the cell can rapidly adapt to lower or higher demands simply by changing the availability of this one protein. This would not be possible if Munc18 (i.e. the upstream element) would be the rate-limiting element, hence this configuration renders the system flexible to different demands.

Another interesting aspect is that both proteins have a significantly lower abundance compared to their putative partners in the course of SV fusion (e.g. SNAREs). In line with this, over-expressing each of the two separately leads to increases in neurotransmitter release (Toonen et al., 2006b; van de Bospoort et al., 2012). Hence, the docking and priming function carried out by Munc13 and -18 could potentially be a rate-limiting for vesicle fusion.

Rab3a has been shown to regulate the release probability of SVs (Schluter et al., 2004) but the exact mechanism is still unknown. I found it to be one of the most abundant pre-synaptic proteins with 30736 molecules which are all localized to the SV cluster (see Figure 3-13 and 3-14). Although it is a soluble protein and only associated with vesicles Takamori and colleagues still found approximately 10 copies on purified SVs. Regarding that (i) changes in the composition of the cytosol cause Rab3a to dissociate from the vesicles (Fischer von Mollard et al., 1991) and that (ii) 10 copies still remained on vesicles after purification it can be expected that substantially larger amounts are associated with the vesicle cluster *in vivo*.

Exocytosis – vesicle fusion

Fusion of SVs is known to be mediated by two target (t-) and one vesicular (v-) SNARE proteins. One of the t-SNAREs is generally from the SNAP protein family of which SNAP 23, 25 and 29 were found in neurons both in previous studies and by us. SNAP 23 and 29 are ubiquitously expressed (Jahn and Scheller, 2006) and were found in low amounts (266 and 78 molecules per synapse respectively) in the synaptosome preparations. According to the stainings (see Figure 3-13 and 3-14) they are most likely localized to vesicles, endosomes and the plasma membrane. In regard of the low amounts I found for both of them in the synapse it can be expected that they at most serve a supportive function for SNAP 25 and are not crucial for pre-synaptic neurotransmitter release (Sorensen et al., 2003; Chen et al., 1999).

In comparison, SNAP 25 is expected to be one of the key elements of the neuronal SNARE complex and with 132090 copies it is the most abundant pre-synaptic protein I investigated. The protein is apparently not involved in spontaneous vesicle fusion and has been

demonstrated to be essential for calcium evoked neurotransmitter release (Washbourne et al., 2001; Bronk et al., 2007). However, the vast amount of SNAP 25 present in synapses which is in line with previous studies (Walch-Solimena et al., 1995; Knowles et al., 2010), indicates that SNAP 25 is presumably not the limiting factor in SNARE complex assembly (see discussion of CSP for alternative ideas on this topic). In line with this, it was shown that not only deletion but also over-expression of SNAP 25 caused a perturbation of SV release (Low et al., 1999). Interestingly, silencing of SNAP 25 has both been reported to reduce secretion in PC12 cells (Cahill et al., 2006) but also to increase the calcium responsiveness of neurons (Condliffe et al., 2010). These results suggest that the amount of SNAP 25 crucial for SV fusion lies somewhere between the extremes; or in other words: that not all SNAP 25 molecules in the synapse are needed for SNARE complex formation and that the remaining molecules might serve another distinct function. It would be very interesting to determine the critical amount of SNAP 25 molecules directly needed for SV fusion. This could for example be achieved by applying defined amounts of neurotoxins (Lang and Jahn, 2008) to sequentially titrate the amount of functional SNAP 25 in the synapse and observe synaptic function in parallel (e.g. using electrophysiology or microscopy assays for vesicle recycling). According to recent findings on the number of SNARE complexes needed for vesicle fusion (Mohrmann et al., 2010; Sinha et al., 2011; van den Bogaart et al., 2010) it has to be expected that only a minor fraction of the SNAP 25 molecules I found is directly involved in SV fusion (see also Bethani et al., 2009). In view of these findings, it is tempting to postulate alternative scenarios for the distinct function of the vast amount of remaining SNAP 25 molecules: in respect of the silencing studies (Cahill et al., 2006; Condliffe et al., 2010) it seems unlikely that the rest of the molecules are only a reserve pool for SNARE complex formation. As illustrated in Figure 3-17, a substantial fraction of the plasma membrane is covered with SNAP 25 molecules when placing the determined copy numbers into the average pre-synaptic terminal. Thus, it could be assumed that SNAP 25 somehow shields the membrane from intra-synaptic components and proteins. The pre-synaptic terminal is a very confined space in which processes have to occur at specific sites (e.g. SV fusion at the AZ). The lawn of SNAP 25 on the plasma membrane may ensure that vesicles do not just fuse randomly everywhere in the terminal but only at specific sites under defined conditions (see also 4.2.2). This hypothesis could be tested by observing potential changes in neuronal secretion sites in cells with reduced SNAP 25 levels or upon acute SNAP 25 ablation by neurotoxins (see above).

The second t-SNARE important for neuronal exocytosis is Syntaxin 1 which I found to be present in 20096 copies per pre-synaptic terminal. According to the stainings (see Figure 3-13) the majority of the molecules are residing in the plasma membrane while some are also associated to SVs (6 molecules according to Takamori et al., 2006) and to recycling endosomes (Hoopmann et al., 2010; Uytterhoeven et al., 2011). The majority of the molecules in the plasma membrane (67 %) has been demonstrated to be arranged in 50 – 60 nm clusters on the plasma membrane (Sieber et al., 2007) in PIP2 dependent patches (van den Bogaart et al., 2011). The remaining molecules diffuse freely in the plasma membrane and are in a dynamic equilibrium with the ones in the cluster. Interestingly, the molecules within the clusters are functionally inactive due to steric hindrance (Sieber et al., 2007). This suggests that the free molecules are the ones involved in SNARE complex formation (see also Yang et al., 2012). Although Syntaxin 1 is generally accepted to be an essential component of the synaptic SNARE complex (Jahn and Scheller, 2006) transgenic mice are perfectly healthy and do not display major defects in neurotransmitter release (Fujiwara et al., 2006). As for the other two major neuronal SNAREs (see above and below) also Syntaxin 1 is highly abundant and the function of this superabundance is not yet clear especially regarding the just mentioned inactivity of the molecules within a cluster (Sieber et al., 2007). According to the abundance of free Syntaxin 1 outlined above, we estimate approximately 5800 copies freely diffusing in the plasma membrane (33% of the fraction residing in the plasma membrane, Sieber et al., 2007). It is well known that Munc18 binds to Syntaxin 1 prior to SNARE complex formation (Ma et al., 2012) and interestingly the amount of free Syntaxin 1 molecules in the plasma membrane correlates remarkably well with its putative interaction partner Munc18 (4253 molecules, see discussion above).

The most prominent neuronal v-SNARE is VAMP 2 (also called Synaptobrevin 2) of which I found 26448 copies per synaptosome. Another neuronal v-SNARE which was studied here is VAMP 1. Its function is largely overlapping with VAMP 2 but it shows a slightly different expression pattern in the brain which is probably also a reason why I found it to be significantly less abundant than VAMP 2 (3884 molecules). Genetic deletion of VAMP 2 leads to a drastic reduction of spontaneous and particularly of evoked neurotransmitter release (Schoch et al., 2001). The amount of VAMP 2 I determined for a single pre-synaptic terminal correlates well with Takamori et al., 2006 who found approximately 70 copies on a SV. Although, VAMP 2 is known to mainly reside on vesicles some molecules are also expected to be found on the plasma

membrane (e.g. AZ and peri-AZ) and on recycling endosomes (Hoopmann et al., 2010; Uytterhoeven et al., 2011). Nevertheless, as for the other neuronal SNARE proteins, the question remains why there are so many of them if apparently only a minor fraction is needed.

In summary, the three key molecules in SV fusion, SNAP 25, Syntaxin 1 and VAMP 2, are all present in ample amounts at a pre-synaptic terminal. Nevertheless, several recent studies could show that between 1 and 3 SNARE complexes are sufficient for fusion of a single vesicle (Mohrmann et al., 2010; Sinha et al., 2011; van den Bogaart et al., 2010). Moreover, it has at least been demonstrated for Syntaxin 1 that the majority of the molecules reside in clusters where its overt function is impeded due to steric hindrance (Sieber et al., 2007). These findings raise the question why the cell would produce such vast amounts of protein? Assuming that a neuron has been shaped throughout evolution into a reliable signaling unit that uses its resources efficiently allows only one conclusion: the protein ensembles serve a specific function distinct from the overt protein function. To address this I would like to get back to an idea that was briefly mentioned in the discussion of SNAP 25 and can be extended to all three SNAREs: maybe the SNAREs are so highly abundant to prevent fusion at most sites and only allow it at very few specialized sites (active zones)? The ample amounts of molecules pave the entire plasma membrane with protein clusters composed of fusion-incompetent molecules most likely organized in clusters (Bar-On et al., 2012; Sieber et al., 2007). Vesicle fusion on the other hand can only take place at specific sites (the AZ) that contain (a) individual SNARE molecules and (b) sufficient amounts of co-factors (e.g. CSP) to stabilize and activate them. The excess amounts of proteins could serve an important function for the spatial organization of SV exo- and endocytosis. Recent evidence to support this theory has demonstrated that spots with low SNARE density are preferred fusion sites of secretory vesicles in PC12 cells (Yang et al., 2012). In addition (see again the discussion of SNAP 25 above), these blocked sites could easily be transferred into fusion sites if necessary by dissociating the clusters and recruiting accessory proteins.

SNARE co-factors

The SNARE co-factors α -SNAP and NSF disassemble cis-SNARE complexes after vesicle fusion and thus are key factors for providing free SNARE proteins for further vesicle release (Jahn and Scheller, 2006). I found them both to be organized within the vesicle cluster and around the AZ (see Figures 3-13 and 3-14). The quantitative immunoblots revealed that a single

synaptosome contains approximately 4065 NSF and 1151 α -SNAP molecules. A functional unit for disassembling a neuronal SNARE complex consists of an NSF hexamer and two α -SNAP molecules (Jahn and Scheller, 2006; Jahn and Fasshauer, 2012). Taking this into account I report an almost perfect 1:1 stoichiometry for the functional units of these two proteins.

It has long been known that Complexins are able to bind to SNARE complexes (Bracher et al., 2002; Chen et al., 2002). Studies with transgenic mice have further proposed a function for Complexin in triggering calcium dependent neurotransmitter release (Xue et al., 2010; Yang et al., 2010a). Recently, evidence is accumulating that Complexins are the functional clamp on SNARE complexes inhibiting uncontrolled fusion and being released upon entry of calcium into the terminal (Kummel et al., 2011; Li et al., 2011; Malsam et al., 2012; Martin et al., 2011). This is further supported by experiments demonstrating that over-expression of Complexin causes an inhibition of exocytosis (Liu et al., 2007). I found the two predominant neuronal isoforms Complexin I and II to be present in very low amounts at a pre-synaptic terminal – 132 and 114 copies respectively. In the neuron, Complexin has been reported to be majorly present in the axon (Denker et al., 2011b) and the stainings revealed that most of the synaptic Complexin molecules are associated with the SV cluster (see Figure 3-13 and 3-14). This observation is in agreement with studies addressing the functional organization of Complexins that could show that the protein is buffered and sequestered by the SV (Denker et al., 2011b; Wragg et al., 2013). In respect of the low amount of SVs used for neurotransmitter release *in vivo* (Denker et al., 2011a; Marra et al., 2012) such a low amount of Complexin molecules would be more than sufficient for clamping the few vesicles ready for release (Trigo et al., 2012; Rosenmund and Stevens, 1996). The low amounts of Complexins in a pre-synaptic terminal also offers a possible explanation for the high release rates observed in neuronal preparations when stimulated *in vitro* (Ikeda and Bekkers, 2009): *in vivo* the number of Complexin molecules is sufficient to clamp the few vesicles needed for neurotransmitter release (Denker et al., 2011a). In contrast, an artificial stimulation paradigm *in vitro* is able to exceed physiological stimulation paradigms and thus mobilizes substantially more vesicles (via phosphorylation of Synapsins). Since the Complexin in the terminal is not sufficient to clamp all but only a few vesicles, those which are not clamped do now readily fuse with the plasma-membrane. In other words – the lack of endogenous Complexin in the pre-synaptic terminal enables excessive SV release upon stimulations which exceed physiological conditions.

I found the vesicular protein CSP in approximately 941 copies per pre-synaptic terminal. The protein is well known for its chaperoning function of SNAP 25 and is important for its stability and therefore ultimately for the ability to form SNARE complexes (Sharma et al., 2011; Sharma et al., 2010). The large amounts of SNAP 25 I found per pre-synaptic terminal already indicated the need of a mechanism to regulate the amount of active SNAP 25 in order to maintain time and site specific vesicle fusion. This regulating function could possibly be performed by CSP. The protein could serve as a bottleneck for functionally available SNAP 25 molecules. In agreement with this theory, over-expression of CSP leads to an increase in calcium dependent exocytosis (Chamberlain and Burgoyne, 1998) indicating that an increased availability of CSP increases the amount of fusion competent SNARE complexes. Interestingly, a very recent study also reports an interaction of CSP with Dynamin 1 (Zhang et al., 2012). In fact, this study shows that CSP is a regulator of Dynamin polymerization which is crucial for pinching off of the vesicle. Considering the evidently essential role of CSP for the function of both SNAP 25 and Dynamin 1 imposes the thought that CSP could actually be an important link regulating the spatio-temporal coupling of SV exo- and endocytosis. Further, it is tempting to speculate that CSP might not only be a link between exo- and endocytosis but also a proteinaceous balancing element of the two processes. Regarding that both processes indirectly depend on CSP and that CSP is only present in low amounts at the synapse, the following model could be envisioned: CSP-stabilized and thus activated SNAP 25 is needed at the AZ for SV fusion. This automatically brings CSP in close proximity to potential endocytic sites next to the AZ – the peri-AZs. However, the CSP is still bound to SNAP 25 and is only freed after SNARE complex assembly and fusion of the vesicle. At this point compensatory endocytosis is initiated which can only be completed by CSP stabilized Dynamin which mediates scission of the newly formed vesicle. Hence, the amount of active Dynamin is directly dependent on the availability of CSP and it is possible that the availability of CSP at endocytic sites depends directly on the fusion of vesicles. I am well aware that this model is highly speculative and that there is no direct prove for it so far. Nevertheless, it is in agreement with what is known about SV recycling and offers a possible mechanism linking and balancing the processes of vesicle fusion and retrieval in a physiological context.

Endocytosis – initiation of pit formation

It is commonly accepted that the local lipid composition is an important regulator in membrane trafficking. In neurons, PIP₂ has been reported to be a key player in early stages of Clathrin mediated endocytosis (Wenk and De Camilli, 2004) presumably by targeting AP2 and other endocytic factors to the plasma membrane (Gaidarov and Keen, 1999; Honing et al., 2005). Among others PIP₂ is generated by PIPK I γ which has been found to be concentrated to the plasma membrane in pre-synaptic terminals and is an essential factor for Clathrin mediated endocytosis (Wenk et al., 2001). Congruently, I found 466 copies of PIPK I γ per synaptosome and they appear to be organized mainly around the AZ (see Figure 3-13). Despite the fact that it seems to hold such an important function in endocytosis its number is quite low. However, as it is an enzyme catalyzing the phosphorylation of PIP to PIP₂, the amount of molecules I found is sufficient to sequentially phosphorylate multiple proteins.

Epsin 1 was found in only 93 copies per synapse and mainly arranged in the vesicle cluster and around the AZ (see Figure 3-13). Epsin 1 is recruited to endocytic sites by binding to PIP₂ and directly modifies the curvature of the plasma membrane (Ford et al., 2002). It can thus be regarded as a coordinating element for curvature generation preceding the assembly of the Clathrin coat and might majorly be involved in determining the size of the endocytosed vesicle (Jakobsson et al., 2008). Although it seems to play a central role in initiation of Clathrin mediated endocytosis I only found it in very low amounts at the synapse. It is likely that this is due to the generally low need of endocytosis under physiological conditions (Denker et al., 2011a; Marra et al., 2012). Assuming that only approximately 5% of the vesicles are needed for neurotransmission renders the number reported in this study reasonable for proper function *in vivo*. Furthermore, it is in agreement with my findings on the number of Clathrin coats possibly formed (see below) ranging between 3 and 7 vesicles at a time.

The role of Intersectin cannot be assigned to a single step in Clathrin mediated endocytosis. It is a large scaffolding protein concentrating several endocytic proteins to specific sites during the entire course of membrane retrieval (Pechstein et al., 2010b; Koh et al., 2004). In this respect, Intersectin has for instance been shown to be involved in fission of vesicles by regulating the recruitment of Dynamin to the neck of the vesicle (Evergren et al., 2007b; Winther et al., 2013). On the other hand, it serves as an essential part during early vesicle formation in conjunction with AP2 (Pechstein et al., 2010a). In addition, further interactions with for example Epsin, EPS15, Amphiphysin (Pechstein et al., 2010b) and SCAMP 1 (Fernandez-

Chacon et al., 2000) have also been reported in the past. It is still debated whether Intersectin might also be involved in coupling exo- and endocytosis potentially via its interaction with SNAP 25 (Okamoto et al., 1999). As outlined in this paragraph, many different interaction partners for Intersectin are known. However, so far neither the precise mechanisms nor their stoichiometry is known which makes it difficult to put the amount of molecules I found (3097) into a relevant synaptic context.

Information on the function of SCAMP 1 is rather scarce in the literature besides that it is expected to be involved in Clathrin recruitment during endocytosis (Fernandez-Chacon et al., 2000). Nevertheless, I found 14595 molecules per pre-synaptic terminal which are expected to reside mostly in endosomal compartments (Fernandez-Chacon and Sudhof, 2000; Fernandez-Chacon et al., 2000). This is quite an impressive amount regarding that the function of the protein is not yet known and that Takamori et al., 2006 only found about 1 copy per vesicle. It will be interesting to see how the number I determined will relate to future studies investigating function further.

Endocytosis – formation of a Clathrin coated vesicle

CALM and AP180 are expected to be functional homologs which are differentially expressed during development: CALM is down- and AP180 up-regulated during the first couple of weeks after birth (personal communication with Prof. Volker Haucke). In line with this I only found 3 CALM molecules while AP180 was quite abundant with 5182 molecules in the synapses of 6 week old rats. AP180 is a cargo specific protein involved in endocytic sorting of SVs. In this respect, it recently has been demonstrated to be a specific adaptor for VAMP 2 during endocytosis (Koo et al., 2011). This is an interesting finding and might possibly explain the large amounts found in a single synapse. According to Takamori et al., 2006 a SV is equipped with approximately 70 copies of VAMP 2. If all these VAMP 2 molecules are targeted to the vesicle via AP180 the amount I found is sufficient to equip approximately 74 vesicles with VAMP 2 (assuming a 1:1 stoichiometry of VAMP 2 and AP180). This seems reasonable and would be amply sufficient to supply the vesicles with VAMP 2 during physiological conditions.

Another prominent adaptor protein in SV recycling is AP2. Interestingly, the recruitment of AP2 to the plasma membrane seems to be dependent on PIP₂ (Honing et al., 2005). On the other hand, it has also been demonstrated to interact with the PIPK I γ at the plasma membrane and therefore control the spatio-temporal synthesis of PIP₂ (Krauss et al., 2003). In this respect,

AP2 appears to be involved in a positive feedback loop which is most probably essential for Clathrin mediated endocytosis (see above). Further, it is known that two AP2 molecules bind one Clathrin triskelion during formation of the coated pit/ vesicle at the plasma membrane (Cocucci et al., 2012). Since it has been reported to be involved in interactions with multiple endocytic proteins (McMahon and Boucrot, 2011; Perrais and Merrifield, 2005) it is difficult to elaborate on the number function relation of this protein in the pre-synaptic terminal. However, the high abundance I found (23247 molecules per synapse) seems to support the theory of AP2 being a major protein interaction hub in vesicle endocytosis as enough molecules are provided for multiple interaction partners (see also Boucrot et al., 2010).

To my knowledge SGIP1 α is expected to be involved in endocytosis by interacting with Eps15 and phospholipids (Uezu et al., 2007). However, the exact mechanism or even the nature of the interaction is not known. Therefore, it is impossible to discuss its role in the pre-synaptic terminal. I found approximately 3382 copies per synapse and the only thing I can possibly conclude is that it is present in substantial amounts and therefore its role within the synapse might not be negligible. It will be interesting to evaluate these findings in regard to future studies which might further elucidate the proteins function.

Clathrin has been found almost 40 years ago to be essential for coating of vesicles involved in intracellular trafficking (Pearse, 1976). I found 2054 Clathrin heavy chain and 811 light chain molecules per synapse in the synaptosomes. The functional unit of Clathrin which actually forms the coat is referred to as Clathrin triskelia which are a complex of three Clathrin heavy chain and three light chain molecules (Musacchio et al., 1999). In the literature the amount of Clathrin triskelia needed to coat a SV varies between 40 (Cheng et al., 2007) and 100 (McMahon and Boucrot, 2011). This is probably due to the fact that many studies so far have been performed on artificial vesicles of defined diameters (Cheng et al., 2007). Unlike a SV these organelles are not peppered with integral membrane proteins and accessory factors which will most likely increase the net diameter of the vesicle, hence it has to be assumed that more triskelia are needed for a Clathrin coat *in vivo* (McMahon and Boucrot, 2011). Nonetheless, the question whether 40 or 100 triskelia coat a single SV seems irrelevant as in both cases the amount of vesicles which could potentially be coated simultaneously is relatively low – i.e. 3 to 7 vesicles respectively. Regarding the copy numbers reported in this study, it is obvious that Clathrin light chain is the limiting factor for the formation of triskelia as it is substantially lower in abundance compared to the heavy chain. In regard of the few triskelia potentially present in a

pre-synaptic terminals, it is tempting to speculate that not Clathrin mediated endocytosis but rather kiss-and-run (transient fusion) is the main mechanism of membrane retrieval in neurons (Klingauf et al., 1998; Rizzoli and Jahn, 2007). However, it has been demonstrated in multiple independent studies that kiss-and-run does not play a role during physiological conditions while Clathrin mediated endocytosis remains the main retrieval mechanism (e.g. Granseth et al., 2006; Newton et al., 2006; Granseth et al., 2007; Wienisch and Klingauf, 2006; Dickman et al., 2005). Further, the amount of Clathrin I found is generally sufficient to maintain neurotransmitter release *in vivo* (Denker et al., 2011a; Marra et al., 2012). Nevertheless, my findings offer a potential explanation for the occurrence of large membrane invaginations (bulk endocytosis) upon intense stimulation (Clayton et al., 2008; Clayton and Cousin, 2009). The limited amount of Clathrin triskelia can only compensate for a few vesicles at a time. Therefore, the inability to immediately retrieve all membrane as Clathrin coated vesicles could force the membrane to form large bulk structures. These membrane invaginations could be regarded as an internal membrane storage which is slowly catabolized by Clathrin mediated endocytosis from the bulk (Ferguson et al., 2007) as Clathrin triskelia become accessible. The necessity to form a membrane bulk upon exocytosis is an extreme situation for which the neuron is most likely not made but nevertheless able to compensate.

Endocytosis – scission of the vesicle

Endophilin is a BAR domain protein which generally bind to curved lipid bilayers and function as curvature sensors and inducers (Frost et al., 2009). Deletion of Endophilin I to III leads to accumulation of Clathrin coated vesicles rather than pits and impaired neurotransmission which imply that the protein is involved in a late stage during endocytosis – maybe via priming coated vesicles for uncoating (Milosevic et al., 2011). In this study I found Endophilin – as expected from the literature – to be largely overlapping in distribution with its interaction partners Dynamin and Amphiphysin. Further, I found approximately 2524 molecules which results in 1262 dimers assuming that the functional units of Endophilins are dimers. Although these amounts are in a similar range to the amounts of Amphiphysin and Dynamin (see below) it is difficult to put them in relation to each other. Unfortunately it is not clear how exactly and in what stoichiometry Endophilin is involved in the late stages of endocytosis. Therefore, it is difficult to relate my findings to the not yet entirely understood physiological role of Endophilin in the pre-synaptic terminal.

The interaction of Amphiphysin and Dynamin has been reported to be essential for scission of the newly formed vesicle and therefore ultimately for neurotransmission (Shupliakov et al., 1997; Di Paolo et al., 2002). In agreement with the fact that the two proteins form heterodimers (Wigge et al., 1997) I found them to be largely overlapping in distribution (see Figure 3-13) and to be present in similar amounts at a synaptic terminal: Amphiphysin at 1194 and Dynamin at 2326 copies per synapse. Studies on Dynamin 1 KO mice have revealed that neurotransmission particularly during more intense stimulation paradigms is impaired in mice lacking the protein (Ferguson et al., 2007). Dynamin is known to be important for the final step in scission of the endocytosed vesicle: it forms a helical ring around the neck of the vesicle and constriction of this ring ultimately pinches off the new vesicle (Ferguson and De Camilli, 2012). The ring is composed of approximately 14 Dynamin homo-dimers. Unfortunately it is not yet known how many of these rings are needed for proper scission of the vesicles (Chappie et al., 2011). Ultrastructural investigations of synapses in the temperature sensitive Dynamin mutant *shibire* revealed that between one and two rings can be found around each neck at non-permissive temperatures (Koenig and Ikeda, 1989). However, as this is a non-functional phenotype it is difficult to directly draw conclusions from it for the situation *in vivo*. Nevertheless, it suggests that at maximum two Dynamin rings are formed around the neck of the vesicle during scission *in vivo* (otherwise they would have observed intermediates with more than two rings). In conjunction with a recent study that proposed that at least one ring is needed for scission (Morlot et al., 2012) it can be concluded that between one and two rings are sufficient for scission of a vesicle. In regard to the amount of molecules I found, the average synapse contains enough Dynamin to make rings for 42 (two turns) to 83 (one turn) vesicle necks. Again, this is not sufficient for the entire population of vesicles in a synapse which (i) indicates that not all SVs are used for neurotransmitter release (Denker et al., 2011a; Marra et al., 2012) and (ii) the need of bulk endocytosis upon intense stimulation (Clayton and Cousin, 2009) as described for Clathrin above. The amount of Dynamin available to form helices could further be regulated by CSP. Similar to its function for SNAP 25 (see above), CSP also seems to regulate the formation of Dynamin polymers (i.e. helices/ rings, Zhang et al., 2012). Therefore, CSP is in direct control of how much Dynamin is available to the newly endocytosed vesicles. For further speculations of the possible role of CSP linking the functions of SNAP 25 and Dynamin refer to the discussion of CSP above.

Endocytosis – uncoating of the new vesicle

The only protein I investigated that is involved in uncoating of the Clathrin coated vesicle is Hsc70 (8210 molecules per synapse). It is recruited to the vesicle by Auxilin where the uncoating process is expected to start from the former neck of the vesicle which is devoid of Clathrin (Chappell et al., 1986; Rothnie et al., 2011; Cremona et al., 1999). Hsc70 is also involved in chaperoning of SNAP 25 together with CSP (see discussion of CSP). It is difficult to directly relate the number of Hsc70 molecules to its chaperoning function of SNAP 25 since it is almost 10-fold more abundant than its partner CSP. Again, it is possible that CSP is the limiting element and directly determines the amount of SNAP 25 available to form SNARE complexes (see discussion of CSP above). Concerning its function in endocytosis, it is known that three Hsc70 molecules are interacting with one Auxilin molecule to disassemble one Clathrin triskelia (Cremona et al., 1999; Rothnie et al., 2011). Unfortunately, I was not able to quantify Auxilin but the number of Hsc70 molecules is sufficient to uncoat between 27 and 68 vesicles (depending on amount of triskelia see (Cheng et al., 2007; McMahon and Boucrot, 2011) simultaneously providing that all molecules are available at the respective endocytic sites.

Endocytosis – integration of the new vesicle in the cluster

Syndapin has been proposed to link vesicle endocytosis with the cytoskeleton and therefore possibly mediating the integration of newly formed vesicles into the cluster (Kessels and Qualmann, 2004). It is expected to be essential for the recruitment of Dynamin to the Clathrin coated vesicle as its KO closely resembles the phenotype of Dynamin mutants (Qualmann et al., 1999; Koch et al., 2011). In this study I found 3201 Syndapin 1 molecules per average brain synapse. Although the direct mechanism of interaction between Syndapin and Dynamin is still not clear they are similarly abundant (compare with 2326 Dynamin molecules) and distributed (depicted in Figures 3-13 and 3-14).

Vesicular pumps/ transporters

The proton pump vATPase is a protein not specific to SVs but universally expressed in eukaryotic cells (Finbow and Harrison, 1997). Its function is to establish a proton gradient between the respective organelle and its surrounding which is used to transport for instance transmitters into the vesicle lumen (Saw et al., 2011). A previous study found 1.4 vATPase protein complexes per single SV (Takamori et al., 2006). In comparison, I found approximately

2186 molecules of the 116 kDa isoform $\alpha 1$ which is a central part of the multi-subunit protein and likely represents a good estimate for the total amount of vATPase present in the preparations. In agreement with the literature (see above) I expect not all pumps to reside on SVs but also on other intracellular organelles (e.g. endosomes, lysosomes, trafficking vesicles etc.). This is also evident at the density distributions for this protein (see Figure 3-13 and 3-14) which indicates that the protein is localized to vesicles as well as to structures behind and next to the vesicle cluster (regarded as endosomal compartments). Therefore, I conclude that the copy number I report for the vATPase seems to correlate with its proposed function and distribution.

In glutamatergic synapses the uptake and storage of neurotransmitters is mediated by two differentially expressed non-overlapping transporters VGlut 1 and 2 (Fremeau et al., 2001). In this respect, a study using transgenic VGlut 1 mutants has demonstrated that VGluts directly determines the efficiency of neurotransmitter release by regulating the amount of Glutamate in the vesicles (Wojcik et al., 2004). In the quantitative approach I determined the abundance of both isoforms together and found 8254 copies per synapse which almost exclusively seem to be localized to vesicles (see Figure 3-13, the protein is not present in the NMJs which are cholinergic synapses). Assuming that the different types of synapses (VGlut1 or 2 positive) contain equal amounts of the respective protein I conclude that the copy number presented in this study is representative for the average synapse (i.e. a VGlut1 synapse would contain 8254 molecules of VGlut1 and a VGlut2 synapse the same amount of VGlut2). Unfortunately, it is difficult to evaluate the physiological relevance of the copy number for the synapse. Despite the fact that Takamori et al., 2006 found “only” approximately 10 molecules per SV a recent study has proposed that this might be an underestimate due to the fast refilling of vesicles (15 s) with Glutamate (Hori and Takahashi, 2012). Moreover, as stated before my synaptosome preparations do not solely contain glutamatergic synapses. As I used both cortex and cerebellum as starting material for the purification, it has to be expected that my number is underestimating the real amount of vGluts in the average glutamatergic synapse. Also, some molecules can be expected to reside on recycling endosomes and in the plasma membrane. Although it is difficult to assess the precise number of vGluts the amount presented here provides a reasonable estimate and underlines the importance of this protein for neurotransmission at chemical synapses.

Endosomal proteins

The first evidence for recycling of SV material via endosomes was found three decades ago by Heuser and Reese (Heuser et al., 1979). Since then the role of endosomes in the recycling of synaptic vesicles has been a matter of debate (Rizzoli and Betz, 2005). Several recent studies have proposed that a small fraction of SVs does indeed undergo endosomal recycling upon endocytosis (Hoopmann et al., 2010; Rizzoli et al., 2006; Schmidt and Haucke, 2007; Uytterhoeven et al., 2011). In regard of these findings, I also decided to address several endosomal SNARE proteins (the copy numbers found per pre-synaptic terminal are in brackets behind the protein): Syntaxin 6 (122 molecules), Syntaxin 7 (79 molecules), Syntaxin 13 (879), Syntaxin 16 (91 molecules), VAMP 4 (101 molecules) and Vti1 A (51 molecules). Strikingly, these endosomal SNARE proteins are all present in low and very similar amounts. This nicely demonstrates that there are most likely not very many endosomes within a pre-synaptic terminal and that those are only sufficient to recycle a minor fraction of all vesicles via endosomal compartments (Hoopmann et al., 2010). Importantly, the amount of vesicles which could be recycled via endosomes appears to be comparable in number to the amount of vesicles which have recently been reported to maintain synaptic activity *in vivo* (Denker et al., 2011a; Marra et al., 2012). The least abundant of the molecules listed above – Vti1 A – has further been proposed to be specific for a separate pool of vesicles which selectively maintains spontaneous fusion (Ramirez et al., 2012). Although this scenario is not negated by the amount of Vti1 A per synapse it is important to emphasize this is a highly controversial topic and that multiple studies have demonstrated that the very same vesicles drive active and spontaneous release (e.g. Wilhelm et al., 2010; Groemer and Klingauf, 2007; Hua et al., 2010)

I also investigated two endosomal Rab proteins namely Rab5 and 7. While the former is mainly involved in membrane trafficking to and from early endosomes the latter has been assigned to regulate trafficking at late endosomes as well as at lysosomes (Stenmark, 2009). I found Rab7 approximately 7-fold more abundant than Rab5 with 4457 and 634 molecules per pre-synaptic terminal, respectively. The precise role of both Rab5 and 7 in the synapse is not yet completely understood. Therefore, it is difficult to relate their copy numbers to the functional organization of the synapse.

Disease-related proteins

Although APP is expected to play a role in neuronal plasticity (Turner et al., 2003) and synapse formation (Priller et al., 2006) it is best known for its potentially central role in Alzheimer's disease pathogenesis (Haass and Selkoe, 2007). In the so called amyloidogenic pathway APP is sequentially cleaved by the β - and γ -secretases. This leads to the generation of so called amyloid β which is thought to aggregate into plaques which cause neurodegeneration and ultimately Alzheimer's disease (Haass and Selkoe, 2007). According to this model not only APP but also the two secretases seem to hold crucial positions in the course of dementia. I quantified both APP and β -secretase and found 6284 and 116 molecules per pre-synaptic terminal respectively. It is well known that both proteins reach the synapse in different transport vesicles (Cole and Vassar, 2007). Compared to APP, the β -secretase is only scarcely transported up and down the axons (Goldsbury et al., 2007). The limited trafficking of the β -secretase is most likely also due to the fact that the protein is quite stable having a half life of approximately nine hours (Puglielli et al., 2003). These findings help to understand the low amounts in a synapse: (i) it is a very stable protein and thus has a low turn over and (ii) the protein is an enzyme which is only needed in low amounts as it catalyzes multiple reactions (in this case the cleavage of APP) in a short time.

On the other hand, APP seems to be quite abundant and it is frequently transported antero- and retrograde along the axon in distinct carrier vesicles (Kaether et al., 2000). The trafficking of APP and its presence on SVs has been controversially discussed in the past two decades (Marquez-Sterling et al., 1997; Cirrito et al., 2008; Cirrito et al., 2005). Recently it could be demonstrated that APP is indeed present on SVs and that cleavage products are released during exocytosis (Groemer et al., 2011). In the quantitative immunoblots I have used an antibody for detection of APP which is directed against the N-terminal part of the protein. It is important to keep in mind that APP is a trans-membrane protein with the N-terminal being outside of the cell (assuming the protein to reside in the plasma membrane, Groemer et al., 2011). Upon cleavage by the secretases (irrespective if it follows the non- or the amyloidogenic pathway) the N-terminal part is released to the extracellular space and most likely lost during the process of synaptosome purification. Therefore, only a small fraction of the APP molecules might have been quantified and peptides present in the terminal i.e. the full length fraction of the protein (Marcello et al., 2012). In this respect, it is tempting to further speculate on the central role of APP in Alzheimer's disease pathogenesis: a protein which is so highly abundant

and has such a rapid synaptic turnover (Kaether et al., 2000) also has the potential to deliver cleavage products – in large amounts – which can aggregate and impair the synaptic physiology. In other words – the rapid turnover of APP is naturally accompanied by the production of large amounts of side products in a short time. This renders the processing of APP as intrinsically prone to cause neurodegeneration as potentially toxic side products can accumulate relatively fast (such as A β).

Similar to APP, the precise function of α -Synuclein has not yet been clarified. It is still most discussed concerning its involvement in Parkinson's disease as it is the main component of the aggregates and deposits which are expected to cause neurodegeneration (Marques and Outeiro, 2012). Another line of evidence links α -Synuclein to actually prevent neurodegeneration in conjunction with CSP (Chandra et al., 2005) and to promote the assembly of SNARE complexes (Burre et al., 2010). Unfortunately little is known about the precise mechanisms of how α -Synuclein may act as a neuro-protectant or as a toxic element in the synapse. Especially the link between these two possible roles remains elusive. Although the α -Synuclein concentration I determined per synapse has recently been confirmed (Westphal and Chandra, 2013) it is difficult to relate amount per synaptic terminal (i.e. 3168 molecules) to any of the two models. However, conclusions which I could draw from this data are that (a) α -Synuclein is highly localized to SVs (see Figure 3-13 and Bellani et al., 2010) and (b) that the protein is relatively abundant which could indicate that it indeed fulfills an important function in the synapse and (similar to APP) might be prone to produce toxic aggregates to its large turnover.

4.2.1 Bottlenecks as control elements for pre-synaptic function

The discussion of the quantification results in the context of the proteins' role within the pre-synaptic terminal (see above) suggests that several key processes in synaptic function might be controlled by bottlenecks. A bottleneck in a biological system can be regarded as the limiting factor which is crucial for a particular process and limits it by its abundance. In this respect, a good experimental approach to determine a bottleneck is over-expression: if a certain protein is the limiting factor in a physiological process, this process will be enhanced/ accelerated upon over-expression of the respective protein.

In the previous section I discussed the copy numbers in the physiological context of synaptic function. Doing so, I pointed out several proteins which could potentially serve as

bottlenecks for the processes they are involved in – for instance: (i) Munc18a in priming and docking of synaptic vesicles, (ii) CSP as a crucial stabilizer for SNARE complex assembly (via SNAP 25) and scission of the vesicle (via Dynamin), (iii) Clathrin for the formation of coated vesicles during endocytosis, (iv) Epsin during initiation of pit formation (v) Complexin as a fusion clamp on SNARE complexes and (vi) endosomal SNARE proteins for accurate sorting of SV material. In regard to these findings it may be hypothesized that neurotransmission is controlled by several consecutive processes which are all governed by separate bottlenecks that define their spatio-temporal timing. The major advantages of using bottlenecks to control entire systems are (1) that it is easier to control the expression and function of a single protein compared to several and most importantly (2) that it makes the system extremely flexible. As for example the expression of one protein is the limiting factor it is also possible to up- and down-regulate the system simply by changing the expression of this protein.

Although my data supports a model involving multiple bottlenecks for neurotransmission it certainly does not prove it beyond reasonable doubt. In order to test this hypothesis more thoroughly, further studies will have to investigate synaptic physiology upon modulating the abundance of certain proteins. This could ideally be achieved in an acute fashion, for instance, by using clostridial neurotoxins to reduce the amount of functional SNARE molecules available. Unfortunately, it will most likely not be possible to acutely modulate the availability of every synaptic protein. In such cases genetic modifications (knock out/ down/ in) could be used instead. However, I would like to mention that genetic modifications usually affect an organism or a cell well before the actual experiment. Therefore, it can not be excluded that phenotypes observed upon such modification are substantially biased by adaptive mechanisms to the modification.

The above outlined speculations are based on the set of proteins addressed in this study. Although I expect to have covered the majority of the proteins thought to be essential for neurotransmission, it is likely that several proteins might still be missing (or are even unknown) which could also function as bottlenecks and majorly steer synaptic function.

4.2.2 SV release is blocked everywhere but at distinct sites

It is generally believed that chemical synapses are tightly controlled neuronal compartments, designed only for one purpose – to release neurotransmitter. However, the data presented in this study gives room for a modified interpretation of the processes within a pre-

synaptic terminal. The vast amount of proteins I report – especially for the synaptic SNARE proteins – raises the question if the synapse is solely made to release:

As outlined in 4.2.1 all three neuronal SNARE proteins are extremely abundant although several studies have shown that few complexes are already sufficient to mediate fusion of a vesicle (Mohrmann et al., 2010; Sinha et al., 2011; van den Bogaart et al., 2010). Moreover, the excess proteins do not seem to support but rather to prevent fusion by being organized in clusters on the plasma membrane where their overt function is sterically blocked (Sieber et al., 2007). At a first glance it seems rather counterintuitive to produce many copies of a certain protein which than inhibit each other. However, as speculated in 4.2.1 this could be a mean to block vesicle fusion everywhere but at specific sites (i.e. the AZ). The data presented in this thesis offers several more examples of proteins where super-abundance is not directly linked to the overt protein function (see also AP2, Rab3, and Synapsin etc.). The SNARE proteins are simply the most extreme case I investigated and are a set of very well characterized proteins which allows more reliable predictions concerning their number-function relation.

Another example for synaptic superabundance without a direct link to physiological function is the large number of SVs present in a synapse. It recently has been demonstrated that only a minor fraction of the SVs within a terminal actually release neurotransmitter *in vivo* (Denker et al., 2011a; Marra et al., 2012). The rest of the vesicles do not participate in transmitter release but function as a molecular buffer retaining soluble proteins concentrated in the synaptic terminal (Denker et al., 2011b). Interestingly, the majority of the vesicles also seem to be integrated in a rigid network composed of accessory proteins and large amounts of Synapsin molecules (see Hirokawa et al., 1989; Siksou et al., 2007 and Figure 3-18) which actually renders these vesicles immobile, hence fusion-incompetent.

Why would a neuron produce large excess amounts of proteins that are apparently not functional? And why does the terminal need vast amounts of SVs which can only be released upon very intense (likely non-physiological) stimulations? These observations are difficult to explain with the notion that a synapse is built for neurotransmitter release. Therefore, I would like to extend our current model of synaptic physiology: chemical synapses are not primarily built for release, but to block release everywhere but at very distinct sites.

This model does certainly not change most interpretations of previous studies on synaptic physiology; it changes our perception of the synapse and has the potential to give rise to new innovative approaches to further elucidate the function of a pre-synaptic terminal.

4.2.3 The synapse – more than just the sum of its parts

Today's research has a very mechanistic focus. The main goal of many studies is usually to understand a defined interaction which could possibly be the base of an entire cascade of processes. In a way this philosophy is a rather reductionistic approach aiming to understand an entire system by simply knowing the properties of any single interaction within it. This philosophy bears a major strength – i.e. by reducing the scope to an individual and possibly isolated mechanism it is likely to reveal all its properties as other cellular parameters are taken out of the equation. Unfortunately this also delineates its major weakness – i.e. rendering it extremely difficult to fit the findings into a physiologically relevant context. On the contrary, this study was designed to be purely descriptive in order to provide a concise picture of the pre-synaptic terminal. As it is crucial to know the composition and functional organization of a system in order to understand it entirely, I am here providing a set of data which could help to put findings about single mechanisms and interactions into the physiological context of an entire synapse (see discussion of the individual proteins in section 4.2).

The data presented in this thesis allows for the first time to determine the role of the spatio-temporal availability of proteins for synaptic function. In the course of my work I provided several examples where the availability of a protein serves as a direct mechanism to control synaptic processes (e.g. SNARE proteins, CSP, Clathrin). These observations could only be made by investigating the molecular composition of a synapse and were thus missed by previous studies addressing synaptic regulation by investigating the specific functions of individual proteins. In regard to my findings, I propose that synaptic function is primarily regulated by the abundance rather than by the function of individual proteins. This model is substantially simpler compared to other regulatory mechanisms proposed in the past: no complex control elements are required since regulating the availability of certain key proteins is sufficient to steer the entire system. The model provides a novel approach towards understanding synaptic physiology as it focuses on the stoichiometry of the different proteins and the synapse as a whole – it demonstrates that the synapse is substantially more than just the sum of its parts.

5. Conclusion and Outlook

The purpose of this study was to describe the architecture of a pre-synaptic terminal of a central neuron. Using purified synaptosomes from rat cortex and cerebellum (see 3.1), I first addressed the ultrastructure of a pre-synaptic terminal. Using 3D reconstruction EM I determined the physical characteristics of the average brain synapse (see 3.2). Next, I calculated absolute copy numbers per single pre-synaptic terminal for 59 proteins using quantitative immunoblots (see 3.3). As I was not only interested in the protein amounts but also in their organization within a synapse, I turned to super resolution STED microscopy to assess the synaptic distribution of these proteins. For this I used two prominent model systems – primary hippocampal cultures as central and mouse NMJs as peripheral synapses (see 3.4). Finally, the data we obtained from all three approaches – the ultrastructural as well as protein numbers and distribution – was used to generate a graphical model of the average pre-synaptic terminal. By providing this concise picture of a pre-synaptic terminal this data will contribute significantly to our understanding of the synapse. It can be used as a reference for the multiple functional studies on single synaptic proteins and will help to put these findings in relation to each other. In this respect, my data may provide the framework for understanding the physiology of a synapse in which functional studies could be fitted in order to draw the big picture.

Furthermore, this data can be used to speculate about general principles that govern pre-synaptic function (see 4.2.2 and 4.2.3). I found enormous amounts of molecules for some proteins and comparably little for several of their functional partners. This suggests that synaptic function is not controlled by specific mechanisms but by the abundance of binding partners. It seems as if an interaction of several proteins (e.g. assembly of a Clathrin coat) solely depends on the availability of the participating molecules and not on their specific interactions. Also, the high abundance of proteins within a pre-synaptic terminal provides a new perspective for our general understanding of synaptic function. Several elements (SNARE proteins, Synapsins etc.) seem to be so abundant as to block or at least restrict vesicle fusion. Only distinct sites (AZ) coinciding with a specific protein and ion environment are able to overcome the block and fuse vesicles with the plasma membrane.

For a methodological outlook of this study it would be interesting to test the distribution information obtained with STED microscopy with a different super resolution system. Since new imaging systems with increased resolutions are almost published every month it would be

worthwhile to reinvestigate the distribution of synaptic proteins in order to get a sharper image of the pre-synaptic organization at some point in the future.

The methods used in this study could of course be extended to other neuronal compartments or even different cell types that can be purified to a certain degree. Hence, it could also be used to describe the composition of several other compartments such as for example mitochondria or PSDs. Unfortunately, the approach I chose here is still extremely laborious but a potential access to fast quantification tools would allow to address different systems. In this respect, a novel and exciting approach to address the composition of cellular compartments without the tedious purification steps has just been introduced by Alice Ting and colleagues (Rhee et al., 2013). In their study they report the use of a genetically encoded biotinylating enzyme which can specifically be targeted to certain cellular compartments. All proteins in the vicinity of the enzyme (i.e. in the same compartment) are then biotinylated and thus can be extracted from a cell homogenate with Streptavidin beads. Next, the pulled down proteins are subjected to mass spectrometry for proteomic and possibly even quantitative analysis. If this technique proves to be applicable to a wide variety of cells it will provide a significant leap towards understanding the molecular composition of different cell types and provide a valuable tool to compare healthy and diseased cells on a proteomic level.

Last but not least I would like to mention one more potential outlook of this project: we would like to ideally make the data accessible and editable to the entire scientific community. It could be organized as an open source internet platform/ database on which people have the chance to access all information displayed in this thesis as well as add new findings (e.g. new protein numbers or revised organization etc.) to it. By combining compositional and possibly also functional information, such a data base would provide a comprehensive image of a pre-synaptic terminal – or in other words: a NANOMAP of the synapse.

Bibliography

Amin, N.D., Zheng, Y.L., Kesavapany, S., Kanungo, J., Guszczynski, T., Sihag, R.K., Rudrabhatla, P., Albers, W., Grant, P., and Pant, H.C. (2008). Cyclin-dependent kinase 5 phosphorylation of human septin SEPT5 (hCDCrel-1) modulates exocytosis. *J Neurosci* 28, 3631-3643.

Angaut-Petit, D., Molgo, J., Connold, A.L., and Faille, L. (1987). The levator auris longus muscle of the mouse: a convenient preparation for studies of short- and long-term presynaptic effects of drugs or toxins. *Neurosci Lett* 82, 83-88.

Anggono, V., Smillie, K.J., Graham, M.E., Valova, V.A., Cousin, M.A., and Robinson, P.J. (2006). Syndapin I is the phosphorylation-regulated dynamin I partner in synaptic vesicle endocytosis. *Nat Neurosci* 9, 752-760.

Aponte, Y., Bischofberger, J., and Jonas, P. (2008). Efficient Ca²⁺ buffering in fast-spiking basket cells of rat hippocampus. *J Physiol* 586, 2061-2075.

Augustin, I., Rosenmund, C., Sudhof, T.C., and Brose, N. (1999). Munc13-1 is essential for fusion competence of glutamatergic synaptic vesicles. *Nature* 400, 457-461.

Bai, F., and Witzmann, F.A. (2007). Synaptosome proteomics. *Subcell Biochem* 43, 77-98.

Bajjalieh, S.M., Peterson, K., Shinghal, R., and Scheller, R.H. (1992). SV2, a brain synaptic vesicle protein homologous to bacterial transporters. *Science* 257, 1271-1273.

Baneyx, F. (1999). Recombinant protein expression in *Escherichia coli*. *Curr Opin Biotechnol* 10, 411-421.

Bar-On, D., Wolter, S., van de Linde, S., Heilemann, M., Nudelman, G., Nachliel, E., Gutman, M., Sauer, M., and Ashery, U. (2012). Super-resolution imaging reveals the internal architecture of nano-sized syntaxin clusters. *The Journal of biological chemistry* 287, 27158-27167.

Baumert, M., Maycox, P.R., Navone, F., De Camilli, P., and Jahn, R. (1989). Synaptobrevin: an integral membrane protein of 18,000 daltons present in small synaptic vesicles of rat brain. *The EMBO journal* **8**, 379-384.

Baumert, M., Takei, K., Hartinger, J., Burger, P.M., Fischer von Mollard, G., Maycox, P.R., De Camilli, P., and Jahn, R. (1990). P29: a novel tyrosine-phosphorylated membrane protein present in small clear vesicles of neurons and endocrine cells. *J Cell Biol* **110**, 1285-1294.

Beites, C.L., Campbell, K.A., and Trimble, W.S. (2005). The septin Sept5/CDCrel-1 competes with alpha-SNAP for binding to the SNARE complex. *Biochem J* **385**, 347-353.

Beites, C.L., Xie, H., Bowser, R., and Trimble, W.S. (1999). The septin CDCrel-1 binds syntaxin and inhibits exocytosis. *Nat Neurosci* **2**, 434-439.

Bellani, S., Sousa, V.L., Ronzitti, G., Valtorta, F., Meldolesi, J., and Chieregatti, E. (2010). The regulation of synaptic function by alpha-synuclein. *Commun Integr Biol* **3**, 106-109.

Bellocchio, E.E., Reimer, R.J., Fremeau, R.T., Jr., and Edwards, R.H. (2000). Uptake of glutamate into synaptic vesicles by an inorganic phosphate transporter. *Science* **289**, 957-960.

Benfenati, F., Greengard, P., Brunner, J., and Bahler, M. (1989). Electrostatic and hydrophobic interactions of synapsin I and synapsin I fragments with phospholipid bilayers. *J Cell Biol* **108**, 1851-1862.

Benfenati, F., Valtorta, F., Rubenstein, J.L., Gorelick, F.S., Greengard, P., and Czernik, A.J. (1992). Synaptic vesicle-associated Ca²⁺/calmodulin-dependent protein kinase II is a binding protein for synapsin I. *Nature* **359**, 417-420.

Bennett, M.K., Garcia-Ararras, J.E., Elferink, L.A., Peterson, K., Fleming, A.M., Hazuka, C.D., and Scheller, R.H. (1993). The syntaxin family of vesicular transport receptors. *Cell* **74**, 863-873.

Bennett, M.V., and Zukin, R.S. (2004). Electrical coupling and neuronal synchronization in the Mammalian brain. *Neuron* **41**, 495-511.

Bergsman, J.B., and Tsien, R.W. (2000). Syntaxin modulation of calcium channels in cortical synaptosomes as revealed by botulinum toxin C1. *J Neurosci* 20, 4368-4378.

Bethani, I., Werner, A., Kadian, C., Geumann, U., Jahn, R., and Rizzoli, S.O. (2009). Endosomal fusion upon SNARE knockdown is maintained by residual SNARE activity and enhanced docking. *Traffic* 10, 1543-1559.

Betz, A., Okamoto, M., Benseler, F., and Brose, N. (1997). Direct interaction of the rat unc-13 homologue Munc13-1 with the N terminus of syntaxin. *The Journal of biological chemistry* 272, 2520-2526.

Bewick, G.S. (2003). Maintenance of transmitter release from neuromuscular junctions with different patterns of usage "in vivo". *J Neurocytol* 32, 473-487.

Blondeau, F., Ritter, B., Allaire, P.D., Wasiak, S., Girard, M., Hussain, N.K., Angers, A., Legendre-Guillemain, V., Roy, L., Boismenu, D., *et al.* (2004). Tandem MS analysis of brain clathrin-coated vesicles reveals their critical involvement in synaptic vesicle recycling. *Proc Natl Acad Sci U S A* 101, 3833-3838.

Bloom, O., Evergren, E., Tomilin, N., Kjaerulff, O., Low, P., Brodin, L., Pieribone, V.A., Greengard, P., and Shupliakov, O. (2003). Colocalization of synapsin and actin during synaptic vesicle recycling. *J Cell Biol* 161, 737-747.

Boersema, P.J., Raijmakers, R., Lemeer, S., Mohammed, S., and Heck, A.J. (2009). Multiplex peptide stable isotope dimethyl labeling for quantitative proteomics. *Nature protocols* 4, 484-494.

Bommert, K., Charlton, M.P., DeBello, W.M., Chin, G.J., Betz, H., and Augustine, G.J. (1993). Inhibition of neurotransmitter release by C2-domain peptides implicates synaptotagmin in exocytosis. *Nature* 363, 163-165.

Bonanomi, D., Benfenati, F., and Valtorta, F. (2006). Protein sorting in the synaptic vesicle life cycle. *Prog Neurobiol* 80, 177-217.

Borst, J.G., and Soria van Hoeve, J. (2012). The calyx of held synapse: from model synapse to auditory relay. *Annu Rev Physiol* 74, 199-224.

Boucrot, E., Saffarian, S., Zhang, R., and Kirchhausen, T. Roles of AP-2 in clathrin-mediated endocytosis. *PLoS One* 5, e10597.

Boucrot, E., Saffarian, S., Zhang, R., and Kirchhausen, T. (2010). Roles of AP-2 in clathrin-mediated endocytosis. *PLoS One* 5, e10597.

Bracher, A., Kadlec, J., Betz, H., and Weissenhorn, W. (2002). X-ray structure of a neuronal complexin-SNARE complex from squid. *The Journal of biological chemistry* 277, 26517-26523.

Brodin, L., Low, P., and Shupliakov, O. (2000). Sequential steps in clathrin-mediated synaptic vesicle endocytosis. *Curr Opin Neurobiol* 10, 312-320.

Bronk, P., Deak, F., Wilson, M.C., Liu, X., Sudhof, T.C., and Kavalali, E.T. (2007). Differential effects of SNAP-25 deletion on Ca²⁺-dependent and Ca²⁺-independent neurotransmission. *J Neurophysiol* 98, 794-806.

Bucci, C., Thomsen, P., Nicoziani, P., McCarthy, J., and van Deurs, B. (2000). Rab7: a key to lysosome biogenesis. *Mol Biol Cell* 11, 467-480.

Buckley, K., and Kelly, R.B. (1985). Identification of a transmembrane glycoprotein specific for secretory vesicles of neural and endocrine cells. *J Cell Biol* 100, 1284-1294.

Burger, P.M., Mehl, E., Cameron, P.L., Maycox, P.R., Baumert, M., Lottspeich, F., De Camilli, P., and Jahn, R. (1989). Synaptic vesicles immunisolated from rat cerebral cortex contain high levels of glutamate. *Neuron* 3, 715-720.

Burgoyne, R.D., Barclay, J.W., Ciufo, L.F., Graham, M.E., Handley, M.T., and Morgan, A. (2009). The functions of Munc18-1 in regulated exocytosis. *Ann N Y Acad Sci* 1152, 76-86.

Burre, J., Beckhaus, T., Schagger, H., Corvey, C., Hofmann, S., Karas, M., Zimmermann, H., and Volkandt, W. (2006). Analysis of the synaptic vesicle proteome using three gel-based protein separation techniques. *Proteomics* 6, 6250-6262.

Burre, J., Sharma, M., and Sudhof, T.C. (2012). Systematic mutagenesis of alpha-synuclein reveals distinct sequence requirements for physiological and pathological activities. *J Neurosci* 32, 15227-15242.

Burre, J., Sharma, M., Tsetsenis, T., Buchman, V., Etherton, M.R., and Sudhof, T.C. (2010). Alpha-synuclein promotes SNARE-complex assembly in vivo and in vitro. *Science* 329, 1663-1667.

Burre, J., and Volkandt, W. (2007). The synaptic vesicle proteome. *J Neurochem* 101, 1448-1462.

Cahill, A.L., Herring, B.E., and Fox, A.P. (2006). Stable silencing of SNAP-25 in PC12 cells by RNA interference. *BMC Neurosci* 7, 9.

Calakos, N., and Scheller, R.H. (1994). Vesicle-associated membrane protein and synaptophysin are associated on the synaptic vesicle. *The Journal of biological chemistry* 269, 24534-24537.

Cameron, P.L., Sudhof, T.C., Jahn, R., and De Camilli, P. (1991). Colocalization of synaptophysin with transferrin receptors: implications for synaptic vesicle biogenesis. *J Cell Biol* 115, 151-164.

Cano, R., Torres-Benito, L., Tejero, R., Biea, A.I., Ruiz, R., Betz, W.J., and Tabares, L. (2013). Structural and functional maturation of active zones in large synapses. *Mol Neurobiol* 47, 209-219.

Castle, A., and Castle, D. (2005). Ubiquitously expressed secretory carrier membrane proteins (SCAMPs) 1-4 mark different pathways and exhibit limited constitutive trafficking to and from the cell surface. *Journal of cell science* *118*, 3769-3780.

Cesca, F., Baldelli, P., Valtorta, F., and Benfenati, F. (2010). The synapsins: key actors of synapse function and plasticity. *Prog Neurobiol* *91*, 313-348.

Chamberlain, L.H., and Burgoyne, R.D. (1998). Cysteine string protein functions directly in regulated exocytosis. *Mol Biol Cell* *9*, 2259-2267.

Chandra, S., Gallardo, G., Fernandez-Chacon, R., Schluter, O.M., and Sudhof, T.C. (2005). Alpha-synuclein cooperates with CSPalpha in preventing neurodegeneration. *Cell* *123*, 383-396.

Chang, W.P., and Sudhof, T.C. (2009). SV2 renders primed synaptic vesicles competent for Ca²⁺-induced exocytosis. *J Neurosci* *29*, 883-897.

Chapman, E.R. (2008). How does synaptotagmin trigger neurotransmitter release? *Annual review of biochemistry* *77*, 615-641.

Chapman, E.R., Hanson, P.I., An, S., and Jahn, R. (1995). Ca²⁺ regulates the interaction between synaptotagmin and syntaxin 1. *The Journal of biological chemistry* *270*, 23667-23671.

Chappell, T.G., Welch, W.J., Schlossman, D.M., Palter, K.B., Schlesinger, M.J., and Rothman, J.E. (1986). Uncoating ATPase is a member of the 70 kilodalton family of stress proteins. *Cell* *45*, 3-13.

Chappie, J.S., Mears, J.A., Fang, S., Leonard, M., Schmid, S.L., Milligan, R.A., Hinshaw, J.E., and Dyda, F. (2011). A pseudoatomic model of the dynamin polymer identifies a hydrolysis-dependent powerstroke. *Cell* *147*, 209-222.

Chen, D., Minger, S.L., Honer, W.G., and Whiteheart, S.W. (1999). Organization of the secretory machinery in the rodent brain: distribution of the t-SNAREs, SNAP-25 and SNAP-23. *Brain Res* 831, 11-24.

Chen, M.S., Obar, R.A., Schroeder, C.C., Austin, T.W., Poodry, C.A., Wadsworth, S.C., and Vallee, R.B. (1991). Multiple forms of dynamin are encoded by shibire, a *Drosophila* gene involved in endocytosis. *Nature* 351, 583-586.

Chen, X., Barg, S., and Almers, W. (2008). Release of the styryl dyes from single synaptic vesicles in hippocampal neurons. *J Neurosci* 28, 1894-1903.

Chen, X., Nelson, C.D., Li, X., Winters, C.A., Azzam, R., Sousa, A.A., Leapman, R.D., Gainer, H., Sheng, M., and Reese, T.S. (2011). PSD-95 is required to sustain the molecular organization of the postsynaptic density. *J Neurosci* 31, 6329-6338.

Chen, X., Tomchick, D.R., Kovrigin, E., Arac, D., Machius, M., Sudhof, T.C., and Rizo, J. (2002). Three-dimensional structure of the complexin/SNARE complex. *Neuron* 33, 397-409.

Chen, Y., Gan, B.Q., and Tang, B.L. (2010). Syntaxin 16: unraveling cellular physiology through a ubiquitous SNARE molecule. *J Cell Physiol* 225, 326-332.

Cheng, D., Hoogenraad, C.C., Rush, J., Ramm, E., Schlager, M.A., Duong, D.M., Xu, P., Wijayawardana, S.R., Hanfelt, J., Nakagawa, T., *et al.* (2006). Relative and absolute quantification of postsynaptic density proteome isolated from rat forebrain and cerebellum. *Mol Cell Proteomics* 5, 1158-1170.

Cheng, Y., Boll, W., Kirchhausen, T., Harrison, S.C., and Walz, T. (2007). Cryo-electron tomography of clathrin-coated vesicles: structural implications for coat assembly. *J Mol Biol* 365, 892-899.

Cheung, W.T., Richards, D.E., and Rogers, J.H. (1993). Calcium binding by chick calretinin and rat calbindin D28k synthesised in bacteria. *Eur J Biochem* 215, 401-410.

Chin, D., and Means, A.R. (2000). Calmodulin: a prototypical calcium sensor. *Trends in cell biology* 10, 322-328.

Chiu, C.S., Jensen, K., Sokolova, I., Wang, D., Li, M., Deshpande, P., Davidson, N., Mody, I., Quick, M.W., Quake, S.R., *et al.* (2002). Number, density, and surface/cytoplasmic distribution of GABA transporters at presynaptic structures of knock-in mice carrying GABA transporter subtype 1-green fluorescent protein fusions. *J Neurosci* 22, 10251-10266.

Chiu, C.S., Kartalov, E., Unger, M., Quake, S., and Lester, H.A. (2001). Single-molecule measurements calibrate green fluorescent protein surface densities on transparent beads for use with 'knock-in' animals and other expression systems. *J Neurosci Methods* 105, 55-63.

Cho, K.O., Hunt, C.A., and Kennedy, M.B. (1992). The rat brain postsynaptic density fraction contains a homolog of the *Drosophila* discs-large tumor suppressor protein. *Neuron* 9, 929-942.

Chretien, D., and Fuller, S.D. (2000). Microtubules switch occasionally into unfavorable configurations during elongation. *J Mol Biol* 298, 663-676.

Chua, C.E., and Tang, B.L. (2008). Syntaxin 16 is enriched in neuronal dendrites and may have a role in neurite outgrowth. *Mol Membr Biol* 25, 35-45.

Cirrito, J.R., Kang, J.E., Lee, J., Stewart, F.R., Verges, D.K., Silverio, L.M., Bu, G., Mennerick, S., and Holtzman, D.M. (2008). Endocytosis is required for synaptic activity-dependent release of amyloid-beta in vivo. *Neuron* 58, 42-51.

Cirrito, J.R., Yamada, K.A., Finn, M.B., Sloviter, R.S., Bales, K.R., May, P.C., Schoepp, D.D., Paul, S.M., Mennerick, S., and Holtzman, D.M. (2005). Synaptic activity regulates interstitial fluid amyloid-beta levels in vivo. *Neuron* 48, 913-922.

Clayton, E.L., and Cousin, M.A. (2009). The molecular physiology of activity-dependent bulk endocytosis of synaptic vesicles. *J Neurochem* 111, 901-914.

Clayton, E.L., Evans, G.J., and Cousin, M.A. (2008). Bulk synaptic vesicle endocytosis is rapidly triggered during strong stimulation. *J Neurosci* 28, 6627-6632.

Cocucci, E., Aguet, F., Boulant, S., and Kirchhausen, T. (2012). The first five seconds in the life of a clathrin-coated pit. *Cell* 150, 495-507.

Cole, S.L., and Vassar, R. (2007). The Alzheimer's disease beta-secretase enzyme, BACE1. *Mol Neurodegener* 2, 22.

Collin, T., Marty, A., and Llano, I. (2005). Presynaptic calcium stores and synaptic transmission. *Curr Opin Neurobiol* 15, 275-281.

Collins, B.M., McCoy, A.J., Kent, H.M., Evans, P.R., and Owen, D.J. (2002). Molecular architecture and functional model of the endocytic AP2 complex. *Cell* 109, 523-535.

Conchello, J.A., and Lichtman, J.W. (2005). Optical sectioning microscopy. *Nature methods* 2, 920-931.

Conde, C., and Caceres, A. (2009). Microtubule assembly, organization and dynamics in axons and dendrites. *Nature reviews* 10, 319-332.

Condliffe, S.B., Corradini, I., Pozzi, D., Verderio, C., and Matteoli, M. (2010). Endogenous SNAP-25 regulates native voltage-gated calcium channels in glutamatergic neurons. *The Journal of biological chemistry* 285, 24968-24976.

Connors, B.W., and Long, M.A. (2004). Electrical synapses in the mammalian brain. *Annual review of neuroscience* 27, 393-418.

Coppola, T., Perret-Menoud, V., Luthi, S., Farnsworth, C.C., Glomset, J.A., and Regazzi, R. (1999). Disruption of Rab3-calmodulin interaction, but not other effector interactions, prevents Rab3 inhibition of exocytosis. *The EMBO journal* 18, 5885-5891.

Coughenour, H.D., Spaulding, R.S., and Thompson, C.M. (2004). The synaptic vesicle proteome: a comparative study in membrane protein identification. *Proteomics* 4, 3141-3155.

Couteaux, R., and Pecot-Dechavassine, M. (1970). [Synaptic vesicles and pouches at the level of "active zones" of the neuromuscular junction]. *C R Acad Sci Hebd Seances Acad Sci D* 271, 2346-2349.

Cremona, O., Di Paolo, G., Wenk, M.R., Luthi, A., Kim, W.T., Takei, K., Daniell, L., Nemoto, Y., Shears, S.B., Flavell, R.A., *et al.* (1999). Essential role of phosphoinositide metabolism in synaptic vesicle recycling. *Cell* 99, 179-188.

Dai, Y., Taru, H., Deken, S.L., Grill, B., Ackley, B., Nonet, M.L., and Jin, Y. (2006). SYD-2 Liprin-alpha organizes presynaptic active zone formation through ELKS. *Nat Neurosci* 9, 1479-1487.

Daly, C., and Ziff, E.B. (2002). Ca²⁺-dependent formation of a dynamin-synaptophysin complex: potential role in synaptic vesicle endocytosis. *The Journal of biological chemistry* 277, 9010-9015.

Dani, A., Huang, B., Bergan, J., Dulac, C., and Zhuang, X. (2010). Superresolution imaging of chemical synapses in the brain. *Neuron* 68, 843-856.

Darchen, F., and Goud, B. (2000). Multiple aspects of Rab protein action in the secretory pathway: focus on Rab3 and Rab6. *Biochimie* 82, 375-384.

Deng, L., Kaeser, P.S., Xu, W., and Sudhof, T.C. (2011). RIM proteins activate vesicle priming by reversing autoinhibitory homodimerization of Munc13. *Neuron* 69, 317-331.

Denker, A., Bethani, I., Krohnert, K., Korber, C., Horstmann, H., Wilhelm, B.G., Barysch, S.V., Kuner, T., Neher, E., and Rizzoli, S.O. (2011a). A small pool of vesicles maintains synaptic activity in vivo. *Proc Natl Acad Sci U S A* 108, 17177-17182.

Denker, A., Krohnert, K., Buckers, J., Neher, E., and Rizzoli, S.O. (2011b). The reserve pool of synaptic vesicles acts as a buffer for proteins involved in synaptic vesicle recycling. *Proc Natl Acad Sci U S A* *108*, 17183-17188.

Desiderio, D.M., and Kai, M. (1983). Preparation of stable isotope-incorporated peptide internal standards for field desorption mass spectrometry quantification of peptides in biologic tissue. *Biomed Mass Spectrom* *10*, 471-479.

Di Paolo, G., Sankaranarayanan, S., Wenk, M.R., Daniell, L., Perucco, E., Caldarone, B.J., Flavell, R., Picciotto, M.R., Ryan, T.A., Cremona, O., *et al.* (2002). Decreased synaptic vesicle recycling efficiency and cognitive deficits in amphiphysin 1 knockout mice. *Neuron* *33*, 789-804.

Dickman, D.K., Horne, J.A., Meinertzhagen, I.A., and Schwarz, T.L. (2005). A slowed classical pathway rather than kiss-and-run mediates endocytosis at synapses lacking synaptojanin and endophilin. *Cell* *123*, 521-533.

Dillon, C., and Goda, Y. (2005). The actin cytoskeleton: integrating form and function at the synapse. *Annual review of neuroscience* *28*, 25-55.

Diril, M.K., Wienisch, M., Jung, N., Klingauf, J., and Haucke, V. (2006). Stonin 2 is an AP-2-dependent endocytic sorting adaptor for synaptotagmin internalization and recycling. *Dev Cell* *10*, 233-244.

Dresbach, T., Hempelmann, A., Spilker, C., tom Dieck, S., Altmann, W.D., Zuschratter, W., Garner, C.C., and Gundelfinger, E.D. (2003). Functional regions of the presynaptic cytomatrix protein bassoon: significance for synaptic targeting and cytomatrix anchoring. *Mol Cell Neurosci* *23*, 279-291.

Dunkley, P.R., Jarvie, P.E., and Robinson, P.J. (2008). A rapid Percoll gradient procedure for preparation of synaptosomes. *Nature protocols* *3*, 1718-1728.

Eberhard, M., and Erne, P. (1994). Calcium and magnesium binding to rat parvalbumin. *Eur J Biochem* 222, 21-26.

Edeling, M.A., Smith, C., and Owen, D. (2006). Life of a clathrin coat: insights from clathrin and AP structures. *Nature reviews* 7, 32-44.

Elferink, L.A., Trimble, W.S., and Scheller, R.H. (1989). Two vesicle-associated membrane protein genes are differentially expressed in the rat central nervous system. *The Journal of biological chemistry* 264, 11061-11064.

Evergren, E., Benfenati, F., and Shupliakov, O. (2007a). The synapsin cycle: a view from the synaptic endocytic zone. *Journal of neuroscience research* 85, 2648-2656.

Evergren, E., Gad, H., Walther, K., Sundborger, A., Tomilin, N., and Shupliakov, O. (2007b). Intersectin is a negative regulator of dynamin recruitment to the synaptic endocytic zone in the central synapse. *J Neurosci* 27, 379-390.

Fejtova, A., and Gundelfinger, E.D. (2006). Molecular organization and assembly of the presynaptic active zone of neurotransmitter release. *Results Probl Cell Differ* 43, 49-68.

Ferguson, S.M., Brasnjo, G., Hayashi, M., Wolfel, M., Collesi, C., Giovedi, S., Raimondi, A., Gong, L.W., Ariel, P., Paradise, S., *et al.* (2007). A selective activity-dependent requirement for dynamin 1 in synaptic vesicle endocytosis. *Science* 316, 570-574.

Ferguson, S.M., and De Camilli, P. (2012). Dynamin, a membrane-remodelling GTPase. *Nature reviews* 13, 75-88.

Ferguson, S.M., Raimondi, A., Paradise, S., Shen, H., Mesaki, K., Ferguson, A., Destaing, O., Ko, G., Takasaki, J., Cremona, O., *et al.* (2009). Coordinated actions of actin and BAR proteins upstream of dynamin at endocytic clathrin-coated pits. *Dev Cell* 17, 811-822.

Fernandez-Chacon, R., Achiriloaie, M., Janz, R., Albanesi, J.P., and Sudhof, T.C. (2000). SCAMP1 function in endocytosis. *The Journal of biological chemistry* 275, 12752-12756.

Fernandez-Chacon, R., and Sudhof, T.C. (2000). Novel SCAMPs lacking NPF repeats: ubiquitous and synaptic vesicle-specific forms implicate SCAMPs in multiple membrane-trafficking functions. *J Neurosci* 20, 7941-7950.

Fernandez-Chacon, R., Wolfel, M., Nishimune, H., Tabares, L., Schmitz, F., Castellano-Munoz, M., Rosenmund, C., Montesinos, M.L., Sanes, J.R., Schneggenburger, R., *et al.* (2004). The synaptic vesicle protein CSP alpha prevents presynaptic degeneration. *Neuron* 42, 237-251.

Fernandez, I., Arac, D., Ubach, J., Gerber, S.H., Shin, O., Gao, Y., Anderson, R.G., Sudhof, T.C., and Rizo, J. (2001). Three-dimensional structure of the synaptotagmin 1 C2B-domain: synaptotagmin 1 as a phospholipid binding machine. *Neuron* 32, 1057-1069.

Finbow, M.E., and Harrison, M.A. (1997). The vacuolar H⁺-ATPase: a universal proton pump of eukaryotes. *Biochem J* 324 (Pt 3), 697-712.

Fischer von Mollard, G., Sudhof, T.C., and Jahn, R. (1991). A small GTP-binding protein dissociates from synaptic vesicles during exocytosis. *Nature* 349, 79-81.

Flucher, B.E., and Daniels, M.P. (1989). Distribution of Na⁺ channels and ankyrin in neuromuscular junctions is complementary to that of acetylcholine receptors and the 43 kd protein. *Neuron* 3, 163-175.

Ford, M.G., Mills, I.G., Peter, B.J., Vallis, Y., Praefcke, G.J., Evans, P.R., and McMahon, H.T. (2002). Curvature of clathrin-coated pits driven by epsin. *Nature* 419, 361-366.

Fornasiero, E.F., Raimondi, A., Guarnieri, F.C., Orlando, M., Fesce, R., Benfenati, F., and Valtorta, F. (2012). Synapsins contribute to the dynamic spatial organization of synaptic vesicles in an activity-dependent manner. *J Neurosci* 32, 12214-12227.

Foster, D.M., and Sherrington, C. (1897). A textbook of physiology, part three: The central nervous system, 7th edn (London, MacMillan & Co. Ltd).

Fountoulakis, M., Schuller, E., Hardmeier, R., Berndt, P., and Lubec, G. (1999). Rat brain proteins: two-dimensional protein database and variations in the expression level. *Electrophoresis* *20*, 3572-3579.

Fremeau, R.T., Jr., Troyer, M.D., Pahner, I., Nygaard, G.O., Tran, C.H., Reimer, R.J., Bellocchio, E.E., Fortin, D., Storm-Mathisen, J., and Edwards, R.H. (2001). The expression of vesicular glutamate transporters defines two classes of excitatory synapse. *Neuron* *31*, 247-260.

Frerking, M., Borges, S., and Wilson, M. (1997). Are some minis multiquantal? *J Neurophysiol* *78*, 1293-1304.

Frost, A., Unger, V.M., and De Camilli, P. (2009). The BAR domain superfamily: membrane-molding macromolecules. *Cell* *137*, 191-196.

Fujiwara, T., Mishima, T., Kofuji, T., Chiba, T., Tanaka, K., Yamamoto, A., and Akagawa, K. (2006). Analysis of knock-out mice to determine the role of HPC-1/syntaxin 1A in expressing synaptic plasticity. *J Neurosci* *26*, 5767-5776.

Furshpan, E.J., and Potter, D.D. (1959). Transmission at the giant motor synapses of the crayfish. *J Physiol* *145*, 289-325.

Gaidarov, I., and Keen, J.H. (1999). Phosphoinositide-AP-2 interactions required for targeting to plasma membrane clathrin-coated pits. *J Cell Biol* *146*, 755-764.

Galbraith, C.G., and Galbraith, J.A. (2011). Super-resolution microscopy at a glance. *Journal of cell science* *124*, 1607-1611.

Galli, T., McPherson, P.S., and De Camilli, P. (1996). The V0 sector of the V-ATPase, synaptobrevin, and synaptophysin are associated on synaptic vesicles in a Triton X-100-resistant, freeze-thawing sensitive, complex. *The Journal of biological chemistry* *271*, 2193-2198.

Gennaro, J.F., Jr., Nastuk, W.L., and Rutherford, D.T. (1978). Reversible depletion of synaptic vesicles induced by application of high external potassium to the frog neuromuscular junction. *J Physiol* *280*, 237-247.

George, J.M., Jin, H., Woods, W.S., and Clayton, D.F. (1995). Characterization of a novel protein regulated during the critical period for song learning in the zebra finch. *Neuron* *15*, 361-372.

Geppert, M., Archer, B.T., 3rd, and Sudhof, T.C. (1991). Synaptotagmin II. A novel differentially distributed form of synaptotagmin. *The Journal of biological chemistry* *266*, 13548-13552.

Geppert, M., Goda, Y., Hammer, R.E., Li, C., Rosahl, T.W., Stevens, C.F., and Sudhof, T.C. (1994). Synaptotagmin I: a major Ca²⁺ sensor for transmitter release at a central synapse. *Cell* *79*, 717-727.

Gerber, S.A., Rush, J., Stemman, O., Kirschner, M.W., and Gygi, S.P. (2003). Absolute quantification of proteins and phosphoproteins from cell lysates by tandem MS. *Proc Natl Acad Sci U S A* *100*, 6940-6945.

Gitler, D., Takagishi, Y., Feng, J., Ren, Y., Rodriguiz, R.M., Wetsel, W.C., Greengard, P., and Augustine, G.J. (2004). Different presynaptic roles of synapsins at excitatory and inhibitory synapses. *J Neurosci* *24*, 11368-11380.

Giudici, M.L., Emson, P.C., and Irvine, R.F. (2004). A novel neuronal-specific splice variant of Type I phosphatidylinositol 4-phosphate 5-kinase isoform gamma. *Biochem J* *379*, 489-496.

Goldsbury, C., Mocanu, M.M., Thies, E., Kaether, C., Haass, C., Keller, P., Biernat, J., Mandelkow, E., and Mandelkow, E.M. (2006). Inhibition of APP trafficking by tau protein does not increase the generation of amyloid-beta peptides. *Traffic* *7*, 873-888.

Goldsbury, C., Thies, E., Konzack, S., and Mandelkow, E.M. (2007). Quantification of amyloid precursor protein and tau for the study of axonal traffic pathways. *J Neurosci* *27*, 3357-3363.

Gordon, S.L., Leube, R.E., and Cousin, M.A. (2011). Synaptophysin is required for synaptobrevin retrieval during synaptic vesicle endocytosis. *J Neurosci* 31, 14032-14036.

Granseth, B., Odermatt, B., Royle, S.J., and Lagnado, L. (2006). Clathrin-mediated endocytosis is the dominant mechanism of vesicle retrieval at hippocampal synapses. *Neuron* 51, 773-786.

Granseth, B., Odermatt, B., Royle, S.J., and Lagnado, L. (2007). Clathrin-mediated endocytosis: the physiological mechanism of vesicle retrieval at hippocampal synapses. *J Physiol* 585, 681-686.

Granseth, B., Odermatt, B., Royle, S.J., and Lagnado, L. (2009). Comment on "The dynamic control of kiss-and-run and vesicular reuse probed with single nanoparticles". *Science* 325, 1499; author reply 1499.

Gray, E.G., and Whittaker, V.P. (1962). The isolation of nerve endings from brain: an electron-microscopic study of cell fragments derived by homogenization and centrifugation. *J Anat* 96, 79-88.

Groemer, T.W., and Klingauf, J. (2007). Synaptic vesicles recycling spontaneously and during activity belong to the same vesicle pool. *Nat Neurosci* 10, 145-147.

Groemer, T.W., Thiel, C.S., Holt, M., Riedel, D., Hua, Y., Huve, J., Wilhelm, B.G., and Klingauf, J. (2011). Amyloid precursor protein is trafficked and secreted via synaptic vesicles. *PLoS One* 6, e18754.

Groffen, A.J., Friedrich, R., Brian, E.C., Ashery, U., and Verhage, M. (2006). DOC2A and DOC2B are sensors for neuronal activity with unique calcium-dependent and kinetic properties. *J Neurochem* 97, 818-833.

Groffen, A.J., Martens, S., Arazola, R.D., Cornelisse, L.N., Lozovaya, N., de Jong, A.P., Goriounova, N.A., Habets, R.L., Takai, Y., Borst, J.G., *et al.* (2010). Doc2b Is a High-Affinity Ca²⁺ Sensor for Spontaneous Neurotransmitter Release. *Science*.

Gulyas-Kovacs, A., de Wit, H., Milosevic, I., Kochubey, O., Toonen, R., Klingauf, J., Verhage, M., and Sorensen, J.B. (2007). Munc18-1: sequential interactions with the fusion machinery stimulate vesicle docking and priming. *J Neurosci* 27, 8676-8686.

Gundelfinger, E.D., and Fejtova, A. (2011). Molecular organization and plasticity of the cytomatrix at the active zone. *Curr Opin Neurobiol* 22, 423-430.

Haass, C., and Selkoe, D.J. (2007). Soluble protein oligomers in neurodegeneration: lessons from the Alzheimer's amyloid beta-peptide. *Nature reviews* 8, 101-112.

Haiech, J., Derancourt, J., Pechere, J.F., and Demaille, J.G. (1979). Magnesium and calcium binding to parvalbumins: evidence for differences between parvalbumins and an explanation of their relaxing function. *Biochemistry* 18, 2752-2758.

Halling, D.B., Aracena-Parks, P., and Hamilton, S.L. (2005). Regulation of voltage-gated Ca²⁺ channels by calmodulin. *Sci STKE* 2005, re15.

Han, K., and Kim, E. (2008). Synaptic adhesion molecules and PSD-95. *Prog Neurobiol* 84, 263-283.

Harris, K.M., Jensen, F.E., and Tsao, B. (1992). Three-dimensional structure of dendritic spines and synapses in rat hippocampus (CA1) at postnatal day 15 and adult ages: implications for the maturation of synaptic physiology and long-term potentiation. *J Neurosci* 12, 2685-2705.

Hauke, V., Neher, E., and Sigrist, S.J. (2011). Protein scaffolds in the coupling of synaptic exocytosis and endocytosis. *Nature reviews* 12, 127-138.

He, L., Wu, X.S., Mohan, R., and Wu, L.G. (2006). Two modes of fusion pore opening revealed by cell-attached recordings at a synapse. *Nature* *444*, 102-105.

Hell, S.W., and Wichmann, J. (1994). Breaking the diffraction resolution limit by stimulated emission: stimulated emission depletion microscopy. *Opt Lett* *19*, 780 - 782.

Helmchen, F., Imoto, K., and Sakmann, B. (1996). Ca²⁺ buffering and action potential-evoked Ca²⁺ signaling in dendrites of pyramidal neurons. *Biophys J* *70*, 1069-1081.

Henne, W.M., Boucrot, E., Meinecke, M., Evergren, E., Vallis, Y., Mittal, R., and McMahon, H.T. FCHO proteins are nucleators of clathrin-mediated endocytosis. *Science* *328*, 1281-1284.

Henne, W.M., Boucrot, E., Meinecke, M., Evergren, E., Vallis, Y., Mittal, R., and McMahon, H.T. (2010). FCHO proteins are nucleators of clathrin-mediated endocytosis. *Science* *328*, 1281-1284.

Heuser, J.E., Reese, T.S., Dennis, M.J., Jan, Y., Jan, L., and Evans, L. (1979). Synaptic vesicle exocytosis captured by quick freezing and correlated with quantal transmitter release. *J Cell Biol* *81*, 275-300.

Hirokawa, N., Sobue, K., Kanda, K., Harada, A., and Yorifuji, H. (1989). The cytoskeletal architecture of the presynaptic terminal and molecular structure of synapsin 1. *J Cell Biol* *108*, 111-126.

Honing, S., Ricotta, D., Krauss, M., Spate, K., Spolaore, B., Motley, A., Robinson, M., Robinson, C., Haucke, V., and Owen, D.J. (2005). Phosphatidylinositol-(4,5)-bisphosphate regulates sorting signal recognition by the clathrin-associated adaptor complex AP2. *Mol Cell* *18*, 519-531.

Hoopmann, P., Punge, A., Barysch, S.V., Westphal, V., Buckers, J., Opazo, F., Bethani, I., Lauterbach, M.A., Hell, S.W., and Rizzoli, S.O. (2010). Endosomal sorting of readily releasable synaptic vesicles. *Proc Natl Acad Sci U S A* *107*, 19055-19060.

Hori, T., and Takahashi, T. (2012). Kinetics of synaptic vesicle refilling with neurotransmitter glutamate. *Neuron* 76, 511-517.

Hormuzdi, S.G., Filippov, M.A., Mitropoulou, G., Monyer, H., and Bruzzone, R. (2004). Electrical synapses: a dynamic signaling system that shapes the activity of neuronal networks. *Biochim Biophys Acta* 1662, 113-137.

Horvath, C.A., Vanden Broeck, D., Boulet, G.A., Bogers, J., and De Wolf, M.J. (2007). Epsin: inducing membrane curvature. *Int J Biochem Cell Biol* 39, 1765-1770.

Hsu, S.C., Hazuka, C.D., Roth, R., Foletti, D.L., Heuser, J., and Scheller, R.H. (1998). Subunit composition, protein interactions, and structures of the mammalian brain sec6/8 complex and septin filaments. *Neuron* 20, 1111-1122.

Hua, Y., Sinha, R., Martineau, M., Kahms, M., and Klingauf, J. (2010). A common origin of synaptic vesicles undergoing evoked and spontaneous fusion. *Nat Neurosci* 13, 1451-1453.

Huang, B., Babcock, H., and Zhuang, X. (2010). Breaking the diffraction barrier: super-resolution imaging of cells. *Cell* 143, 1047-1058.

Huang, B., Wang, W., Bates, M., and Zhuang, X. (2008). Three-dimensional super-resolution imaging by stochastic optical reconstruction microscopy. *Science* 319, 810-813.

Huang, F., Khvorova, A., Marshall, W., and Sorkin, A. (2004). Analysis of clathrin-mediated endocytosis of epidermal growth factor receptor by RNA interference. *The Journal of biological chemistry* 279, 16657-16661.

Hudmon, A., and Schulman, H. (2002). Neuronal CA2+/calmodulin-dependent protein kinase II: the role of structure and autoregulation in cellular function. *Annual review of biochemistry* 71, 473-510.

Hunt, C.A., Schenker, L.J., and Kennedy, M.B. (1996). PSD-95 is associated with the postsynaptic density and not with the presynaptic membrane at forebrain synapses. *J Neurosci* *16*, 1380-1388.

Igarashi, M., and Watanabe, M. (2007). Roles of calmodulin and calmodulin-binding proteins in synaptic vesicle recycling during regulated exocytosis at submicromolar Ca²⁺ concentrations. *Neurosci Res* *58*, 226-233.

Ikeda, K., and Bekkers, J.M. (2009). Counting the number of releasable synaptic vesicles in a presynaptic terminal. *Proc Natl Acad Sci U S A* *106*, 2945-2950.

Illinger, D., Kubina, M., Duportail, G., Poindron, P., Bartholeyns, J., and Kuhry, J.G. (1989). TMA-DPH a fluorescent probe of membrane dynamics in living cells. How to use it in phagocytosis. *Cell Biophys* *14*, 17-26.

Inoue, E., Deguchi-Tawarada, M., Takao-Rikitsu, E., Inoue, M., Kitajima, I., Ohtsuka, T., and Takai, Y. (2006). ELKS, a protein structurally related to the active zone protein CAST, is involved in Ca²⁺-dependent exocytosis from PC12 cells. *Genes Cells* *11*, 659-672.

Jahn, R., and Fasshauer, D. (2012). Molecular machines governing exocytosis of synaptic vesicles. *Nature* *490*, 201-207.

Jahn, R., and Scheller, R.H. (2006). SNAREs--engines for membrane fusion. *Nature reviews* *7*, 631-643.

Jahn, R., Schiebler, W., Ouimet, C., and Greengard, P. (1985). A 38,000-dalton membrane protein (p38) present in synaptic vesicles. *Proc Natl Acad Sci U S A* *82*, 4137-4141.

Jakobsson, J., Gad, H., Andersson, F., Low, P., Shupliakov, O., and Brodin, L. (2008). Role of epsin 1 in synaptic vesicle endocytosis. *Proc Natl Acad Sci U S A* *105*, 6445-6450.

Janz, R., Goda, Y., Geppert, M., Missler, M., and Sudhof, T.C. (1999a). SV2A and SV2B function as redundant Ca²⁺ regulators in neurotransmitter release. *Neuron* 24, 1003-1016.

Janz, R., Sudhof, T.C., Hammer, R.E., Unni, V., Siegelbaum, S.A., and Bolshakov, V.Y. (1999b). Essential roles in synaptic plasticity for synaptogyrin I and synaptophysin I. *Neuron* 24, 687-700.

Jia, J.Y., Lamer, S., Schumann, M., Schmidt, M.R., Krause, E., and Haucke, V. (2006). Quantitative proteomics analysis of detergent-resistant membranes from chemical synapses: evidence for cholesterol as spatial organizer of synaptic vesicle cycling. *Mol Cell Proteomics* 5, 2060-2071.

Johnston, P.A., and Sudhof, T.C. (1990). The multisubunit structure of synaptophysin. Relationship between disulfide bonding and homo-oligomerization. *The Journal of biological chemistry* 265, 8869-8873.

Jongsma, A.P., Hijmans, W., and Ploem, J.S. (1971). Quantitative immunofluorescence. Standardization and calibration in microfluorometry. *Histochemie* 25, 329-343.

Jordan, B.A., Fernholz, B.D., Boussac, M., Xu, C., Grigorean, G., Ziff, E.B., and Neubert, T.A. (2004). Identification and verification of novel rodent postsynaptic density proteins. *Mol Cell Proteomics* 3, 857-871.

Jung, J.J., Inamdar, S.M., Tiwari, A., and Choudhury, A. (2012). Regulation of intracellular membrane trafficking and cell dynamics by syntaxin-6. *Biosci Rep* 32, 383-391.

Jung, N., and Haucke, V. (2007). Clathrin-mediated endocytosis at synapses. *Traffic* 8, 1129-1136.

Kaesler, P.S., Deng, L., Chavez, A.E., Liu, X., Castillo, P.E., and Sudhof, T.C. (2009). ELKS2 α /CAST deletion selectively increases neurotransmitter release at inhibitory synapses. *Neuron* 64, 227-239.

Kaesler, P.S., Deng, L., Wang, Y., Dulubova, I., Liu, X., Rizo, J., and Sudhof, T.C. (2011). RIM proteins tether Ca²⁺ channels to presynaptic active zones via a direct PDZ-domain interaction. *Cell* *144*, 282-295.

Kaether, C., Skehel, P., and Dotti, C.G. (2000). Axonal membrane proteins are transported in distinct carriers: a two-color video microscopy study in cultured hippocampal neurons. *Mol Biol Cell* *11*, 1213-1224.

Kammermeier, P.J. (2006). Surface clustering of metabotropic glutamate receptor 1 induced by long Homer proteins. *BMC Neurosci* *7*, 1.

Kandel, E.R. (2000). *Principles of neural science*, 4. edn (New York, NY. [u.a.], McGraw-Hill).

Kessels, M.M., and Qualmann, B. (2004). The syndapin protein family: linking membrane trafficking with the cytoskeleton. *Journal of cell science* *117*, 3077-3086.

Kessels, M.M., and Qualmann, B. (2006). Syndapin oligomers interconnect the machineries for endocytic vesicle formation and actin polymerization. *The Journal of biological chemistry* *281*, 13285-13299.

Kirkpatrick, D.S., Gerber, S.A., and Gygi, S.P. (2005). The absolute quantification strategy: a general procedure for the quantification of proteins and post-translational modifications. *Methods (San Diego, Calif)* *35*, 265-273.

Kittler, J.T., and Moss, S.J. (2003). Modulation of GABA_A receptor activity by phosphorylation and receptor trafficking: implications for the efficacy of synaptic inhibition. *Curr Opin Neurobiol* *13*, 341-347.

Kjaerulff, O., Brodin, L., and Jung, A. (2010). The structure and function of endophilin proteins. *Cell Biochem Biophys* *60*, 137-154.

Klingauf, J., Kavalali, E.T., and Tsien, R.W. (1998). Kinetics and regulation of fast endocytosis at hippocampal synapses. *Nature* 394, 581-585.

Knowles, M.K., Barg, S., Wan, L., Midorikawa, M., Chen, X., and Almers, W. (2010). Single secretory granules of live cells recruit syntaxin-1 and synaptosomal associated protein 25 (SNAP-25) in large copy numbers. *Proc Natl Acad Sci U S A* 107, 20810-20815.

Koch, D., Spiwox-Becker, I., Sabanov, V., Sinning, A., Dugladze, T., Stellmacher, A., Ahuja, R., Grimm, J., Schuler, S., Muller, A., *et al.* (2011). Proper synaptic vesicle formation and neuronal network activity critically rely on syndapin I. *The EMBO journal* 30, 4955-4969.

Koenig, J.H., and Ikeda, K. (1989). Disappearance and reformation of synaptic vesicle membrane upon transmitter release observed under reversible blockage of membrane retrieval. *J Neurosci* 9, 3844-3860.

Koh, T.W., Verstreken, P., and Bellen, H.J. (2004). Dap160/intersectin acts as a stabilizing scaffold required for synaptic development and vesicle endocytosis. *Neuron* 43, 193-205.

Koo, S.J., Markovic, S., Puchkov, D., Mahrenholz, C.C., Beceren-Braun, F., Maritzen, T., Dervedde, J., Volkmer, R., Oschkinat, H., and Haucke, V. (2011). SNARE motif-mediated sorting of synaptobrevin by the endocytic adaptors clathrin assembly lymphoid myeloid leukemia (CALM) and AP180 at synapses. *Proc Natl Acad Sci U S A* 108, 13540-13545.

Koo, S.J., Puchkov, D., and Haucke, V. (2012). AP180 and CALM: Dedicated endocytic adaptors for the retrieval of synaptobrevin 2 at synapses. *Cell Logist* 1, 168-172.

Krauss, M., Kinuta, M., Wenk, M.R., De Camilli, P., Takei, K., and Haucke, V. (2003). ARF6 stimulates clathrin/AP-2 recruitment to synaptic membranes by activating phosphatidylinositol phosphate kinase type Igamma. *J Cell Biol* 162, 113-124.

Kreykenbohm, V., Wenzel, D., Antonin, W., Atlachkine, V., and von Mollard, G.F. (2002). The SNAREs vti1a and vti1b have distinct localization and SNARE complex partners. *European journal of cell biology* *81*, 273-280.

Kummel, D., Krishnakumar, S.S., Radoff, D.T., Li, F., Giraudo, C.G., Pincet, F., Rothman, J.E., and Reinisch, K.M. (2011). Complexin cross-links prefusion SNAREs into a zigzag array. *Nature structural & molecular biology* *18*, 927-933.

Kwon, S.E., and Chapman, E.R. (2012). Glycosylation is dispensable for sorting of synaptotagmin 1 but is critical for targeting of SV2 and synaptophysin to recycling synaptic vesicles. *The Journal of biological chemistry* *287*, 35658-35668.

Lang, T., and Jahn, R. (2008). Core proteins of the secretory machinery. *Handb Exp Pharmacol*, 107-127.

Lenzi, D., Runyeon, J.W., Crum, J., Ellisman, M.H., and Roberts, W.M. (1999). Synaptic vesicle populations in saccular hair cells reconstructed by electron tomography. *J Neurosci* *19*, 119-132.

Li, F., Pincet, F., Perez, E., Giraudo, C.G., Taresté, D., and Rothman, J.E. (2011). Complexin activates and clamps SNAREpins by a common mechanism involving an intermediate energetic state. *Nature structural & molecular biology* *18*, 941-946.

Liu, J., Guo, T., Wu, J., Bai, X., Zhou, Q., and Sui, S.F. (2007). Overexpression of complexin in PC12 cells inhibits exocytosis by preventing SNARE complex recycling. *Biochemistry (Mosc)* *72*, 439-444.

Loewi, O. (1926). About the vagus-substance. *Naturwissenschaften* *14*, 994-995.

Loschberger, A., van de Linde, S., Dabauvalle, M.C., Rieger, B., Heilemann, M., Krohne, G., and Sauer, M. (2012). Super-resolution imaging visualizes the eightfold symmetry of gp210 proteins around the nuclear pore complex and resolves the central channel with nanometer resolution. *Journal of cell science* *125*, 570-575.

Low, P., Norlin, T., Risinger, C., Larhammar, D., Pieribone, V.A., Shupliakov, O., and Brodin, L. (1999). Inhibition of neurotransmitter release in the lamprey reticulospinal synapse by antibody-mediated disruption of SNAP-25 function. *European journal of cell biology* 78, 787-793.

Ma, C., Li, W., Xu, Y., and Rizo, J. (2011). Munc13 mediates the transition from the closed syntaxin-Munc18 complex to the SNARE complex. *Nature structural & molecular biology* 18, 542-549.

Ma, C., Su, L., Seven, A.B., Xu, Y., and Rizo, J. (2012). Reconstitution of the vital functions of Munc18 and Munc13 in neurotransmitter release. *Science* 339, 421-425.

Mallard, F., Tang, B.L., Galli, T., Tenza, D., Saint-Pol, A., Yue, X., Antony, C., Hong, W., Goud, B., and Johannes, L. (2002). Early/recycling endosomes-to-TGN transport involves two SNARE complexes and a Rab6 isoform. *J Cell Biol* 156, 653-664.

Malsam, J., Parisotto, D., Bharat, T.A., Scheutzow, A., Krause, J.M., Briggs, J.A., and Sollner, T.H. (2012). Complexin arrests a pool of docked vesicles for fast Ca²⁺-dependent release. *The EMBO journal* 31, 3270-3281.

Marcello, E., Epis, R., Saraceno, C., and Di Luca, M. (2012). Synaptic dysfunction in Alzheimer's disease. *Adv Exp Med Biol* 970, 573-601.

Maritzen, T., Koo, S.J., and Haucke, V. (2012). Turning CALM into excitement: AP180 and CALM in endocytosis and disease. *Biol Cell* 104, 588-602.

Marques, O., and Outeiro, T.F. (2012). Alpha-synuclein: from secretion to dysfunction and death. *Cell Death Dis* 3, e350.

Marquez-Sterling, N.R., Lo, A.C., Sisodia, S.S., and Koo, E.H. (1997). Trafficking of cell-surface beta-amyloid precursor protein: evidence that a sorting intermediate participates in synaptic vesicle recycling. *J Neurosci* 17, 140-151.

Marra, V., Burden, J.J., Thorpe, J.R., Smith, I.T., Smith, S.L., Hausser, M., Branco, T., and Staras, K. (2012). A preferentially segregated recycling vesicle pool of limited size supports neurotransmission in native central synapses. *Neuron* *76*, 579-589.

Martin, A.R. (1994). Amplification of neuromuscular transmission by postjunctional folds. *Proc Biol Sci* *258*, 321-326.

Martin, J.A., Hu, Z., Fenz, K.M., Fernandez, J., and Dittman, J.S. (2011). Complexin has opposite effects on two modes of synaptic vesicle fusion. *Curr Biol* *21*, 97-105.

Marz, K.E., Lauer, J.M., and Hanson, P.I. (2003). Defining the SNARE complex binding surface of alpha-SNAP: implications for SNARE complex disassembly. *The Journal of biological chemistry* *278*, 27000-27008.

Matthew, W.D., Tsavaler, L., and Reichardt, L.F. (1981). Identification of a synaptic vesicle-specific membrane protein with a wide distribution in neuronal and neurosecretory tissue. *J Cell Biol* *91*, 257-269.

Mayer, M.L. (2005). Glutamate receptor ion channels. *Curr Opin Neurobiol* *15*, 282-288.

McMahon, H.T., Bolshakov, V.Y., Janz, R., Hammer, R.E., Siegelbaum, S.A., and Sudhof, T.C. (1996). Synaptophysin, a major synaptic vesicle protein, is not essential for neurotransmitter release. *Proc Natl Acad Sci U S A* *93*, 4760-4764.

McMahon, H.T., and Boucrot, E. (2011). Molecular mechanism and physiological functions of clathrin-mediated endocytosis. *Nature reviews* *12*, 517-533.

Merrifield, C.J., Feldman, M.E., Wan, L., and Almers, W. (2002). Imaging actin and dynamin recruitment during invagination of single clathrin-coated pits. *Nature cell biology* *4*, 691-698.

Miller, T.M., and Heuser, J.E. (1984). Endocytosis of synaptic vesicle membrane at the frog neuromuscular junction. *J Cell Biol* 98, 685-698.

Milosevic, I., Giovedi, S., Lou, X., Raimondi, A., Collesi, C., Shen, H., Paradise, S., O'Toole, E., Ferguson, S., Cremona, O., *et al.* (2011). Recruitment of endophilin to clathrin-coated pit necks is required for efficient vesicle uncoating after fission. *Neuron* 72, 587-601.

Mohrmann, R., de Wit, H., Verhage, M., Neher, E., and Sorensen, J.B. (2010). Fast vesicle fusion in living cells requires at least three SNARE complexes. *Science* 330, 502-505.

Monici, M. (2005). Cell and tissue autofluorescence research and diagnostic applications. *Biotechnol Annu Rev* 11, 227-256.

Morciano, M., Beckhaus, T., Karas, M., Zimmermann, H., and Volkandt, W. (2009). The proteome of the presynaptic active zone: from docked synaptic vesicles to adhesion molecules and maxi-channels. *J Neurochem* 108, 662-675.

Morciano, M., Burre, J., Corvey, C., Karas, M., Zimmermann, H., and Volkandt, W. (2005). Immunolocalization of two synaptic vesicle pools from synaptosomes: a proteomics analysis. *J Neurochem* 95, 1732-1745.

Morgan, J.R., Prasad, K., Hao, W., Augustine, G.J., and Lafer, E.M. (2000). A conserved clathrin assembly motif essential for synaptic vesicle endocytosis. *J Neurosci* 20, 8667-8676.

Morley, B.J., Kemp, G.E., and Salvaterra, P. (1979). alpha-Bungarotoxin binding sites in the CNS. *Life Sci* 24, 859-872.

Morlot, S., Galli, V., Klein, M., Chiaruttini, N., Manzi, J., Humbert, F., Dinis, L., Lenz, M., Cappello, G., and Roux, A. (2012). Membrane shape at the edge of the dynamin helix sets location and duration of the fission reaction. *Cell* 151, 619-629.

Moser, T., Brandt, A., and Lysakowski, A. (2006). Hair cell ribbon synapses. *Cell and tissue research* 326, 347-359.

Mostowy, S., and Cossart, P. (2012). Septins: the fourth component of the cytoskeleton. *Nature reviews* 13, 183-194.

Motley, A., Bright, N.A., Seaman, M.N., and Robinson, M.S. (2003). Clathrin-mediated endocytosis in AP-2-depleted cells. *J Cell Biol* 162, 909-918.

Mullock, B.M., Smith, C.W., Ihrke, G., Bright, N.A., Lindsay, M., Parkinson, E.J., Brooks, D.A., Parton, R.G., James, D.E., Luzio, J.P., *et al.* (2000). Syntaxin 7 is localized to late endosome compartments, associates with Vamp 8, and is required for late endosome-lysosome fusion. *Mol Biol Cell* 11, 3137-3153.

Murakami, K., Yasunaga, T., Noguchi, T.Q., Gomibuchi, Y., Ngo, K.X., Uyeda, T.Q., and Wakabayashi, T. (2010). Structural basis for actin assembly, activation of ATP hydrolysis, and delayed phosphate release. *Cell* 143, 275-287.

Musacchio, A., Smith, C.J., Roseman, A.M., Harrison, S.C., Kirchhausen, T., and Pearse, B.M. (1999). Functional organization of clathrin in coats: combining electron cryomicroscopy and X-ray crystallography. *Mol Cell* 3, 761-770.

Mutch, S.A., Gadd, J.C., Fujimoto, B.S., Kensel-Hammes, P., Schiro, P.G., Bajjalieh, S.M., and Chiu, D.T. (2011a). Determining the number of specific proteins in cellular compartments by quantitative microscopy. *Nature protocols* 6, 1953-1968.

Mutch, S.A., Kensel-Hammes, P., Gadd, J.C., Fujimoto, B.S., Allen, R.W., Schiro, P.G., Lorenz, R.M., Kuyper, C.L., Kuo, J.S., Bajjalieh, S.M., *et al.* (2011b). Protein quantification at the single vesicle level reveals that a subset of synaptic vesicle proteins are trafficked with high precision. *J Neurosci* 31, 1461-1470.

Nagy, A., Baker, R.R., Morris, S.J., and Whittaker, V.P. (1976). The preparation and characterization of synaptic vesicles of high purity. *Brain Res* 109, 285-309.

Neher, E., and Sakaba, T. (2008). Multiple roles of calcium ions in the regulation of neurotransmitter release. *Neuron* 59, 861-872.

Newton, A.J., Kirchhausen, T., and Murthy, V.N. (2006). Inhibition of dynamin completely blocks compensatory synaptic vesicle endocytosis. *Proc Natl Acad Sci U S A* 103, 17955-17960.

Nicholls, D.G. (1978). Calcium transport and proton electrochemical potential gradient in mitochondria from guinea-pig cerebral cortex and rat heart. *Biochem J* 170, 511-522.

Nikolov, M., Schmidt, C., and Urlaub, H. (2012). Quantitative mass spectrometry-based proteomics: an overview. *Methods Mol Biol* 893, 85-100.

Nonet, M.L., Holgado, A.M., Brewer, F., Serpe, C.J., Norbeck, B.A., Holleran, J., Wei, L., Hartwig, E., Jorgensen, E.M., and Alfonso, A. (1999). UNC-11, a *Caenorhabditis elegans* AP180 homologue, regulates the size and protein composition of synaptic vesicles. *Mol Biol Cell* 10, 2343-2360.

Nusser, Z. (1999). A new approach to estimate the number, density and variability of receptors at central synapses. *Eur J Neurosci* 11, 745-752.

Okamoto, M., Schoch, S., and Sudhof, T.C. (1999). EHS1/intersectin, a protein that contains EH and SH3 domains and binds to dynamin and SNAP-25. A protein connection between exocytosis and endocytosis? *The Journal of biological chemistry* 274, 18446-18454.

Opazo, F., Levy, M., Byrom, M., Schafer, C., Geisler, C., Groemer, T.W., Ellington, A.D., and Rizzoli, S.O. (2012). Aptamers as potential tools for super-resolution microscopy. *Nature methods* 9, 938-939.

Opazo, F., Punge, A., Bückers, J., Hoopmann, P., Kastrup, L., Hell, S.W., and Rizzoli, S.O. (2010). Limited intermixing of synaptic vesicle components upon vesicle recycling. *Traffic*.

Orenbuch, A., Shalev, L., Marra, V., Sinai, I., Lavy, Y., Kahn, J., Burden, J.J., Staras, K., and Gitler, D. (2012). Synapsin selectively controls the mobility of resting pool vesicles at hippocampal terminals. *J Neurosci* 32, 3969-3980.

Pakkenberg, B., and Gundersen, H.J. (1997). Neocortical neuron number in humans: effect of sex and age. *J Comp Neurol* 384, 312-320.

Pang, Z.P., Bacaj, T., Yang, X., Zhou, P., Xu, W., and Sudhof, T.C. (2011). Doc2 supports spontaneous synaptic transmission by a Ca²⁺-independent mechanism. *Neuron* 70, 244-251.

Pang, Z.P., Melicoff, E., Padgett, D., Liu, Y., Teich, A.F., Dickey, B.F., Lin, W., Adachi, R., and Sudhof, T.C. (2006a). Synaptotagmin-2 is essential for survival and contributes to Ca²⁺ triggering of neurotransmitter release in central and neuromuscular synapses. *J Neurosci* 26, 13493-13504.

Pang, Z.P., Sun, J., Rizo, J., Maximov, A., and Sudhof, T.C. (2006b). Genetic analysis of synaptotagmin 2 in spontaneous and Ca²⁺-triggered neurotransmitter release. *The EMBO journal* 25, 2039-2050.

Pearse, B.M. (1976). Clathrin: a unique protein associated with intracellular transfer of membrane by coated vesicles. *Proc Natl Acad Sci U S A* 73, 1255-1259.

Pechstein, A., Bacetic, J., Vahedi-Faridi, A., Gromova, K., Sundborger, A., Tomlin, N., Krainer, G., Vorontsova, O., Schafer, J.G., Owe, S.G., *et al.* (2010a). Regulation of synaptic vesicle recycling by complex formation between intersectin 1 and the clathrin adaptor complex AP2. *Proc Natl Acad Sci U S A* 107, 4206-4211.

Pechstein, A., Shupliakov, O., and Haucke, V. (2010b). Intersectin 1: a versatile actor in the synaptic vesicle cycle. *Biochem Soc Trans* 38, 181-186.

Pelassa, I., and Lagnado, L. (2011). Synaptic ribbons: machines for priming vesicle release? *Curr Biol* 21, R819-821.

Peng, J., Kim, M.J., Cheng, D., Duong, D.M., Gygi, S.P., and Sheng, M. (2004). Semiquantitative proteomic analysis of rat forebrain postsynaptic density fractions by mass spectrometry. *The Journal of biological chemistry* 279, 21003-21011.

Pennuto, M., Dunlap, D., Contestabile, A., Benfenati, F., and Valtorta, F. (2002). Fluorescence resonance energy transfer detection of synaptophysin I and vesicle-associated membrane protein 2 interactions during exocytosis from single live synapses. *Mol Biol Cell* 13, 2706-2717.

Perin, M.S., Fried, V.A., Stone, D.K., Xie, X.S., and Sudhof, T.C. (1991). Structure of the 116-kDa polypeptide of the clathrin-coated vesicle/synaptic vesicle proton pump. *The Journal of biological chemistry* 266, 3877-3881.

Perrais, D., and Merrifield, C.J. (2005). Dynamics of endocytic vesicle creation. *Dev Cell* 9, 581-592.

Pfriege, F.W. (2003). Role of cholesterol in synapse formation and function. *Biochim Biophys Acta* 1610, 271-280.

Phillips, G.R., Florens, L., Tanaka, H., Khaing, Z.Z., Fidler, L., Yates, J.R., 3rd, and Colman, D.R. (2005). Proteomic comparison of two fractions derived from the transsynaptic scaffold. *Journal of neuroscience research* 81, 762-775.

Phillips, G.R., Huang, J.K., Wang, Y., Tanaka, H., Shapiro, L., Zhang, W., Shan, W.S., Arndt, K., Frank, M., Gordon, R.E., *et al.* (2001). The presynaptic particle web: ultrastructure, composition, dissolution, and reconstitution. *Neuron* 32, 63-77.

Prekeris, R., Klumperman, J., Chen, Y.A., and Scheller, R.H. (1998). Syntaxin 13 mediates cycling of plasma membrane proteins via tubulovesicular recycling endosomes. *J Cell Biol* 143, 957-971.

Priller, C., Bauer, T., Mitteregger, G., Krebs, B., Kretzschmar, H.A., and Herms, J. (2006). Synapse formation and function is modulated by the amyloid precursor protein. *J Neurosci* 26, 7212-7221.

Puglielli, L., Ellis, B.C., Saunders, A.J., and Kovacs, D.M. (2003). Ceramide stabilizes beta-site amyloid precursor protein-cleaving enzyme 1 and promotes amyloid beta-peptide biogenesis. *The Journal of biological chemistry* 278, 19777-19783.

Qualmann, B., Roos, J., DiGregorio, P.J., and Kelly, R.B. (1999). Syndapin I, a synaptic dynamin-binding protein that associates with the neural Wiskott-Aldrich syndrome protein. *Mol Biol Cell* 10, 501-513.

Quetglas, S., Iborra, C., Sasakawa, N., De Haro, L., Kumakura, K., Sato, K., Leveque, C., and Seagar, M. (2002). Calmodulin and lipid binding to synaptobrevin regulates calcium-dependent exocytosis. *The EMBO journal* 21, 3970-3979.

Rabilloud, T. (2009). Membrane proteins and proteomics: love is possible, but so difficult. *Electrophoresis* 30 Suppl 1, S174-180.

Raingo, J., Khvotchev, M., Liu, P., Darios, F., Li, Y.C., Ramirez, D.M., Adachi, M., Lemieux, P., Toth, K., Davletov, B., *et al.* (2012). VAMP4 directs synaptic vesicles to a pool that selectively maintains asynchronous neurotransmission. *Nat Neurosci* 15, 738-745.

Ramirez, D.M., Khvotchev, M., Trauterman, B., and Kavalali, E.T. (2012). Vti1a identifies a vesicle pool that preferentially recycles at rest and maintains spontaneous neurotransmission. *Neuron* 73, 121-134.

Ramon y Cajal, S. (1894). La fine structure des centres nerveux. *Proceedings of the Royal Society of London* 55, 444-468.

Raptis, A., Torrejon-Escribano, B., Gomez de Aranda, I., and Blasi, J. (2005). Distribution of synaptobrevin/VAMP 1 and 2 in rat brain. *J Chem Neuroanat* 30, 201-211.

Reisinger, C., Yelamanchili, S.V., Hinz, B., Mitter, D., Becher, A., Bigalke, H., and Ahnert-Hilger, G. (2004). The synaptophysin/synaptobrevin complex dissociates independently of neuroexocytosis. *J Neurochem* 90, 1-8.

Rhee, H.W., Zou, P., Udeshi, N.D., Martell, J.D., Mootha, V.K., Carr, S.A., and Ting, A.Y. (2013). Proteomic Mapping of Mitochondria in Living Cells via Spatially Restricted Enzymatic Tagging. *Science*.

Ries, J., Kaplan, C., Platonova, E., Eghlidi, H., and Ewers, H. (2012). A simple, versatile method for GFP-based super-resolution microscopy via nanobodies. *Nature methods* 9, 582-584.

Rittweger, E., Han, K.Y., Irvine, S.E., Eggeling, C., and Hell, S.W. (2009). STED microscopy reveals crystal colour centres with nanometric resolution. *Nature Biophotonics* 2.

Rizzoli, S.O., Bethani, I., Zwillig, D., Wenzel, D., Siddiqui, T.J., Brandhorst, D., and Jahn, R. (2006). Evidence for early endosome-like fusion of recently endocytosed synaptic vesicles. *Traffic* 7, 1163-1176.

Rizzoli, S.O., and Betz, W.J. (2005). Synaptic vesicle pools. *Nature reviews* 6, 57-69.

Rizzoli, S.O., and Jahn, R. (2007). Kiss-and-run, collapse and 'readily retrievable' vesicles. *Traffic* 8, 1137-1144.

Roos, J., and Kelly, R.B. (1999). The endocytic machinery in nerve terminals surrounds sites of exocytosis. *Curr Biol* 9, 1411-1414.

Rosenmund, C., and Stevens, C.F. (1996). Definition of the readily releasable pool of vesicles at hippocampal synapses. *Neuron* 16, 1197-1207.

Rothnie, A., Clarke, A.R., Kuzmic, P., Cameron, A., and Smith, C.J. (2011). A sequential mechanism for clathrin cage disassembly by 70-kDa heat-shock cognate protein (Hsc70) and auxilin. *Proc Natl Acad Sci U S A* *108*, 6927-6932.

Roux, A., Uyhazi, K., Frost, A., and De Camilli, P. (2006). GTP-dependent twisting of dynamin implicates constriction and tension in membrane fission. *Nature* *441*, 528-531.

Royle, S.J., and Lagnado, L. (2010). Clathrin-mediated endocytosis at the synaptic terminal: bridging the gap between physiology and molecules. *Traffic* *11*, 1489-1497.

Saheki, Y., and De Camilli, P. (2012). Synaptic vesicle endocytosis. *Cold Spring Harb Perspect Biol* *4*, a005645.

Sakaba, T., and Neher, E. (2001). Calmodulin mediates rapid recruitment of fast-releasing synaptic vesicles at a calyx-type synapse. *Neuron* *32*, 1119-1131.

Sala, C., Roussignol, G., Meldolesi, J., and Fagni, L. (2005). Key role of the postsynaptic density scaffold proteins Shank and Homer in the functional architecture of Ca²⁺ homeostasis at dendritic spines in hippocampal neurons. *J Neurosci* *25*, 4587-4592.

Sankaranarayanan, S., Atluri, P.P., and Ryan, T.A. (2003). Actin has a molecular scaffolding, not propulsive, role in presynaptic function. *Nat Neurosci* *6*, 127-135.

Santoni, V., Molloy, M., and Rabilloud, T. (2000). Membrane proteins and proteomics: un amour impossible? *Electrophoresis* *21*, 1054-1070.

Saw, N.M., Kang, S.Y., Parsaud, L., Han, G.A., Jiang, T., Grzegorzczak, K., Surkont, M., Sun-Wada, G.H., Wada, Y., Li, L., *et al.* (2011). Vacuolar H⁽⁺⁾-ATPase subunits Voa1 and Voa2 cooperatively regulate secretory vesicle acidification, transmitter uptake, and storage. *Mol Biol Cell* *22*, 3394-3409.

Scales, S.J., Yoo, B.Y., and Scheller, R.H. (2001). The ionic layer is required for efficient dissociation of the SNARE complex by alpha-SNAP and NSF. *Proc Natl Acad Sci U S A* *98*, 14262-14267.

Schagger, H. (2006). Tricine-SDS-PAGE. *Nature protocols* *1*, 16-22.

Schagger, H., and von Jagow, G. (1987). Tricine-sodium dodecyl sulfate-polyacrylamide gel electrophoresis for the separation of proteins in the range from 1 to 100 kDa. *Anal Biochem* *166*, 368-379.

Schiavini, D.G., Puel, J.M., Averous, S.A., and Bazex, J.A. (1989). Quantitative western immunoblotting analysis in survey of human immunodeficiency virus-seropositive patients. *J Clin Microbiol* *27*, 2062-2066.

Schikorski, T., and Stevens, C.F. (1997). Quantitative ultrastructural analysis of hippocampal excitatory synapses. *J Neurosci* *17*, 5858-5867.

Schlossman, D.M., Schmid, S.L., Braell, W.A., and Rothman, J.E. (1984). An enzyme that removes clathrin coats: purification of an uncoating ATPase. *J Cell Biol* *99*, 723-733.

Schluter, O.M., Khvotchev, M., Jahn, R., and Sudhof, T.C. (2002). Localization versus function of Rab3 proteins. Evidence for a common regulatory role in controlling fusion. *The Journal of biological chemistry* *277*, 40919-40929.

Schluter, O.M., Schmitz, F., Jahn, R., Rosenmund, C., and Sudhof, T.C. (2004). A complete genetic analysis of neuronal Rab3 function. *J Neurosci* *24*, 6629-6637.

Schmid, E.M., and McMahon, H.T. (2007). Integrating molecular and network biology to decode endocytosis. *Nature* *448*, 883-888.

Schmidt, C., and Urlaub, H. (2012). Absolute quantification of proteins using standard peptides and multiple reaction monitoring. *Methods Mol Biol* *893*, 249-265.

Schmidt, M.R., and Haucke, V. (2007). Recycling endosomes in neuronal membrane traffic. *Biol Cell* 99, 333-342.

Schmidt, R., Wurm, C.A., Jakobs, S., Engelhardt, J., Egner, A., and Hell, S.W. (2008). Spherical nanosized focal spot unravels the interior of cells. *Nature methods*.

Schoch, S., Deak, F., Konigstorfer, A., Mozhayeva, M., Sara, Y., Sudhof, T.C., and Kavalali, E.T. (2001). SNARE function analyzed in synaptobrevin/VAMP knockout mice. *Science* 294, 1117-1122.

Schuske, K.R., Richmond, J.E., Matthies, D.S., Davis, W.S., Runz, S., Rube, D.A., van der Blik, A.M., and Jorgensen, E.M. (2003). Endophilin is required for synaptic vesicle endocytosis by localizing synaptojanin. *Neuron* 40, 749-762.

Schwaller, B. (2010). Cytosolic Ca²⁺ buffers. *Cold Spring Harb Perspect Biol* 2, a004051.

Schwaller, B. (2011). The use of transgenic mouse models to reveal the functions of Ca²⁺ buffer proteins in excitable cells. *Biochim Biophys Acta* 1820, 1294-1303.

Schwaller, B., Durussel, I., Jermann, D., Herrmann, B., and Cox, J.A. (1997). Comparison of the Ca²⁺-binding properties of human recombinant calretinin-22k and calretinin. *The Journal of biological chemistry* 272, 29663-29671.

Schwaller, B., Meyer, M., and Schiffmann, S. (2002). 'New' functions for 'old' proteins: the role of the calcium-binding proteins calbindin D-28k, calretinin and parvalbumin, in cerebellar physiology. Studies with knockout mice. *Cerebellum* 1, 241-258.

Schwanhausser, B., Busse, D., Li, N., Dittmar, G., Schuchhardt, J., Wolf, J., Chen, W., and Selbach, M. (2011). Global quantification of mammalian gene expression control. *Nature* 473, 337-342.

Scott, D., and Roy, S. (2012). alpha-Synuclein inhibits intersynaptic vesicle mobility and maintains recycling-pool homeostasis. *J Neurosci* 32, 10129-10135.

Serulle, Y., Sugimori, M., and Llinas, R.R. (2007). Imaging synaptosomal calcium concentration microdomains and vesicle fusion by using total internal reflection fluorescent microscopy. *Proc Natl Acad Sci U S A* 104, 1697-1702.

Sharma, M., Burre, J., Bronk, P., Zhang, Y., Xu, W., and Sudhof, T.C. (2011). CSPalpha knockout causes neurodegeneration by impairing SNAP-25 function. *The EMBO journal* 31, 829-841.

Sharma, M., Burre, J., and Sudhof, T.C. (2010). CSPalpha promotes SNARE-complex assembly by chaperoning SNAP-25 during synaptic activity. *Nature cell biology* 13, 30-39.

Sheng, M., and Hoogenraad, C.C. (2007). The postsynaptic architecture of excitatory synapses: a more quantitative view. *Annual review of biochemistry* 76, 823-847.

Sheng, Z.H., Rettig, J., Takahashi, M., and Catterall, W.A. (1994). Identification of a syntaxin-binding site on N-type calcium channels. *Neuron* 13, 1303-1313.

Shupliakov, O., Haucke, V., and Pechstein, A. (2011). How synapsin I may cluster synaptic vesicles. *Semin Cell Dev Biol* 22, 393-399.

Shupliakov, O., Low, P., Grabs, D., Gad, H., Chen, H., David, C., Takei, K., De Camilli, P., and Brodin, L. (1997). Synaptic vesicle endocytosis impaired by disruption of dynamin-SH3 domain interactions. *Science* 276, 259-263.

Sieber, J.J., Willig, K.I., Kutzner, C., Gerding-Reimers, C., Harke, B., Donnert, G., Rammner, B., Eggeling, C., Hell, S.W., Grubmuller, H., *et al.* (2007). Anatomy and dynamics of a supramolecular membrane protein cluster. *Science* 317, 1072-1076.

Siksou, L., Rostaing, P., Lechaire, J.P., Boudier, T., Ohtsuka, T., Fejtova, A., Kao, H.T., Greengard, P., Gundelfinger, E.D., Triller, A., *et al.* (2007). Three-dimensional architecture of presynaptic terminal cytomatrix. *J Neurosci* 27, 6868-6877.

Simonsen, A., Bremnes, B., Ronning, E., Aasland, R., and Stenmark, H. (1998). Syntaxin-16, a putative Golgi t-SNARE. *European journal of cell biology* 75, 223-231.

Sinha, R., Ahmed, S., Jahn, R., and Klingauf, J. (2011). Two synaptobrevin molecules are sufficient for vesicle fusion in central nervous system synapses. *Proc Natl Acad Sci U S A*.

Slepnev, V.I., and De Camilli, P. (2000). Accessory factors in clathrin-dependent synaptic vesicle endocytosis. *Nature reviews* 1, 161-172.

Smith, S.M., Renden, R., and von Gersdorff, H. (2008). Synaptic vesicle endocytosis: fast and slow modes of membrane retrieval. *Trends Neurosci* 31, 559-568.

Sollner, T., Bennett, M.K., Whiteheart, S.W., Scheller, R.H., and Rothman, J.E. (1993a). A protein assembly-disassembly pathway in vitro that may correspond to sequential steps of synaptic vesicle docking, activation, and fusion. *Cell* 75, 409-418.

Sollner, T., Whiteheart, S.W., Brunner, M., Erdjument-Bromage, H., Geromanos, S., Tempst, P., and Rothman, J.E. (1993b). SNAP receptors implicated in vesicle targeting and fusion. *Nature* 362, 318-324.

Sorensen, J.B., Nagy, G., Varoqueaux, F., Nehring, R.B., Brose, N., Wilson, M.C., and Neher, E. (2003). Differential control of the releasable vesicle pools by SNAP-25 splice variants and SNAP-23. *Cell* 114, 75-86.

Spacek, J., and Harris, K.M. (1998). Three-dimensional organization of cell adhesion junctions at synapses and dendritic spines in area CA1 of the rat hippocampus. *J Comp Neurol* 393, 58-68.

Staudt, T., Lang, M.C., Medda, R., Engelhardt, J., and Hell, S.W. (2007). 2,2'-thiodiethanol: a new water soluble mounting medium for high resolution optical microscopy. *Microscopy research and technique* 70, 1-9.

Steegmaier, M., Klumperman, J., Foletti, D.L., Yoo, J.S., and Scheller, R.H. (1999). Vesicle-associated membrane protein 4 is implicated in trans-Golgi network vesicle trafficking. *Mol Biol Cell* 10, 1957-1972.

Stenmark, H. (2009). Rab GTPases as coordinators of vesicle traffic. *Nature reviews* 10, 513-525.

Stenmark, H., Parton, R.G., Steele-Mortimer, O., Lutcke, A., Gruenberg, J., and Zerial, M. (1994). Inhibition of rab5 GTPase activity stimulates membrane fusion in endocytosis. *The EMBO journal* 13, 1287-1296.

Stenmark, H., Vitale, G., Ullrich, O., and Zerial, M. (1995). Rabaptin-5 is a direct effector of the small GTPase Rab5 in endocytic membrane fusion. *Cell* 83, 423-432.

Sterling, P., and Matthews, G. (2005). Structure and function of ribbon synapses. *Trends Neurosci* 28, 20-29.

Stevens, J., and Rogers, J.H. (1997). Chick calretinin: purification, composition, and metal binding activity of native and recombinant forms. *Protein Expr Purif* 9, 171-181.

Stevens, T.J., and Arkin, I.T. (2000). Do more complex organisms have a greater proportion of membrane proteins in their genomes? *Proteins* 39, 417-420.

Su, Q., Mochida, S., Tian, J.H., Mehta, R., and Sheng, Z.H. (2001). SNAP-29: a general SNARE protein that inhibits SNARE disassembly and is implicated in synaptic transmission. *Proc Natl Acad Sci U S A* 98, 14038-14043.

Sudhof, T.C. (2004). The synaptic vesicle cycle. *Annual review of neuroscience* 27, 509-547.

Sudhof, T.C. (2012). The presynaptic active zone. *Neuron* 75, 11-25.

Sudhof, T.C., and Rizo, J. (1996). Synaptotagmins: C2-domain proteins that regulate membrane traffic. *Neuron* 17, 379-388.

Sudhof, T.C., and Rizo, J. (2011). Synaptic vesicle exocytosis. *Cold Spring Harb Perspect Biol* 3.

Sudhof, T.C., and Rothman, J.E. (2009). Membrane fusion: grappling with SNARE and SM proteins. *Science* 323, 474-477.

Sugiyama, Y., Kawabata, I., Sobue, K., and Okabe, S. (2005). Determination of absolute protein numbers in single synapses by a GFP-based calibration technique. *Nature methods* 2, 677-684.

Sun, J.Y., Wu, X.S., and Wu, L.G. (2002). Single and multiple vesicle fusion induce different rates of endocytosis at a central synapse. *Nature* 417, 555-559.

Sundborger, A., Soderblom, C., Vorontsova, O., Evergren, E., Hinshaw, J.E., and Shupliakov, O. (2011). An endophilin-dynamin complex promotes budding of clathrin-coated vesicles during synaptic vesicle recycling. *Journal of cell science* 124, 133-143.

Sweitzer, S.M., and Hinshaw, J.E. (1998). Dynamin undergoes a GTP-dependent conformational change causing vesiculation. *Cell* 93, 1021-1029.

Takamori, S., Holt, M., Stenius, K., Lemke, E.A., Gronborg, M., Riedel, D., Urlaub, H., Schenck, S., Brugger, B., Ringler, P., *et al.* (2006). Molecular anatomy of a trafficking organelle. *Cell* 127, 831-846.

Takamori, S., Rhee, J.S., Rosenmund, C., and Jahn, R. (2000). Identification of a vesicular glutamate transporter that defines a glutamatergic phenotype in neurons. *Nature* 407, 189-194.

Tanaka, J., Matsuzaki, M., Tarusawa, E., Momiyama, A., Molnar, E., Kasai, H., and Shigemoto, R. (2005). Number and density of AMPA receptors in single synapses in immature cerebellum. *J Neurosci* 25, 799-807.

Tang, B.L., Tan, A.E., Lim, L.K., Lee, S.S., Low, D.Y., and Hong, W. (1998). Syntaxin 12, a member of the syntaxin family localized to the endosome. *The Journal of biological chemistry* 273, 6944-6950.

Taylor, M.J., Lampe, M., and Merrifield, C.J. (2012). A feedback loop between dynamin and actin recruitment during clathrin-mediated endocytosis. *PLoS Biol* 10, e1001302.

Tebar, F., Bohlander, S.K., and Sorkin, A. (1999). Clathrin assembly lymphoid myeloid leukemia (CALM) protein: localization in endocytic-coated pits, interactions with clathrin, and the impact of overexpression on clathrin-mediated traffic. *Mol Biol Cell* 10, 2687-2702.

Teng, H., and Wilkinson, R.S. (2000). Clathrin-mediated endocytosis near active zones in snake motor boutons. *J Neurosci* 20, 7986-7993.

Thiel, G. (1993). Synapsin I, synapsin II, and synaptophysin: marker proteins of synaptic vesicles. *Brain Pathol* 3, 87-95.

Thiele, C., Hannah, M.J., Fahrenholz, F., and Huttner, W.B. (2000). Cholesterol binds to synaptophysin and is required for biogenesis of synaptic vesicles. *Nature cell biology* 2, 42-49.

Tobaben, S., Thakur, P., Fernandez-Chacon, R., Sudhof, T.C., Rettig, J., and Stahl, B. (2001). A trimeric protein complex functions as a synaptic chaperone machine. *Neuron* 31, 987-999.

Toomre, D., and Bewersdorf, J. (2010). A new wave of cellular imaging. *Annu Rev Cell Dev Biol* 26, 285-314.

Toonen, R.F., Kochubey, O., de Wit, H., Gulyas-Kovacs, A., Konijnenburg, B., Sorensen, J.B., Klingauf, J., and Verhage, M. (2006a). Dissecting docking and tethering of secretory vesicles at the target membrane. *The EMBO journal* 25, 3725-3737.

Toonen, R.F., Wierda, K., Sons, M.S., de Wit, H., Cornelisse, L.N., Brussaard, A., Plomp, J.J., and Verhage, M. (2006b). Munc18-1 expression levels control synapse recovery by regulating readily releasable pool size. *Proc Natl Acad Sci U S A* *103*, 18332-18337.

Towbin, H., Staehelin, T., and Gordon, J. (1989). Immunoblotting in the clinical laboratory. *J Clin Chem Clin Biochem* *27*, 495-501.

Trevaskis, J., Walder, K., Foletta, V., Kerr-Bayles, L., McMillan, J., Cooper, A., Lee, S., Bolton, K., Prior, M., Fahey, R., *et al.* (2005). Src homology 3-domain growth factor receptor-bound 2-like (endophilin) interacting protein 1, a novel neuronal protein that regulates energy balance. *Endocrinology* *146*, 3757-3764.

Trigo, F.F., Sakaba, T., Ogden, D., and Marty, A. (2012). Readily releasable pool of synaptic vesicles measured at single synaptic contacts. *Proc Natl Acad Sci U S A* *109*, 18138-18143.

Trimble, W.S., Cowan, D.M., and Scheller, R.H. (1988). VAMP-1: a synaptic vesicle-associated integral membrane protein. *Proc Natl Acad Sci U S A* *85*, 4538-4542.

Turner, P.R., O'Connor, K., Tate, W.P., and Abraham, W.C. (2003). Roles of amyloid precursor protein and its fragments in regulating neural activity, plasticity and memory. *Prog Neurobiol* *70*, 1-32.

Uezu, A., Horiuchi, A., Kanda, K., Kikuchi, N., Umeda, K., Tsujita, K., Suetsugu, S., Araki, N., Yamamoto, H., Takenawa, T., *et al.* (2007). SGIP1alpha is an endocytic protein that directly interacts with phospholipids and Eps15. *The Journal of biological chemistry* *282*, 26481-26489.

Ungewickell, E., Ungewickell, H., Holstein, S.E., Lindner, R., Prasad, K., Barouch, W., Martin, B., Greene, L.E., and Eisenberg, E. (1995). Role of auxilin in uncoating clathrin-coated vesicles. *Nature* *378*, 632-635.

Urushihara, H., and Yanagisawa, K. (1987). Fusion of cell ghosts with intact cells in *Dictyostelium discoideum*: differential response of opposite mating-type cells. *Differentiation* *35*, 176-180.

Uytterhoeven, V., Kuenen, S., Kasprowicz, J., Miskiewicz, K., and Verstreken, P. (2011). Loss of skywalker reveals synaptic endosomes as sorting stations for synaptic vesicle proteins. *Cell* 145, 117-132.

Vagin, O., Kraut, J.A., and Sachs, G. (2009). Role of N-glycosylation in trafficking of apical membrane proteins in epithelia. *Am J Physiol Renal Physiol* 296, F459-469.

van de Bospoort, R., Farina, M., Schmitz, S.K., de Jong, A., de Wit, H., Verhage, M., and Toonen, R.F. (2012). Munc13 controls the location and efficiency of dense-core vesicle release in neurons. *J Cell Biol* 199, 883-891.

van den Bogaart, G., Holt, M.G., Bunt, G., Riedel, D., Wouters, F.S., and Jahn, R. (2010). One SNARE complex is sufficient for membrane fusion. *Nature structural & molecular biology* 17, 358-364.

van den Bogaart, G., Meyenberg, K., Risselada, H.J., Amin, H., Willig, K.I., Hubrich, B.E., Dier, M., Hell, S.W., Grubmuller, H., Diederichsen, U., *et al.* (2011). Membrane protein sequestering by ionic protein-lipid interactions. *Nature* 479, 552-555.

van der Blied, A.M., and Meyerowitz, E.M. (1991). Dynamin-like protein encoded by the *Drosophila shibire* gene associated with vesicular traffic. *Nature* 351, 411-414.

Varoqueaux, F., Sigler, A., Rhee, J.S., Brose, N., Enk, C., Reim, K., and Rosenmund, C. (2002). Total arrest of spontaneous and evoked synaptic transmission but normal synaptogenesis in the absence of Munc13-mediated vesicle priming. *Proc Natl Acad Sci U S A* 99, 9037-9042.

Vassar, R., Bennett, B.D., Babu-Khan, S., Kahn, S., Mendiaz, E.A., Denis, P., Teplow, D.B., Ross, S., Amarante, P., Loeloff, R., *et al.* (1999). Beta-secretase cleavage of Alzheimer's amyloid precursor protein by the transmembrane aspartic protease BACE. *Science* 286, 735-741.

Vautrin, J., and Mambrini, J. (1989). Synaptic current between neuromuscular junction folds. *J Theor Biol* *140*, 479-498.

Verhage, M., de Vries, K.J., Roshol, H., Burbach, J.P., Gispen, W.H., and Sudhof, T.C. (1997). DOC2 proteins in rat brain: complementary distribution and proposed function as vesicular adapter proteins in early stages of secretion. *Neuron* *18*, 453-461.

Verhage, M., Maia, A.S., Plomp, J.J., Brussaard, A.B., Heeroma, J.H., Vermeer, H., Toonen, R.F., Hammer, R.E., van den Berg, T.K., Missler, M., *et al.* (2000). Synaptic assembly of the brain in the absence of neurotransmitter secretion. *Science* *287*, 864-869.

Verhage, M., and Sorensen, J.B. (2008). Vesicle docking in regulated exocytosis. *Traffic* *9*, 1414-1424.

Vervaeke, K., Lorincz, A., Gleeson, P., Farinella, M., Nusser, Z., and Silver, R.A. (2010). Rapid desynchronization of an electrically coupled interneuron network with sparse excitatory synaptic input. *Neuron* *67*, 435-451.

Vincendon, G., Morgan, I.G., Gombos, G., and Breckenridge, W.C. (1972). [Comparative study of the composition of the synaptic vesicles and synaptosomal plasma membranes of the rat brain]. *J Physiol (Paris)* *65*, Suppl 1:173A.

Volkmandt, W., and Karas, M. (2012). Proteomic analysis of the presynaptic active zone. *Exp Brain Res* *217*, 449-461.

Walch-Solimena, C., Blasi, J., Edelmann, L., Chapman, E.R., von Mollard, G.F., and Jahn, R. (1995). The t-SNAREs syntaxin 1 and SNAP-25 are present on organelles that participate in synaptic vesicle recycling. *J Cell Biol* *128*, 637-645.

Walter, A.M., Groffen, A.J., Sorensen, J.B., and Verhage, M. (2011). Multiple Ca²⁺ sensors in secretion: teammates, competitors or autocrats? *Trends Neurosci* *34*, 487-497.

Wan, Q.F., Zhou, Z.Y., Thakur, P., Vila, A., Sherry, D.M., Janz, R., and Heidelberger, R. (2010). SV2 acts via presynaptic calcium to regulate neurotransmitter release. *Neuron* 66, 884-895.

Wang, Y.V., Wade, M., Wong, E., Li, Y.C., Rodewald, L.W., and Wahl, G.M. (2007). Quantitative analyses reveal the importance of regulated Hdmx degradation for p53 activation. *Proc Natl Acad Sci U S A* 104, 12365-12370.

Washbourne, P., Cansino, V., Mathews, J.R., Graham, M., Burgoyne, R.D., and Wilson, M.C. (2001). Cysteine residues of SNAP-25 are required for SNARE disassembly and exocytosis, but not for membrane targeting. *Biochem J* 357, 625-634.

Weldon, S., Ambroz, K., Schutz-Geschwender, A., and Olive, D.M. (2008). Near-infrared fluorescence detection permits accurate imaging of loading controls for Western blot analysis. *Anal Biochem* 375, 156-158.

Welzel, O., Henkel, A.W., Stroebel, A.M., Jung, J., Tischbirek, C.H., Ebert, K., Kornhuber, J., Rizzoli, S.O., and Groemer, T.W. (2011). Systematic heterogeneity of fractional vesicle pool sizes and release rates of hippocampal synapses. *Biophys J* 100, 593-601.

Wenk, M.R., and De Camilli, P. (2004). Protein-lipid interactions and phosphoinositide metabolism in membrane traffic: insights from vesicle recycling in nerve terminals. *Proc Natl Acad Sci U S A* 101, 8262-8269.

Wenk, M.R., Pellegrini, L., Klenchin, V.A., Di Paolo, G., Chang, S., Daniell, L., Arioka, M., Martin, T.F., and De Camilli, P. (2001). PIP kinase Iγ is the major PI(4,5)P₂ synthesizing enzyme at the synapse. *Neuron* 32, 79-88.

Westphal, C.H., and Chandra, S.S. (2013). Monomeric Synucleins Generate Membrane Curvature. *The Journal of biological chemistry* 288, 1829-1840.

Wienisch, M., and Klingauf, J. (2006). Vesicular proteins exocytosed and subsequently retrieved by compensatory endocytosis are nonidentical. *Nat Neurosci* 9, 1019-1027.

Wigge, P., Kohler, K., Vallis, Y., Doyle, C.A., Owen, D., Hunt, S.P., and McMahon, H.T. (1997). Amphiphysin heterodimers: potential role in clathrin-mediated endocytosis. *Mol Biol Cell* *8*, 2003-2015.

Wilhelm, B.G., Groemer, T.W., and Rizzoli, S.O. (2010). The same synaptic vesicles drive active and spontaneous release. *Nat Neurosci* *13*, 1454-1456.

Willem, M., Lammich, S., and Haass, C. (2009). Function, regulation and therapeutic properties of beta-secretase (BACE1). *Semin Cell Dev Biol* *20*, 175-182.

Willig, K.I., Rizzoli, S.O., Westphal, V., Jahn, R., and Hell, S.W. (2006). STED microscopy reveals that synaptotagmin remains clustered after synaptic vesicle exocytosis. *Nature* *440*, 935-939.

Willox, A.K., and Royle, S.J. (2012). Stonin 2 is a major adaptor protein for clathrin-mediated synaptic vesicle retrieval. *Curr Biol* *22*, 1435-1439.

Winther, A.M., Jiao, W., Vorontsova, O., Rees, K.A., Koh, T.W., Sopova, E., Schulze, K.L., Bellen, H.J., and Shupliakov, O. (2013). The dynamin-binding domains of Dap160/Intersectin affect bulk membrane retrieval in synapses. *Journal of cell science*.

Wojcik, S.M., Rhee, J.S., Herzog, E., Sigler, A., Jahn, R., Takamori, S., Brose, N., and Rosenmund, C. (2004). An essential role for vesicular glutamate transporter 1 (VGLUT1) in postnatal development and control of quantal size. *Proc Natl Acad Sci U S A* *101*, 7158-7163.

Wragg, R.T., Snead, D., Dong, Y., Ramlall, T.F., Menon, I., Bai, J., Eliezer, D., and Dittman, J.S. (2013). Synaptic vesicles position complexin to block spontaneous fusion. *Neuron* *77*, 323-334.

Wu, L.G., and Betz, W.J. (1999). Spatial variability in release at the frog neuromuscular junction measured with FM1-43. *Can J Physiol Pharmacol* *77*, 672-678.

Wu, W., and Wu, L.G. (2007). Rapid bulk endocytosis and its kinetics of fission pore closure at a central synapse. *Proc Natl Acad Sci U S A* *104*, 10234-10239.

Xing, Y., Bocking, T., Wolf, M., Grigorieff, N., Kirchhausen, T., and Harrison, S.C. (2010). Structure of clathrin coat with bound Hsc70 and auxilin: mechanism of Hsc70-facilitated disassembly. *The EMBO journal* 29, 655-665.

Xu, T., and Bajjalieh, S.M. (2001). SV2 modulates the size of the readily releasable pool of secretory vesicles. *Nature cell biology* 3, 691-698.

Xue, M., Craig, T.K., Xu, J., Chao, H.T., Rizo, J., and Rosenmund, C. (2010). Binding of the complexin N terminus to the SNARE complex potentiates synaptic-vesicle fusogenicity. *Nature structural & molecular biology* 17, 568-575.

Yamauchi, T. (2005). Neuronal Ca²⁺/calmodulin-dependent protein kinase II--discovery, progress in a quarter of a century, and perspective: implication for learning and memory. *Biol Pharm Bull* 28, 1342-1354.

Yang, L., Dun, A.R., Martin, K.J., Qiu, Z., Dunn, A., Lord, G.J., Lu, W., Duncan, R.R., and Rickman, C. (2012). Secretory Vesicles Are Preferentially Targeted to Areas of Low Molecular SNARE Density. *PLoS One* 7, e49514.

Yang, X., Kaeser-Woo, Y.J., Pang, Z.P., Xu, W., and Sudhof, T.C. (2010a). Complexin clamps asynchronous release by blocking a secondary Ca²⁺ sensor via its accessory alpha helix. *Neuron* 68, 907-920.

Yang, Y.M., Fedchyshyn, M.J., Grande, G., Aitoubah, J., Tsang, C.W., Xie, H., Ackerley, C.A., Trimble, W.S., and Wang, L.Y. (2010b). Septins regulate developmental switching from microdomain to nanodomain coupling of Ca²⁺ influx to neurotransmitter release at a central synapse. *Neuron* 67, 100-115.

Yao, J., Gaffaney, J.D., Kwon, S.E., and Chapman, E.R. (2011). Doc2 is a Ca²⁺ sensor required for asynchronous neurotransmitter release. *Cell* 147, 666-677.

Yao, J., Nowack, A., Kensel-Hammes, P., Gardner, R.G., and Bajjalieh, S.M. (2010). Cotrafficking of SV2 and synaptotagmin at the synapse. *J Neurosci* 30, 5569-5578.

Yeh, F.L., Dong, M., Yao, J., Tepp, W.H., Lin, G., Johnson, E.A., and Chapman, E.R. (2010). SV2 mediates entry of tetanus neurotoxin into central neurons. *PLoS Pathog* 6, e1001207.

Yoshimura, Y., Yamauchi, Y., Shinkawa, T., Taoka, M., Donai, H., Takahashi, N., Isobe, T., and Yamauchi, T. (2004). Molecular constituents of the postsynaptic density fraction revealed by proteomic analysis using multidimensional liquid chromatography-tandem mass spectrometry. *J Neurochem* 88, 759-768.

Zhang, Q., Li, Y., and Tsien, R.W. (2009). The dynamic control of kiss-and-run and vesicular reuse probed with single nanoparticles. *Science* 323, 1448-1453.

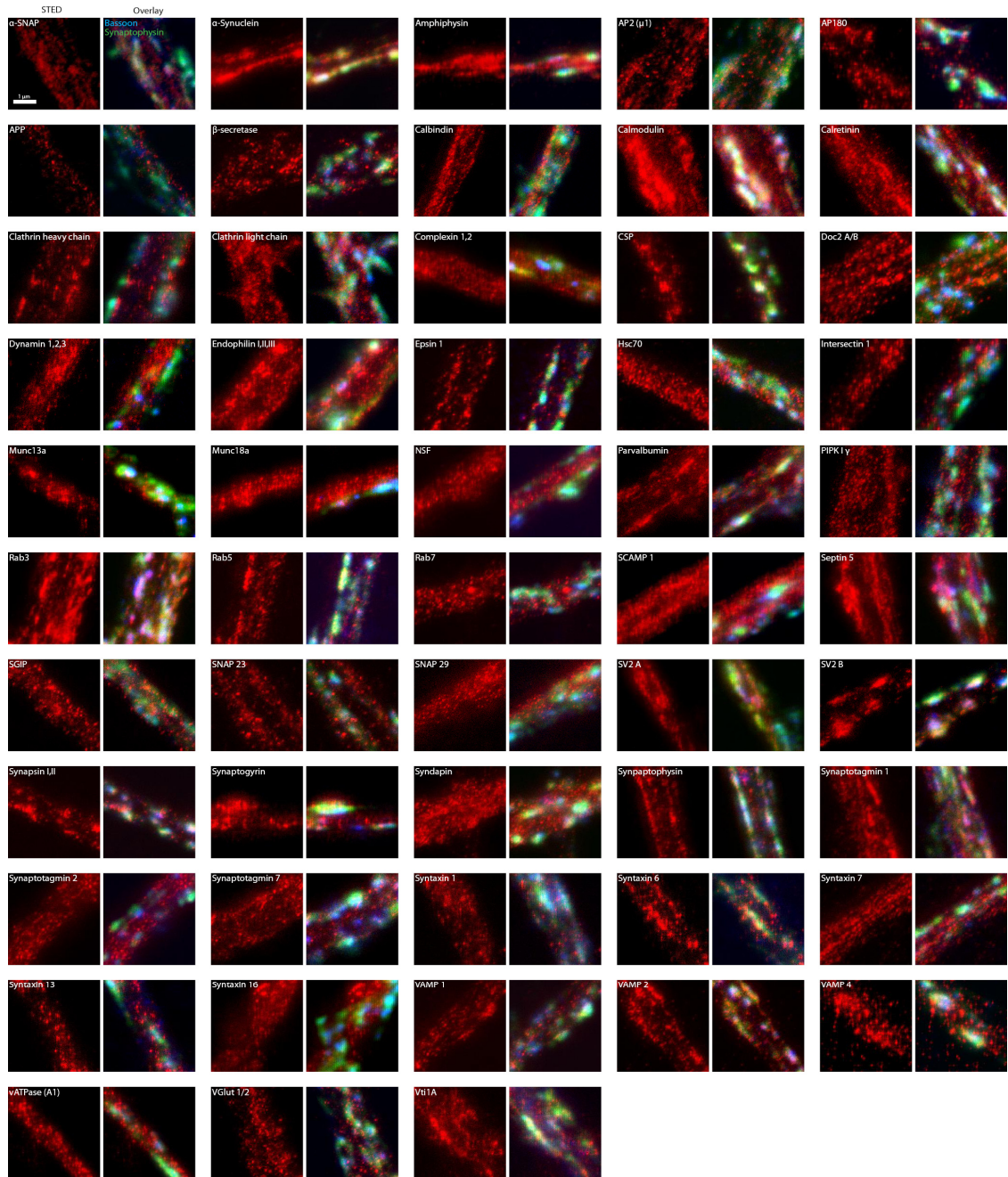
Zhang, Y.Q., Henderson, M.X., Colangelo, C.M., Ginsberg, S.D., Bruce, C., Wu, T., and Chandra, S.S. (2012). Identification of CSPalpha clients reveals a role in dynamin 1 regulation. *Neuron* 74, 136-150.

Ziff, E.B. (1997). Enlightening the postsynaptic density. *Neuron* 19, 1163-1174.

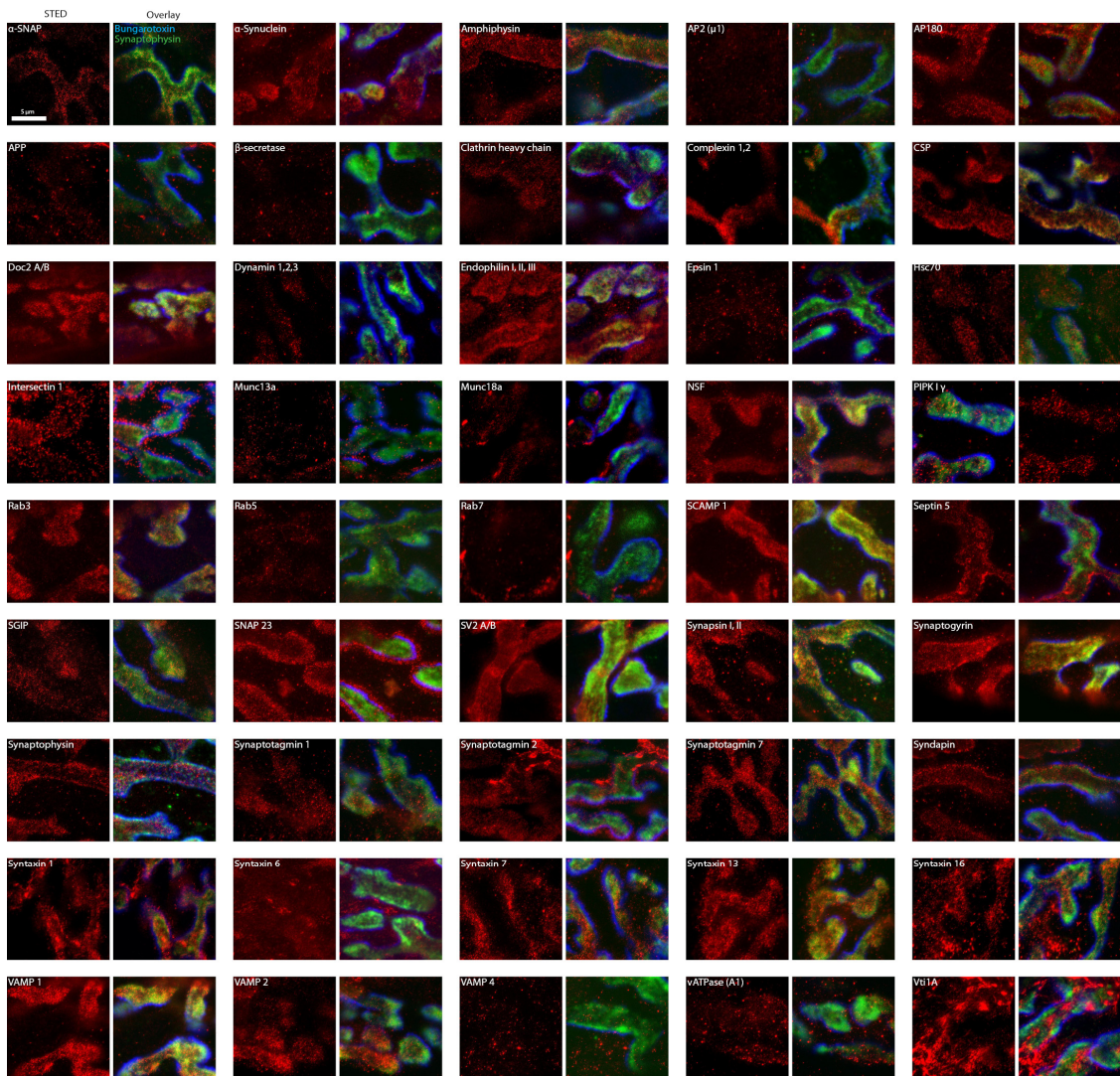
Zilly, F.E., Sorensen, J.B., Jahn, R., and Lang, T. (2006). Munc18-bound syntaxin readily forms SNARE complexes with synaptobrevin in native plasma membranes. *PLoS Biol* 4, e330.

Appendix

Appendix 1



Appendix 2



Curriculum Vitae

Benjamin Wilhelm

born 18th of December 1984 in Kassel

Personal Data

Address: Marienstr. 6
37073 Göttingen
Email: benni.wilhelm@gmx.de

Education

04/ 10 – 04/ 13 **Georg-August University Göttingen**, Göttingen
Neuroscience (International Max Planck Research School)
Dr. rer. nat.
10/ 08 – 03/ 10 **Georg-August University Göttingen**, Göttingen
Neuroscience (International Max Planck Research School)
Master of Science
08/ 97 – 06/ 04 Gymnasium Mellendorf, Wedemark
Allgemeine Hochschulreife
10/ 01 – 06/ 02 New Plymouth High School, New Plymouth, ID, USA
High School Diploma

Research Experience

04/ 10 – 04/ 13 **European Neuroscience Institute**, Göttingen
PhD student, Department: STED Microscopy of Synaptic Function
10/ 09 – 03/ 10 **European Neuroscience Institute**, Göttingen
Master's, Department: STED Microscopy of Synaptic Function
08/ 07 – 10/ 07 **Harvard University**, Cambridge, MA, USA
Internship, Department for Molecular and Cellular Biology
08/ 06 – 07/ 08 **Max Planck Institute for biophysical chemistry**, Göttingen
Internship, Department: Membranbiophysics

Stipends and Awards

06/ 11: Participation at the **Lindau Nobel Laureate Meeting**
04/ 11 – 04/ 13 PhD Fellowship from the **Boehringer Ingelheim Foundation**
11/ 10 – 04/ 11 **Excellence Stipend** from GGNB
06/ 08 – 04/ 10 **German National Academic Foundation**

Engagements

05/ 11 Organizer of the scientific conference "**Neurizons 2011**"
11/ 10 – 11/ 12: Campus Captain for **Teach First Germany**
08/ 08 – 04/ 13 **Student representative** MSc/PhD Neuroscience Program

Publications

Denker A, Bethani I, Kröhnert K, Körber C, Horstman H, Wilhelm BG, Barysch SV, Kuner T, Neher E and Rizzoli SO (2011) A small pool of vesicles maintains synaptic activity in vivo. **PNAS**, 108(41): 17177-82.

Wilhelm BG, Zhang W and Rizzoli SO (2011) Zur Synapse, bitte! **Gehirn und Geist**, 7-8: 68-73

Groemer TW, Thiel CS, Holt M, Riedel D, Hua Y, Hüve J, Wilhelm BG and Klingauf J (2011) Amyloid precursor protein is trafficked and secreted via synaptic vesicles. **PLoS one**, 6(4): e18754.

Wilhelm BG, Groemer TW and Rizzoli SO (2010) The same synaptic vesicles drive active and spontaneous release. **Nature Neuroscience**. 12:1454-1456